Contents of issue 5 vol. XLVI

Polish Academy of Sciences

Institute of Fundamental Technological Research

Archives of Mechanics

Archiwum Mechaniki Stosowanej

volume 46 issue 5

Polish Scientific Publishers PWN

Warszawa 1994

ARCHIVES OF MECHANICS IS DEVOTED TO
Theory of elasticity and plasticity • Theory of nonclassical continua • Physics of continuous media • Mechanics of discrete media • Nonlinear mechanics • Rheology • Fluid gas-mechanics • Rarefied gas • Thermodynamics

---

Printed in Poland, Editorial Office: Świętokrzyska 21,
00-049 Warszawa (Poland)

Arkuszy wydawniczych 14,75. Arkuszy drukarskich 13.
Papier offset. kl. III 70 g. B1. Oddano do składania w październiku 1994 r.
Druk ukończono w styczniu 1995 r.
Skład i łamanie: IPPT PAN
Druk i oprawa: Drukarnia Braci Grodzickich, Żabieniec ul. Przelotowa 7

Arch. Mech., 46, 5, pp. 611–623, Warszawa 1994

Inequalities for the effective transport coefficients of two-component composite materials

S. TOKARZEWSKI (WARSZAWA)

WE DERIVE the inequalities satisfied by the convergents of a continued fraction of type S, constructed for the effective physical properties of two-component composite materials. These inequalities represent the upper and lower bounds for the principal values of second-rank tensors representing the effective transport coefficients. The correspondence between continued fractions bounds and the bounds obtained by means of variational methods has been shown. As an example of application, we calculate the sequence of lower and upper bounds for the effective conductivity of isotropic composite, consisting of inclusions, regularly spaced in the matrix material.

1. Introduction

THE MATHEMATICAL properties of Padé approximants for Stieltjes functions have been extensively investigated in recent years [1–3, 12, 17]. One of the most important results presented in mathematical literature states that the sequence of Padé approximants represented by the convergents of a continued fraction of type S form the upper and lower bounds uniformly approaching the Stieltjes function. Moreover, these bounds are the best in respect to the given number of power series coefficients [1, theorem 15.2].

In 1978 BERGMAN proved [4], that the effective transport coefficients of a two-phase composite materials represented by eigenvalues of a second-rank tensor have Stieltjes-function representation. Hence all theoretical results for Padé approximants to Stieltjes functions [1–3, 9, 12, 17] can be directly applied to the theory of inhomogeneous media on order to determine the lower and upper bounds for the effective transport coefficients of composite materials.

The main aim of this paper is to derive, on the basis of the results reported in the literature [1, theorem 15.2] and in BERGMAN'S paper [4], the general inequalities determining, in terms of the convergents of S-continued fractions, the upper and lower bounds for the effective transport coefficients of two-component inhomogeneous media.

The problem we are investigating has been extensively studied, for instance in the references quoted below; of these, BERGMAN [4–8], FELDERHOF [10], MCPHEDRAN *et al.* [14] and MILTON [15] are particularly relevant to the present work.

To illustrate the S-continued fraction method presented in this paper, the bounds for the effective conductivity coefficients for both the square and hexagonal array of cylinders have been calculated in the form of the convergents of the S-continued fraction.

2. Basic assumptions, definitions and notations

We will consider the composite consisting of inclusions of conductivity λ_2 embedded in a matrix material of conductivity λ_1. The bulk effective conductivity constant λ_e is defined by the linear relationship between the volume-averaged temperature gradient $<\nabla \mathbf{T}>$ and the volume-averaged heat flux $<\mathbf{J}>$.

$$<\mathbf{J}> = \lambda_e <\nabla \mathbf{T}> . \tag{2.1}$$

The matrix and the inclusion volume fractions will be denoted by p_1 and p_2. In general λ_e will be a second-rank symmetric tensor, even when λ_1 and λ_2 are both scalars, and will depend not only on the precise microstructure, but also on the macroscopic shape of the sample and on the boundary conditions fulfilled by the fields $<\nabla \mathbf{T}>$ and $<\mathbf{J}>$. However, the only physical situations where λ_e is really interesting are those where the microstructure, as well as the boundary conditions, are sufficiently uniform so that λ_e is an intensive quantity, i.e., independent of the total size and shape of the sample and of the precise value $<\nabla \mathbf{T}>$. Even in that case, $\lambda_e(\lambda_1, \lambda_2)$ will still be a tensor function in general, the precise form of which depends on the precise microgeometry. Consider the four power expansions of the effective conductivity λ_e [4]

$$F_j(z_j) = \sum_{n=1}^{\infty} c_{nj}(z_j)^n, \qquad j = 1,2,3,4, \tag{2.2}$$

a) for $j = 1$

$$F_1 = \frac{\lambda_e}{\lambda_1} - 1, \qquad z_1 = h - 1,$$

b) for $j = 2$

$$F_2 = \frac{\lambda_2}{\lambda_e} - 1, \qquad z_2 = h - 1,$$

c) for $j = 3$

$$F_3 = \frac{\lambda_e}{\lambda_2} - 1, \qquad z_3 = l - 1,$$

d) for $j = 4$

$$F_4 = \frac{\lambda_1}{\lambda_e} - 1, \qquad z_4 = l - 1,$$

where

$$h = \lambda_2/\lambda_1, \qquad l = 1/h = \lambda_1/\lambda_2 . \tag{2.3}$$

It has been proved in the literature [1, theorem 15.2], that for real, nonnegative z_j, $j = 1,2,3,4$, the following convergents

$$[M + 1/M](z_j) = \frac{g_{1j}z_j}{1} + \ldots + \frac{g_{(2M)j}z_j}{1} + \frac{g_{(2M+1)j}z_j}{1}, \tag{2.4}$$

and

$$[M/M](z_j) = \frac{g_{1j}z_j}{1} + \ldots + \frac{g_{(2M-1)j}z_j}{1} + \frac{g_{(2M)j}z_j}{1} \tag{2.5}$$

of the S-continued fraction for Stieltjes series (2.2) form the sequences of upper bounds (2.4)

$$[M + 1/M](z_j) \geq F_j(z_j), \qquad j = 1,2,3,4 \tag{2.6}$$

and lower bounds (2.5)

$$[M/M](z_j) \leq F_j(z_j), \qquad j = 1,2,3,4, \tag{2.7}$$

uniformly converging to the function $F_j(z_j)$, $j = 1,2,3,4$. Due to $(2.2)_{a-d}$, the inequalities (2.6) and (2.7) can be rewritten as follows: for $h \geq 1$

$$\lambda_1[R + 1/R](z_1) \geq \lambda_e \geq \lambda_2 \{[R + 1/R](z_2)\}^{-1}, \tag{2.8}$$

$$\lambda_1[R/R](z_1) \leq \lambda_e \leq \lambda_2 \{[R/R](z_2)\}^{-1}; \tag{2.9}$$

for $0 \leq h \leq 1$

$$\lambda_2[R + 1/R](z_3) \geq \lambda_e \geq \lambda_1 \{[R + 1/R](z_4)\}^{-1}, \tag{2.10}$$

$$\lambda_2[R/R](z_3) \leq \lambda_e \leq \lambda_1 \{[R/R](z_4)\}^{-1}, \tag{2.11}$$

where for convenience the substitutions

$$[R + 1/R] = 1 + [M + 1/M], \qquad [R/R] = 1 + [M/M] \tag{2.12}$$

have been made. It is necessary to notice that rational functions $[R + 1/R]$ and $[R/R]$ are Padé approximants to the series representing λ_e/λ_k and λ_k/λ_e, $k = 1,2$ $(2.2)_{a-d}$, respectively.

3. General lower and upper bounds

In this section we will prove two important theorems establishing general inequalities satisfied by convergents of S-continued fraction to Stieltjes series. These inequalities represent general upper and lower bounds for the effective physical properties of two-phase composites.

THEOREM 1. *The convergents of S-continued fractions $[M + 1/M](z_1)$ and $[M + 1/M](z_2)$ to power expansions of Stieltjes series $(2.2)_a$ and $(2.2)_b$, respectively, obey the following inequalities valid for $h \geq 0$,*

$$\lambda_1 \{1 + [M + 1/M](z_1)\} \geq \lambda_e \geq \lambda_2 \{1 + [M + 1/M](z_2)\}^{-1}, \tag{3.1}$$

where the effective conductivity λ_e stands for the limit as M goes to infinity of

$$\lambda_1\{1 + [M + 1/M](z_1)\} \qquad \text{or} \qquad \lambda_2\{1 + [M + 1/M](z_2)\}^{-1}.$$

These inequalities form the best upper and lower bounds which can be obtained by means of a given, odd number of coefficients of series of $(2.2)_a$ *and* $(2.2)_b$, *and that the use of additional coefficients (higher M) improves the bounds.*

P r o o f. On the basis of $(2.2)_a$, $(2.2)_c$ and (2.2) we can write

$$l \cdot \left(1 + \sum_{n=1}^{\infty} c_{n1}\left(l^{-1} - 1\right)^n\right) = 1 + \sum_{n=1}^{\infty} c_{n3}(l-1)^n. \tag{3.2}$$

By differentiating both sides of (3.2) n times with respect to l, we obtain for $l = 1$

$$\frac{1}{n!}\frac{\partial^n}{\partial l^n}\left\{l \cdot \left(1 + \sum_{j=1}^{\infty} c_{j1}\left(l^{-1} - 1\right)^j\right)\right\}_{l=1} = c_{n3}. \tag{3.3}$$

It is necessary to notice that

$$\frac{1}{n!}\frac{\partial^n}{\partial l^n}\{l \cdot [R + 1/R](z_1)\}_{l=1} = c_{n3}, \qquad z_1 = l^{-1} - 1, \tag{3.4}$$

because the rational function $[R + 1/R](z_1)$, $z_1 = h - 1$ is a Padé approximant to the series $1 + \sum_{n=1}^{\infty} c_{n1}(h-1)^n$. Additionally we have

$$\frac{1}{n!}\frac{\partial^n}{\partial l^n}\{[R + 1/R](z_3)\}_{l=1} = c_{n3}, \qquad z_3 = l^{-1} - 1. \tag{3.5}$$

Due to (3.4) and (3.5) we can write

$$\lambda_1[R + 1/R](z_1) = \lambda_2[R + 1/R](z_3). \tag{3.6}$$

Using identical argumentations one can prove that

$$\lambda_2\{[R + 1/R](z_2)\}^{-1} = \lambda_1\{[R + 1/R](z_4)\}^{-1}. \tag{3.7}$$

Equalities (3.6)–(3.7), inequalities (2.8)–(2.11), relation (2.12) and inequalities (2.6)–(2.7) lead directly to the Theorem 1.

THEOREM 2. *The S-fractions convergents $[M/M](z_1)$ and $[M/M](z_2)$ for power expansions of the Stieltjes series* $(2.2)_a$ *and* $(2.2)_b$ *satisfy the following inequalities*

$$\lambda_1\{1 + [M/M](z_1)\} \leq \lambda_e \leq \lambda_2\{1 + [M/M](z_2)\}^{-1}, \tag{3.8}$$

and for $0 \leq h \leq 1$

$$\lambda_1\{1 + [M/M](z_1)\} \geq \lambda_e \geq \lambda_2\{1 + [M/M](z_2)\}^{-1}, \tag{3.9}$$

where the effective conductivity λ_e *stands for the limit as* M *goes to infinity of* $\lambda_1\{1 + [M/M](z_1)\}$ *or* $\lambda_2\{1 + [M/M](z_2)\}^{-1}$. *These inequalities form the best upper and lower bounds which can be obtained by means of a given, even number of coefficients of series of* $(2.2)_a$ *and* $(2.2)_b$, *and that the use of additional coefficients (higher* M*) improves the bounds.*

P r o o f. On the basis of $(2.2)_a$ and $(2.2)_d$ we can write

$$\left\{\sum_{n=1}^{\infty} c_{n1}\left(l^{-1}-1\right)^n\right\}^{-1} = \sum_{n=1}^{\infty} c_{n4}(l-1)^n. \tag{3.10}$$

By differentiating both sides of (3.10) n times with respect to l, we obtain for $l = 1$

$$\frac{1}{n!}\frac{\partial^n}{\partial l^n}\left\{\sum_{j=1}^{\infty} c_{j1}(z_1)^j\right\}^{-1} = c_{n4}, \qquad z_1 = l^{-1} - 1. \tag{3.11}$$

Due to the definition of Padé approximants to power series and on the basis of (3.10) – (3.11) we have

$$\frac{\partial^n}{\partial l^n}\left\{[R/R]\left(l^{-1}-1\right)\right\}_{l=1}^{-1} = \frac{\partial^n}{\partial l}\{[R/R](l-1)\}_{l=1} = n!\, c_{n4}. \tag{3.12}$$

Hence we can write

$$[R/R](z_1) = \{[R/R](z_4)\}^{-1}. \tag{3.13}$$

Using identical arguments the following equality can be proved

$$\{[R/R](z_2)\}^{-1} = [R/R](z_3). \tag{3.14}$$

Equalities (3.13) – (3.14), inequalities (2.8) – (2.11), relation (2.12) and inequalities (2.6) – (2.7) lead directly to the Theorem 2. The Theorems 1, 2 determine, by means of convergents of S-continued fraction, the best upper and lower bounds for the effective transport coefficients of two-phase composite materials with respect to the given odd (Theorem 1) and even (Theorem 2) number of coefficients of power series $(2.2)_a$ and $(2.2)_b$. The coefficients of $(2.2)_b$ are uniquely determined by the coefficients of $(2.2)_a$ by means of the following recurrence formula

$$c_{02} = 1, \qquad c_{12} = 1 - c_{11}, \qquad c_{N2} = -\sum_{k=1}^{N} c_{k1}\, c_{(N-k)2}. \tag{3.15}$$

Due to relation (3.15), only power series $(2.2)_a$ is needed in the S-continued fraction approach to the study of upper and lower bounds for the effective transport constants.

4. Examples of applications

For macroscopically isotropic, two-component composite materials the first two coefficients of power series $(2.2)_a$ are as follows [4]:

$$\frac{\lambda_e}{\lambda_1} - 1 = p_2(h-1) - \frac{1}{d}p_1p_2(h-1)^2 + \dots , \tag{4.1}$$

where p_1 and p_2 denote the volume fractions of inclusions and of the matrix, respectively. Parameter d takes the value $d = 2$ for a two-dimensional case, and $d = 3$ for three-dimensional case. By using the recurrence formula (3.15), one can calculate the series $(2.2)_b$.

$$\frac{\lambda_2}{\lambda_e} - 1 = p_1(h-1) - \frac{d-1}{d}p_1p_2(h-1)^2 + \dots . \tag{4.2}$$

The S-continued fractions corresponding to the series (4.1) and (4.2) are as follows:

$$\frac{\lambda_e}{\lambda_1} - 1 = \frac{p_2z_1}{1} + \frac{(p_1/d)z_1}{1} + \dots \tag{4.3}$$

and

$$\frac{\lambda_2}{\lambda_e} - 1 = \frac{p_1z_2}{1} + \frac{[(d-1)/d]p_2z_2}{1} + \dots . \tag{4.4}$$

The first term of S-continued fraction in (4.3), and the first term in (4.4), lead to the upper and lower bounds (Theorem 1)

$$(p_1/\lambda_1 + p_2/\lambda_2)^{-1} \leq \lambda_e \leq p_1\lambda_1 + p_2\lambda_2 , \tag{4.5}$$

known as WIENER'S bounds [18]. By taking into account the two terms on the right-hand side of (4.3) and of (4.4), we obtain (Theorem 2) the following bounds: for $h = \lambda_2/\lambda_1 \geq 1$

$$\lambda_1 + \frac{p_2}{1/(\lambda_2 - \lambda_1) + p_1/(d \cdot \lambda_1)} \leq \lambda_e \leq \lambda_2 + \frac{p_1}{1/(\lambda_1 - \lambda_2) + p_2/(d \cdot \lambda_2)} \tag{4.6}$$

and for $h = \lambda_2/\lambda_1 \leq 1$

$$\lambda_1 + \frac{p_2}{1/(\lambda_2 - \lambda_1) + p_1/(d \cdot \lambda_1)} \geq \lambda_e \geq \lambda_2 + \frac{p_1}{1/(\lambda_1 - \lambda_2) + p_2/(d \cdot \lambda_2)} . \tag{4.7}$$

Inequalities (4.6)–(4.7) are HASHIN–SHTRIKMAN bounds [11]. If more than two terms of S-fractions (4.3)–(4.4) are available, the bounds are improved. To illustrate this fact we investigate a square and hexagonal array of cylinders. We

assume the unit distance between the centers of neighbouring of cylinders. The conductivities of the cylinders and of the surrounding matrix are specified by their ratio h. The ratio λ_e/λ_1 of the effective conductivity to that of the matrix has been evaluated with the aid of the algorithm reported in paper [13]. The numerical calculations have been carried out for both square ($p_2 = 0.75$) and hexagonal ($p_2 = 0.88$) arrays of cylinders. For a square array we have obtained:

1) the power series $(2.2)_a$

$$\frac{\lambda_e}{\lambda_1} - 1 = 0.75z_1 - 0.0937z_1^2 + 0.0301z_1^3 - 0.0153z_1^4 + 0.0092z_1^5 + \ldots; \tag{4.8}$$

2) the power series $(2.2)_b$

$$\frac{\lambda_2}{\lambda_e} - 1 = 0.25z_2 - 0.0937z_2^2 + 0.0636z_2^3 - 0.0488z_2^4 + 0.0400z_2^5 + \ldots; \tag{4.9}$$

3) the S-continued fraction (2.4) corresponding to (4.8)

$$\frac{\lambda_e}{\lambda_1} - 1 = \frac{0.750z_1}{1} + \frac{0.125z_1}{1} + \frac{0.136z_1}{1}\frac{0.304z_1}{1} + \ldots; \tag{4.10}$$

4) the S-continued fraction (2.5) corresponding to (4.9)

$$\frac{\lambda_2}{\lambda_e} - 1 = \frac{0.250z_2}{1} + \frac{0.375z_2}{1} + \frac{0.304z_2}{1} + \frac{0.196z_2}{1} + \ldots; \tag{4.11}$$

For a hexagonal array we have:

1) the power series $(2.2)_a$

$$\frac{\lambda_e}{\lambda_1} - 1 = 0.88z_1 - 0.0528z_1^2 + 0.0109z_1^3 - 0.0050z_1^4 + 0.0030z_1^5 + \ldots; \tag{4.12}$$

2) the power series $(2.2)_b$

$$\frac{\lambda_2}{\lambda_e} - 1 = 0.12z_2 - 0.0528z_2^2 + 0.0419z_2^3 - 0.0360z_2^4 + 0.0321z_2^5 + \ldots; \tag{4.13}$$

3) the S-continued fractions (2.4) to series (4.12)

$$\frac{\lambda_e}{\lambda_1} - 1 = \frac{0.880z_1}{1} + \frac{0.060z_1}{1} + \frac{0.146z_1}{1} + \frac{0.354z_1}{1} + \ldots; \tag{4.14}$$

4) the S-continued fractions (2.5) to series (4.13)

$$\frac{\lambda_2}{\lambda_e} - 1 = \frac{0.120z_2}{1} + \frac{0.440z_2}{1} + \frac{0.354z_2}{1} + \frac{0.146z_2}{1} + \ldots. \tag{4.15}$$

The hierarchy of upper and lower bounds for the effective conductivity of square and hexagonal arrays of cylinders are depicted in Fig. 1 and Fig. 2, respectively. Our numerical results presented in Figs. 1, 2 coincide with the result obtained by means of a variational approach reported in paper [14] in Figs. 2, 4.

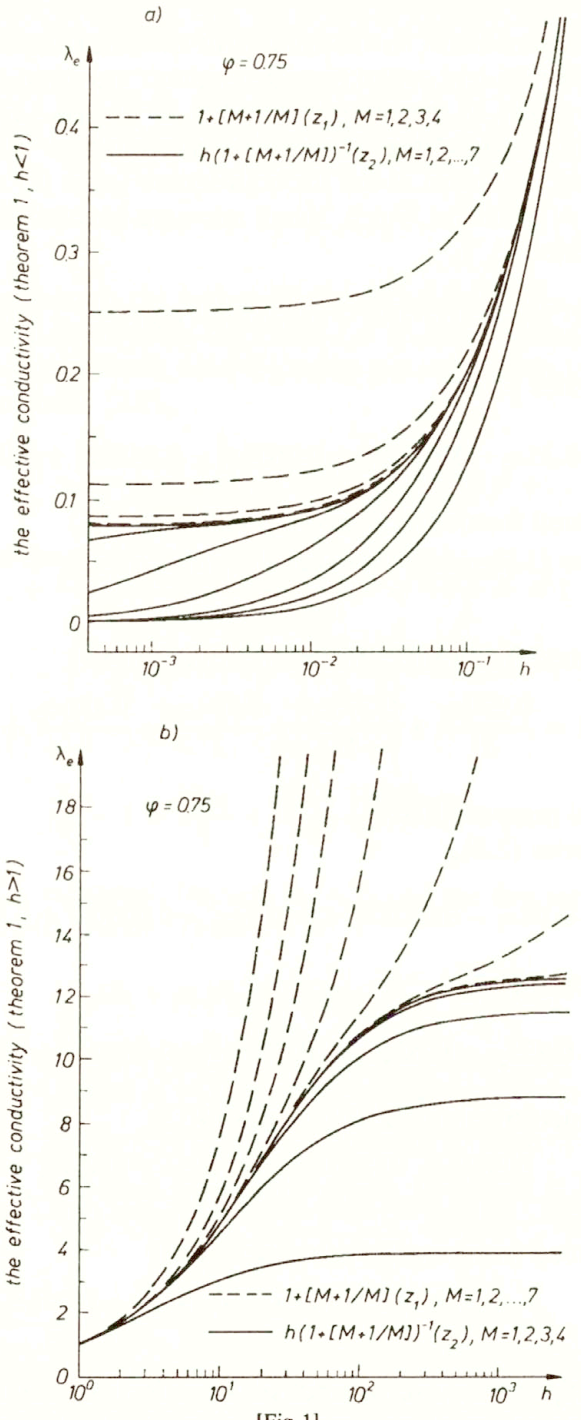

[Fig. 1]

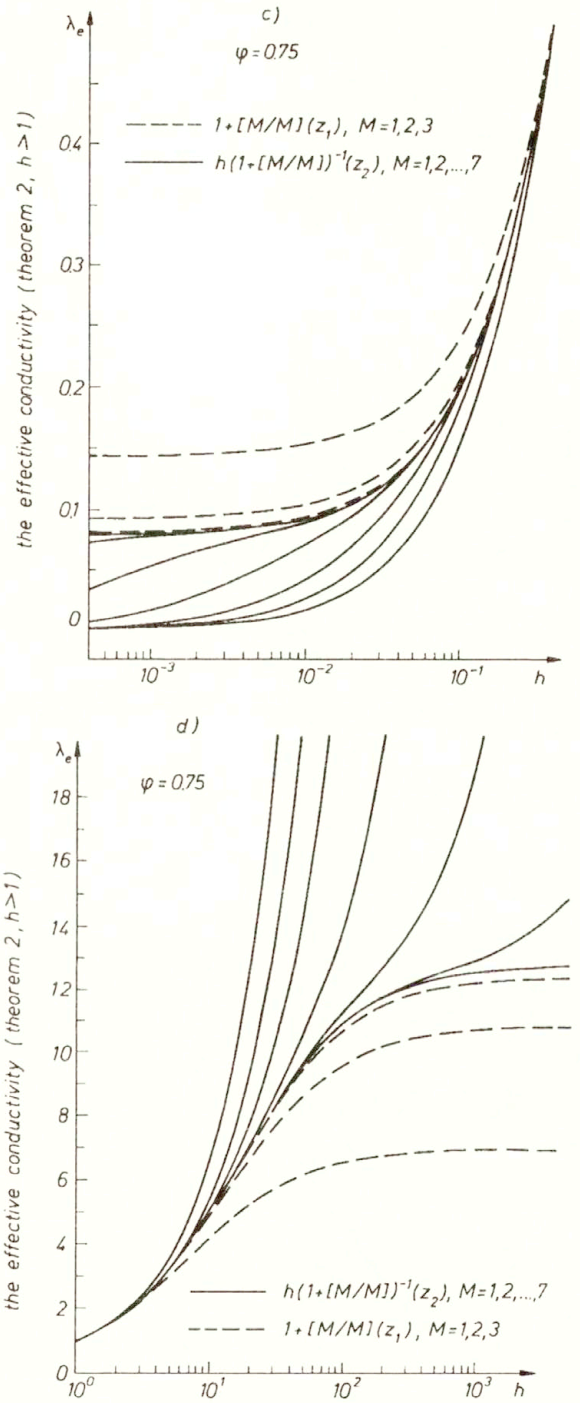

FIG. 1. The hierarchy of upper and lower bounds for the effective conductivity of square array of cylinders represented by a sequence of convergents of S-continued fractions ($\lambda_1 = 1$, φ-volume fraction of cylinders).

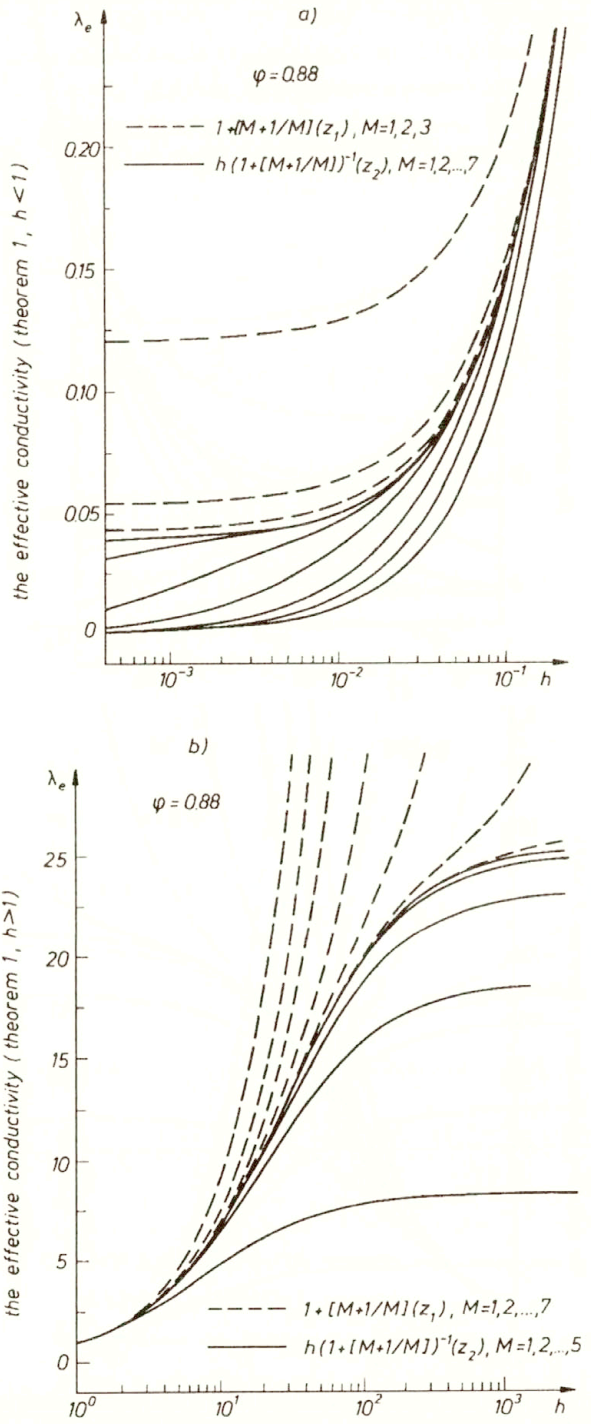

[Fig. 2]

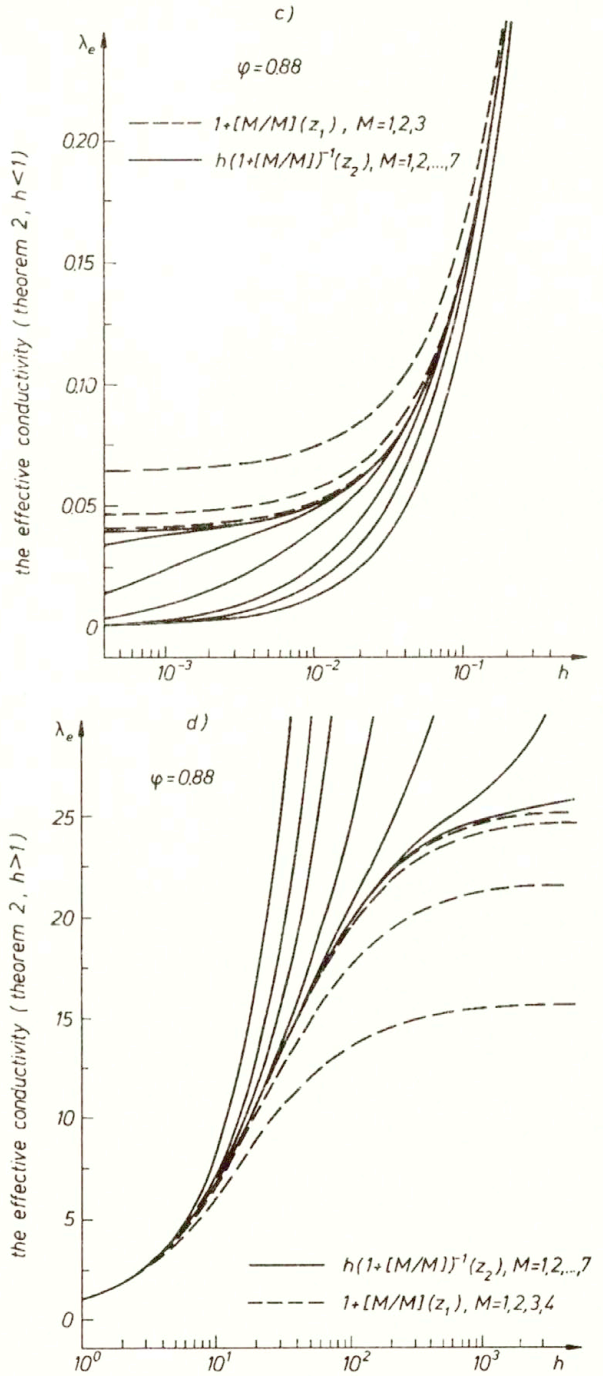

FIG. 2. The hierarchy of upper and lower bounds for the effective conductivity of hexagonal array of cylinders represented by a sequence of convergents of S-continued fractions ($\lambda_1 = 1$, φ-volume fraction of cylinders).

5. Discussion

The macroscopic behaviour of inhomogeneous two-component media has been extensively studied by BERGMAN [4–8], FELDERHOF [10], MCPHEDRAN *et al.* [14] and MILTON [15]. They investigated the problem concerning the bounds for the complex, effective transport coefficients of two-component composite materials. The bounds obtained by them take the form of a nested sequence of lens-shaped regions in the complex plane. For the case of real, effective constants these lens-shaped regions become transformed to finite intervals occupying the positive part of a real axis. The beginning and the end of those intervals indicate lower and upper bounds, respectively. It implies, that the bounds reported in [4–8, 10, 14] are recognizable as lower and upper bounds only after numerical calculations (no general inequalities determining upper or lower bounds).

On the contrary, the Theorems 1, 2 derived in this paper, specify the upper or lower bounds for the effective modulus λ_e depending on $h = \lambda_1/\lambda_2$ and on the order of Padé approximants $[M/M]$, $[M + 1/M]$ to the given, odd or even, number of power series coefficients. This fact distinguishes the results of our work from the results presented in the literature [4–8, 10, 14] and makes Theorems 1, 2, together with the recurrence formula (3.15), a convenient method for investigation of the macroscopic behaviour of two-component composites.

6. Final remarks

The general inequalities obeyed in real domain by one-point Padé approximants to Stieltjes functions reported in the literature [4, Theorem 15.2] have been extended, on account of constraints $(2.2)_{a-d}$, to Padé approximants corresponding to the effective transport coefficients (Theorem 1.2).

On the basis of a given number of power series coefficients $(2.2)_a$, the inequalities (3.1), (3.8)–(3.9) and recurrence formula (3.15) provide, in terms of the convergents of an S-continued fraction, the best upper and lower bounds on the effective transport coefficients such as thermal conductivity, electric permittivity, magnetic permeability, elastic constants and many others.

Acknowledgment

This work was supported by State Committee for Scientific Research through the Grant Nr 3 P404 013 06.

References

1. G.A. BAKER, *Essential of Padé approximants*, Acad. Press, 1975.
2. G.A. BAKER, P. GRAVES-MORRIS, *Padé approximants, part I: Basic theory* (Encyclopedia of Mathematics and its Applications, Vol. 13), Addison-Wesley Publ. Co., 1981.

3. G.A. BAKER, P. GRAVES–MORRIS, *Padé approximants, part II: Extension and application* (Encyclopedia of Mathematics and its Applications, Vol. 14), Addison-Wesley Publ. Co., 1981.
4. D.J. BERGMAN, *The dielectric constant of a composite material – A problem in classical physics*, Phys. Rep., C **43**, 377, 1978.
5. D.J. BERGMAN, *Bounds for the complex dielectric constants of two-component composite material*, Phys. Rev. B, **23**, 6, 3058–3065, 1981.
6. D.J. BERGMAN, *Rigorous bounds for the complex dielectric constants of a two-component composite material*, Ann. Phys., **138**, 78–114, 1982.
7. D.J. BERGMAN, K.J. DUN, *Bulk effective dielectric constants of a composite with periodic microgeometry*, Phys. Rev. B, **45**, 23, 13262–13271, 1992.
8. D.J. BERGMAN, *Hierarchies of Stieltjes functions and their applications to the calculation of bounds for the dielectric constant of a two-component composite medium*, SIAM J. Appl.Math., **53**, 4, 915–930, 1993.
9. A. BULTHEEL, *Laurent series and their Padé approximants*, Birkhauser-Verlag, Basel 1987.
10. B.U. FELDERHOF, *Bounds for the complex dielectric constant of a two-phase composite*, Physica A, **126**, 430–442, 1984.
11. Z. HASHIN, S. SHTRIKMAN, *A variational approach to the theory of the elastic behaviour of polycrystals*, Vol. 10, 343–352, 1962.
12. W.B. JONES, W.J. THRON, *Continued fraction analytic theory and its applications*, (Encyclopedia of Mathematics and its Applications, Vol. 11), Addison-Wesley Publ. Co., 1980.
13. S. MAY, S. TOKARZEWSKI, A. ZACHARA, B. CICHOCKI, *Continued fraction representation for the effective thermal conductivity coefficient of a periodic two component composite*, Int. J. Heat and Mass Transf., [to be published].
14. R.C.MCPHEDRAN, G.W. MILTON, *Bounds and exact theories for the transport properties of inhomogeneous media*, Appl. Phys., A **26**, 207–220, 1981.
15. G.W. MILTON, *Bounds on the complex permittivity of two-component composite material*, J. Appl. Phys., **52**, 8, 5288–5293, 1981.
16. S. TOKARZEWSKI, J. BŁAWZDZIEWICZ, I.V. ANDRIANOV, *Two-point Padé approximants for Stieltjes series*, Reports of Inst. of Fund. Techn. Res., 30/93, Warsaw 1993.
17. H.S. WALL, *Analytic theory of continued fractions*, Van Nostrand, New York 1948.
18. O. WIENER, *Abhandlungen der mathematisch-physischen Klasse der Königlichen Sachsischen Gesellschaft der Wissenschaften*, Vol. 32, 509, 1912.

POLISH ACADEMY OF SCIENCES
INSTITUTE OF FUNDAMENTAL TECHNOLOGICAL RESEARCH

Received March 3, 1994.

Arch. Mech., 46, 5, pp. 625–638, Warszawa 1994

Unsteady compressible boundary layer flow over a rotating sphere

A. CHANDRASEKAR (KHARAGPUR) and G. NATH (BANGALORE)

THE UNSTEADY compressible boundary layer around a rotating sphere in forced flow is investigated. The sphere rotates with an angular velocity which is time-dependent and the free stream flow is assumed to be nonhomentropic. The resulting partial differential equations are solved numerically by the method of finite differences combined with quasi-linearization method. The effect of rotation is an advance of the point of vanishing of longitudinal shear stress further upstream. The skin friction coefficients in the longitudinal and tangential directions are zero at the forward stagnation point, but the heat transfer coefficient is finite. The skin friction parameters in the longitudinal and tangential directions increase with the wall temperature.

1. Introduction

STUDIES RELATING to flow past bodies rotating with uniform angular velocity, other than their inherent interest, have many interesting applications in the fields of turbomachinery, meteorology and astrophysics. Not surprisingly this problem has attracted the attention of many investigators. References to research conducted prior to 1958 can be found in DORFMAN [1], while KREITH [2] has reviewed the work done before 1968.

The problem of a sphere rotating sufficiently fast in a fluid being at rest was first considered by HOWARTH [3]. According to Howarth, the boundary layers on the two hemispheres originate near the vicinity of the poles wherein the flow is similar in nature to the flow generated by an infinite rotating disk. Howarth employed a power series in θ, where θ is the angle measured from the axis of rotation and obtained an approximate solution for the above problem. From considerations of the fluid flux, Howarth stated that fluid would be thrown outwards in the form of a radial jet near the equatorial region. NIGAM [4] suggested a slightly different form of series expansion (in $\sin\theta$) which indicated an outflow near the equator, which exactly balanced the inflow at the poles. Nigam believed that his solution was valid over the whole flow field and the boundary layer equations were sufficient to describe the flow up to the equator. Subsequent theoretical [5–8] and experimental studies [9–11] have not fully cleared the nature of the interaction at the equator.

HOSKIN [12] obtained a solution for the problem of a sphere rotating about an axis aligned with the uniform stream and found that an increase in the angular velocity of the sphere relative to the free stream caused the point of separation to be moved upstream towards the equator. SIEKMANN [13] calculated the heat

transfer by investigating the thermal boundary layer on a rotating sphere in a uniform stream.

DENNIS and INGHAM [14] considered the problem of a rotating sphere (in a fluid at rest) for large values of the Reynolds number. The sphere is started impulsively from rest to rotate with constant angular velocity about a diameter. Their results showed that the steady state profiles were reached earlier ($t = 3$) for the rotational component of velocity (being the primary flow), while for the meridional and radial components the steady state profiles were yet to be reached at $t = 3.7$. For short times, the magnitudes of the radial inflow and outflow velocity components at the edge of the boundary layer are comparable. As time increases, the region of inflow increases whereas the region of outflow decreases. Also there is a moderate increase in the magnitude of the radial inflow velocity as time progresses. However, this can be balanced only by a large increase in the radial outflow near the equator. This rapid increase of the radial velocity at equator, along with narrowing of the region of outflow, is a sufficient evidence of the development of an equatorial jet. Subsequently, DENNIS and INGHAM [15] studied the problem of a sphere which rotates initially with the same angular velocity as the fluid over it, and then is impulsively brought to rest. Near the equator the approach to the steady solution was very rapid, while near the poles the approach was slow. HUSSAINI and SASTRY [16] considered the laminar compressible boundary layer on a rotating sphere and calculated the heat transfer. References [17–18] give information on some of the recent works in rotating sphere problems.

In this paper we have studied the unsteady compressible nonhomentropic boundary layer flow about a rotating sphere of radius R in a forced flow. The flow is assumed to be axisymmetric and subsonic. Both the cases of acceleration and deceleration of the sphere have been considered. The parameters which appear in this study are a rotation parameter λ, Mach number M_∞, Prandtl number Pr, Eckert number E and the Reynolds numbers Re and $\overline{\mathrm{Re}}$. λ, E, Re and $\overline{\mathrm{Re}}$ are defined as $\lambda = (\Omega R/u_\infty)^2$, $E = (\gamma - 1)M_\infty^2$, $\mathrm{Re} = u_\infty R\rho_e/\mu_e$ and $\overline{\mathrm{Re}} = u_\infty \rho \bar{x}/\mu_e$. Subscripts ∞ and e refer to conditions at the free stream and the edge of the boundary layer. $\gamma = c_p/c_v$ is the ratio of specific heats at constant pressure to that at constant volume. Ω is the angular velocity of the sphere while ρ_e and μ_e refer to density and viscosity, respectively, $\bar{x} = x/R$ where x is the coordinate measured from the lower stagnation point (cf. Fig. 1) and R is the sphere radius.

For a rotating sphere [19] we have

$$\begin{aligned} \bar{x} &= x/R, \qquad r(\bar{x}) = R\sin\bar{x}, \\ u_{es}(\bar{x}) &= u_\infty(B_1\sin\bar{x} + B_2\sin^3\bar{x}), \\ B_1 &= 1.5 - (139/660)M_\infty^2, \\ B_2 &= (243/352)M_\infty^2. \end{aligned} \tag{1.1}$$

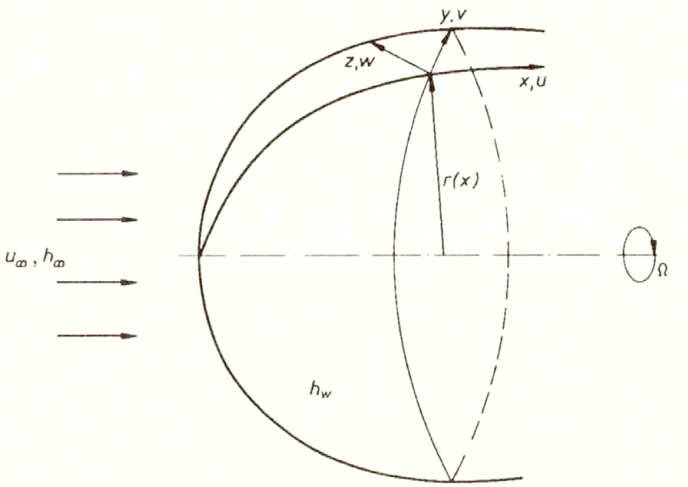

FIG. 1. Physical model and coordinate system.

The assumption of homentropic flow leads to vanishing of the p_t term in the energy equation. Since we are considering nonhomentropic flow, we retain p_t in the energy equation. Since the velocity and pressure are related at the edge of the boundary layer, we have allowed the velocity at the edge of the boundary layer u_e to vary with time. For simplicity we have assumed $u_e(\bar{x}, t) = u_{es}(\bar{x})\phi(t)$ and that $\phi(t)$ has the same form as that of the sphere unsteadiness. Since a nonhomentropic flow is considered, enthalpy h_e is given by [20]

$$h_e = h_\infty \left[1 + 2^{-1}(\gamma - 1)\mathrm{M}_\infty^2(1 - u_{es}^2/u_\infty^2)\right]. \tag{1.2}$$

2. Governing equations

We consider the problem of an unsteady compressible boundary layer flow over a rotating sphere in forced flow (Fig. 1). The sphere rotates with an angular velocity which is time-dependent. The flow is assumed to be axisymmetric and subsonic, while the freestream flow is taken to be nonhomentropic. All quantities are independent of y due to axisymmetry. The aim of the present investigation is to understand as to what extent the rotation affects the heat transfer and skin friction.

The governing boundary layer equations are [13, 20, 21, 22]

$$(\rho r)_t + (\rho r u)_x + (\rho r w)_z = 0, \tag{2.1}$$

$$\rho(u_t + uu_x + wu_z - r^{-1}v^2 r_x) = -p_x + (\mu u_z)_z, \tag{2.2}$$

$$\rho(v_t + uv_x + wv_z + uvr^{-1}r_x) = (\mu v_z)_z, \tag{2.3}$$

$$\rho(h_t + uh_x + wh_z) = (p_t + up_x) + (\mu \mathrm{Pr}^{-1}h_z)_z + \mu\left[(u_z)^2 + (v_z)^2\right], \tag{2.4}$$

$$\rho \propto h^{-1}, \tag{2.5}$$

$$\mu \propto h^{\omega}, \tag{2.6}$$

subject to initial and boundary conditions

$$\begin{aligned}
&u(x,z,0) = u_i(x,z), \qquad v(x,z,0) = v_i(x,z),\\
&w(x,z,0) = w_i(x,z), \qquad h(x,z,0) = h_i(x,z),\\
&u(x,0,t) = 0, \qquad v(x,0,t) = \Omega r(x)\phi(t), \qquad w(x,0,t) = 0,\\
&h(x,0,t) = h_w(x), \qquad u(x,\infty,t) = u_e(x,t) = u_{es}(x)\phi(t),\\
&v(x,\infty,t) = 0, \qquad h(x,\infty,t) = h_e(x),
\end{aligned} \tag{2.7}$$

where u, v and w are the components of velocity along the coordinates chosen in the longitudinal, transverse and normal directions to the surface, with x being measured from the lower stagnation point and $r(x)$ being the distance of the body from the axis (see Fig. 1). The enthalpy is denoted by h while μ and ν are the coefficient of viscosity and kinematic viscosity. $\phi(t)$ is a function of time to introduce unsteadiness. ω is a constant which occurs in the viscosity-enthalpy relationship. The subscript e and w denote conditions at the edge of the boundary layer and at the wall, respectively. The subscripts x, z and t denote partial derivatives. Since we are concerned with subsonic flow in the present problem, the fluid medium can be assumed as one which has constant gas properties. Hence Pr = constant; $\rho \propto h^{-1}$ and from Chapman's law $\mu \propto h$ i.e. $\omega = 1$ and hence $N = \mu\rho(\mu_e\rho_e)^{-1} = 1$. We have solved the equations (A.7) to (A.9) (see the Appendix) subject to (A.13), with unity replacing N. We have taken $\phi(t^*)$ to be of the form

$$\phi(t^*) = 1 \pm \varepsilon t^{*2}, \qquad \varepsilon = 0.1, \tag{2.8}$$

where plus sign implies that the angular velocity of the sphere is increasing with time t^*, and minus sign implies that it is decreasing. However, as mentioned earlier, we have assumed $u_e(x,t^*) = u_{es}(x)(1 + \varepsilon t^{*2})$, $\varepsilon = 0.1$, to allow for the variation of u_e with time. The steady state equations with $N = 1$, $M_\infty = 0$, $\alpha_4 = \alpha_3 = 0$, $\alpha_1 = \alpha$ and $2\alpha_2 = \alpha_1$ reduce to those equations solved by KUMARI and NATH [22] for the incompressible flow. Also equations (A.7) and (A.9) for $\alpha_1 = \lambda = S = 0$ reduce to those of VASANTHA and NATH [23] who studied the flow over a stationary sphere. For stationary case, equation (A.8) is not required. The initial conditions are given by steady state equations (A.7)–(A.9), by putting $\phi = 1$ and $F_t^* = S_t^* = g_t^* = \phi_t^* = 0$.

The skin friction coefficients and the Nusselt number are given by

$$\begin{aligned}
(\mathrm{Re})^{1/2}C_x = {} & 2^{1/2}\sin\bar{x}(1+\cos\bar{x})(B_1 + B_2\sin^2\bar{x})^2\Big[(B_1/3)(2+\cos\bar{x})\\
& +(B_2/15)(1-\cos\bar{x})(8+9\cos\bar{x}+3\cos^2\bar{x})\Big]^{-1/2}(F_\eta)_w,
\end{aligned} \tag{2.9}$$

(2.9) [cont.]

$$(\mathrm{Re})^{1/2}C_y = (2\lambda)^{1/2}(1+\cos\bar{x})\phi(t^*)(B_1\sin\bar{x} + B_2\sin^3\bar{x}) \times\Big[(B_1/3)(2+\cos\bar{x}) + (B_2/15)(1-\cos\bar{x}) \times(8+9\cos\bar{x}+3\cos^2\bar{x})\Big]^{-1/2}(S_\eta)_w,$$

$$(\mathrm{Re})^{1/2}Nu(\overline{\mathrm{Re}})^{-1} = 2^{-1/2}\Big[1+2^{-1}(\gamma-1)\mathrm{M}_\infty^2\Big\{1 -(B_1\sin\bar{x}+B_2\sin^3\bar{x})^2\Big\}\Big] \times(1+\cos\bar{x})(B_1+B_2\sin^2\bar{x})(g_0-1)^{-1}\,[(B_1/3)(2+\cos\bar{x}) +(B_2/15)(1-\cos\bar{x})(8+9\cos\bar{x}+3\cos^2\bar{x})\Big]^{-1/2}(g_\eta)_w$$

where

$$C_x = 2\mu(u_z)_w(\rho_e u_\infty^2)^{-1}, \qquad C_y = 2\mu(v_z)_w(\rho_e u_\infty^2)^{-1},$$

$$\mathrm{Nu} = \bar{x}(h_w - h_\infty)^{-1}(h_z)_w.$$

3. Results and discussions

The method of finite differences in combination with the quasi-linearization method [24] is employed for the numerical work. The aim of the numerical method is to solve the system of partial differential equations (A.7) – (A.9) which govern the unsteady compressible boundary layer flow over a rotating sphere, subject to boundary conditions (A.13). The governing equations were first linearized using the method of quasi-linearization, and then an implicit finite difference scheme was applied as described in [23]. The resulting system of linear algebraic equations was solved using block elimination method [25]. Numerical computations were carried out for Mach number equal to 0.4 and Prandtl number equal to 0.72, and for various values of rotation parameter λ (0, 4, 10) and g_0 (0.5, 1.5). The grid sizes were chosen, respectively, as $\delta\bar{x} = 0.05$, $\delta\eta = 0.05$ and $\delta t^* = 0.1$. η_∞ was taken equal to 4 and was found to be adequate. The above grid sizes were found suitable, because similar results were obtained with reduced grid size. The grid size in the $\bar{x}$ direction was progressively reduced and in the neighbourhood of vanishing longitudinal shear stress $(F_\eta)_w$, $\delta(\bar{x})$ was taken as 0.0005. Results of LEE *et al.* [21] and KUMARI and NATH [22] were recovered as the steady-state case of our results, and the comparison is shown in Fig. 2. The unsteady-state results for the stationary sphere ($\lambda = 0$) have been compared with those of VASANTHA and NATH [23] and they are found to be in excellent agreement. The comparison is shown in Fig. 3.

Figure 4 illustrates the effect of rotation parameter λ on skin friction ($(F_\eta)_w$, $(S_\eta)_w$) and heat transfer ($(g_\eta)_w$) for $\mathrm{M}_\infty = 0.4$, $g_0 = 0.5$ (cold wall), $t^* =$

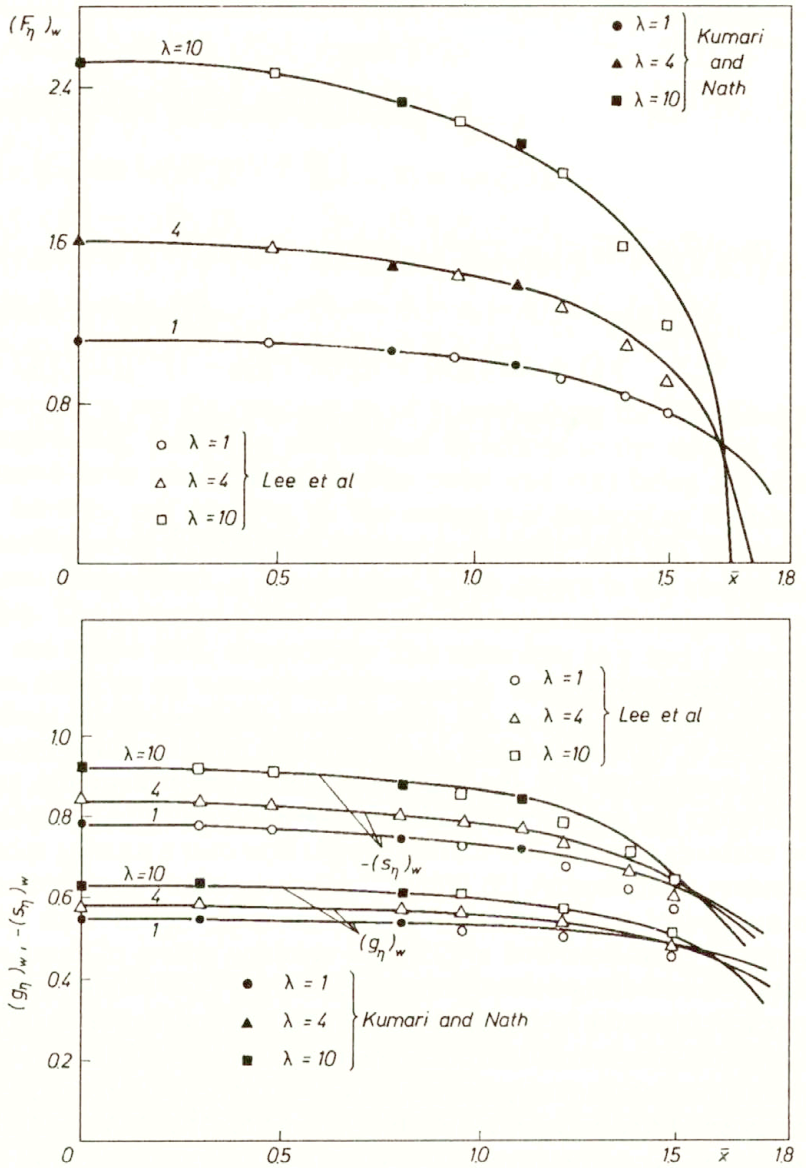

FIG. 2. Comparison of steady state results for longitudinal shear stress $(F_\eta)_w$, tangential shear stress $-(S_\eta)_w$ and heat transfer parameter $(g_\eta)_w$.

0.2, $\phi(t^*) = 1 + \varepsilon t^{*2}$, $\varepsilon = 0.1$. It is seen from Fig. 4 that an increase in the rotation parameter λ causes the point of zero skin friction in the longitudinal direction ($(F_\eta)_w$) to be moved upstream, due to centrifugal acceleration on the boundary layer which tends to push the fluid towards the equator. However, the tangential shear stress ($-(S_\eta)_w$) does not vanish simultaneously with the longitudinal shear stress. A similar trend has been observed by LEE *et al.* [21]

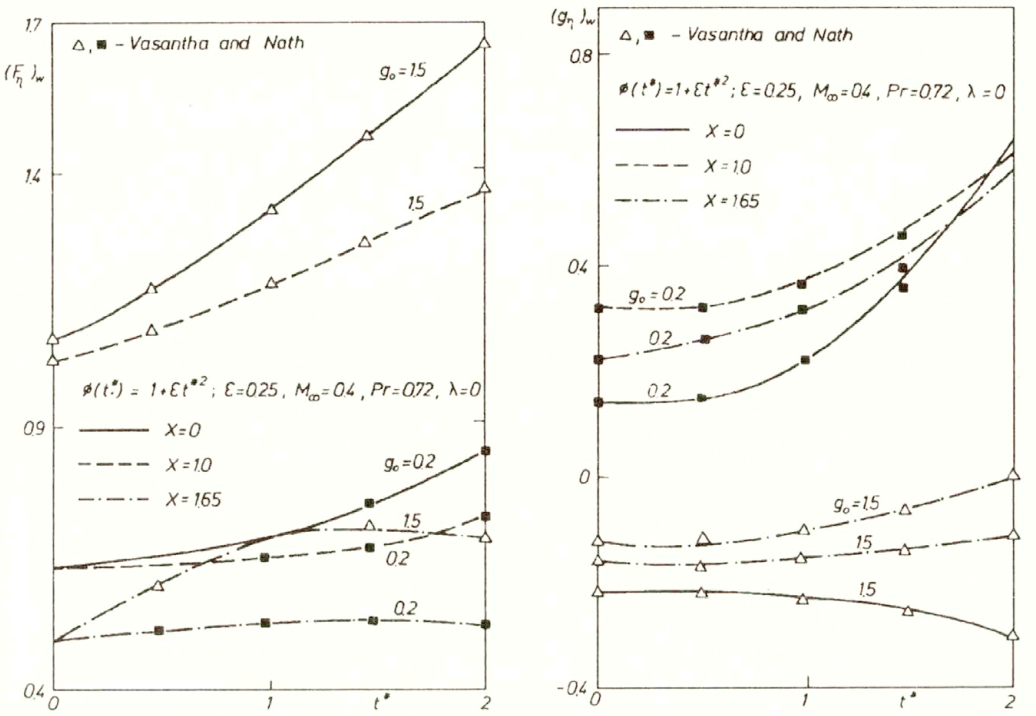

FIG. 3. Comparison of unsteady state results for longitudinal shear stress $(F_\eta)_w$ and heat transfer parameter $(g_\eta)_w$.

and KUMARI and NATH [22] for a steady-state case. It is also observed that the rotation parameter λ increases the skin friction $((F_\eta)_w)$, $-(S_\eta)_w$) in the region of favourable pressure gradient ($\bar{x} \leq \pi/2$) due to the acceleration of the fluid which reduces the boundary layer thickness. In the region of adverse pressure gradient ($\bar{x} \geq \pi/2$), λ increases the boundary layer thickness which in turn reduces the skin friction. For a given viscous dissipation parameter (E), the heat transfer $(g_\eta)_w$ increases with λ, and its effect is more pronounced for $\bar{x} \geq 0.4$. The percentage increase of heat transfer with λ (as seen in Fig. 4) is 7.7% at $\bar{x} = 0.2$, 33% at $\bar{x} = 0.6$ and 70% at $\bar{x} = 1.2$, respectively.

It may be remarked that vanishing of wall shear stress in unsteady two-dimensional and axisymmetric flows on a fixed wall does not imply separation, in contrast to the steady flow. Therefore there is a difference between the point of separation and point of zero skin friction in unsteady flows. For high Reynolds number, in the flow over bodies the effect of viscosity is generally limited to a thin layer, the boundary layer, adjacent to the surface. Within the boundary layer, where the momentum of the fluid has been reduced in overcoming viscous forces, the remaining momentum may be insufficient to allow the flow to proceed into the region of increasing pressure. At the point on the body where this condition holds true, the boundary layer separates from the surface. Downstream of this

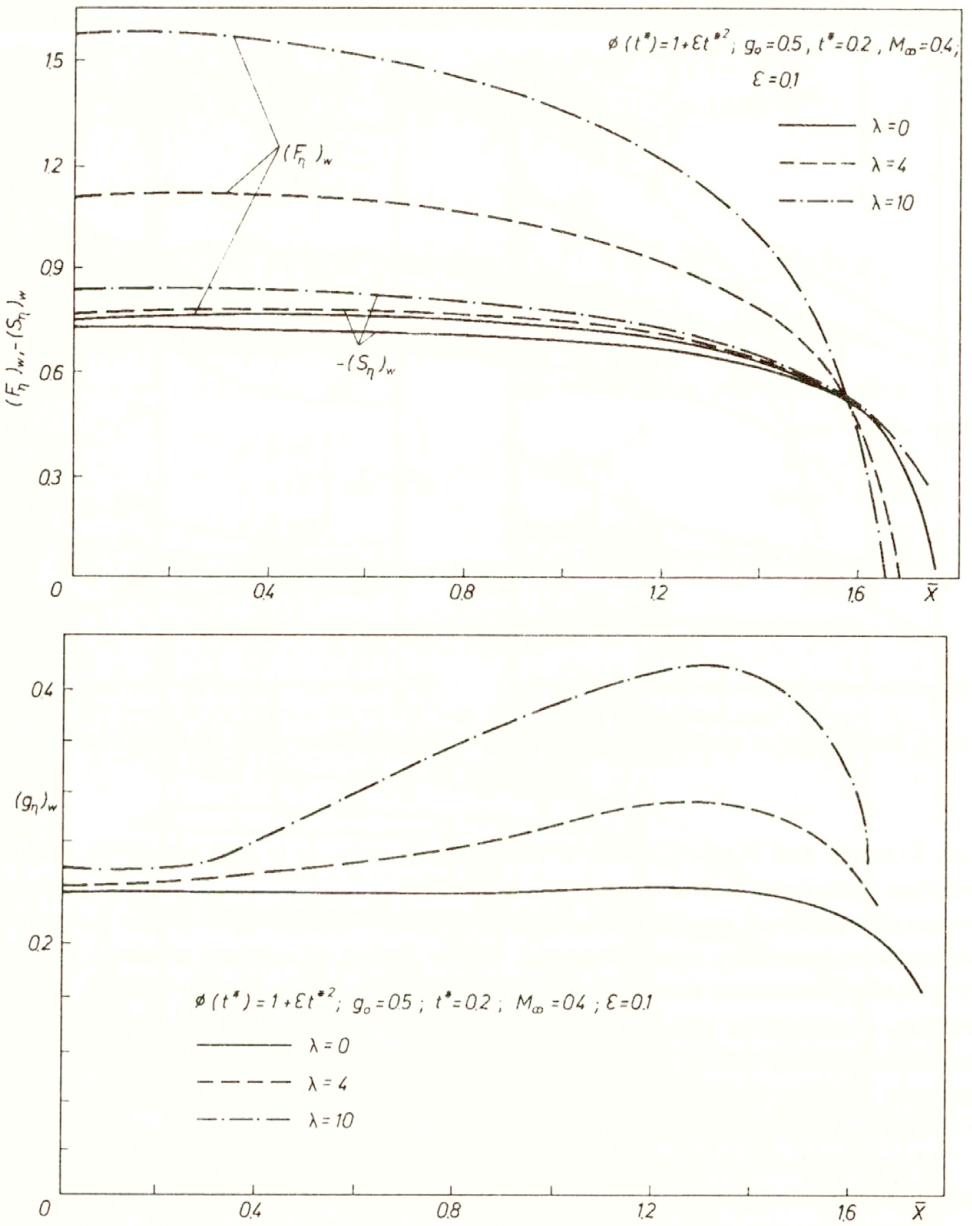

FIG. 4. Effect of the rotation parameter λ on the skin friction and heat transfer parameters $(F_\eta)_w$, $-(S_\eta)_w$, $(g_\eta)_w$.

point, the boundary layer fluid passes over a region of recirculating flow. The point at which the boundary layer breaks away from the surface, and which divides the region of downstream directed flow, where the viscous effect is quite limited in extent from the region of recirculation flow, is known as the point of

separation. For steady two-dimensional or axisymmetric flow over a fixed wall, the point of vanishing shear (zero skin friction) coincides with the point of separation. For unsteady two-dimensional or axisymmetric flow over a fixed wall, the point of zero skin friction at the wall does not coincide with the point of separation. The physical symptom of separation in unsteady two-dimensional or axisymmetric flow over a fixed wall is the simultaneous vanishing of velocity and shear stress away from the wall in a coordinate system moving with separation. The detailed discussion of the phenomenon of separation for unsteady flows is given by SEARS and TELIONIS [26], WILLIAMS [27], VAN DOMMELAN and SHEN [28] and SMITH [29].

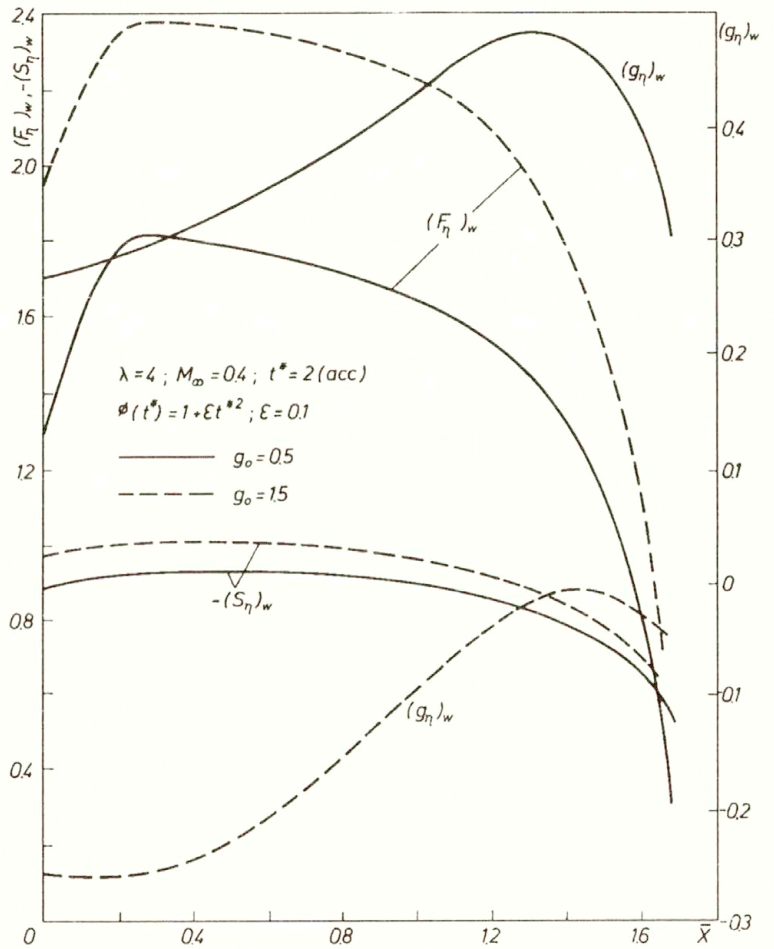

FIG. 5. Effect of the wall temperature g_0 on the skin friction and heat transfer parameters $(F_\eta)_w$, $-(S_\eta)_w$, $(g_\eta)_w$.

Figure 5 depicts the effect of the wall temperature g_0 on the skin friction parameters in x and y directions ($(F_\eta)_w$, $-(S_\eta)_w$) and heat transfer parameter

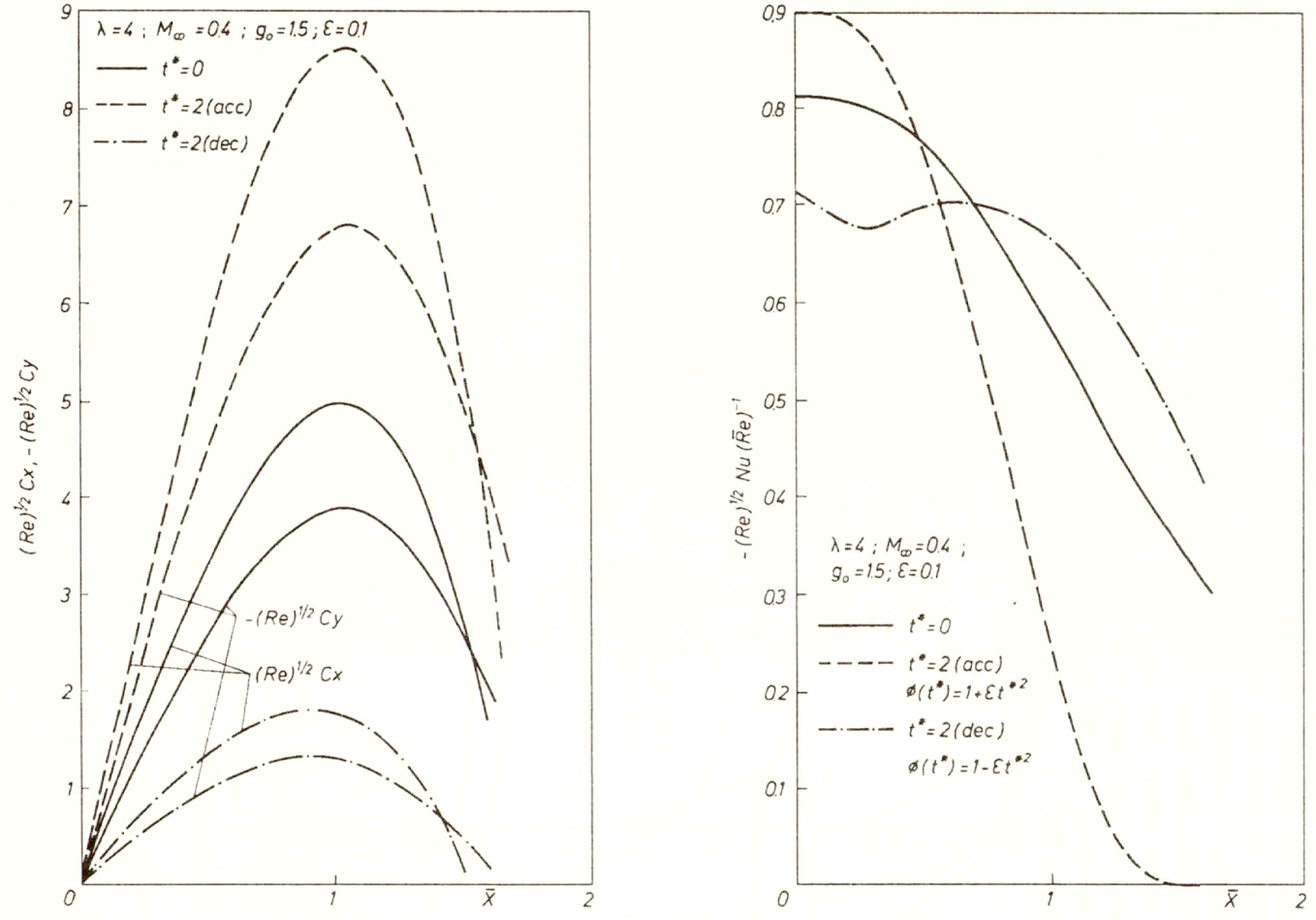

FIG. 6. Effect of accelerating and decelerating angular velocity of the sphere on the skin friction and heat transfer coefficients $(\mathrm{Re})^{1/2}C_x$, $-(\mathrm{Re})^{1/2}C_y$, $-(\mathrm{Re})^{1/2}\mathrm{Nu}(\overline{\mathrm{Re}})^{-1}$.

$(g_\eta)_w$ for $\lambda = 4$ and $t^* = 2$ (accelerating case). The skin friction parameters increase with the wall temperature. The reason for this behaviour is that the temperature near the wall increases with g_0, which reduces the density of the fluid near the wall. Consequently, the less dense fluid is more accelerated than the more dense fluid. This in turn increases the skin friction parameters. For cold wall ($g_0 < 1$) the heat is transferred from the fluid to the wall ($(g_\eta)_w > 0$), but for hot wall ($g_0 > 1$) the direction of the transfer of heat changes ($(g_\eta)_w < 0$). For a given g_0 and t^*, the skin friction parameters $(F_\eta)_w$ and $-(S_\eta)_w$ decrease with the longitudinal distance $\bar{x}$. The heat transfer parameter $(g_\eta)_w$ for a cold wall increases with $\bar{x}$ in the region of favourable pressure gradient and decreases in the region of adverse pressure gradient, while for the hot wall the behaviour is opposite.

The skin friction coefficients in x and y directions $((\mathrm{Re})^{1/2}C_x, -(\mathrm{Re})^{1/2}C_y)$ and heat transfer coefficient $(-\mathrm{Re}^{1/2}\mathrm{Nu}(\overline{\mathrm{Re}})^{-1})$ for both accelerating and decelerating cases are shown in Fig. 6 for $\lambda = 4$ and $g_0 = 1.5$. The skin friction coefficients are zero at $\bar{x} = 0$ and attain maximum values in the neighbourhood of $\bar{x} = 1$ and then decrease. The maximum values of the skin friction coefficients for accelerating flow are greater than those of decelerating flow. Unlike the skin friction coefficients, the heat transfer coefficient is finite at $\bar{x} = 0$ and, in general, decreases with $\bar{x}$.

4. Conclusions

The effect of rotation consists in the advance of the point of vanishing longitudinal shear stress further upstream. At the point where the longitudinal shear stress vanishes, the tangential shear stress is non-zero. The skin friction coefficients in the longitudinal and tangential directions are zero at the forward stagnation point ($\bar{x} = 0$), but the heat transfer coefficient is finite. Also, the skin friction parameters in the longitudinal and tangential directions increase with the wall temperature. The extension of this work to include rotating fluid will be a subject of a later study. Also the non-symmetric flow above a rotating disk is currently being investigated.

Appendix

At the edge of the boundary layer, velocity and enthalpy obey the following relations:

$$(u_e)_t + u_e(u_e)_x = -\rho_e^{-1}p_x, \tag{A.1}$$

$$\rho_e u_e(h_e)_x = [(p_t) + u_e(p)_x]. \tag{A.2}$$

Making use of (A.1) and (A.2) in Eqs. (2.2) and (2.4), we get the following momentum and energy equations:

$$u_t + uu_x + wu_z - r^{-1}v^2 r_x = \rho_e \rho^{-1}[(u_e)_t + u_e(u_e)_x] + \left(\mu\rho^{-1}u_z\right)_z, \tag{A.3}$$

$$h_t + uh_x + wh_z = \rho_e\rho^{-1}[u_e(h_e)_x + (u_e - u)\{(u_e)_t + u_e(u_e)_x\}] + (\mu \mathrm{Pr}^{-1}\rho^{-1}h_z)_z + \rho^{-1}\mu\left[(u_z)^2 + (v_z)^2\right]. \tag{A.4}$$

The following transformations as in [23] are employed

$$\xi = \int_0^x \rho_e u_{es}\mu_e r^2\, dx,$$

$$\eta = u_{es}(2\xi)^{-1/2}\int_0^z (\rho r)\, dz,$$

$$t^* = u_\infty t/R,$$

$$f(\xi,\eta,t^*) = (2\xi)^{-1/2}\psi(x,z,t), \tag{A.5}$$

$$S(\xi,\eta,t^*) = v(x,z,t)/[\Omega r\phi(t^*)],$$

$$g(\xi,\eta,t^*) = h(x,z,t)/h_e(x),$$

where the velocity components are related to stream function as

$$\rho ur = \psi_z, \tag{A.6}$$

$$\rho wr = -\left[\psi_x + \{\eta(2\xi)^{1/2}u_{es}\}_t\right].$$

Substituting (A.5) and (A.6) in Eqs. (2.1), (2.3), (A.3) and (A.4), we obtain the following set of partial differential equations:

$$(NF_\eta)_\eta - \alpha F_t^* - \beta F^2 + fF_\eta + \alpha_1 S^2\phi^2 + \left[\alpha\, d\phi/dt^* + \beta\phi^2\right] g = 2\xi(FF_\xi - f_\xi F_\eta), \tag{A.7}$$

$$(NS_\eta)_\eta - \alpha S_t^* - \alpha\phi^{-1}S\, d\phi/dt^* - 2\alpha_2 SF + fS_\eta = 2\xi(FS_\xi - f_\xi S_\eta), \tag{A.8}$$

$$(N\mathrm{Pr}^{-1}g_\eta)_\eta + N(F_\eta)^2u_{es}^2/h_e + \lambda N\alpha_5\phi^2(S_\eta)^2 + \alpha_3\phi^2(\phi - F)g + \alpha(\phi - F)g(d\phi/dt^*)u_{es}^2/h_e + \alpha_4\phi g - \alpha g_t^* - \alpha_4 gF + fg_\eta = 2\xi(Fg_\xi - f_\xi g_\eta), \tag{A.9}$$

$$\rho/\rho_e = h_e/h, \tag{A.10}$$

$$\mu/\mu_e = (h/h_e)^\omega, \tag{A.11}$$

where

$$
\begin{aligned}
&\alpha = 2\xi u_\infty (R u_{es}^2 \rho_e \mu_e r^2)^{-1}, \\
&\beta = 2\xi u_{es}^{-1}(u_{es})_\xi, \qquad \alpha_1 = 2\xi \Omega^2 (u_{es}^3 \rho_e \mu_e r)^{-1} r_x, \\
&\alpha_2 = 2\xi (r^3 u_{es} \rho_e \mu_e)^{-1} r_x, \qquad \alpha_3 = 2\xi h_e^{-1} u_{es}(u_{es})_\xi, \\
&\alpha_4 = 2\xi h_e^{-1}(h_e)_\xi, \qquad \alpha_5 = u_\infty^2 r^2 (h_e R^2)^{-1}, \\
&\lambda = \Omega^2 R^2 u_\infty^{-2}, \qquad N = \mu\rho(\mu_e \rho_e)^{-1}, \qquad f = \int_0^\eta F\, d\eta .
\end{aligned} \tag{A.12}
$$

The relevant boundary conditions are

$$
\begin{aligned}
&F(\xi,0,t^*) = 0, \qquad S(\xi,0,t^*) = 1, \qquad g(\xi,0,t^*) = g_w, \\
&F(\xi,\infty,t^*) = \phi(t^*), \qquad S(\xi,\infty,t^*) = 0, \qquad g(\xi,\infty,t^*) = 1,
\end{aligned} \tag{A.13}
$$

where

$$g_w = h_w (h_e)^{-1}$$

and is given by

$$g_w = g_0 \left[1 + 2^{-1}(\gamma - 1)\mathrm{M}_\infty^2 (1 - u_{es}^2/u_\infty^2)\right]^{-1}, \qquad g_0 = h_w/h_\infty . \tag{A.14}$$

One gets the following expressions for the sphere:

$$
\begin{aligned}
&\xi = \rho_e \mu_e u_\infty R^3 c_2^2 c_1, \qquad \alpha = 2c_3^{-2} c_4^{-2} c_1, \\
&\beta = 2\cos\bar{x}\, c_3^{-2} c_4^{-2} c_1 (B_1 + 3B_2 \sin^2\bar{x}), \\
&\alpha_1 = 2\lambda \cos\bar{x}\, c_3^{-2} c_4^{-3} c_1, \qquad \alpha_2 = 2\cos\bar{x}\, c_3^{-2} c_4^{-1} c_1, \\
&\alpha_3 = \beta E c_5 (B_1 \sin\bar{x} + B_2 \sin^3\bar{x})^2, \\
&\alpha_4 = -2c_2(\gamma - 1)\mathrm{M}_\infty^2 \cos\bar{x}\, c_3^{-1} c_4^{-1} c_5 c_1 \left[B_1^2 + 3B_2^2 \sin^4\bar{x} + 4B_1 B_2 \sin^2\bar{x}\right], \\
&\alpha_5 = E \sin^2\bar{x}\, c_5, \qquad \xi\, \partial/\partial\xi = \sin\bar{x}\, c_3^{-2} c_4^{-1} c_1\, \partial/\partial\bar{x},
\end{aligned} \tag{A.15}
$$

where

$$
\begin{aligned}
&c_1 = (B_1/3)(2 + \cos\bar{x}) + (B_2/15)(1 - \cos\bar{x})(8 + 9\cos\bar{x} + 3\cos^2\bar{x}), \\
&c_2 = 1 - \cos\bar{x}, \qquad c_3 = 1 + \cos\bar{x}, \qquad c_4 = (B_1 + B_2 \sin^2\bar{x}), \\
&c_5 = \left[1 + 2^{-1}(\gamma - 1)\mathrm{M}_\infty^2 \{1 - (B_1 \sin\bar{x} + B_2 \sin^3\bar{x})^2\}\right]^{-1} .
\end{aligned} \tag{A.16}
$$

References

1. L.A. DORFMAN, *Hydrodynamic resistance and heat loss of rotating bodies*, Oliver and Boyd, Edinburgh 1963.
2. F. KREITH, *Advances in Heat Transfer*, 5, 129, 1968.
3. L. HOWARTH, Phil. Mag., **42**, 1308, 1951.
4. S.D. NIGAM, ZAMP, **5**, 151, 1954.
5. K. STEWARTSON, *Boundary layer research*, IUTAM Symp., p. 59, Berlin, Springer Verlag, Berlin 1958.
6. W.H.H. BANKS, Q. J. Mech. Appl. Math., **18**, 443, 1965.
7. W.H.H. BANKS, Acta Mech., **24**, 273, 1976.
8. R. MANOHAR, ZAMP, **18**, 320, 1967.
9. F. KREITH, L.G. ROBERTS, J.A. SULLIVAN and S.N. SINHA, Int. J. Heat Mass Transfer, **6**, 881, 1963.
10. F.P. BOWDEN and R.G. LORD, Proc. Roy. Soc., London, **271A**, 143, 1963.
11. O. SAWATZKI, Acta Mech., **9**, 159, 1971.
12. N.E. HOSKIN, *In 50 Jahre Grenzschichtforschung*, p. 127, Friedr. Vieweg u Sohn., Braunschweig 1959.
13. I. SIEKMANN, ZAMP, **13**, 468, 1962.
14. S.C.R. DENNIS and D.B. INGHAM, Phys. Fluids, **22**, 1, 1979.
15. S.C.R. DENNIS and D.B. INGHAM, J. Fluid Mech., **123**, 219, 1982.
16. M.Y. HUSSAINI and M.S. SASTRY, J. Heat Transfer, **98**, 533, 1976.
17. M.A.I. EL-SHAARAVI, M.F. EL-REFATE and S.A. EL-BEDEAWI, J. Fluid Engng., **107**, 97, 1985.
18. P. CHANDRAN and P. KUMAR, Int. J. Engng. Sci., **24**, 685, 1986.
19. C.F. CARRIER and C.E. PEARSON, *Partial differential equations: theory and technique*, p. 136, Academic Press, New York 1976.
20. H. SCHLICHTING, *Boundary layer theory*, 7th Ed., McGraw Hill, New York 1979.
21. M.H. LEE, D.R. JENG and K.T. DEWITT, J. Heat Transfer, **100**, 496, 1978.
22. M. KUMARI and G. NATH, Arch. Mech., **34**, 147, 1982.
23. R. VASANTHA and G. NATH, Acta Mech., **57**, 215, 1985.
24. K. INOUYE and A. TATA, AIAA J., **12**, 558, 1974.
25. R.S. VARGA, *Matrix iterative analysis*, Prentice Hall, Englewood Cliff, New York 1962.
26. W.R. SEARS and D.P. TELIONIS, SIAM J. Appl. Math., **28**, 215, 1975.
27. J.C. WILLIAMS, Ann. Rev. Fluid Mech., **9**, 113, 1977.
28. L.L. VAN DOMMELEN and S.F. SHEN, AIAAJ., **21**, 358, 1983.
29. F.T. SMITH Ann. Rev. Fluid Mech., **18**, 197, 1986.

DEPARTMENT OF PHYSICS AND METEOROLOGY
INDIAN INSTITUTE OF TECHNOLOGY, KHARAGPUR
and
DEPARTMENT OF APPLIED MATHEMATICS
INDIAN INSTITUTE OF SCIENCE, BANGALORE, INDIA.

Received March 8, 1994.

Arch. Mech., 46, 5, pp. 639–651, Warszawa 1994

Numerical investigation of the two-dimensional shock wave reflection

K. KANTIEM (WARSZAWA)

A SERIES OF NUMERICAL boundary conditions describing the shock wave reflection on an oblique wall is considered. The cases of an adiabatic slip wall, adiabatic no-slip wall, isothermal no-slip and a certain mixture between them are tested and the resulting density profiles for the test gas argon are presented.

1. Introduction

THE MAIN OBJECTIVE of the present paper is the investigation of the numerical boundary conditions for the two-dimensional shock wave reflection from an oblique wall. In order to take into consideration effects caused by viscosity and heat-conductivity, we describe the motion of the test gas argon by the Navier–Stokes equations. Depending on the concrete choice of conditions on the wall, we should obtain phenomena like the Mach reflection or the formation of a boundary layer [3, 7]. The equations are solved by a stable finite-difference method.

The aim is to find numerical boundary conditions which applied to calculations of the reflection of gas flow, lead to a good agreement with experimental results. The next step is the analysis of the numerical stability of solutions including the suggested boundary conditions [5].

Although there exist many results concerning the well-posedness of boundary-value problems for hyperbolic systems with non-characteristic boundaries [8], as well as with uniformly characteristic boundaries [10], and for incompletely parabolic equations including Navier–Stokes equations with non-characteristic boundaries [11], they are not applicable in the case of reflection of gas flow from a wall, since we are dealing here with a characteristic but not uniformly characteristic boundary. The same problem appears for the stability analysis of numerical boundary conditions concerning the non-viscous flow, since the theory in [4] and [12] assumes non-characteristic boundaries.

2. Formulation of the problem

In this section we present the Navier–Stokes equations and the numerical problem including the initial and boundary conditions.

2.1. Navier–Stokes equations

The two-dimensional Navier–Stokes equations are of the (dimensionless) form

$$\frac{\partial U}{\partial t} + \frac{\partial F}{\partial x} + \frac{\partial G}{\partial y} - \frac{\partial F^D}{\partial x} - \frac{\partial G^D}{\partial y} = 0,$$

where

$$U = \begin{pmatrix} \rho \\ \rho u \\ \rho v \\ \rho\left(\dfrac{u^2+v^2}{2} + \dfrac{T}{\gamma(\gamma-1)}\right) \end{pmatrix},$$

$$F = \begin{pmatrix} \rho u \\ \rho\left(u^2 + \dfrac{T}{\gamma}\right) \\ \rho u v \\ \rho u\left(\dfrac{u^2+v^2}{2} + \dfrac{T}{\gamma-1}\right) \end{pmatrix},$$

$$G = \begin{pmatrix} \rho v \\ \rho u v \\ \rho\left(v^2 + \dfrac{T}{\gamma}\right) \\ \rho v\left(\dfrac{u^2+v^2}{2} + \dfrac{T}{\gamma-1}\right) \end{pmatrix},$$

$$F^D = \frac{1}{\mathrm{Re}} \begin{pmatrix} 0 \\ \mu\left(\dfrac{\partial u}{\partial x} - \dfrac{1}{2}\dfrac{\partial v}{\partial y}\right) \\ \dfrac{3}{4}\mu\left(\dfrac{\partial u}{\partial y} + \dfrac{\partial v}{\partial x}\right) \\ \mu\left(u\left(\dfrac{\partial u}{\partial x} - \dfrac{1}{2}\dfrac{\partial v}{\partial y}\right) + \dfrac{3}{4}v\left(\dfrac{\partial u}{\partial y} + \dfrac{\partial v}{\partial x}\right)\right) + \dfrac{\kappa}{\mathrm{Pr}(\gamma-1)}\dfrac{\partial T}{\partial x} \end{pmatrix},$$

$$G^D = \frac{1}{\mathrm{Re}} \begin{pmatrix} 0 \\ \dfrac{3}{4}\mu\left(\dfrac{\partial u}{\partial y} + \dfrac{\partial v}{\partial x}\right) \\ \mu\left(\dfrac{\partial v}{\partial y} - \dfrac{1}{2}\dfrac{\partial u}{\partial x}\right) \\ \mu\left(v\left(\dfrac{\partial v}{\partial y} - \dfrac{1}{2}\dfrac{\partial u}{\partial x}\right) + \dfrac{3}{4}u\left(\dfrac{\partial u}{\partial y} + \dfrac{\partial v}{\partial x}\right)\right) + \dfrac{\kappa}{\mathrm{Pr}(\gamma-1)}\dfrac{\partial T}{\partial y} \end{pmatrix},$$

with ρ denoting density, u and v – velocity components in x and y direction, respectively, μ – coefficient of viscosity, κ – coefficient of heat-conductivity, T – temperature, $\gamma = c_p/c_v$, where c_p, c_v – specific heat at constant pressure and volume. Assuming a linear dependence on temperature for viscosity $\mu(T)$ and heat-conductivity $\kappa(T)$, we can substitute μ and κ by T in the dimensionless form of the Navier–Stokes equations.

For convenience we introduce the following notation:

$$\tau_{11} = \left(\frac{\partial u}{\partial x} - \frac{1}{2}\frac{\partial v}{\partial y}\right),$$

$$\tau_{12} = \tau_{21} = \frac{3}{4}\left(\frac{\partial u}{\partial y} + \frac{\partial v}{\partial x}\right),$$

$$\tau_{22} = \left(\frac{\partial v}{\partial y} - \frac{1}{2}\frac{\partial u}{\partial x}\right),$$

$$q_1 = \frac{\partial T}{\partial x}, \qquad q_2 = \frac{\partial T}{\partial y}.$$

2.2. Finite-difference scheme

The calculations have been carried out with the two-step second order MAC CORMACK difference scheme [9]

$$U^*_{i,j} = U^n_{i,j} - \frac{\Delta t}{\Delta x}\left((F - F^D)^n_{i+1,j} - (F - F^D)^n_{i,j}\right) - \frac{\Delta t}{\Delta y}\left((G - G^D)^n_{i,j+1} - (G - G^D)^n_{i,j}\right),$$

$$U^{n+1}_{i,j} = \frac{1}{2}\left\{U^n_{i,j} + U^*_{i,j} - \frac{\Delta t}{\Delta x}\left((F - F^D)^*_{i,j} - (F - F^D)^*_{i-1,j}\right) - \frac{\Delta t}{\Delta y}\left((G - G^D)^*_{i,j} - (G - G^D)^*_{i,j-1}\right)\right\},$$

where

$$(F - F^D)^n_{i,j} = F(U^n_{i,j}) - F^D(U^n_{i,j})$$

and

$$(G - G^D)^n_{i,j} = G(U^n_{i,j}) - G^D(U^n_{i,j}).$$

The derivatives in the dissipative parts F^D and G^D are approximated by backward differences in the first step and forward differences in the second step.

The scheme is considered on a rectangular mesh in the $(\overline{x}, \overline{y})$-plane, $\overline{x}_i = \frac{x_i}{\lambda} = i\frac{\Delta x}{\lambda} = i\Delta\overline{x}$, $\overline{y}_i = \frac{y_i}{\lambda} = j\frac{\Delta y}{\lambda} = j\Delta\overline{y}$ for $i = 0, \ldots, n_{\max}$, $j = 0, \ldots, m_{\max}$, where λ is the mean free path. The computational domain is bounded by the wall on the x-axis

$$\{(\overline{x}, \overline{y}) : 0 \leq \overline{x} < n\Delta\overline{x}, \quad \overline{y} = 0\},$$

where $n\Delta\bar{x}$ is a meshpoint on the x-axis, $0 < n < n_{\max}$, and the artificial boundaries

$$\left\{(\bar{x},\bar{y}) : \bar{x} = 0, \quad 0 \le \bar{y} \le m_{\max}\Delta\bar{y}\right\},$$
$$\left\{(\bar{x},\bar{y}) : \bar{x} = n_{\max}\Delta\bar{x}, \quad 0 \le \bar{y} \le m_{\max}\Delta\bar{y}\right\},$$
$$\left\{(\bar{x},\bar{y}) : 0 \le \bar{x} \le n_{\max}\Delta\bar{x}, \quad \bar{y} = m_{\max}\Delta\bar{y}\right\},$$
$$\left\{(\bar{x},\bar{y}) : n\Delta\bar{x} < \bar{x} \le n_{\max}\Delta\bar{x}, \quad \bar{y} = 0\right\}.$$

The position of the wall and the incident shock wave is as presented in Fig. 1.

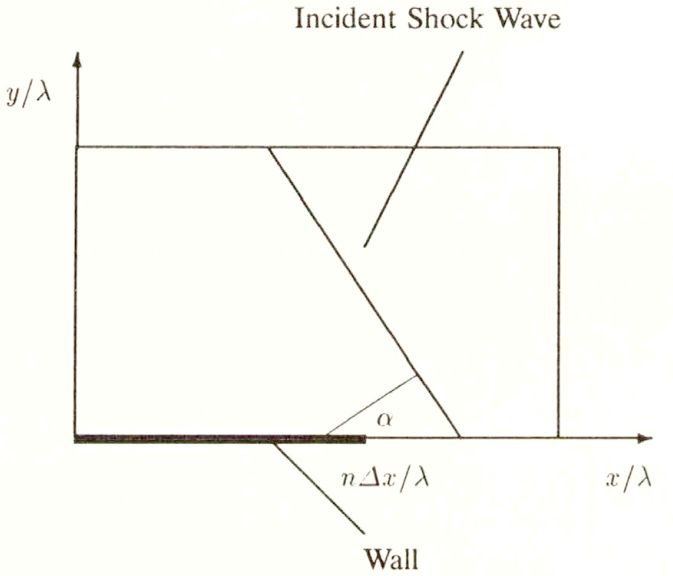

FIG. 1.

2.3. Initial conditions

The initial shock moves toward the wall located on the x-axis. The angle between the direction of motion and the x-axis is α.

For a given state of the gas (ρ_1, u_1, v_1, T_1) far before the shock we obtain the state far behind the shock (ρ_2, u_2, v_2, T_2) by means of the Rankine–Hugoniot conditions. The initial structure of the incident shock is assumed in the form proposed by TAYLOR [2]. Although these formulas are valid only for weak shocks, and a more appropriate structure could be obtained from the numerical solution of the stationary one-dimensional Navier–Stokes equations, we follow the reasoning used in [14]. There, the authors observed that the shock profiles which were initiated by the two mentioned procedures converged to each other after a sufficiently long time.

2.4. Boundary conditions on the artificial boundaries

On the artificial boundaries we assume that the gradient of all physical variables in the direction parallel to the incident shock front is zero. Therefore we obtain the values of (ρ, u, v, T) by shifting the corresponding (possibly interpolated) values from inside the computational domain along a line parallel to the incident shock front. Of course, this procedure introduces an error in the region of the boundary near the point $(\overline{x}, \overline{y}) = (n\Delta\overline{x}, 0)$, but that has no influence on the stability behaviour of the conditions on the wall.

3. Conditions on the wall

Generally the numerical boundary conditions can be divided into two classes:

• The so-called physical boundary conditions imposed by the considered physical situation, independently of any numerical method used. Their number should be equal to the number of conditions obtained by the analysis of well-posedness of the problem [1, 16]. Since for the Navier–Stokes equations, the well-posedness problem is still open, we assume that the physical boundary conditions for the Navier–Stokes equations reduce to physical boundary conditions for the Euler equations with vanishing viscous terms. Especially in the case of inflow/outflow boundaries, this assumption prevents the development of non-physical boundary layers. However, in the case of a solid wall, the boundary layers can be expected [13].

• If not all variables are specified by the physical conditions, appropriate artificial or soft boundary conditions have to be introduced in order to determine the remaining variables on the boundary. These additional conditions should correspond to the considered physical situation, and they must not provide any additional constraints on the physical variables. The soft boundary conditions may depend on the numerical method and on the equations considered.

Below we present a technique of specifying the boundary conditions proposed in [15]. Then we discuss the application of this method to the considered boundary conditions including such typical physical situations as the adiabatic slip, adiabatic no-slip and the isothermal no-slip wall, as well as a class of boundary conditions which represent a combination of the conditions for the adiabatic slip and the isothermal no-slip wall.

Following [15] let us notice that

$$\frac{\partial G(U)}{\partial y} = PP^{-1}R\frac{\partial V}{\partial y} = PB\frac{\partial V}{\partial y} = PT^{-1}\Lambda T\frac{\partial V}{\partial y},$$

where $\Lambda = \operatorname{diag}(\lambda_1, \lambda_2, \lambda_3, \lambda_4)$ and λ_i are the eigenvalues of the matrix $B = P^{-1}R$. The rows of T are the corresponding left eigenvectors l_i. P is defined as $\frac{\partial U}{\partial t} = P\frac{\partial V}{\partial t}$ and $V = (\rho, u, v, T)'$.

With

$$\mathcal{L}_i = \lambda_i l_i \frac{\partial V}{\partial y}, \qquad i = 1, \ldots, 4$$

we can rewrite the Navier–Stokes equations following the procedure in [17]:

$$\frac{\partial U}{\partial t} + \frac{\partial F}{\partial x} + PT^{-1} \begin{pmatrix} \mathcal{L}_1 \\ \mathcal{L}_2 \\ \mathcal{L}_3 \\ \mathcal{L}_4 \end{pmatrix} - \frac{\partial F^D}{\partial x} - \frac{\partial G^D}{\partial y} = 0$$

or

$$(1) \qquad \frac{\partial \rho}{\partial t} + \frac{\partial (\rho u)}{\partial x} + d_1 = 0,$$

$$(2) \qquad \frac{\partial (\rho u)}{\partial t} + \frac{\partial \left[\rho \left(u^2 + \frac{T}{\gamma}\right)\right]}{\partial x} + u d_1 + \rho d_4 - \frac{1}{\mathrm{Re}} \frac{\partial (\mu \tau_{11})}{\partial x} - \frac{1}{\mathrm{Re}} \frac{\partial (\mu \tau_{12})}{\partial y} = 0,$$

$$(3) \qquad \frac{\partial (\rho v)}{\partial t} + \frac{\partial (\rho u v)}{\partial x} + v d_1 + \rho d_3 - \frac{1}{\mathrm{Re}} \frac{\partial (\mu \tau_{21})}{\partial x} - \frac{1}{\mathrm{Re}} \frac{\partial (\mu \tau_{22})}{\partial y} = 0,$$

$$(4) \qquad \frac{\partial}{\partial t}\left[\rho \left(\frac{u^2 + v^2}{2} + \frac{T}{\gamma(\gamma - 1)}\right)\right] + \frac{\partial}{\partial x}\left[\rho u \left(\frac{u^2 + v^2}{2} + \frac{T}{\gamma - 1}\right)\right]$$
$$+ \frac{u^2 + v^2}{2} d_1 + \frac{d_2}{\gamma - 1} + \rho v d_3 + \rho u d_4$$
$$- \frac{1}{\mathrm{Re}} \frac{\partial}{\partial x}\left(\mu u \tau_{11} + \mu v \tau_{12} + \frac{\kappa}{\mathrm{Pr}(\gamma - 1)} q_1\right)$$
$$- \frac{1}{\mathrm{Re}} \frac{\partial}{\partial y}\left(\mu u \tau_{21} + \mu v \tau_{22} + \frac{\kappa}{\mathrm{Pr}(\gamma - 1)} q_2\right) = 0,$$

where

$$d = \begin{pmatrix} d_1 \\ d_2 \\ d_3 \\ d_4 \end{pmatrix} = \begin{pmatrix} \frac{1}{T\gamma}\left(\mathcal{L}_2 + \frac{1}{2}(\mathcal{L}_1 + \mathcal{L}_4)\right) \\ \frac{1}{2\gamma}(\mathcal{L}_1 + \mathcal{L}_4) \\ \frac{1}{2\rho\gamma\sqrt{T}}(\mathcal{L}_4 - \mathcal{L}_1) \\ \mathcal{L}_3 \end{pmatrix}.$$

$\mathcal{L}_i$, $i = 1, \ldots, 4$ are the amplitudes of characteristic waves associated with the characteristic velocity λ_i for the hyperbolic part of the equations. The technique described in [15] is based on the estimation of unknown incoming wave amplitudes ($\lambda_i > 0$) in terms of known outgoing wave amplitudes ($\lambda_i < 0$), using the so-called local associated one-dimensional inviscid (LODI) relations. In order to obtain the LODI relations, the flow is supposed to be locally inviscid

and one-dimensional near the boundary, hence neglecting transverse and viscous terms in the Navier–Stokes equations they are of the form:

$$\frac{\partial \rho}{\partial t} + \frac{1}{T\gamma}\left(\mathcal{L}_2 + \frac{1}{2}(\mathcal{L}_1 + \mathcal{L}_4)\right) = 0, \tag{5}$$

$$\begin{aligned} \frac{\partial u}{\partial t} + \mathcal{L}_3 &= 0, \\ \frac{\partial v}{\partial t} + \frac{1}{2\rho\gamma\sqrt{T}}(\mathcal{L}_4 - \mathcal{L}_1) &= 0, \\ \frac{\partial T}{\partial t} + \frac{\gamma - 1}{2\rho\gamma}(\mathcal{L}_1 + \mathcal{L}_4) - \frac{\mathcal{L}_2}{\rho\gamma} &= 0. \end{aligned} \tag{6}$$

The method consists now of the following steps:

- For each physical boundary condition imposed for the Euler equations, eliminate the corresponding equation from (1)...(4) and use the corresponding LODI relations (5)...$(6)_{1-3}$ in order to express the unknown values $\mathcal{L}_i$ by known $\mathcal{L}_i$.
- Use the remaining equations (1)...(4) combined with the values of $\mathcal{L}_i$ obtained in the previous step for the approximation of the normal first order derivatives, and the remaining physical boundary conditions of the Navier–Stokes equations, for the approximation of the second order derivatives in order to calculate the remaining variables.

Following the instruction we neglect (3) since $v_{|W} = 0$ is a natural boundary condition for the Euler equations. The eigenvalues are $\lambda_1 = v - \sqrt{T}$, $\lambda_2 = \lambda_3 = v$, $\lambda_4 = v + \sqrt{T}$, and for $v_{|W} = 0$ the only positive eigenvalue is $\lambda_4 = \sqrt{T}$. Then we obtain from $(6)_2$ the identity $\mathcal{L}_4 = \mathcal{L}_1$. This should be the only Euler boundary condition in order to get a well-posed Euler problem (see also [6]).

We consider now the following situations:

3.1. Adiabatic slip wall

The boundary conditions are $v_{|W} = 0$, $(\tau_{12})_{|W} = 0$, $(q_2)_{|W} = 0$, and from (1), (2), (4) with $\mathcal{L}_4 = \mathcal{L}_1$, we are able to calculate the values for (ρ, u, v, T) on the boundary.

Let us also mention another idea of obtaining the boundary conditions for the adiabatic slip wall, which has its origin in the fact that the interaction of two symmetric shock waves is equivalent to the reflection of a shock from a wall situated in the plane of symmetry. Obviously, this is true only for inviscid, non-conducting gases and can be applied if viscosity effects and heat-conductivity are negligibly small. Indeed, the boundary conditions generated in this way are stable since they appear to be a simple application of the stable MacCormack method with extrapolated values $\rho_{i,-1} = \rho_{i,1}$, $u_{i,-1} = u_{i,1}$, $v_{i,-1} = -v_{i,1}$, $T_{i,-1} = T_{i,1}$ [5].

3.2. Adiabatic no-slip wall

Here the conditions are expressed by $u_{|W} = v_{|W} = 0$, $(q_2)_{|W} = 0$. Since $u_{|W} = 0$, we should neglect (2) and equation $(6)_1$ indicates the already known relation $\mathcal{L}_3 = 0$, since $\lambda_3 = v_{|W} = 0$.

3.3. Isothermal no-slip wall

The conditions proposed in [15] are $u_{|W} = v_{|W} = 0$, $T_{|W} = T_1$. As described in the above mentioned procedure, we neglect (2) and (3) since $u_{|W} = v_{|W} = 0$ and from $(6)_{1,2}$ we get $\mathcal{L}_3 = 0$, $\mathcal{L}_4 = \mathcal{L}_1$. Since $T_{|W} = T_1$ we should neglect (4), and from $(6)_3$ we get, with $\mathcal{L}_2 = 0$ and $\mathcal{L}_4 = \mathcal{L}_1$, that $\mathcal{L}_4 = \mathcal{L}_1 = 0$.

Let us emphasize that for vanishing viscous terms the reduced boundary conditions for the no-slip walls are not the boundary conditions for the Euler equations, since $u_{|W} = 0$ is a typical viscous assumption. Nevertheless, this condition does not introduce any new restrictions on $\mathcal{L}_3$ since it is zero because of $\lambda_3 = v_{|W} = 0$. The case of the isothermal wall is more problematic since the condition $T_{|W} = T_1$ imposes a further restriction on the values of $\mathcal{L}_i$ namely $\mathcal{L}_1 = \mathcal{L}_4 = 0$.

Now we present an idea of the boundary conditions which arise in a series of experiments on the reflection of shock waves from a wall in rarefied gases [18], and they are given by

$$
\begin{aligned}
u_{|W} - u_i &= \beta(u_{\text{isn}} - u_i), \\
T_{|W} - T_i &= \beta(T_{\text{isn}} - T_i).
\end{aligned}
\tag{7}
$$

Here u_{isn} and T_{isn} are the boundary values of tangential velocity and temperature on an isothermal no-slip wall, i.e. $u_{\text{isn}} = 0$, $T_{\text{isn}} = T_1$. u_i and T_i are values inside the flow near the wall. β is a number between 0 and 1.

Let us notice that these conditions are an intermediate state between the adiabatic slip wall ($\beta = 0$) and the isothermal no-slip wall ($\beta = 1$). If $\beta \to 0$ would correspond to vanishing viscous terms, the conditions (7) would reduce to boundary conditions for the Euler equations and, therefore, they would satisfy the assumption for the physical boundary conditions made above. However, we do not know the dependence of β on the viscosity and heat-conductivity coefficients.

Density was obtained from Eq. (1) with $\mathcal{L}_1 = \mathcal{L}_4$.

We are aware of the inaccuracy of this procedure determining the density. The problem is that this type of boundary conditions for u and T does not allow for the use of the method proposed in [15], since we do not know anything about their first order normal or time derivatives, and therefore we can not exploit the appropriate LODI equations. More useful boundary conditions should be given for the expressions q_i and τ_{ij}, since their application in the second order derivatives in Eqs. (1), (2), (4) would guarantee the transition into the Euler conditions for vanishing viscous terms.

4. Numerical results and discussion

Now we present the numerical results systematically. The figures show the density profiles of the reflected shock wave after a certain time interval.

First we have used the boundary conditions for the adiabatic slip wall. The procedures give identical stable results. In Fig. 2 we see the regular reflection of the shock for Mach number before the shock 2.05 and $\alpha = 60°$. Figures 3 and 4 show the single Mach reflection for Mach numbers 3.5 and 5.0 and $\alpha = 10°$ and 20°, respectively.

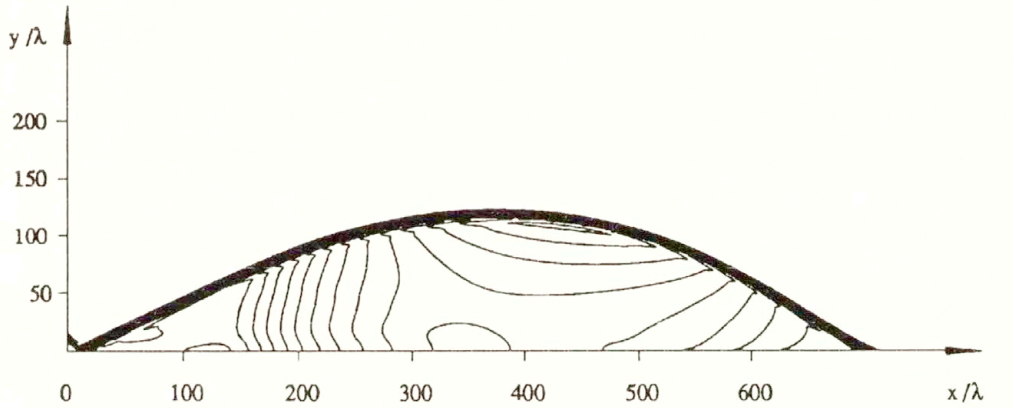

FIG. 2. Adiabatic slip wall. Data before the shock: $M = 2.05$, $p = 20000\,\text{Pa}$, $T = 297\,\text{K}$, $\alpha = 60°$.

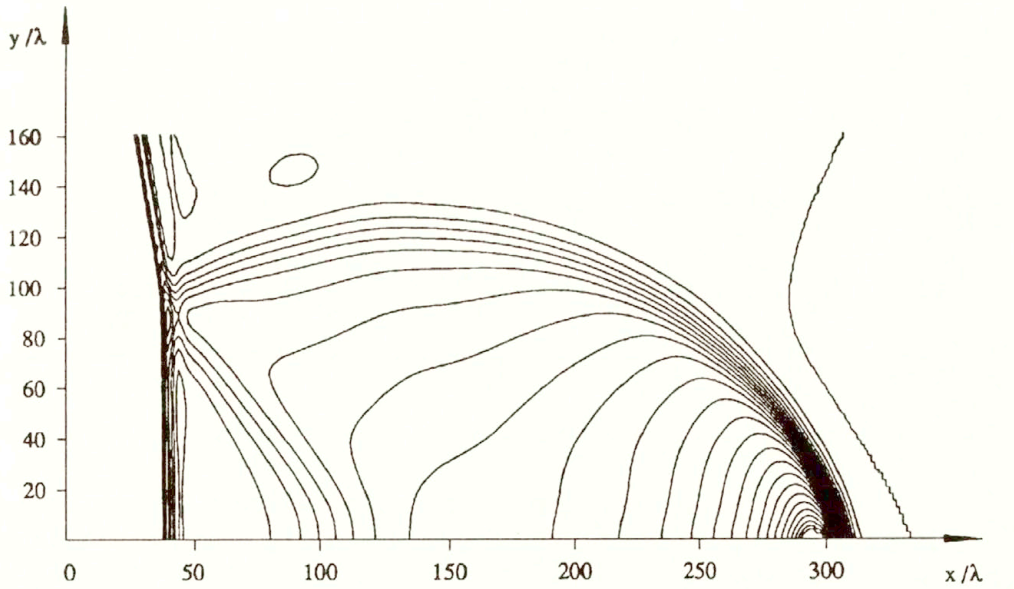

FIG. 3. Adiabatic slip wall. Data before the shock: $M = 3.5$, $p = 1000\,\text{Pa}$, $T = 300\,\text{K}$, $\alpha = 10°$.

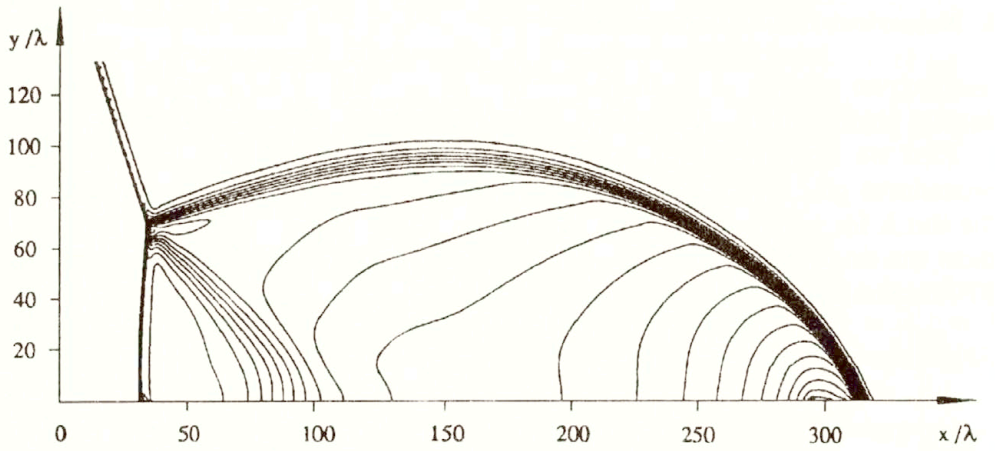

FIG. 4. Adiabatic slip wall. Data before the shock: $M = 5.0$, $p = 1000\,\text{Pa}$, $T = 300\,\text{K}$, $\alpha = 20°$.

Using this type of boundary conditions we achieve a good agreement with results of the shock tube experiments for dense gases (see [3]).

Although the conditions for the adiabatic no-slip wall used in Fig. 5 are stable, we see that the decrease of density near the boundary questions the physical significance of these conditions for the shock wave reflection. The Mach number before the shock is here 2.8, the angle $\alpha = 25°$.

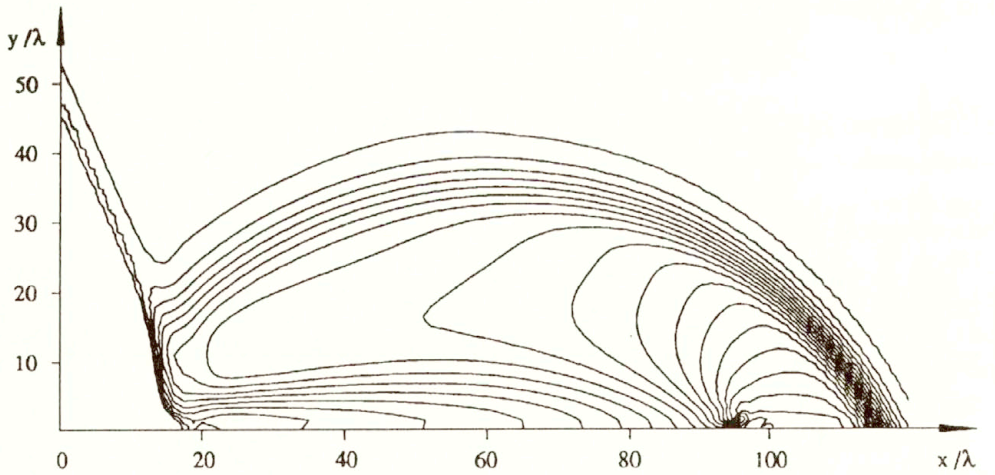

FIG. 5. Adiabatic no-slip wall. Data before the shock: $M = 2.8$, $p = 7.33\,\text{Pa}$, $T = 297\,\text{K}$, $\alpha = 25°$.

Let us present the shock wave reflection using conditions (7) which are a combination of the adiabatic slip and the isothermal no-slip boundary conditions. For Mach number before the shock 2.8, $\alpha = 25°$ and $\beta = 0.2$ we obtain Fig. 6. Figure 6 shows a considerable but smooth increase of density near the boundary for small β, in contrast to non-smooth jumps developing for β near 1.

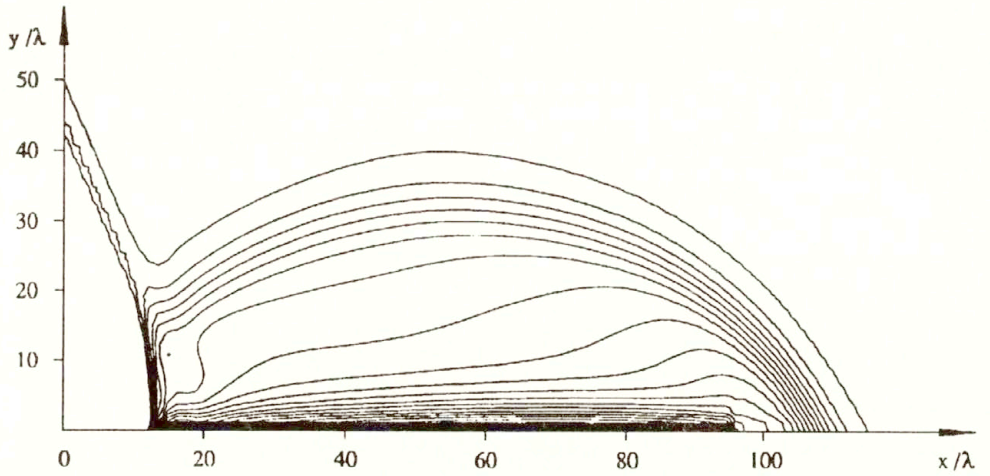

FIG. 6. Proposal. Data before the shock: $M = 2.8$, $p = 7.33\,\text{Pa}$, $T = 297\,\text{K}$, $\alpha = 25°$, $\beta = 0.2$.

Using the same boundary conditions (7) with Mach number 2.8, $\alpha = 60°$ and $\beta = 0.3$, we get the results presented in Fig. 7. Figure 7b shows an enlargement of the reflection area of the shock wave near the boundary. The values describing the levels are related to the quotient $(\rho - \rho_1)/(\rho_2 - \rho_1)$.

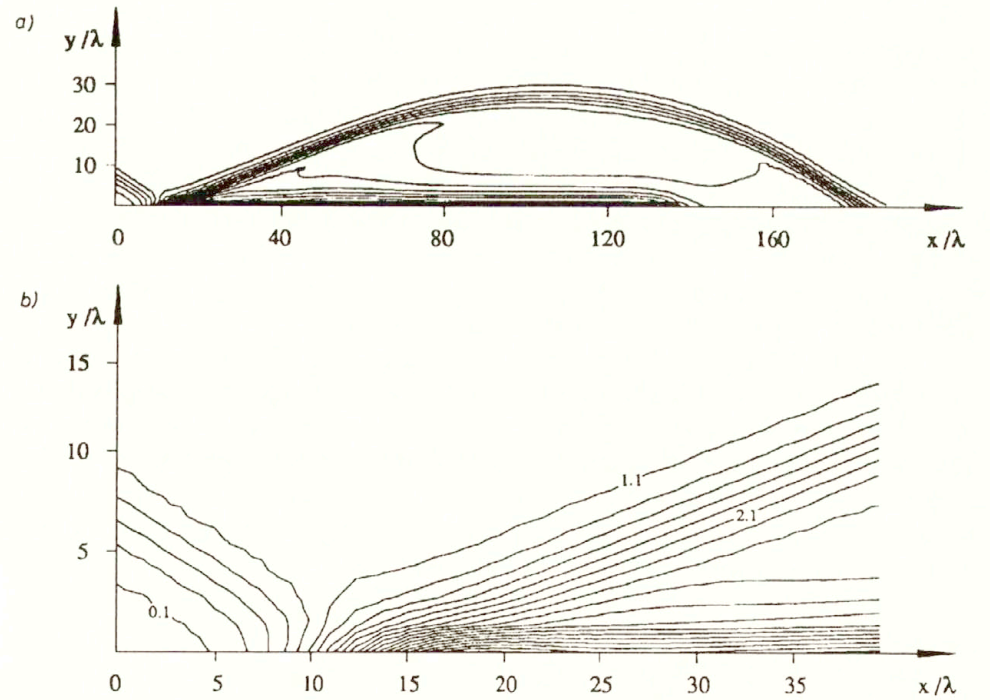

FIG. 7. Proposal. Data before the shock: $M = 2.8$, $p = 7.33\,\text{Pa}$, $T = 297\,\text{K}$, $\alpha = 60°$, $\beta = 0.3$.

Here we recognize the same structure of density profiles as that shown by the results of the shock tube experiments for rarefied gases in Fig. 8 [18]. Also important is here the good agreement of the angles between the wall and the reflected shock in the experimental and numerical results.

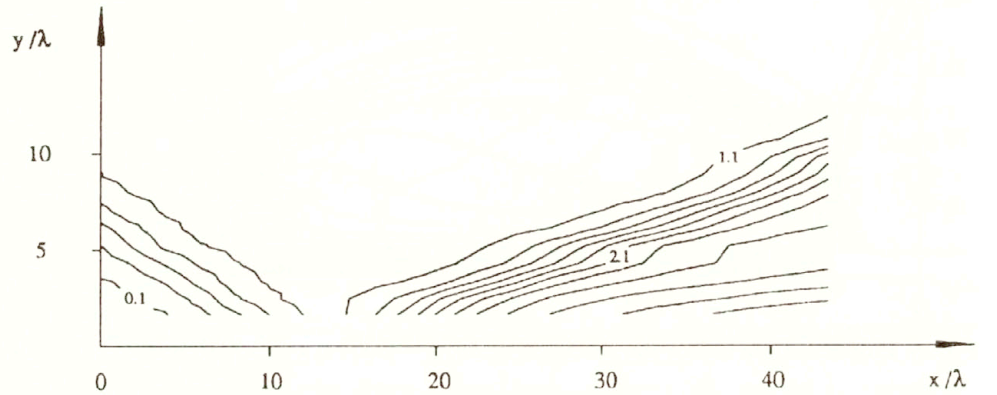

FIG. 8. Experimental results [18]. Data before the shock: $M = 2.8$, $p = 7.33\,\text{Pa}$, $T = 297\,\text{K}$, $\alpha = 60°$.

5. Summary

We see that the application of the procedure proposed in [15] for the classical physical situations of the adiabatic slip, adiabatic no-slip and the isothermal no-slip wall gives different results. For the adiabatic slip wall we get stable boundary conditions and a good agreement with shock tube experiments for dense gases [3]. The conditions of the adiabatic no-slip wall are also stable, but the decrease of density near the boundary makes the usefulness of these conditions for the shock wave reflection questionable. Problems occur in the formulation of boundary conditions for the isothermal no-slip wall, since the LODI relations introduce an additional restriction on the equations. Numerical experiments show that solutions including these conditions are unstable.

The crucial point is the investigation of a new class of boundary conditions (7) which allow for the consideration of a decisive wider range of physical situations. These boundary conditions represent a combination between the conditions for the adiabatic slip and isothermal no-slip wall, depending on parameter β. For an appropriately small but nonzero β we get a good agreement of the numerical and experimental results concerning the density levels, and the reflection angles of the shock wave in the case of rarefied gases [18].

Acknowledgment

The author expresses her gratitude to Prof. A. PALCZEWSKI for many important advices and discussion, and acknowledges Prof. Z. WALENTA for an important sug-

gestion related to the physical motivation of the boundary condition considered in the paper.

References

1. P. DUTT, *Stable boundary conditions and difference schemes for Navier–Stokes equations*, SIAM J. Numer. Anal., **25**, 2, 245–267, 1988.
2. W. FISZDON, *The structure of plane shock waves* [in:] Rarefied Gas Flow Theory, W. FISZDON [Ed.], Springer Verlag, Wien 1981.
3. H. M. GLAZ, P. COLELLA, I.I. GLASS, R.L. DESCHAMBAULT, *A numerical study of oblique shock-wave reflections with experimental comparisons*, Proc. Roy. Soc. Lond., A **398**, 117-140, 1985.
4. B. GUSTAFSSON, H.-O. KREISS, A. SUNDSTRÖM, *Stability theory of difference approximations for mixed initial-boundary value problems II*, Math. Comp., **26**, 119, 649–686, 1972.
5. K. KANTIEM, *On numerical stability of boundary conditions for the equations of fluid mechanics*, Ph. D. Thesis, Warsaw University, 1994.
6. K. KANTIEM and W. ZAJĄCZKOWSKI, *The existence and uniqueness of solutions of equations for ideal compressible polytropic fluids* [to appear].
7. M. N. KOGAN, *The dynamics of rarefied gases* [in Russian], Nauka, Moskva 1967.
8. H.-O. KREISS, *Initial boundary value problems for hyperbolic systems*, Comm. Pure Appl. Math., **23**, 277–298, 1970.
9. R. W. MAC CORMACK, *Numerical solution of the interaction of a shock wave with a laminar boundary layer*, Proc. 2nd Intern. Conference on Numerical Methods in Fluid Dynamics, Lecture Notes in Physics 8, 151–163, 1970.
10. A. MAJDA and S. OSHER, *Initial boundary value problems for hyperbolic equations with uniformly characteristic boundary*, Comm. Pure Appl. Math., **28**, 607–675, 1975.
11. D. MICHELSON, *Initial boundary value problems for incomplete singular perturbations of hyperbolic systems*, J. D'Analyse Mathematique, **53**, 1989.
12. D. MICHELSON, *Stability theory of difference approximations for multidimensional initial-boundary value problems*, Math. Comp., **40**, 161, 1–45, 1983.
13. J. OLIGER and A. SUNDSTRÖM, *Theoretical and practical aspects of some initial-boundary value problems in fluid dynamics*, SIAM J. Appl. Math., **35**, 3, 419–446, 1978.
14. A. PALCZEWSKI, W. STASIAK, *Numerical investigation of the one-dimensional shock wave reflection in a perfect gas*, Arch. Mech., **42**, 6, 667–677, 1990.
15. T.J. POINSOT and S.K. LELE, *Boundary conditions for direct simulations of compressible viscous flows*, J. Comp. Phys., **101**, 104–129, 1992.
16. J. STRIKWERDA, *Initial boundary value problems for incompletely parabolic systems*, Comm. Pure Appl. Math., **30**, 797–822, 1977.
17. K.W. THOMPSON, *Time-dependent boundary conditions for hyperbolic systems*, J. Comp. Phys., **68**, 1–24, 1987.
18. Z.A. WALENTA [private communication].

INSTITUTE OF APPLIED MATHEMATICS AND MECHANICS
WARSAW UNIVERSITY, WARSZAWA.

Received March 23, 1994.

Arch. Mech., 46, 5, pp. 653–668, Warszawa 1994

Dynamic stress intensity factors at two collinear cracks in two bonded dissimilar elastic half-planes

S. ITOU (YOKOHAMA) and Q. RENGEN (BEIJING)

DYNAMIC STRESSES in two bonded dissimilar half-planes weakened by two equal and collinear cracks are determined. The two cracks are placed in parallel with the interface of the two half-planes. Internal pressure is applied suddenly to the surfaces of the cracks. Application of the Fourier and Laplace transforms reduces the problem to the solution of dual integral equations in the Laplace transform domain. To solve the equations, the differences in the crack surface displacements are expanded in a series of functions which are automatically zero outside the cracks. The unknown coefficients in the series are solved using the Schmidt method. The stress intensity factors defined in the Laplace transform domain are inverted numerically in the physical space. Numerical calculations are carried out for the bonded composite materials made of a ceramic half-plane and steel half-plane.

1. Introduction

MANY STATIC PROBLEMS have been solved for a crack or cracks in two bonded elastic dissimilar half-planes, as seen in a recent book dealing with the stress intensity factors [1]. Especially, studies by Ishida and Noguchi are extremely helpful regarding this question. To solve the problems, they have used the body force method [2]. Quite recently, the stress intensity factors around an arbitrary array of cracks in bonded dissimilar half-planes have been treated by ISHIDA and NOGUCHI [3].

Regarding the dynamic crack problem for the composite materials, research has not been progressed as much as its statical counterpart because of the greater complexities. SIH and CHEN originally solved the dynamic problem for the composite materials with a crack [4]. They determined the transient dynamic stress field around a finite crack placed in the mid-surface in an infinite elastic layer sandwiched between two elastic half-planes. They also treated the axisymmetric dynamic crack problem concerning a penny-shaped crack in an infinite elastic layer sandwiched between two elastic half-spaces [5]. The dynamic stress intensity factor has been given for the case in which the material property of the cracked layer and that of the half-planes obey the theory of elasticity of orthotropic bodies [6]. Recently, the dynamic stress field around a rectangular crack in an infinite elastic layer sandwiched between two elastic half-spaces has been solved [7].

All of these problems deal with a single crack in composite materials. If some cracks exist in composite materials, we must reveal the mutual effect of the dynamic stress intensity factors. Focusing attention on that aspect of the subject, the dynamic stress intensity factors around two coplanar cracks in an orthotropic layer sandwiched between two isotropic half-planes have been worked out [8].

In the study, two cracks are placed at the mid-surface of the layer so as to be symmetrical with respect to the mid-surface.

Composite materials are occasionally weakened by cracks near the interface. In the present paper, the dynamic stress intensity factors appearing at two equal and collinear cracks in two bonded dissimilar half-planes are determined. Internal pressure is applied suddenly to the surfaces of the cracks. The problem is non-symmetric with respect to the plane, on which the cracks exist. Using the Fourier and Laplace transforms, the boundary conditions are reduced to dual integral equations in the Laplace transform domain. To solve the equations, the differences in the displacements at the interface are expanded in a series of functions which are automatically zero outside the cracks. The unknown coefficients in the series are determined using the Schmidt method [9].

Numerical calculations are carried out for the composite materials made of a ceramic half-plane and steel half-plane.

2. Fundamental equations

The two cracks are placed on the x-axis from $-b$ to $-a$ and from a to b with reference to the rectangular coordinate system (x, y) as shown in Fig. 1. The two

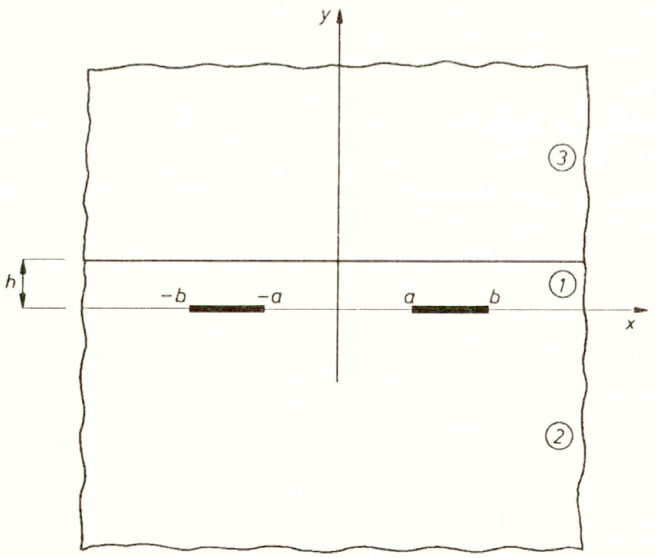

FIG. 1. Geometry and coordinate system.

half-planes are bonded at $y = h$. We consider the problem in a plane strain condition. For convenience, we have called the layer which occupies $0 \leq y \leq h$ Layer ①, the lower half-plane which occupies $y \leq 0$ Half-plane ②, and the upper half-plane which occupies $h \leq y$ Half-plane ③.

The equations of motion are reduced to:

$$\left(\partial^2/\partial x^2 + \partial^2/\partial y^2 - 1/c_{1i}^2\,\partial^2/\partial t^2\right)\phi_i = 0,$$
$$\left(\partial^2/\partial x^2 + \partial^2/\partial y^2 - 1/c_{2i}^2\,\partial^2/\partial t^2\right)\psi_i = 0, \tag{2.1}$$

with

$$c_{1i}^2 = 2(1-\nu_i)\mu_i/\{(1-2\nu_i)\rho_i\}, \qquad c_{2i}^2 = \mu_i/\rho_i, \tag{2.2}$$

where c_{1i} and c_{2i} are the dilatational and shear wave velocities, respectively, μ_i the modulus of elasticity in shear, ν_i the Poisson's ratio, ρ_i the density of the material, and the subscript $i = 1$ means that the corresponding values are those for Layer ①. The values of Half-plane ② and those of Half-plane ③ are also denoted by the subscript $i = 2$ and $i = 3$, respectively.

Displacements u_i, v_i and stresses τ_{xxi}, τ_{yyi}, τ_{xyi} are expressed in terms of ϕ_i and ψ_i as follows:

$$u_i = \partial\phi_i/\partial x - \partial\psi_i/\partial y, \qquad v_i = \partial\psi_i/\partial x + \partial\phi_i/\partial y, \tag{2.3}$$

$$\begin{aligned}
\tau_{xxi} &= -2\mu_i\partial^2\phi_i/\partial y^2 + \rho_i\partial^2\phi_i/\partial t^2 - 2\mu_i\partial^2\psi_i/\partial x\partial y,\\
\tau_{yyi} &= -2\mu_i\partial^2\phi_i/\partial x^2 + \rho_i\partial^2\phi_i/\partial t^2 + 2\mu_i\partial^2\psi_i/\partial x\partial y,\\
\tau_{xyi} &= 2\mu_i\partial^2\phi_i/\partial x\partial y + \mu_i(\partial^2\psi_i/\partial x^2 - \partial^2\psi_i/\partial y^2).
\end{aligned} \tag{2.4}$$

3. Boundary conditions

Consider an incident stress wave which propagates through upper half-plane at right angle to the x-axis. It is expressed as:

$$\tau_{yy3}^{(i)} = pH(y + c_{13}t) \tag{3.1}$$

where p is the constant, $H(t)$ the Heaviside unit step function, time t is zero when the wave front reaches the cracks and the superscript "(i)" means that the corresponding value is that of the incident stress field. The incident wave is reflected and refracted in a complicated manner at the interface $y = h$. However, it is likely that a stress wave which is similar to Eq. (3.1) passes across the cracks. Therefore, the stress intensity factors can be obtained by solving the problem with the following boundary conditions:

$$\tau_{yy1} = \tau_{yy3}, \quad \tau_{xy1} = \tau_{xy3}, \quad u_1 = u_3, \quad v_1 = v_3 \quad \text{at} \quad y = h, \quad |x| < \infty, \tag{3.2}$$

$$\tau_{yy1}^0 = \tau_{yy2}^0, \quad \tau_{xy1}^0 = \tau_{xy2}^0, \quad \text{at} \quad y = 0, \quad |x| < \infty, \tag{3.3}$$

$$\tau_{yy1}^0 = \tau_{yy2}^0 = -pH(t), \quad \tau_{xy1}^0 = \tau_{xy2}^0 = 0 \quad \text{at} \quad y = 0, \quad a < |x| < b, \tag{3.4}$$

$$u_1^0 = u_2^0, \quad v_1^0 = v_2^0 \quad \text{at} \quad y = 0, \quad 0 \le |x| < a, \quad b < |x|, \tag{3.5}$$

where superscript "0" denotes the values at $y = 0$.

4. Analysis

To find the solution, the Laplace transforms were used

$$g^*(s) = \int_0^\infty g(t)\exp(-st)\,dt,$$
$$g(t) = 1/(2\pi i)\int_{Br.} g^*(s)\exp(st)\,ds \tag{4.1}$$

and the Fourier transforms

$$\overline{f}(\xi) = \int_{-\infty}^{\infty} f(x)\exp(i\,\xi x)\,dx,$$
$$f(x) = 1/(2\pi)\int_{-\infty}^{\infty} \overline{f}(\xi)\exp(-i\,\xi x)\,d\xi. \tag{4.2}$$

Applying Eqs. (4.1) and (4.2) to Eq. (2.1) we obtain

$$(d^2/dy^2 - \xi^2 - s^2/c_{1i}^2)\overline{\phi}_i^* = 0,$$
$$(d^2/dy^2 - \xi^2 - \varepsilon_i^2\, s^2/c_{1i}^2)\overline{\psi}_i^* = 0, \tag{4.3}$$

with

$$\varepsilon_i^2 = 2(1-\nu_i)/(1-2\nu_i). \tag{4.4}$$

The solutions of Eq. (4.3) have the following forms for Layer ①, Half-plane ② and Half-plane ③, respectively,

$$\overline{\phi}_1^* = A_{11}\sinh(\gamma_{11}y) + A_{21}\cosh(\gamma_{11}y),$$
$$\overline{\psi}_1^* = B_{11}\sinh(\gamma_{21}y) + B_{21}\cosh(\gamma_{21}y), \tag{4.5}$$

$$\overline{\phi}_2^* = C_{12}\exp(\gamma_{12}y), \qquad \overline{\psi}_2^* = D_{12}\exp(\gamma_{22}y), \tag{4.6}$$

$$\overline{\phi}_3^* = C_{13}\exp(-\gamma_{13}y), \qquad \overline{\psi}_3^* = D_{13}\exp(-\gamma_{23}y), \tag{4.7}$$

with

$$\gamma_{1i} = (\xi^2 + s^2/c_{1i}^2)^{1/2}, \qquad \gamma_{2i} = (\xi^2 + \varepsilon_i^2 s^2/c_{1i})^{1/2}, \tag{4.8}$$

where $A_{11}, A_{21}, \ldots, D_{13}$ are the unknown coefficients.

Applying Eqs. (4.1) and (4.2) to Eqs. (2.3) and (2.4), we obtain

$$\overline{u}_i^* = -i\xi\overline{\phi}_i^* - d\overline{\psi}_i^*/dy, \qquad \overline{v}_i^* = d\overline{\phi}_i^*/dy - i\xi\overline{\psi}_i^*, \tag{4.9}$$

$$\begin{aligned}
\overline{\tau}_{xxi}^* &= -2\mu_i d^2\overline{\phi}_i^*/dy^2 + \mu_i\varepsilon_i^2 s^2/c_{1i}^2\phi_i + 2\mu_i i\xi d\overline{\psi}_i^*/dy, \\
\overline{\tau}_{yyi}^* &= 2\mu_i\xi^2\overline{\phi}_i^* + \mu_i\varepsilon_i^2 s^2/c_{1i}^2\phi_i - 2\mu_i i\xi d\overline{\psi}_i^*/dy, \\
\overline{\tau}_{xyi}^* &= -2i\mu_i\xi d\overline{\psi}_i^*/dy + \mu_i(-\xi^2\overline{\psi}_i^* - d^2\overline{\psi}_i^*/dy^2).
\end{aligned} \tag{4.10}$$

Substituting Eqs. (4.5), (4.6) and (4.7) into Eqs. (4.9) and (4.10), we can express the displacements and the stresses in the Laplace transform domain. With use of Eqs. (3.2) and (3.3), coefficients $B_{11}, B_{21}, C_{12}, D_{12}, C_{13}, D_{13}$ are represented by coefficients A_{11} and A_{21} as follows:

$$\begin{vmatrix} C_{13} \\ iD_{13} \\ iB_{11} \\ iB_{21} \\ C_{12} \\ iD_{12} \end{vmatrix} = \begin{vmatrix} f_1 & f_2 \\ f_3 & f_4 \\ f_5 & f_6 \\ f_7 & f_8 \\ f_9 & f_{10} \\ f_{11} & f_{12} \end{vmatrix} \begin{vmatrix} A_{11} \\ A_{21} \end{vmatrix}, \tag{4.11}$$

where $f_1, f_2, \ldots, f_{12}$ are given in Appendix A. Now, all of the stresses and displacements can be only expressed by coefficients A_{11} and A_{21}. For example, $\overline{\tau}_{yy1}^{0*}$, $\overline{\tau}_{xy1}^{0*}$, $\overline{u}_1^{0*}$, $\overline{v}_1^{0*}$ are written in the form

$$\begin{aligned}
\overline{\tau}_{yy1}^{0*}/(2\mu_1) &= A_{11}K_1^{(1)} + A_{21}K_2^{(1)}, \\
\overline{\tau}_{xy1}^{0*}/(2\mu_1) &= iA_{11}K_3^{(1)} + iA_{21}K_4^{(1)},
\end{aligned} \tag{4.12}$$

$$\begin{aligned}
-i\overline{u}_1^{0*} &= A_{11}K_5^{(1)} + iA_{21}K_6^{(1)}, \\
\overline{v}_1^{0*} &= A_{11}K_7^{(1)} + iA_{21}K_8^{(1)},
\end{aligned} \tag{4.13}$$

where functions $K_1^{(1)}, K_2^{(1)}, \ldots, K_8^{(1)}$ are given in Appendix B.

For convenience, we represent coefficients A_{11} and A_{21} by $\overline{u}_1^{0*}$ and $\overline{v}_1^{0*}$ with use of Eqs. (4.13). Then, stresses $\overline{\tau}_{yy1}^{0*}$ and $\overline{\tau}_{xy1}^{0*}$ are given by

$$\begin{aligned}
\overline{\tau}_{yy1}^{0*} &= -i\overline{u}_1^{0*}r_1^{(1)} + \overline{v}_1^{0*}r_2^{(1)}, \\
\overline{\tau}_{xy1}^{0*} &= \overline{u}_1^{0*}r_3^{(1)} + i\overline{v}_1^{0*}r_4^{(1)},
\end{aligned} \tag{4.14}$$

where $r_1^{(1)}, r_2^{(1)}, r_3^{(1)}, r_4^{(1)}$ are given in Appendix C. Similarly, displacements $\overline{u}_2^{0*}$ and $\overline{v}_2^{0*}$ are represented by $\overline{u}_1^{0*}$ and $\overline{v}_1^{0*}$ as follows:

$$\begin{aligned}
\overline{u}_2^{0*} &= i(-i\overline{u}_1^{0*})L_1^{(2)} + i\overline{v}_1^{0*}L_2^{(2)}, \\
\overline{v}_2^{0*} &= (-i\overline{u}_1^{0*})L_3^{(2)} + \overline{v}_1^{0*}L_4^{(2)},
\end{aligned} \tag{4.15}$$

where functions $L_1^{(2)}, L_2^{(2)}, L_3^{(2)}, L_4^{(2)}$ are given in Appendix D.

Here, we expand the differences of the displacements at $y = 0$ in the Laplace transform domain into the series

$$
\begin{aligned}
\pi(v_1^{0*} - v_2^{0*}) &= \sum_{n=1}^{\infty} c_n \frac{1}{2n} \sin\left\{ n \sin^{-1}\left[\frac{a+b-2|x|}{b-a}\right] - n\frac{\pi}{2} \right\} \\
&\qquad\qquad \text{for} \quad a < |x| < b, \\
&= 0 \qquad \text{for} \quad 0 \le |x| < a, \quad b < |x|, \\
\pi(u_1^{0*} - u_2^{0*}) &= \sum_{n=1}^{\infty} d_n \frac{1}{2n} \sin\left\{ n \sin^{-1}\left[\frac{a+b-2|x|}{b-a}\right] - n\frac{\pi}{2} \right\} \operatorname{sgn}(x) \\
&\qquad\qquad \text{for} \quad a < |x| < b, \\
&= 0 \qquad \text{for} \quad 0 \le |x| < a, \quad b < |x|,
\end{aligned}
\tag{4.16}
$$

with

$$
\begin{aligned}
\operatorname{sgn}(x) &= -1 \qquad \text{for} \quad x < 0, \\
&= 0 \qquad \text{for} \quad x = 0, \\
&= 1 \qquad \text{for} \quad x > 0,
\end{aligned}
\tag{4.17}
$$

and c_n, d_n are the unknown coefficients. Differences in displacements $(v_1^{0*} - v_2^{0*})$ and $(u_1^{0*} - u_2^{0*})$ are written in the form of Eq. (4.16). Then, the boundary condition (3.5) is satisfied automatically; the remaining boundary condition is only Eq. (3.4). The Fourier transforms of Eq. (4.16) are

$$
\begin{aligned}
\bar{v}^{0*} - \bar{v}_2^{0*} &= \sum_{n=1}^{\infty} c_n \frac{1}{\xi} \sin\left\{ \frac{(a+b)\xi}{2} - n\frac{\pi}{2} \right\} J_n\left\{ \frac{(b-a)\xi}{2} \right\}, \\
-i(\bar{u}_1^{0*} - \bar{u}_2^{0*}) &= \sum_{n=1}^{\infty} d_n \frac{-1}{\xi} \cos\left\{ \frac{(a+b)\xi}{2} - n\frac{\pi}{2} \right\} J_n\left\{ \frac{(b-a)\xi}{2} \right\},
\end{aligned}
\tag{4.18}
$$

where $J_n(x)$ are Bessel functions.

Substituting Eq. (4.18) into Eq. (4.15), $\bar{v}_2^{0*}$ and $\bar{u}_2^{0*}$ can be eliminated and then $\bar{v}_1^{0*}$ and $\bar{u}_1^{0*}$ are represented by coefficients c_n and d_n.

Therefore, all the stresses and displacements are expressed in terms of coefficients c_n and d_n only. For example, stresses τ_{yy1}^{0*} and τ_{xy1}^{0*} are as follows:

$$
\begin{aligned}
\tau_{yy1}^{0*} &= \sum_{n=1}^{\infty} c_n \frac{1}{\pi} \int_0^{\infty} \frac{Q_1(\xi)}{\xi} \sin\left\{ \frac{(a+b)\xi}{2} - n\frac{\pi}{2} \right\} J_n\left\{ \frac{(b-a)\xi}{2} \right\} \cos(\xi x)\, d\xi \\
&\quad + \sum_{n=1}^{\infty} d_n \frac{1}{\pi} \int_0^{\infty} \frac{Q_2(\xi)}{\xi} \cos\left\{ \frac{(a+b)\xi}{2} - n\frac{\pi}{2} \right\} J_n\left\{ \frac{(b-a)\xi}{2} \right\} \cos(\xi x)\, d\xi,
\end{aligned}
\tag{4.19}
$$

$$\tau_{xy1}^{0*} = \sum_{n=1}^{\infty} c_n \frac{1}{\pi} \int_0^{\infty} \frac{Q_3(\xi)}{\xi} \sin\left\{\frac{(a+b)\xi}{2} - n\frac{\pi}{2}\right\} J_n\left\{\frac{(b-a)\xi}{2}\right\} \sin(\xi x)\, d\xi$$

$$+ \sum_{n=1}^{\infty} d_n \frac{1}{\pi} \int_0^{\infty} \frac{Q_4(\xi)}{\xi} \cos\left\{\frac{(a+b)\xi}{2} - n\frac{\pi}{2}\right\} J_n\left\{\frac{(b-a)\xi}{2}\right\} \sin(\xi x)\, d\xi, \tag{4.19 [cont.]}$$

where $Q_j(\xi)$ $(j = 1, 2, 3, 4)$ are given in Appendix E. Functions $Q_j(\xi)$ behave for a large value of ξ

$$Q_j(\xi)/\xi \to Q_j^L + Q_j^0/\xi, \tag{4.20}$$

where Q_j^L and Q_j^0 are constants given by

$$\begin{aligned} Q_j^L &= \{Q_j(\xi_L) - Q_j(\xi_L - \varepsilon)\}/\varepsilon, \\ Q_j^0 &= Q_j(\xi_L) - Q_j^L \xi_L, \end{aligned} \tag{4.21}$$

with ξ_L being a large value of ξ and ε being an arbitrary small value.

Finally, the remaining boundary condition (3.4) can be reduced to

$$\begin{aligned} &\sum_{n=1}^{\infty} c_n F_n(x) + \sum_{n=1}^{\infty} d_n G_n(x) = -p/s, \\ &\sum_{n=1}^{\infty} c_n H_n(x) + \sum_{n=1}^{\infty} d_n I_n(x) = 0, \end{aligned} \qquad \text{for} \quad a < x < b, \tag{4.22}$$

where functions $F_n(x), G_n(x), H_n(x), I_n(x)$ are given in Appendix F. Here, the following relationships have been used,

$$\begin{aligned} &\int_0^{\infty} J_n(\alpha\xi)\{\cos(\beta\xi),\ \sin(\beta\xi)\}\, d\xi \\ &= 1/(\alpha^2 - \beta^2)^{1/2}\left[\cos\{n \sin^{-1}(\beta/\alpha)\},\ \sin\{n \sin^{-1}(\beta/\alpha)\}\right] \quad \text{for} \quad \alpha > \beta; \\ &= \{-\alpha^n \sin(n\pi/2),\ \alpha^n \cos(n\pi/2)\} \\ &\qquad / \left[(\beta^2 - \alpha^2)^{1/2}\{\beta + (\beta^2 - \alpha^2)^{1/2}\}^n\right] \quad \text{for} \quad \beta > \alpha. \end{aligned} \tag{4.23}$$

$$\begin{aligned} &\int_0^{\infty} \xi^{-1} J_n(\alpha\xi)\{\cos(\beta\xi),\ \sin(\beta\xi)\}\, d\xi \\ &= n^{-1}\left[\cos\{n \sin^{-1}(\beta/\alpha)\},\ \sin\{n \sin^{-1}(\beta/\alpha)\}\right] \quad \text{for} \quad \alpha > \beta; \\ &= n^{-1}\alpha^n\{\cos(n\pi/2),\ \sin(n\pi/2)\} \\ &\qquad /\{\beta + (\beta^2 - \alpha^2)^{1/2}\}^n \quad \text{for} \quad \beta > \alpha. \end{aligned} \tag{4.24}$$

Now, Eq. (4.22) can be solved for coefficients c_n and d_n using the Schmidt method [9].

5. Stress intensity factors

Coefficients c_n and d_n are known so that the entire stress field can be determined. Regarding the crack problem, it is important to know the values of the stress intensity factors determined from the stresses around the crack tips. With the use of Eqs. (4.19) and (4.23), the stress intensity factors can be expressed in the Laplace transform domain by

$$
\begin{aligned}
K_{1a}^{*} &= \tau_{yy1}^{0*}\{2\pi(a-x)\}^{1/2}\Big|_{x\to a-} = \sum_{n=1}^{\infty} c_n Q_1^L/\{2\pi(b-a)\}^{1/2},\\
K_{2a}^{*} &= \tau_{xy1}^{0*}\{2\pi(a-x)\}^{1/2}\Big|_{x\to a-} = \sum_{n=1}^{\infty} d_n(-Q_4^L)/\{2\pi(b-a)\}^{1/2},\\
K_{1b}^{*} &= \tau_{yy1}^{0*}\{2\pi(x-b)\}^{1/2}\Big|_{x\to b+} = \sum_{n=1}^{\infty} c_n(-1)^n Q_1^L/\{2\pi(b-a)\}^{1/2},\\
K_{2b}^{*} &= \tau_{xy1}^{0*}\{2\pi(x-b)\}^{1/2}\Big|_{x\to b+} = \sum_{n=1}^{\infty} d_n(-1)^{n+1} Q_4^L/\{2\pi(b-a)\}^{1/2}.
\end{aligned}
\tag{5.1}
$$

The Laplace inverse transformations in Eq. (5.1) are carried out by the numerical method provided by MILLER and GUY [10].

6. Numerical examples and results

We consider the composite materials made of the ceramic half-plane with the material constants $\mu_i = 119.7\,\mathrm{GN/m^2}$, $\rho_i = 3.15 \times 10^3\,\mathrm{kg/m^3}$, $\nu_i = 0.27$ and the steel half-plane with the material constants $\mu_i = 79.2\,\mathrm{GN/m^2}$, $\rho_i = 7.70 \times 10^3\,\mathrm{kg/m^3}$, $\nu_i = 0.30$. Numerical calculations are carried out for two cases. One of them is the case in which the upper half-plane is steel and the lower cracked half-plane is ceramic. We call this Case 1. Another is the case in which the upper half-plane is ceramic and the lower cracked half-plane is steel. We call this Case 2.

The semi-infinite integrals which appear in $F_n(x)$, $G_n(x)$, $H_n(x)$, $I_n(x)$ in Eq. (4.22) are easily evaluated using Filon's method because the integrands decay rapidly. By breaking off the infinite series in Eq. (4.22) at term of $n = 10$, the Schmidt method is applied. It has been verified in each numerical calculation that the values of the l.h.s. in Eq. (4.22) agree well with those of r.h.s.

In Figs. 2 and 3, the results of K_{1a} and K_{1b} are shown for Case 1 versus $c_{11}t/\{(b-a)/2\}$. The results of K_{1a} and K_{1b} for Case 2 are plotted in Figs. 4 and 5. In these, the straight lines are the corresponding static values which are

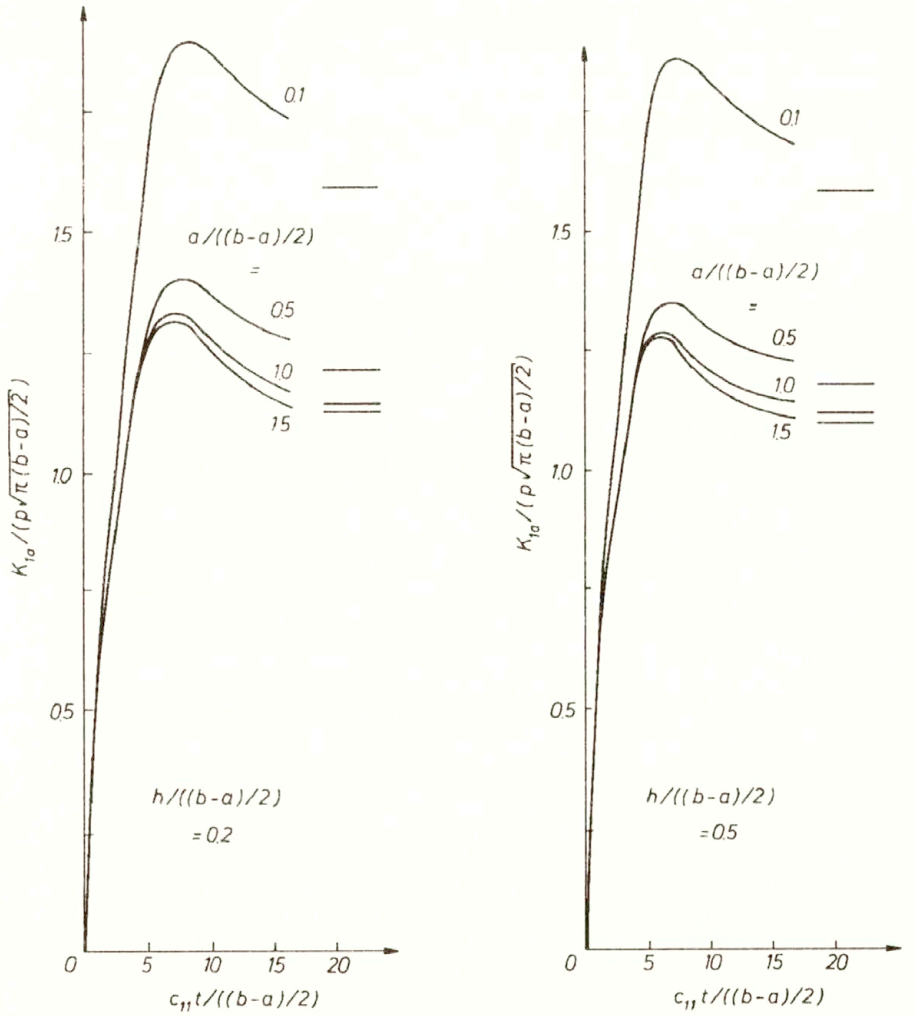

FIG. 2. Stress intensity factor K_{1a} for Case 1 (Upper half-plane of steel is bonded to the lower cracked half-plane of ceramics).

calculated by the authors separately. The values of K_{2a} and K_{2b} are not shown because they are very small.

The curves of K_{1a} and K_{1b} for $a/\{(b-a)/2\} = 1.5$ are close to those for $a/\{(b-a)/2\} = 1.0$ regardless of the values of $h/\{(b-a)/2\}$. Therefore, the results for $a/\{(b-a)/2\} = 1.5$ can be considered as the results of the stress intensity factors around a single crack in two bonded dissimilar elastic half-planes. In addition, it can be seen from the figures that the peak values of the dynamic stress intensity factors are about 1.15 or 1.25 times larger than those of the corresponding static values.

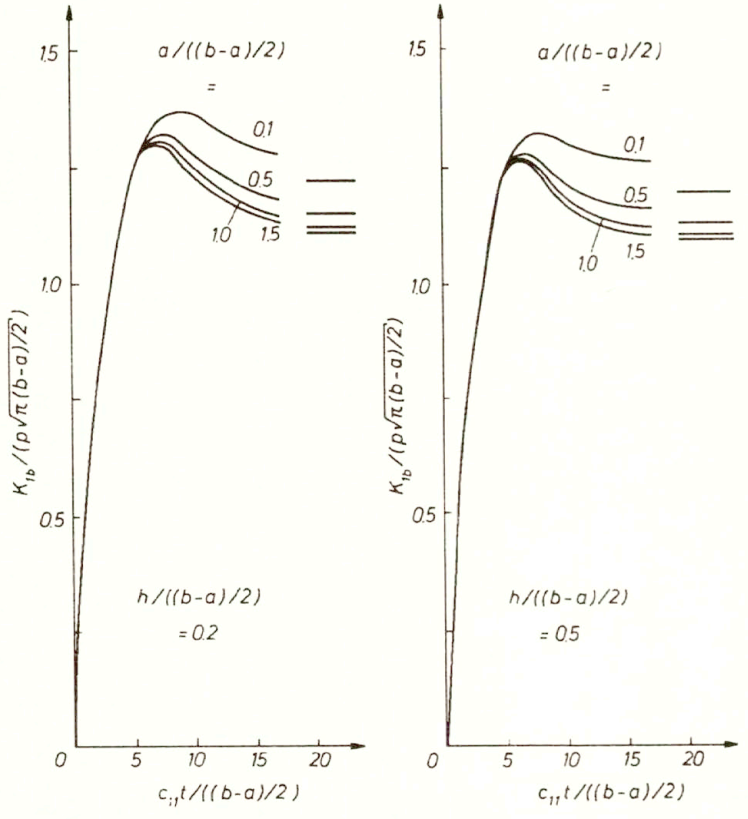

FIG. 3. Stress intensity factor K_{1b} for Case 1 (Upper half-plane of steel is bonded to the lower cracked half-plane of ceramics).

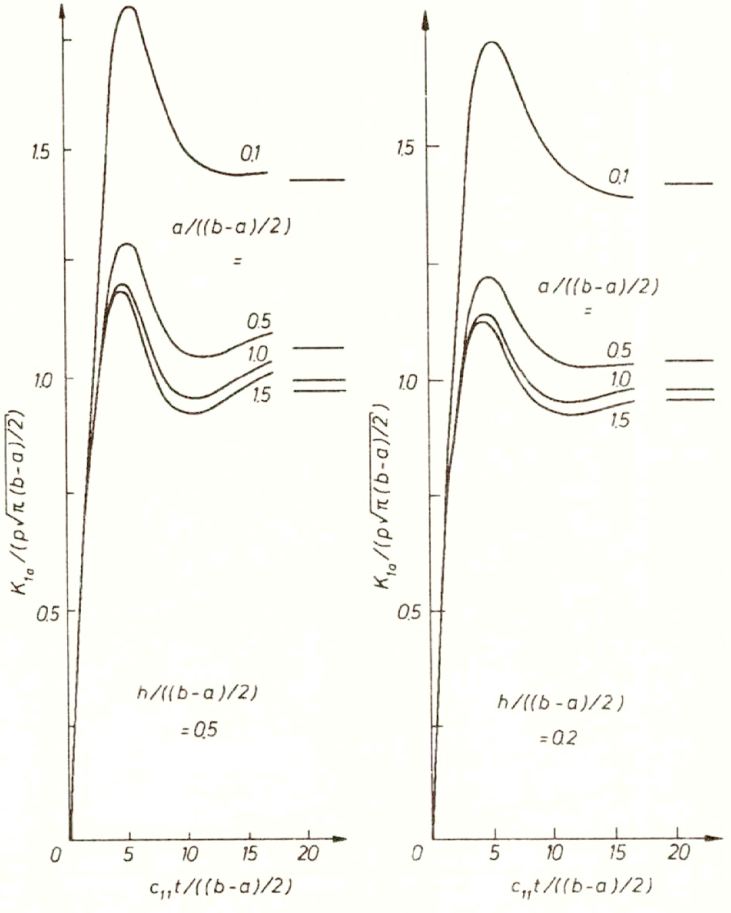

FIG. 4. Stress intensity factor K_{1a} for Case 2 (Upper half-plane of ceramics is bonded to the lower cracked half-plane of steel).

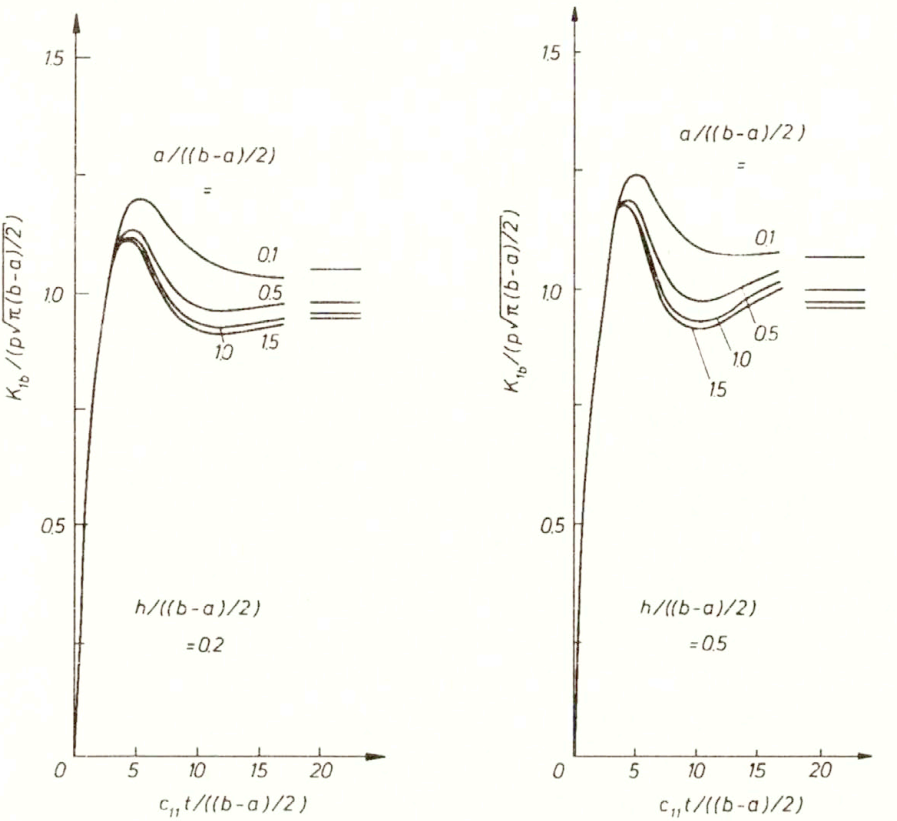

FIG. 5. Stress intensity factor K_{1b} for Case 2 (Upper half-plane of ceramics is bonded to the lower cracked half-plane of steel).

Appendix A

$$f_{i+2(k-1)} = \begin{vmatrix} a_{11} & \dots & a_{1i-1} & b_{1k} & a_{1i+1} & \dots & a_{16} \\ a_{21} & \dots & a_{2i-1} & b_{2k} & a_{2i+1} & \dots & a_{26} \\ a_{31} & \dots & a_{3i-1} & b_{3k} & a_{3i+1} & \dots & a_{36} \\ a_{41} & \dots & a_{4i-1} & b_{4k} & a_{4i+1} & \dots & a_{46} \\ a_{51} & \dots & a_{5i-1} & b_{5k} & a_{5i+1} & \dots & a_{56} \\ a_{61} & \dots & a_{6i-1} & b_{6k} & a_{6i+1} & \dots & a_{66} \end{vmatrix} / \Delta \tag{A.1}$$

$$\text{for} \quad (i = 1, 2, \dots, 6), \quad (k = 1, 2)$$

with

$$\Delta = |a_{ij}| \quad \text{for} \quad (i, j = 1, 2, \dots, 6), \tag{A.2}$$

$$
\begin{aligned}
a_{11} &= -2\mu_3\left\{\xi^2 + \varepsilon_3^2 s^2/(2c_{13}^2)\right\}\exp(-\gamma_{13}h),\\
a_{12} &= -2\mu_3\xi\gamma_{23}\exp(-\gamma_{23}h),\\
a_{13} &= -2\mu_1\xi\gamma_{21}\cosh(\gamma_{21}h),\\
a_{14} &= -2\mu_1\xi\gamma_{21}\sinh(\gamma_{21}h), \qquad a_{15} = 0, \qquad a_{16} = 0,\\
b_{11} &= -2\mu_1\left\{\xi^2 + \varepsilon_1^2 s^2/(2c_{11}^2)\right\}\sinh(\gamma_{11}h),\\
b_{12} &= -2\mu_1\left\{\xi^2 + \varepsilon_1^2 s^2/(2c_{11}^2)\right\}\cosh(\gamma_{11}h),\\
a_{21} &= 2\mu_3\xi\gamma_{13}\exp(-\gamma_{13}h),\\
a_{22} &= \mu_3(\xi^2 + \gamma_{23}^2)\exp(-\gamma_{23}h),\\
a_{23} &= -\mu_3(\xi^2 + \gamma_{21}^2)\sinh(\gamma_{21}h),\\
a_{24} &= -\mu_1(\xi^2 + \gamma_{21}^2)\cosh(\gamma_{21}h), \qquad a_{25} = 0, \qquad a_{26} = 0,\\
b_{21} &= -2\mu_1\xi\gamma_{11}\cosh(\gamma_{11}h),\\
b_{22} &= -2\mu_1\xi\gamma_{11}\sinh(\gamma_{11}h),\\
a_{31} &= -\xi\exp(-\gamma_{13}h), \qquad a_{32} = -\gamma_{23}\exp(-\gamma_{23}h),\\
a_{33} &= -\gamma_{21}\cosh(\gamma_{21}h), \qquad a_{34} = -\gamma_{21}\sinh(\gamma_{21}h),\\
a_{35} &= 0, \qquad a_{36} = 0, \qquad b_{31} = -\xi\sinh(\gamma_{11}h),\\
b_{32} &= -\xi\cosh(\gamma_{11}h), \qquad a_{41} = \gamma_{13}\exp(-\gamma_{13}h),\\
a_{42} &= \xi\exp(-\gamma_{23}h), \qquad a_{43} = -\xi\sinh(\gamma_{21}h),\\
a_{44} &= -\xi\cosh(\gamma_{21}h), \qquad a_{45} = 0, \qquad a_{46} = 0,\\
b_{41} &= -\gamma_{11}\cosh(\gamma_{11}h), \qquad b_{42} = -\gamma_{11}\sinh(\gamma_{11}h),\\
a_{51} &= 0, \qquad a_{52} = 0, \qquad a_{53} = -2\mu_1\xi\gamma_{21},\\
a_{54} &= 0, \qquad a_{55} = -2\mu_2\{\xi^2 + \varepsilon_2^2 s^2/(2c_{12}^2)\},\\
a_{56} &= 2\mu_2\xi\gamma_{22}, \qquad b_{51} = 0,\\
b_{52} &= -2\mu_1\{\xi^2 + \varepsilon_1^2 s^2/(2c_{11}^2)\}, \qquad a_{61} = 0,\\
a_{62} &= 0, \qquad a_{63} = 0, \qquad a_{64} = -\mu_1(\xi^2 + \gamma_{21}^2),\\
a_{65} &= -2\mu_2\xi\gamma_{12}, \qquad a_{66} = -\mu_2(\xi^2 + \gamma_{22}^2),\\
b_{61} &= -2\mu_1\xi\gamma_{11}, \qquad b_{62} = 0.
\end{aligned}
\tag{A.3}
$$

Appendix B

$$
\begin{aligned}
K_1^{(1)} &= -\xi\gamma_{21}f_5, \qquad K_2^{(1)} = -\xi\gamma_{21}f_6 + \{\xi^2 + \varepsilon_1^2 s^2/(2c_{11}^2)\},\\
K_3^{(1)} &= \xi\gamma_{11} + (\xi^2 + \gamma_{21}^2)f_7/2, \qquad K_4^{(1)} = (\xi^2 + \gamma_{21}^2)f_8/2,\\
K_5^{(1)} &= \gamma_{21}f_5, \qquad K_6^{(1)} = -\xi + \gamma_{21}f_6,\\
K_7^{(1)} &= \gamma_{11} - \xi f_7, \qquad K_8^{(1)} = -\xi f_8.
\end{aligned}
\tag{B.1}
$$

Appendix C

$$
\begin{aligned}
r_1^{(1)} &= 2\mu_1 \left(K_1^{(1)} K_8^{(1)} - K_2^{(1)} K_7^{(1)}\right) / \Delta_1, \\
r_2^{(1)} &= 2\mu_1 \left(-K_1^{(1)} K_6^{(1)} + K_2^{(1)} K_5^{(1)}\right) / \Delta_1, \\
r_3^{(1)} &= 2\mu_1 \left(K_3^{(1)} K_8^{(1)} - K_4^{(1)} K_7^{(1)}\right) / \Delta_1, \\
r_4^{(1)} &= 2\mu_1 \left(-K_3^{(1)} K_6^{(1)} + K_4^{(1)} K_5^{(1)}\right) / \Delta_1, \\
\Delta_1 &= K_5^{(1)} K_8^{(1)} - K_6^{(1)} K_7^{(1)}.
\end{aligned} \tag{C.1}
$$

Appendix D

$$
\begin{aligned}
L_2^{(1)} &= \left(K_8^{(1)} K_5^{(2)} - K_7^{(1)} K_6^{(2)}\right) / \Delta_1, \\
L_2^{(2)} &= \left(-K_6^{(1)} K_5^{(2)} + K_5^{(1)} K_6^{(2)}\right) / \Delta_1, \\
L_3^{(2)} &= \left(K_8^{(1)} K_7^{(2)} - K_7^{(1)} K_8^{(2)}\right) / \Delta_1, \\
L_4^{(2)} &= \left(-K_6^{(1)} K_7^{(2)} + K_5^{(1)} K_8^{(2)}\right) / \Delta_1,
\end{aligned} \tag{D.1}
$$

with

$$
\begin{aligned}
K_5^{(2)} &= -\xi f_9 + \gamma_{22} f_{11}, \qquad & K_6^{(2)} &= -\xi f_{10} + \gamma_{22} f_{12}, \\
K_7^{(2)} &= \gamma_{12} f_9 - \xi f_{11}, \qquad & K_8^{(2)} &= \gamma_{12} f_{10} - \xi f_{12}.
\end{aligned} \tag{D.2}
$$

Appendix E

$$
\begin{aligned}
Q_1(\xi) &= \{r_1^{(1)} L_2^{(2)} + r_2^{(1)} (1 - L_1^{(2)})\} / \Delta_2, \\
Q_2(\xi) &= -\{r_1^{(1)} (1 - L_4^{(2)}) + r_2^{(1)} L_3^{(2)}\} / \Delta_2, \\
Q_3(\xi) &= \{r_3^{(1)} L_2^{(2)} + r_4^{(1)} (1 - L_1^{(2)})\} / \Delta_2, \\
Q_4(\xi) &= -\{r_3^{(1)} (1 - L_4^{(2)}) + r_4^{(1)} L_3^{(2)}\} / \Delta_2,
\end{aligned} \tag{E.1}
$$

$$
\Delta_2 = (1 - L_1^{(2)})(1 - L_4^{(2)}) - L_2^{(2)} L_3^{(2)}. \tag{E.2}
$$

Appendix F

$$
\begin{aligned}
F_n(x) = 1/\pi \int_0^\infty & \{Q_1(\xi)/\xi - Q_1^L - Q_1^0/\xi\} J_n\{(b-a)\xi/2\} \\
& \times \Big\{\cos(n\pi/2)/2\Big[\sin\{(a+b+2x)\xi/2\} + \sin\{(a+b-2x)\xi/2\}\Big] \\
& - \sin(n\pi/2)/2\Big[\cos\{(a+b-2x)\xi/2\} + \cos\{(a+b+2x)\xi/2\}\Big]\Big\}\, d\xi \\
& + Q_1^L/\pi\{\cos(n\pi/2)/2(g_1+g_2) - \sin(n\pi/2)/2(g_3+g_4)\} \\
& + Q_1^0/\pi\{\cos(n\pi/2)/2(g_5+g_6) - \sin(n\pi/2)/2(g_7+g_8)\},
\end{aligned}
$$

$$
\begin{aligned}
G_n(x) = 1/\pi \int_0^\infty & \{Q_2(\xi)/\xi - Q_2^L - Q_2^0/\xi\} J_n\{(b-a)\xi/2\} \\
& \times \Big\{\cos(n\pi/2)/2\Big[\cos\{(a+b-2x)\xi/2\} + \cos\{(a+b+2x)\xi/2\}\Big] \\
& + \sin(n\pi/2)/2\Big[\sin\{(a+b+2x)\xi/2\} + \sin\{(a+b-2x)\xi/2\}\Big]\Big\}\, d\xi \\
& + Q_2^L/\pi\{\cos(n\pi/2)/2(g_3+g_4) + \sin(n\pi/2)/2(g_1+g_2)\} \\
& + Q_2^0/\pi\{\cos(n\pi/2)/2(g_7+g_8) + \sin(n\pi/2)/2(g_5+g_6)\},
\end{aligned}
$$

(F.1)

$$
\begin{aligned}
H_n(x) = 1/\pi \int_0^\infty & \{Q_3(\xi)/\xi - Q_3^L - Q_3^0/\xi\} J_n\{(b-a)\xi/2\} \\
& \times \Big\{\cos(n\pi/2)/2\Big[\cos\{(a+b-2x)\xi/2\} - \cos\{(a+b+2x)\xi/2\}\Big] \\
& - \sin(n\pi/2)/2\Big[\sin\{(a+b+2x)\xi/2\} - \sin\{(a+b-2x)\xi/2\}\Big]\Big\}\, d\xi \\
& + Q_3^L/\pi\{\cos(n\pi/2)/2(g_4-g_3) - \sin(n\pi/2)/2(g_1-g_2)\} \\
& + Q_3^0/\pi\{\cos(n\pi/2)/2(g_8-g_7) - \sin(n\pi/2)/2(g_5-g_6)\},
\end{aligned}
$$

$$
\begin{aligned}
I_n(x) = 1/\pi \int_0^\infty & \{Q_4(\xi)/\xi - Q_4^L - Q_4^0/\xi\} J_n\{(b-a)\xi/2\} \\
& \times \Big\{\cos(n\pi/2)/2\Big[\sin\{(a+b+2x)\xi/2\} - \sin\{(a+b-2x)\xi/2\}\Big] \\
& + \sin(n\pi/2)/2\Big[\cos\{(a+b-2x)\xi/2\} - \cos\{(a+b+2x)\xi/2\}\Big]\Big\}\, d\xi \\
& + Q_4^L/\pi\{\cos(n\pi/2)/2(g_1-g_2) + \sin(n\pi/2)/2(g_1-g_3)\} \\
& + Q_4^0/\pi\{\cos(n\pi/2)/2(g_5-g_6) + \sin(n\pi/2)/2(g_8-g_7)\}
\end{aligned}
$$

with

$$g_1 = \{(b-a)/2\}^n \cos(n\pi/2) / \left\{ \left[\{(a+b+2x)/2\}^2 - \{(b-a)/2\}^2 \right]^{1/2} \times \left[(a+b+2x)/2 + \left[\{(a+b+2x)/2\}^2 - \{(b-a)/2\}^2 \right]^{1/2} \right]^n \right\},$$

$$g_2 = \sin\left[n \sin^{-1}\{(a+b+2x)/(b-a)\} \right] / \left[\{(b-a)/2\}^2 - \{(a+b+2x)/2\}^2 \right]^{1/2},$$

$$g_3 = -\{(b-a)/2\}^n \sin(n\pi/2) / \left\{ \left[\{(a+b+2x)/2\}^2 - \{(b-a)/2\}^2 \right]^{1/2} \times \left[(a+b+2x)/2 + \left[\{(a+b+2x)/2\}^2 - \{(b-a)/2\}^2 \right]^{1/2} \right]^n \right\},$$

(F.2)

$$g_4 = \cos\left[n \sin^{-1}\{(a+b-2x)/(b-a)\} \right] / \left[\{(b-a)/2\}^2 - \{(a+b-2x)/2\}^2 \right]^{1/2},$$

$$g_5 = \{(b-a)/2\}^n \sin(n\pi/2) \Big/ \left\{ n \left[(a+b+2x)/2 + \left[\{(a+b+2x)/2\}^2 - \{(b-a)/2\}^2 \right]^{1/2} \right]^n \right\},$$

$$g_6 = \sin\left[n \sin^{-1}\{(a+b-2x)/(b-a)\} \right] / n,$$

$$g_7 = \{(b-a)/2\}^n \cos(n\pi/2) \Big/ \left\{ n \left[(a+b+2x)/2 + \left[\{(a+b+2x)/2\}^2 - \{(b-a)/2\}^2 \right]^{1/2} \right]^n \right\},$$

$$g_8 = \cos\left[n \sin^{-1}\{(a+b-2x)/(b-a)\} \right] / n.$$

References

1. *Stress intensity factors handbook*, Y. MURAKAMI [Ed.], vol. 1, 427–640, Pergamon Press, Oxford 1987.
2. H. NISITANI and D.H. CHEN, *Body force method* [in Japanese], Baifukan, 39–66, Tokyo 1987.
3. M. ISIDA and H. NOGUCHI, *Arbitrary array of cracks in bonded half-planes subjected to various loadings*, Engng. Fracture Mech., **46**, 365–380, 1993.
4. G.C. SIH and E.P. CHEN, *Normal and shear impact of layered composite with a crack: dynamic stress intensification*, ASME, J. Appl. Mech., **47**, 351–358, 1980.
5. G.C. SIH and E.P. CHEN, *Axisymmetric elastodynamic response from normal and radial impact of layered composites with an embedded penny-shaped crack*, Int. J. Solids Struct., **16**, 1093–1107, 1980.
6. W.T. ANG, *A crack in an anisotropic layered material under the action of impact loading*, ASME J. Appl. Mech., **55**, 120–125, 1988.
7. S. ITOU, *Dynamic stress intensity factors around a rectangular crack in an elastic layer sandwiched between two elastic half-spaces*, Arch. Mech., **44**, 231–241, 1992.

8. S. ITOU, *Dynamic stress intensity factors around two coplanar Griffith cracks in an orthotropic layer sandwiched between two elastic half-planes*, Engng. Fracture Mech., **34**, 1085–1095, 1989.
9. W.F. YAU, *Axisymmetric slipless indentation of an infinite elastic cylinder*, SIAM J. Appl. Math., **15**, 219–227, 1967.
10. M.K. MILLER and W.T. GUY, *Numerical inversion of the Laplace transform by use of Jacobi polynomials*, SIAM J. Num. Anal., **3**, 624–635, 1966.

DEPARTMENT OF MECHANICAL ENGINEERING
KANAGAWA UNIVERSITY, YOKOHAMA, JAPAN
and
DEPARTMENT OF MATHEMATICS AND MECHANICS
UNIVERSITY OF SCIENCE AND TECHNOLOGY BEIJING
XUEYUAN LU, BEIJING, P.R. CHINA.

Received April 18, 1994.

Arch. Mech., 46, 5, pp. 669–683, Warszawa 1994

Objective frame derivatives for the hyperstress and couple stress

B. SVENDSEN (DARMSTADT)

THIS WORK outlines a formulation of objective derivatives for tensors of arbitrary order in linear spaces based on the notions of a frame connection and the associated induced frame derivative. The general results are applied in particular to the formulation of such objective (frame) derivatives for the hyperstress and its associated forms appearing in general models of structured continua, as well as for the couple stress and its associated forms, appearing for example in the Cosserat model.

1. Introduction

THE FORMULATION of rate-type constitutive relations for the various higher-order tensors appearing in different structured media theories (e.g., Cosserat continua, continua with affine structure, polar continua, and so on) requires the use of some kind of "objective" derivative for these tensors in order to satisfy material objectivity. The purpose of this work is to formulate one such type of derivative for such tensors based on the notion of the connection and derivative induced by a time-dependent frame, as discussed in detail in SVENDSEN [1]. In particular, attention is focused in this work on applying this approach to the formulation of objective frame derivatives for the hyperstress and couple stress (e.g., TRUESDELL and NOLL [2, §98 and 127], MURDOCH [3], CAPRIZ [4]), i.e., the third-order tensors.

After briefly defining of the basic mathematical concepts and notation used in this work (Sec. 2), in particular those associated with frames (Sec. 3), the notion of a time-dependent frame, the connection of such a frame, as well as the induced frame derivative, as formulated in detail in SVENDSEN [1], are briefly summarized (Sec. 4). These results are then applied to the formulation of objective frame derivatives for the hyperstress and couple stress (Sec. 5). To facilitate understanding of these results, this frame-based approach is also used to derive the more familiar objective (frame) derivatives for the Cauchy stress, which can be directly compared to those for the hyperstress and couple stress. Finally, well-known special objective derivatives (e.g., Oldroyd) are obtained and discussed in the current frame-based context for the Cauchy stress, hyperstress and couple stress (Sec. 6).

2. Basic mathematical concepts and notation

Let $\mathcal{V}$ and $\mathcal{W}$ be *finite-dimensional* linear spaces, $\mathrm{Bij}(\mathcal{V},\mathcal{W})$ the set of all bijections, $\mathrm{Lin}(\mathcal{V},\mathcal{W})$ the set of all linear mappings, and $\mathrm{Lbj}(\mathcal{V},\mathcal{W}) := \mathrm{Lin}(\mathcal{V},\mathcal{W}) \cap$

$\mathrm{Bij}(\mathcal{V},\mathcal{W})$ the set of all linear bijections (sometimes denoted by $\mathrm{Lis}(\mathcal{V},\mathcal{W})$), between $\mathcal{V}$ and $\mathcal{W}$ (in this latter case, of course, $\dim(\mathcal{V}) = \dim(\mathcal{W})$). Any $\mathbf{L} \in \mathrm{Lis}(\mathcal{V},\mathcal{W})$ induces a dual (linear) mapping

$$\mathbf{L}^* : \mathcal{W}^* \to \mathcal{V}^* \mid \boldsymbol{\sigma} \mapsto \boldsymbol{\sigma}\mathbf{L} =: \mathbf{L}^*\boldsymbol{\sigma} \tag{2.1}$$

between the spaces $\mathcal{V}^* := \mathrm{Lin}(\mathcal{V},\mathbb{R})$ and $\mathcal{W}^* := \mathrm{Lin}(\mathcal{W},\mathbb{R})$ *dual* to $\mathcal{V}$ and $\mathcal{W}$, respectively.

The linear bijection $(\mathbf{v} \mapsto \imath_{\mathbf{v}}) \in \mathrm{Lbj}(\mathcal{V},\mathcal{V}^{**})$ defined by $\imath_{\mathbf{v}}\boldsymbol{\nu} := \boldsymbol{\nu}\mathbf{v}$ for all $\boldsymbol{\nu} \in \mathcal{V}^*$ allows us to *identify* each $\mathbf{v} \in \mathcal{V}$ with an element $\imath_{\mathbf{v}} \in \mathcal{V}^{**}$ of $\mathcal{V}^{**}$, and *vice-versa*. Such a *natural identification* (i.e., independent of any additional structure on the sets involved, e.g., a metric) of elements of one set with those of another one is signified by writing $\mathcal{V}^{**} \cong \mathcal{V}$ (i.e., $\imath_{\mathbf{v}} \cong \mathbf{v}$) in the case of $\mathcal{V}$. *Note that such identifications will often be used implicitly in this work.* In what follows, let $\mathrm{Sym}^+(\mathcal{V},\mathcal{V}^*) := \{\mathbf{M} \in \mathrm{Lin}(\mathcal{V},\mathcal{V}^*) \mid \mathbf{M}^* = \mathbf{M}\,\&\,(\mathbf{M}\mathbf{v})\mathbf{v} > 0\ \forall \mathbf{v} \in \mathcal{V}\backslash\{\mathbf{0}\}\}$ represent the set of all symmetric positive-definite linear mappings between $\mathcal{V}$ and $\mathcal{V}^*$.

Let $\mathcal{U}$ be a linear space. For any bilinear mapping $\boldsymbol{\mu} \in \mathrm{Lin}_2(\mathcal{U}\times\mathcal{V},\mathcal{W})$ or its linear form $\mathsf{L} \in \mathrm{Lin}(\mathcal{V},\mathrm{Lin}(\mathcal{U},\mathcal{W}))$, we define associated mappings $\boldsymbol{\mu}^s \in \mathrm{Lin}_2(\mathcal{V}\times\mathcal{U},\mathcal{W})$ and $\mathsf{L}^s \in \mathrm{Lin}(\mathcal{U},\mathrm{Lin}(\mathcal{V},\mathcal{W}))$ *via*

$$\boldsymbol{\mu}^s(\mathbf{v},\mathbf{u}) := \boldsymbol{\mu}(\mathbf{u},\mathbf{v}) \qquad \text{and} \qquad (\mathsf{L}^s\mathbf{u})\mathbf{v} := (\mathsf{L}\mathbf{v})\mathbf{u} \tag{2.2}$$

for all $\mathbf{u} \in \mathcal{U}$ and $\mathbf{v} \in \mathcal{V}$. Note that $(\mathsf{L}\mathbf{v})\mathbf{u} = \boldsymbol{\mu}(\mathbf{u},\mathbf{v})$, i.e., we are using the convention

$$\mathrm{Lin}(\mathcal{V}_n,\ldots,\mathrm{Lin}(\mathcal{V}_1,\mathcal{W})\ldots) \cong \mathrm{Lin}_n(\mathcal{V}_1\times\mathcal{V}_2\times\ldots\times\mathcal{V}_n,\mathcal{W}) \tag{2.3}$$

in this paper.

Usually the $\binom{p}{q}$ *tensors* (i.e., p-contravariant, q-covariant) on a linear space $\mathcal{V}$ are defined as elements of the set $\mathrm{Lin}_{p+q}(\mathcal{V}^{*p}\times\mathcal{V}^q,\mathbb{R})$ of all $(p+q)$-linear mappings

$$\boldsymbol{\mu} : \mathcal{V}^{*p}\times\mathcal{V}^q \to \mathbb{R} \mid (\boldsymbol{\nu}_1,\ldots,\boldsymbol{\nu}_p,\mathbf{v}_1,\ldots,\mathbf{v}_q) \mapsto a = \mu(\boldsymbol{\nu}_1,\ldots,\boldsymbol{\nu}_p,\mathbf{v}_1,\ldots,\mathbf{v}_q) \tag{2.4}$$

of $\mathcal{V}^{*p}\times\mathcal{V}^q$ (A^p denotes the p-fold Cartesian product of any set A with itself) into $\mathbb{R}$. Any linear bijection $\mathbf{L} \in \mathrm{Lbj}(\mathcal{V},\mathcal{W})$ induces one

$$\mathbf{t}_{\mathbf{L}} : \mathrm{Lin}_{p+q}(\mathcal{V}^{*p}\times\mathcal{V}^q,\mathbb{R}) \to \mathrm{Lin}_{p+q}(\mathcal{W}^{*p}\times\mathcal{W}^q,\mathbb{R}) \mid \mu \mapsto \mathbf{t}_{\mathbf{L}}\mu := \mathbf{t}_{\mathbf{L}}(\mu) \tag{2.5}$$

of $\mathcal{V}$ tensors to $\mathcal{W}$ tensors, defined by

$$(\mathbf{t}_{\mathbf{L}}\mu)(\boldsymbol{\eta}_1,\ldots,\boldsymbol{\eta}_p,\mathbf{w}_1,\ldots,\mathbf{w}_q) := \mu(\mathbf{L}^*\boldsymbol{\eta}_1,\ldots,\mathbf{L}^*\boldsymbol{\eta}_p,\mathbf{L}^{-1}\mathbf{w}_1,\ldots,\mathbf{L}^{-1}\mathbf{w}_q) \tag{2.6}$$

for all $\mu \in \mathrm{Lin}_{p+q}(\mathcal{V}^{*p} \times \mathcal{V}^q, \mathbb{R})$, $\boldsymbol{\eta}_1, \ldots, \boldsymbol{\eta}_p \in \mathcal{W}^*$ and $\mathbf{w}_1, \ldots, \mathbf{w}_q \in \mathcal{W}$. In particular, (2.6) implies $\mathbf{t}_{\mathbf{L}}\mathbf{v} = \mathbf{L}\mathbf{v} \quad \forall \mathbf{v} \in \mathcal{V} \cong \mathcal{V}^{**}$ and $\mathbf{t}_{\mathbf{L}}\boldsymbol{\nu} = \mathbf{L}^{-*}\boldsymbol{\nu} \; \forall \boldsymbol{\nu} \in \mathcal{V}^*$, where $\mathbf{L}^{-*} := \mathbf{L}^{-1*} = \mathbf{L}^{*-1} \in \mathrm{Lbj}(\mathcal{V}^*, \mathcal{W}^*)$. Further, $\mathbf{t}_{\mathbf{L}}^{-1} = \mathbf{t}_{\mathbf{L}^{-1}} \in \mathrm{Lbj}(\mathrm{Lin}_{p+q}(\mathcal{V}^{*p} \times \mathcal{W}^q, \mathbb{R}), \mathrm{Lin}_{p+q}(\mathcal{V}^{*p} \times \mathcal{V}^q, \mathbb{R}))$ for all $\mathbf{L} \in \mathrm{Lbj}(\mathcal{V}, \mathcal{W})$. All of the above results involving $\mathbf{t}$, as well as those to follow, hold of course for the special case $\mathcal{V} = \mathcal{W}$.

If $\dim(\mathcal{V}) = n$, the non-zero elements of the one-dimensional linear space $\mathrm{Skw}_n(\mathcal{V}^n, \mathbb{R})$ of all completely skew-symmetric n-multilinear mappings of $\mathcal{V}$ into $\mathbb{R}$ are called *volume convectors*. An equivalence class $[\omega] := \{\omega' \in \mathrm{Skw}_n(\mathcal{V}^n, \mathbb{R}) \mid \exists\, a > 0 \text{ such that } \omega' = a\omega\}$ of such volume covectors determines an *orientation* of $\mathcal{V}$. Since $\mathrm{Skw}_n(\mathcal{V}^n, \mathbb{R})$ is one-dimensional, there are two such orientations, i.e., $[\omega]$ and $[-\omega]$. By convention, the chosen orientation is called *positive*, and the other *negative*. A linear space $\mathcal{V}$ endowed with a given (i.e., fixed) orientation is called *oriented*. If $\mathcal{V}$ is oriented with orientation $[\omega]$, the *determinant* of any $\mathbf{L} \in \mathrm{Lin}(\mathcal{V}, \mathcal{V})$ is defined by

$$\det(\mathbf{L}) := \frac{\omega(\mathbf{L}\mathbf{v}_1, \ldots, \mathbf{L}\mathbf{v}_n)}{\omega(\mathbf{v}_1, \ldots, \mathbf{v}_n)} \tag{2.7}$$

for all linearly independent $\mathbf{v}_1, \ldots, \mathbf{v}_n \in \mathcal{V}$ and any $\omega \in [\omega]$. Note that (2.6) and (2.7) imply $\mathbf{t}_{\mathbf{L}}\omega = \det(\mathbf{L}^{-1})\omega$ for all $\mathbf{L} \in \mathrm{Lbj}(\mathcal{V}, \mathcal{V})$. For $\mathcal{V}$ and $\mathcal{W}$ oriented with orientations $[\omega_{\mathcal{V}}]$ and $[\omega_{\mathcal{W}}]$, respectively, and $\dim(\mathcal{V}) = \dim(\mathcal{W})$, any $\mathbf{L} \in \mathrm{Lbj}(\mathcal{V}, \mathcal{W})$ is called *orientation-preserving* if $(\mathbf{t}_{\mathbf{L}}\varpi) \in [\omega_{\mathcal{W}}]$ for any $\varpi \in [\omega_{\mathcal{V}}]$. Let $\mathrm{Lbj}^+(\mathcal{V}, \mathcal{W})$ represent the set of all such orientation-preserving linear bijections between two oriented linear spaces $\mathcal{V}$ and $\mathcal{W}$.

An *inner product space* is a linear space $\mathcal{V}$ endowed with the additional structure of a symmetric, positive-definite bilinear mapping $g \in \mathrm{Sym}_2^+(\mathcal{V}^2, \mathbb{R})$, referred to as a *metric* (on $\mathcal{V}$) in this work. On the basis of $g \in \mathrm{Sym}^+(\mathcal{V}^2, \mathbb{R})$, one defines in the usual way an *inner product*

$$\mathbf{v}_1 \cdot \mathbf{v}_2 := g(\mathbf{v}_1, \mathbf{v}_2) = (\mathbf{G}\mathbf{v}_2)\mathbf{v}_1 = (\mathbf{G}\mathbf{v}_1)\mathbf{v}_2 \tag{2.8}$$

of elements $\mathbf{v}_1, \mathbf{v}_2 \in \mathcal{V}$ of $\mathcal{V}$, where $\mathbf{G} \in \mathrm{Sym}^+(\mathcal{V}, \mathcal{V}^*)$ represents the linear form of $g \in \mathrm{Sym}_2^+(\mathcal{V}^2, \mathbb{R})$, and will also be referred to as a metric in this work. Any linear mapping $\mathbf{L} \in \mathrm{Lin}(\mathcal{V}, \mathcal{W})$ between two inner product spaces $\mathcal{V}$ and $\mathcal{W}$ with metrics $g_{\mathcal{V}} \in \mathrm{Sym}^+(\mathcal{V}^2, \mathbb{R})$ and $g_{\mathcal{W}} \in \mathrm{Sym}^+(\mathcal{W}^2, \mathbb{R})$, respectively, induces a linear mapping

$$\mathbf{L}^T := \mathbf{G}_{\mathcal{V}}^{-1}\mathbf{L}^*\mathbf{G}_{\mathcal{W}} \in \mathrm{Lin}(\mathcal{W}, \mathcal{V}), \tag{2.9}$$

called the *transpose* of $\mathbf{L} \in \mathrm{Lin}(\mathcal{V}, \mathcal{W})$. A linear mapping $\mathbf{Q} \in \mathrm{Lin}(\mathcal{V}, \mathcal{W})$ between two inner product spaces $\mathcal{V}$ and $\mathcal{W}$ is called *orthogonal* if

$$\mathbf{Q}^*\mathbf{G}_{\mathcal{W}}\mathbf{Q} = \mathbf{G}_{\mathcal{V}}. \tag{2.10}$$

As usual, let $\mathrm{Orth}(\mathcal{V}, \mathcal{W})$ denote the set of all such linear mappings. From the definition (2.9) of the transpose, it follows that $\mathbf{Q}^*\mathbf{G}_{\mathcal{W}}\mathbf{Q} = \mathbf{G}_{\mathcal{V}}\mathbf{Q}^T\mathbf{Q} = \mathbf{G}_{\mathcal{V}}$ for all

$\mathbf{Q} \in \mathrm{Orth}(\mathcal{V}, \mathcal{W})$, implying $\mathbf{Q}^T\mathbf{Q} = 1_{\mathcal{V}}$, and in particular $\mathbf{Q}^T = \mathbf{Q}^{-1}$ if $\dim(\mathcal{V}) = \dim(\mathcal{W})$. As usual, let

$$
\begin{aligned}
\mathrm{Sym}(\mathcal{V}, \mathcal{V}) &:= \left\{\mathbf{L} \in \mathrm{Lin}(\mathcal{V}, \mathcal{V}) \mid \mathbf{L}^T = \mathbf{L}\right\}, \\
\mathrm{Sym}^+(\mathcal{V}, \mathcal{V}) &:= \{\mathbf{L} \in \mathrm{Sym}(\mathcal{V}, \mathcal{V}) \mid (\mathbf{G}, \mathbf{L}) \in \mathrm{Sym}^+(\mathcal{V}, \mathcal{V}^*)\}, \\
\mathrm{Skw}(\mathcal{V}, \mathcal{V}) &:= \left\{\mathbf{L} \in \mathrm{Lin}(\mathcal{V}, \mathcal{V}) \mid \mathbf{L}^T = -\mathbf{L}\right\}, \\
\mathrm{Orth}^+(\mathcal{V}, \mathcal{V}) &:= \{\mathbf{L} \in \mathrm{Orth}(\mathcal{V}, \mathcal{V}) \mid \det(\mathbf{L}) = +1\},
\end{aligned}
\tag{2.11}
$$

denote the sets of all symmetric, symmetric positive-definite, skew-symmetric, and orientation-preserving orthogonal, linear mappings of $\mathcal{V}$ onto itself, respectively. We will also make use of symmetrization

$$
\mathrm{sym} : \mathrm{Lin}(\mathcal{V}, \mathcal{V}) \to \mathrm{Lin}(\mathcal{V}, \mathcal{V}) \quad | \quad \mathbf{L} \mapsto \frac{1}{2}(\mathbf{L} + \mathbf{L}^T) =: \mathrm{sym}(\mathbf{L}) \tag{2.12}
$$

and skew-symmetrization

$$
\mathrm{skw} : \mathrm{Lin}(\mathcal{V}, \mathcal{V}) \to \mathrm{Lin}(\mathcal{V}, \mathcal{V}) \quad | \quad \mathbf{L} \mapsto \frac{1}{2}(\mathbf{L} - \mathbf{L}^T) =: \mathrm{skw}(\mathbf{L}) \tag{2.13}
$$

operations in this paper.

Since $\dim(\mathcal{V}^*) = \dim(\mathcal{V})$ for finite-dimensional $\mathcal{V}$, the injective elements of $\mathrm{Lin}(\mathcal{V}, \mathcal{V}^*)$ are actually bijective; in particular, since the metric $\mathbf{G} \in \mathrm{Lin}(\mathcal{V}, \mathcal{V}^*)$ is injective by definition, $\mathbf{G} \in \mathrm{Lbj}(\mathcal{V}, \mathcal{V}^*)$ holds. The resulting linear bijections

$$
\mathbf{G} : \mathcal{V} \to \mathcal{V}^* \quad | \quad \mathbf{v} \mapsto \mathbf{G}\mathbf{v} := \mathbf{G}(\mathbf{v}) \tag{2.14}
$$

and

$$
\mathbf{G}^{-1} : \mathcal{V}^* \to \mathcal{V} \quad | \quad \boldsymbol{\nu} \mapsto \mathbf{G}^{-1}\boldsymbol{\nu} := \mathbf{G}^{-1}(\boldsymbol{\nu}) \tag{2.15}
$$

represent the basis of the operation of forming the *associated tensors* (e.g., ABRAHAM *et al.* [5, §5.1]), often called "lowering and raising indices", respectively. By linearity and duality, this operation can be extended to tensors of arbitrary order; indeed, a $(p + q)$ th-order tensor possesses $(p + q)! + 1$ associated forms. Being a linear bijection, the metric $\mathbf{G} \in \mathrm{Sym}^+(\mathcal{V}, \mathcal{V}^*)$ induces alternatively the natural identification $\mathcal{V}^* \cong \mathcal{V}$ (i.e., $\boldsymbol{\nu} \cong \mathbf{G}^{-1}\boldsymbol{\nu}$) or $\mathcal{V} \cong \mathcal{V}^*$ (i.e., $\mathbf{v} \cong \mathbf{G}\mathbf{v} = \mathbf{v}\,\cdot$). Perhaps the most well-known case of this in the literature is the identification or association $\mathbf{G} \cong \mathbf{I}$ of the metric $\mathbf{G}$ itself with the identity linear mapping $\mathbf{I} \in \mathrm{Lin}(\mathcal{V}, \mathcal{V})$ on $\mathcal{V}$, induced *via* $\mathbf{I} = \mathbf{G}\mathbf{G}^{-1}$ or $\mathbf{G} = \mathbf{G}\mathbf{I}$. Unfortunately, this fact has been too often interpreted in the literature to somehow mean that $\mathbf{G}$ and $\mathbf{I}$ are *equal*, something that is simply wrong; indeed, $\mathbf{G} \neq \mathbf{I}$ always holds. Rather than take advantage of $\mathcal{V}^* \cong \mathcal{V}$, as is usually done, we will deal *explicitly* with the associated forms of various tensors that arise naturally in this work.

In the text, we are of course particularly interested in the case when the inner product space $\mathcal{V}$ represents three-dimensional Euclidean vector space. In this case, the metric $\mathbf{G} \in \mathrm{Sym}^+(\mathcal{V}, \mathcal{V}^*)$ induces the compatible volume form

$$\omega_{\mathbf{G}}(\mathbf{v}_1, \mathbf{v}_2, \mathbf{v}_3) := (\mathbf{v}_1 \times \mathbf{v}_2) \cdot \mathbf{v}_3 = (\mathbf{G}(\mathbf{v}_1 \times \mathbf{v}_2))\mathbf{v}_3 \tag{2.16}$$

via (2.8) for all $\mathbf{v}_1, \mathbf{v}_2, \mathbf{v}_3 \in \mathcal{V}$, with $\times$ denoting the Euclidean vector cross-product. For all $\mathbf{Q} \in \mathrm{Orth}^+(\mathcal{V}, \mathcal{V})$, note that $\mathbf{G} = \mathbf{t}_{\mathbf{Q}}\mathbf{G}$ follows from (2.10), and $\mathbf{t}_{\mathbf{Q}}\omega_{\mathbf{G}} = \det(\mathbf{Q}^{-1})\omega_{\mathbf{G}} = \omega_{\mathbf{G}}$ from (2.6), (2.7) and (2.11). In addition, from (2.16), we have the expression

$$\mathbf{v}_1 \times \mathbf{v}_2 = \mathbf{G}^{-1}(\imath_{\mathbf{v}_2}\imath_{\mathbf{v}_1}\omega_{\mathbf{G}}) \tag{2.17}$$

for the Euclidean cross-product of any $\mathbf{v}_1, \mathbf{v}_2 \in \mathcal{V}$, where $\imath_{\mathbf{v}}\mu$ represents the *interior product* of $\mathbf{v} \in \mathcal{V}$ with $\mu \in \mathrm{Lin}_q(\mathcal{V}^q, R)$, defined by $(\imath_{\mathbf{v}}\mu)(\mathbf{v}_1, \ldots, \mathbf{v}_{q-1}) := \mu(\mathbf{v}, \mathbf{v}_1, \ldots, \mathbf{v}_{q-1})$ for all $\mathbf{v}, \mathbf{v}_1, \ldots, \mathbf{v}_{q-1} \in \mathcal{V}$.

3. Frames

Let $\mathcal{V}$ be an n-dimensional linear space and $\mathrm{Frm}\mathcal{V}$ the set of all *frames* of $\mathcal{V}$, i.e., *ordered bases* $\mathbf{b} := (\mathbf{b}_1, \ldots, \mathbf{b}_n) \in \mathrm{Frm}\mathcal{V}$ of $\mathcal{V}$. Of course, the case $n = 3$ is relevant to this work. Each such frame $\mathbf{b} \in \mathrm{Frm}\mathcal{V}$ induces a linear bijection.

$$\theta_{\mathbf{b}} : \mathcal{V} \to \mathbb{R}^n \mid \mathbf{v} \mapsto [\mathbf{v}]_{\mathbf{b}} = \theta_{\mathbf{b}}\mathbf{v}, \tag{3.1}$$

assigning any $\mathbf{v} \in \mathcal{V}$ the $\mathbb{R}^n$-vector $[\mathbf{v}]_{\mathbf{b}} \in \mathbb{R}^n$ of its components *relative to* $\mathbf{b} \in \mathrm{Frm}\mathcal{V}$. In this case, we have $\theta_{\mathbf{b}} \in \mathrm{Lbj}(\mathcal{V}, \mathbb{R}^n)$ and $k_{\mathbf{b}} := \theta_{\mathbf{b}}^{-1} \in \mathrm{Lbj}(\mathbb{R}^n, \mathcal{V})$, such that $k_{\mathbf{b}}\theta_{\mathbf{b}} = 1_{\mathcal{V}}$ and $\theta_{\mathbf{b}}k_{\mathbf{b}} = 1_{\mathbb{R}^n}$, for all $\mathbf{b} \in \mathrm{Frm}\mathcal{V}$. Clearly, any $\mathbf{b} \in \mathrm{Frm}\mathcal{V}$ can be represented *uniquely* by $\theta_{\mathbf{b}}$ or $k_{\mathbf{b}}$, constituting in essence the differential geometric representation of a frame (e.g., SPIVAK [6, V. II, Ch. 8]; see also NOLL [7, §15]), and the one used in this work. Note that any frame $\mathbf{b} \in \mathrm{Frm}\mathcal{V}$ and any linear bijection $\mathbf{L} \in \mathrm{Lbj}(\mathcal{V}, \mathcal{W})$ induce a frame $\mathbf{Lb} := (\mathbf{Lb}_1, \ldots, \mathbf{Lb}_n) \in \mathrm{Frm}\mathcal{W}$ of $\mathcal{W}$, as well as the transformations

$$k_{\mathbf{Lb}} = \mathbf{L}k_{\mathbf{b}}, \qquad \theta_{\mathbf{Lb}} = \theta_{\mathbf{b}}\mathbf{L}^{-1}, \tag{3.2}$$

which we will also use in what follows.

By linearity and duality, (3.1) and its inverse induce the linear bijection

$$\Theta_{\mathbf{b}} : \mathrm{Lin}_{p+q}(\mathcal{V}^{*p} \times \mathcal{V}^q, \mathbb{R}) \to \mathrm{Lin}_{p+q}((\mathbb{R}^{n*})^p \times (\mathbb{R}^n)^q, \mathbb{R}) \mid \mu \mapsto [\mu]_{\mathbf{b}} := \Theta_{\mathbf{b}}\mu, \tag{3.3}$$

defined by $\Theta_{\mathbf{b}} := \mathbf{t}_{\theta_{\mathbf{b}}}$ *via* (2.5) with $\mathcal{W} = \mathbb{R}^n$ for all $\mathbf{b} \in \mathrm{Frm}\mathcal{V}$, i.e.,

$$(\Theta_{\mathbf{b}}\mu)(\nu_1, \ldots, \nu_p, v_1, \ldots, v_q) := \mu(\theta_{\mathbf{b}}^*\nu_1, \ldots, \theta_{\mathbf{b}}^*\nu_p, k_{\mathbf{b}}v_1, \ldots, k_{\mathbf{b}}v_q) \tag{3.4}$$

for all $\mu \in \mathrm{Lin}_{p+q}(\mathcal{V}^{*p} \times \mathcal{V}^q, \mathbb{R})$, $v_1, \ldots, v_p \in \mathbb{R}^n$ and $\nu_1, \ldots, \nu_q \in \mathbb{R}^{n*}$. The $\binom{p}{q}$ $\mathbb{R}^n$ tensor $[\mu]_{\mathbf{b}} \in \mathrm{Lin}_{p+q}((\mathbb{R}^{n*})^p \times (\mathbb{R}^n)^q, \mathbb{R})$ represents then the "components" of $\mu \in \mathrm{Lin}_{p+q}(\mathcal{V}^{*p} \times \mathcal{V}^q, \mathbb{R})$ *relative to* $\mathbf{b} \in \mathrm{Frm}\mathcal{V}$. Note that the dual form of the $\mathbf{b}$-induced linear bijection $k_{\mathbf{b}} \in \mathrm{Lbj}(\mathbb{R}^n, \mathcal{V})$, i.e.,

$$k_{\mathbf{b}}^* : \mathcal{V}^* \to \mathbb{R}^{n*} \,|\boldsymbol{\nu} \mapsto [\boldsymbol{\nu}]_{\mathbf{b}} := k_{\mathbf{b}}^* \boldsymbol{\nu} \tag{3.5}$$

assigns any $\boldsymbol{\nu} \in \mathcal{V}^*$ the $\mathbb{R}^{n*}$-vector $[\boldsymbol{\nu}]_{\mathbf{b}} \in \mathbb{R}^{n*}$ ($\cong \mathbb{R}^n$) of its components *relative to* $\mathbf{b} \in \mathrm{Frm}\mathcal{V}$. In addition, we have $k_{\mathbf{b}}^* \in \mathrm{Lbj}(\mathcal{V}^*, \mathbb{R}^{n*})$ and $\theta_{\mathbf{b}}^* \in \mathrm{Lbj}(\mathbb{R}^{n*}, \mathcal{V}^*)$, such that $k_{\mathbf{b}}^* \theta_{\mathbf{b}}^* = 1_{\mathbb{R}^{n*}}$ and $\theta_{\mathbf{b}}^* k_{\mathbf{b}}^* = 1_{\mathcal{V}^*}$ for all $\mathbf{b} \in \mathrm{Frm}\mathcal{V}$. Letting $k_{\mathbf{b}} := \mathbf{t}_{k_{\mathbf{b}}}$ denote the inverse of $\Theta_{\mathbf{b}}$ *via* (2.5) with $\mathcal{V} = \mathbb{R}^n$ and $\mathcal{W} = \mathcal{V}$ for all $\mathbf{b} \in \mathrm{Frm}\mathcal{V}$, we have $k_{\mathbf{b}} \Theta_{\mathbf{b}} = 1_{\mathrm{Lin}_{p+q}(\mathcal{V}^{*p} \times \mathcal{V}^q, \mathbb{R})}$ and $\Theta_{\mathbf{b}} k_{\mathbf{b}} = 1_{\mathrm{Lin}_{p+q}((\mathbb{R}^{n*})^p \times (\mathbb{R}^n)^q, \mathbb{R})}$.

4. Time-dependent frame, frame connection and derivative

A *time-dependent frame* on an n-dimensional linear space $\mathcal{V}$ consists of n time-dependent C^r ($r \geq 1$) basis vectors $\mathbf{r}_i \in C^r(I, \mathcal{V})$, $i = 1, \ldots, n$, with $I \subset \mathbb{R}$ a time interval. Let $\mathbf{r} := (\mathbf{r}_1, \ldots, \mathbf{r}_n) \in C^r(I, \mathrm{Frm}\mathcal{V})$ denote the corresponding frame. Similarly to its constant counterpart, each such frame $\mathbf{r} \in C^r(I, \mathrm{Frm}\mathcal{V})$ induces the mappings $k_{\mathbf{r}} \in C^r(I, \mathrm{Lbj}(\mathbb{R}^n, \mathcal{V}))$ and $\theta_{\mathbf{r}} \in C^r(I, \mathrm{Lbj}(\mathcal{V}, \mathbb{R}^n))$ such that

$$k_{\mathbf{r}} \theta_{\mathbf{r}} = k_{\mathbf{r}} k_{\mathbf{r}}^{-1} : I \to \mathrm{Lbj}(\mathcal{V}, \mathcal{V}) \quad | \quad t \mapsto 1_{\mathcal{V}} = k_{\mathbf{r}}(t) \theta_{\mathbf{r}}(t) \tag{4.1}$$

and

$$\theta_{\mathbf{r}} k_{\mathbf{r}} = k_{\mathbf{r}}^{-1} k_{\mathbf{r}} : I \to \mathrm{Lbj}(\mathbb{R}^n, \mathbb{R}^n) \quad | \quad t \mapsto 1_{\mathbb{R}^n} = \theta_{\mathbf{r}}(t) k_{\mathbf{r}}(t) \tag{4.2}$$

are *constant* maps, i.e., $(k_{\mathbf{r}} \theta_{\mathbf{r}})[I] = \{1_{\mathcal{V}}\}$ and $(\theta_{\mathbf{r}} k_{\mathbf{r}})[I] = \{1_{\mathbb{R}^n}\}$. Taking the time derivative of either of these two last relations, we obtain

$$\theta_{\mathbf{r}}(\delta k_{\mathbf{r}}) = -(\delta \theta_{\mathbf{r}}) k_{\mathbf{r}}. \tag{4.3}$$

Introducing the time-dependent curve

$$\boldsymbol{\Gamma}_{\mathbf{r}} := (\delta k_{\mathbf{r}}) \theta_{\mathbf{r}} = (\delta k_{\mathbf{r}}) k_{\mathbf{r}}^{-1} \in C^{r-1}(I, \mathrm{Lin}(\mathcal{V}, \mathcal{V})), \tag{4.4}$$

we have

$$\delta k_{\mathbf{r}} = \boldsymbol{\Gamma}_{\mathbf{r}} k_{\mathbf{r}}, \tag{4.5}$$

as well as

$$(\delta \theta_{\mathbf{r}}) = -\theta_{\mathbf{r}} \boldsymbol{\Gamma}_{\mathbf{r}} \tag{4.6}$$

from (4.3). Since $\delta \mathbf{r}_i = \delta(k_\mathbf{r} e_i) = \mathbf{\Gamma}_\mathbf{r} \mathbf{r}_i$ follows from (4.5) for $i = 1, \ldots, n$, $\mathbf{\Gamma}_\mathbf{r}$ represents a *linear connection* for the time-dependent frame $\mathbf{r} \in C^r(I, \mathrm{Frm}\mathcal{V})$. To show how this connection transforms under a change of frame, let $\mathcal{W}$ be a linear space and $\mathbf{Z} \in C^r(I, \mathrm{Lbj}(\mathcal{V}, \mathcal{W}))$ a C^r curve in $\mathrm{Lbj}(\mathcal{V}, \mathcal{W})$; then $\mathbf{Zr} := (\mathbf{Zr}_1, \ldots, \mathbf{Zr}_n) \in C^r(I, \mathrm{Frm}\mathcal{W})$ is a time-dependent frame on $\mathcal{W}$ for all $\mathbf{r} \in C^r(I, \mathrm{Frm}\mathcal{V})$. In this case,

$$k_{\mathbf{Zr}} = \mathbf{Z} k_\mathbf{r} \tag{4.7}$$

holds according to $(3.2)_1$. Taking the time derivative of (4.7) we obtain

$$\delta k_{\mathbf{Zr}} = (\delta \mathbf{Z}) k_\mathbf{r} + \mathbf{Z}(\delta k_\mathbf{r}). \tag{4.8}$$

Substituting (4.5) for $\mathbf{r}$ and $\mathbf{Zr}$ into (4.8), and using (4.7), we have

$$\mathbf{\Gamma}_{\mathbf{Zr}} = (\delta \mathbf{Z}) \mathbf{Z}^{-1} + \mathbf{Z} \mathbf{\Gamma}_\mathbf{r} \mathbf{Z}^{-1}. \tag{4.9}$$

The result (4.9) represents the transformation of the $\mathbf{r}$-connection to the $\mathbf{Zr}$-connection, and has the same form as that for the *Cartan connection* (e.g., SPIVAK [6], V. 2, Ch. 7-8]) of a "moving" frame.

On the basis of the connection and induced "parallel-transport" of a time-dependent frame, a type of covariant (time) derivative of any time-dependent tensor *relative to* a frame can be defined; such a derivative will be called a *frame derivative* in this paper. Logically, this derivative represents the time-rate of change of the quantity in question *relative to* the correspondent frame. A mathematical formulation of this derivative can be found in SVENDSEN [1, §7]. In particular, the frame derivative of a time-dependent $\binom{p}{q}$ tensor $\mu \in C^k(I, \mathrm{Lin}_{p+q}(\mathcal{V}^{*p} \times \mathcal{V}^q, \mathbb{R}))$ with respect to the time-dependent frame $\mathbf{r}$ is given by

$$\begin{aligned}(\delta_\mathbf{r}\mu)(\boldsymbol{\nu}_1, \ldots, \boldsymbol{\nu}_p, \mathbf{v}_1, \ldots, \mathbf{v}_q) = {} & (\delta\mu)(\boldsymbol{\nu}_1, \ldots, \boldsymbol{\nu}_p, \mathbf{v}_1, \ldots, \mathbf{v}_q) \\ & -\mu(\mathbf{\Gamma}_\mathbf{r}^* \boldsymbol{\nu}_1, \ldots, \boldsymbol{\nu}_p, \mathbf{v}_1, \ldots, \mathbf{v}_q) \\ & \vdots \\ & +\mu(\boldsymbol{\nu}_1, \ldots, \boldsymbol{\nu}_p, \mathbf{v}_1, \ldots, \mathbf{\Gamma}_\mathbf{r} \mathbf{v}_q)\end{aligned} \tag{4.10}$$

(SVENDSEN [1, (4.24)]), where

$$\delta_\mathbf{r}\mu := \mathcal{K}_\mathbf{r}[\delta(\Theta_\mathbf{r}\mu)] = \{\mathcal{K}_\mathbf{r} \circ \delta \circ \Theta_\mathbf{r}\}\mu \tag{4.11}$$

represents the frame derivative operator with respect to $\mathbf{r}$, such that

$$\begin{aligned}\delta_\mathbf{r} = \mathcal{K}_\mathbf{r} \circ \delta \circ \Theta_\mathbf{r} : {} & C^k(I, \mathrm{Lin}_{p+q}(\mathcal{V}^{*p} \times \mathcal{V}^q, \mathbb{R})) \to \\ & C^{k-1}(I, \mathrm{Lin}_{p+q}(\mathcal{V}^{*p} \times \mathcal{V}^q, \mathbb{R})),\end{aligned} \tag{4.12}$$

and

$$\Theta_{\mathbf{r}} \circ \delta_{\mathbf{r}} = \delta \circ \Theta_{\mathbf{r}} \tag{4.13}$$

such that $\Theta_{\mathbf{r}}(\delta_{\mathbf{r}}\mu) = \delta(\Theta_{\mathbf{r}}\mu)$ for all $\mu \in C^k(I, \mathrm{Lin}_{p+q}(\mathcal{V}^{*p} \times \mathcal{V}^q, \mathbb{R}))$. Note that a time-dependent tensor $\mu \in C^k(I, \mathrm{Lin}_{p+q}(\mathcal{V}^{*p} \times \mathcal{V}^q, \mathbb{R}))$ is *parallel-transported in time by* $\mathbf{r}$ (i.e., constant in time with respect to $\mathbf{r}$) iff $\delta_{\mathbf{r}}\mu$ vanishes.

As shown in detail in SVENDSEN [1, §8], the frame derivative operator $\delta_{\mathbf{r}}$ transforms *tensorially* under the "action" of any $\mathbf{Z} \in C^r(I, \mathrm{Lbj}(\mathcal{W}, \mathcal{U}))$ on any time-dependent $\binom{p}{q}$ tensor $\mu \in C^k(I, \mathrm{Lin}_{p+q}(\mathcal{W}^p \times \mathcal{W}^{*q}, \mathbb{R}))$ as defined in (2.5), i.e.,

$$\delta_{\mathbf{Zr}}(\mathbf{t}_{\mathbf{Z}}\mu) = \mathbf{t}_{\mathbf{Z}}(\delta_{\mathbf{r}}\mu). \tag{4.14}$$

Last result takes the operator form

$$\delta_{\mathbf{Zr}} \circ \mathbf{t}_{\mathbf{Z}} = \mathbf{t}_{\mathbf{Z}} \circ \delta_{\mathbf{r}} \quad \Rightarrow \quad \delta_{\mathbf{Zr}} = \mathbf{t}_{\mathbf{Z}} \circ \delta_{\mathbf{r}} \circ \mathbf{t}_{\mathbf{Z}^{-1}}, \tag{4.15}$$

which holds on the basis of (4.9) for all time-dependent frames $\mathbf{r}$ and all $\mathbf{Z} \in C^r(I, \mathrm{Lbj}(\mathcal{W}, \mathcal{U}))$. It is because of this property that frame derivatives are "objective", meaning that they transform *tensorially* under the action of any $\mathbf{Z} \in C^r(I, \mathrm{Lbj}(\mathcal{W}, \mathcal{U}))$, in fact in the same fashion as the corresponding tensors themselves, as shown in (4.14).

5. Frame derivatives for the Cauchy stress and hyperstress

The main goal of this section is to derive the frame derivatives for the hyperstress and some of its associated forms using the general result (4.10) for the frame derivative of a $\binom{p}{q}$ time-dependent tensor. To motivate the frame derivatives of the hyperstress so obtained, it is useful to derive in parallel the corresponding expressions for the frame derivatives of the Cauchy stress, which correspond to well-known "objective" derivatives of $\mathbf{T}$ found in the literature (e.g., MARSDEN and HUGHES [8, §1.6]).

Let E represent three-dimensional Euclidean point space, $\mathcal{V}$ the corresponding Euclidean vector space with metric $\mathbf{G} \in \mathrm{Sym}^+(\mathcal{V}, \mathcal{V}^*)$ and compatible volume form $\omega_{\mathbf{G}} \in \mathrm{Skw}_3(\mathcal{V}^3, \mathbb{R})$, and $B \subset E$ a reference configuration of some material body in E. Further, let $\mathbf{F} : I \to \mathrm{Lbj}^+(\mathcal{V}, \mathcal{V})$ be the deformation gradient at a material point with reference location $b \in B$ associated with a motion of the material body relative to B during the time interval $I \subset \mathbb{R}$, $\mathbf{T} : I \to \mathrm{Lin}(\mathcal{V}, \mathcal{V})$ the corresponding Cauchy stress tensor, and $\mathsf{H} : I \to \mathrm{Lin}(\mathcal{V}, \mathrm{Lin}(\mathcal{V}, \mathcal{V}))$ the corresponding hyperstress tensor (see, e.g., TRUESDELL and NOLL [2, §98]), which are defined as follows. For any two tangent vectors $\mathbf{u}, \mathbf{v} \in \mathcal{V}$ (i.e., "line elements")

in the reference configuration B at $b \in B$, $\mathbf{n}da := (\mathbf{Fu}) \times (\mathbf{Fv}) = \mathbf{G}^{-1}(\imath_{\mathbf{Fv}}\imath_{\mathbf{Fu}}\omega_{\mathbf{G}})$ represents the deformed area element (see (3.7)) with unit normal $\mathbf{n}$. In terms of this area element, the standard spatial contact force element takes the form

$$\mathbf{T}\mathbf{n}\,da = \mathbf{T}[(\mathbf{Fu}) \times (\mathbf{Fv})] = (\mathbf{TG}^{-1})(\imath_{\mathbf{Fv}}\imath_{\mathbf{Fu}}\omega_{\mathbf{G}}), \tag{5.1}$$

in which appears an associated form $\mathbf{TG}^{-1} : I \to \mathrm{Lin}(\mathcal{V}^*, \mathcal{V})$ of $\mathbf{T}$. Analogously, the quantity

$$\mathsf{H}\mathbf{n}\,da = \mathsf{H}[(\mathbf{Fu}) \times (\mathbf{Fv})] = (\mathsf{HG}^{-1})(\imath_{\mathbf{Fv}}\imath_{\mathbf{Fu}}\omega_{\mathbf{G}}) \tag{5.2}$$

represents a spatial contact force moment element, where $\mathsf{HG}^{-1} : I \to \mathrm{Lin}(\mathcal{V}^*, \mathrm{Lin}(\mathcal{V}, \mathcal{V}))$ represents an associated form of H. In total, $\mathbf{T}$ possesses three associated forms (i.e., $2! + 1$: $\mathbf{TG}^{-1}$, $\mathbf{GT}$ and $\mathbf{GTG}^{-1}$), and H – seven forms (i.e., $3! + 1$). In this work, attention is confined to the two most common associated forms of each tensor; frame derivatives for the other forms can easily be obtained using the approach presented in this paper.

Analogously to the associated form $\mathbf{TG}^{-1} : I \to \mathrm{Lin}(\mathcal{V}^*, \mathcal{V})$ of the Cauchy stress, we have the associated form $\mathsf{H}_{\mathbf{G}^{-1}} : I \to \mathrm{Lin}(\mathcal{V}^*, \mathrm{Lin}(\mathcal{V}^*, \mathcal{V}))$ of the generalized moment of momentum flux, defined by

$$(\mathsf{H}_{\mathbf{G}^{-1}}\boldsymbol{\nu}_2)\boldsymbol{\nu}_1 := (\mathsf{HG}^{-1}\boldsymbol{\nu}_2)(\mathbf{G}^{-1}\boldsymbol{\nu}_1) \tag{5.3}$$

for all $\boldsymbol{\nu}_1, \boldsymbol{\nu}_2 \in \mathcal{V}^*$. In a similar fashion, the associated form $\mathsf{H}_{\mathbf{G}} : I \to \mathrm{Lin}(\mathcal{V}, \mathrm{Lin}(\mathcal{V}, \mathcal{V}^*))$ of H, defined by

$$(\mathsf{H}_{\mathbf{G}}\mathbf{v}_2)\mathbf{v}_1 := \mathbf{G}((\mathsf{H}\mathbf{v}_2)\mathbf{v}_1) \tag{5.4}$$

for all $\mathbf{v}_1, \mathbf{v}_2 \in \mathcal{V}$, is analogous to the associated form $\mathbf{GT} : I \to \mathrm{Lin}(\mathcal{V}, \mathcal{V}^*)$ of the Cauchy stress. The results to be obtained in what follows for the frame derivative of H and its associated forms apply as well to the "symmetric" and "skew-symmetric" parts of H, i.e., $\mathrm{sym}\mathsf{H} : I \to \mathrm{Lin}(\mathcal{V}, \mathrm{Sym}(\mathcal{V}, \mathcal{V}))$ and $\mathrm{skw}\,\mathsf{H} : I \to \mathrm{Lin}(\mathcal{V}, \mathrm{Skw}(\mathcal{V}, \mathcal{V}))$, respectively, defined by $(\mathrm{sym}\mathsf{H})\mathbf{v} := \mathrm{sym}(\mathsf{H}\mathbf{v})$ and $(\mathrm{skw}\mathsf{H})\mathbf{v} := \mathrm{skw}(\mathsf{H}\mathbf{v})$ for all $\mathbf{v} \in \mathcal{V}$. Note that $\mathsf{M} := \mathrm{skw}\mathsf{H}$ is usually referred to as the couple-stress (e.g., TRUESDELL and NOLL [2, §98]).

Now, since $\mathrm{Lin}(\mathcal{V}^*, \mathcal{V}) \cong \mathrm{Lin}_2(\mathcal{V}^{*2}, \mathbb{R})$, $\mathbf{TG}^{-1}$ can be naturally identified with a $\binom{2}{0}$ tensor $\sigma_{\mathbf{G}^{-1}} : I \to \mathrm{Lin}_2(\mathcal{V}^{*2}, \mathbb{R})$ defined by

$$\sigma_{\mathbf{G}^{-1}}(\boldsymbol{\nu}_1, \boldsymbol{\nu}_2) := \imath_{(\mathbf{TG}^{-1})\boldsymbol{\nu}_2}\boldsymbol{\nu}_1 = \boldsymbol{\nu}_1(\mathbf{TG}^{-1}\boldsymbol{\nu}_2) \tag{5.5}$$

for all $\boldsymbol{\nu}_1, \boldsymbol{\nu}_2 \in \mathcal{V}^*$; likewise, the identification $\mathrm{Lin}(\mathcal{V}^*, \mathrm{Lin}(\mathcal{V}^*, \mathcal{V})) \cong \mathrm{Lin}_2(\mathcal{V}^{*2}, \mathcal{V}) \cong \mathrm{Lin}_3(\mathcal{V}^{*3}, \mathbb{R})$ implies that $\mathsf{H}_{\mathbf{G}^{-1}}$ can be identified with a $\binom{3}{0}$ tensor $h_{\mathbf{G}^{-1}} : I \to \mathrm{Lin}_3(\mathcal{V}^{*3}, \mathbb{R})$ *via*

$$h_{\mathbf{G}^{-1}}(\boldsymbol{\nu}_1, \boldsymbol{\nu}_2, \boldsymbol{\nu}_3) := \imath_{(\mathsf{H}_{\mathbf{G}^{-1}}\boldsymbol{\nu}_3)\boldsymbol{\nu}_2}\boldsymbol{\nu}_1 := \boldsymbol{\nu}_1((\mathsf{H}_{\mathbf{G}^{-1}}\boldsymbol{\nu}_3)\boldsymbol{\nu}_2) \tag{5.6}$$

for all $\boldsymbol{\nu}_1, \boldsymbol{\nu}_2, \boldsymbol{\nu}_3 \in \mathcal{V}^*$. In a similar fashion, $\mathrm{Lin}(\mathcal{V}, \mathcal{V}) \cong \mathrm{Lin}_2(\mathcal{V}^* \times \mathcal{V}, \mathbb{R})$ and $\mathrm{Lin}(\mathcal{V}, \mathrm{Lin}(\mathcal{V}, \mathcal{V})) \cong \mathrm{Lin}_2(\mathcal{V}^2, \mathcal{V}) \cong \mathrm{Lin}_3(\mathcal{V}^* \times \mathcal{V}^2, \mathbb{R})$ imply the existence of the $\binom{1}{1}$ tensor $\sigma : I \to \mathrm{Lin}_2(\mathcal{V}^* \times \mathcal{V}, \mathbb{R})$ and $\binom{1}{2}$ tensor $h : I \to \mathrm{Lin}_3(\mathcal{V}^* \times \mathcal{V}^2, \mathbb{R})$, respectively, defined by

$$\sigma(\boldsymbol{\nu}, \mathbf{v}) := \imath_{\mathbf{T}\mathbf{v}}\boldsymbol{\nu} = \boldsymbol{\nu}(\mathbf{T}\mathbf{v}) \tag{5.7}$$

and

$$h(\boldsymbol{\nu}, \mathbf{v}_1, \mathbf{v}_2) := \imath_{(\mathbf{H}\mathbf{v}_2)\mathbf{v}_1}\boldsymbol{\nu} = \boldsymbol{\nu}((\mathbf{H}\mathbf{v}_2)\mathbf{v}_1), \tag{5.8}$$

respectively, for all $\boldsymbol{\nu} \in \mathcal{V}^*$ and $\mathbf{v}_1, \mathbf{v}_2 \in \mathcal{V}$. Lastly, $\mathrm{Lin}(\mathcal{V}, \mathcal{V}^*) \cong \mathrm{Lin}_2(\mathcal{V}^2, \mathbb{R})$ and $\mathrm{Lin}(\mathcal{V}, \mathrm{Lin}(\mathcal{V}, \mathcal{V}^*)) \cong \mathrm{Lin}_2(\mathcal{V}^2, \mathcal{V}^*) \cong \mathrm{Lin}_3(\mathcal{V}^3, \mathbb{R})$ imply the existence of the $\binom{0}{2}$ tensor $\sigma_{\mathbf{G}} : I \to \mathrm{Lin}_2(\mathcal{V}^2, \mathbb{R})$ and $\binom{0}{3}$ tensor $h_{\mathbf{G}} : I \to \mathrm{Lin}_3(\mathcal{V}^3, \mathbb{R})$, defined by

$$\sigma_{\mathbf{G}}(\mathbf{v}_1, \mathbf{v}_2) := ((\mathbf{G}\mathbf{T})\mathbf{v}_2)\mathbf{v}_1 = (\mathbf{T}\mathbf{v}_2) \cdot \mathbf{v}_1 \tag{5.9}$$

and

$$h_{\mathbf{G}}(\mathbf{v}_1, \mathbf{v}_2, \mathbf{v}_3) := ((\mathbf{H}_{\mathbf{G}}\mathbf{v}_3)\mathbf{v}_2)\mathbf{v}_1 = ((\mathbf{H}\mathbf{v}_3)\mathbf{v}_2) \cdot \mathbf{v}_1, \tag{5.10}$$

respectively, for all $\mathbf{v}_1, \mathbf{v}_2, \mathbf{v}_3 \in \mathcal{V}$.

Let $\mathbf{r} : I \to \mathrm{Frm}\mathcal{V}$ be any differentiable time-dependent frame. From the general result (4.10), we have then

$$\begin{aligned}
(\delta_{\mathbf{r}}\sigma_{\mathbf{G}^{-1}})(\boldsymbol{\nu}_1, \boldsymbol{\nu}_2) &= (\delta\sigma_{\mathbf{G}^{-1}})(\boldsymbol{\nu}_1, \boldsymbol{\nu}_2) - \sigma_{\mathbf{G}^{-1}}(\boldsymbol{\Gamma}_{\mathbf{r}}^*\boldsymbol{\nu}_1, \boldsymbol{\nu}_2) - \sigma_{\mathbf{G}^{-1}}(\boldsymbol{\nu}_1, \boldsymbol{\Gamma}_{\mathbf{r}}^*\boldsymbol{\nu}_2), \\
(\delta_{\mathbf{r}}\sigma)(\boldsymbol{\nu}, \mathbf{v}) &= (\delta\sigma)(\boldsymbol{\nu}, \mathbf{v}) - \sigma(\boldsymbol{\Gamma}_{\mathbf{r}}^*\boldsymbol{\nu}, \mathbf{v}) + \sigma(\boldsymbol{\nu}, \boldsymbol{\Gamma}_{\mathbf{r}}\mathbf{v}), \\
(\delta_{\mathbf{r}}\sigma_{\mathbf{G}})(\mathbf{v}_1, \mathbf{v}_2) &= (\delta\sigma_{\mathbf{G}})(\mathbf{v}_1, \mathbf{v}_2) + \sigma_{\mathbf{G}}(\boldsymbol{\Gamma}_{\mathbf{r}}\mathbf{v}_1, \mathbf{v}_2) + \sigma_{\mathbf{G}}(\mathbf{v}_1, \boldsymbol{\Gamma}_{\mathbf{r}}\mathbf{v}_2),
\end{aligned} \tag{5.11}$$

for the frame derivatives of the Cauchy stress and its two associated forms, as well as those

$$\begin{aligned}
(\delta_{\mathbf{r}}h_{\mathbf{G}^{-1}})(\boldsymbol{\nu}_1, \boldsymbol{\nu}_2, \boldsymbol{\nu}_3) &= (\delta h_{\mathbf{G}^{-1}})(\boldsymbol{\nu}_1, \boldsymbol{\nu}_2, \boldsymbol{\nu}_3) - h_{\mathbf{G}^{-1}}(\boldsymbol{\Gamma}_{\mathbf{r}}^*\boldsymbol{\nu}_1, \boldsymbol{\nu}_2, \boldsymbol{\nu}_3) \\
&\quad - h_{\mathbf{G}^{-1}}(\boldsymbol{\nu}_1, \boldsymbol{\Gamma}_{\mathbf{r}}^*\boldsymbol{\nu}_2, \boldsymbol{\nu}_3) - h_{\mathbf{G}^{-1}}(\boldsymbol{\nu}_1, \boldsymbol{\nu}_2, \boldsymbol{\Gamma}_{\mathbf{r}}^*\boldsymbol{\nu}_3), \\
(\delta_{\mathbf{r}}h)(\boldsymbol{\nu}, \mathbf{v}_1, \mathbf{v}_2) &= (\delta h)(\boldsymbol{\nu}, \mathbf{v}_1, \mathbf{v}_2) - h(\boldsymbol{\Gamma}_{\mathbf{r}}^*\boldsymbol{\nu}, \mathbf{v}_1, \mathbf{v}_2) \\
&\quad + h(\boldsymbol{\nu}, \boldsymbol{\Gamma}_{\mathbf{r}}\mathbf{v}_1, \mathbf{v}_2) + h(\boldsymbol{\nu}, \mathbf{v}_1, \boldsymbol{\Gamma}_{\mathbf{r}}\mathbf{v}_2), \\
(\delta_{\mathbf{r}}h_{\mathbf{G}})(\mathbf{v}_1, \mathbf{v}_2, \mathbf{v}_3) &= (\delta h_{\mathbf{G}})(\mathbf{v}_1, \mathbf{v}_2, \mathbf{v}_3) + h_{\mathbf{G}}(\boldsymbol{\Gamma}_{\mathbf{r}}\mathbf{v}_1, \mathbf{v}_2, \mathbf{v}_3) \\
&\quad + h_{\mathbf{G}}(\mathbf{v}_1, \boldsymbol{\Gamma}_{\mathbf{r}}\mathbf{v}_2, \mathbf{v}_3) + h_{\mathbf{G}}(\mathbf{v}_1, \mathbf{v}_2, \boldsymbol{\Gamma}_{\mathbf{r}}\mathbf{v}_3),
\end{aligned} \tag{5.12}$$

for the hyperstress and its associated forms. Using the relations (5.5), (5.7) and (5.9) between $\sigma_{\mathbf{G}^{-1}}$ and $(\mathbf{T}\mathbf{G}^{-1})$, σ and $\mathbf{T}$, and $\sigma_{\mathbf{G}}$ and $(\mathbf{G}\mathbf{T})$, respectively, the

frame derivatives (5.11) can be written in terms of these latter tensors, i.e.,

$$
\begin{aligned}
\delta_{\mathrm{r}}(\mathbf{T}\mathbf{G}^{-1}) &= \delta(\mathbf{T}\mathbf{G}^{-1}) - \boldsymbol{\Gamma}_{\mathrm{r}}(\mathbf{T}\mathbf{G}^{-1}) - (\mathbf{T}\mathbf{G}^{-1})\boldsymbol{\Gamma}_{\mathrm{r}}^{*},\\
\delta_{\mathrm{r}}\mathbf{T} &= \delta\mathbf{T} - \boldsymbol{\Gamma}_{\mathrm{r}}\mathbf{T} + \mathbf{T}\boldsymbol{\Gamma}_{\mathrm{r}},\\
\delta_{\mathrm{r}}(\mathbf{G}\mathbf{T}) &= \delta(\mathbf{G}\mathbf{T}) + \boldsymbol{\Gamma}_{\mathrm{r}}^{*}(\mathbf{G}\mathbf{T}) + (\mathbf{G}\mathbf{T})\boldsymbol{\Gamma}_{\mathrm{r}}.
\end{aligned}
\tag{5.13}
$$

Likewise, using the relations (5.6), (5.8) and (5.10) between $h_{\mathbf{G}^{-1}}$ and $\mathsf{H}_{\mathbf{G}^{-1}}$, h and H, and $h_{\mathbf{G}}$ and $\mathsf{H}_{\mathbf{G}}$, respectively, (5.12) yields

$$
\begin{aligned}
\delta_{\mathrm{r}}\mathsf{H}_{\mathbf{G}^{-1}} &= \delta\mathsf{H}_{\mathbf{G}^{-1}} - \boldsymbol{\Gamma}_{\mathrm{r}}\mathsf{H}_{\mathbf{G}^{-1}} - (\mathsf{H}^{s}_{\mathbf{G}^{-1}}\boldsymbol{\Gamma}_{\mathrm{r}}^{*})^{s} - \mathsf{H}_{\mathbf{G}^{-1}}\boldsymbol{\Gamma}_{\mathrm{r}}^{*},\\
\delta_{\mathrm{r}}\mathsf{H} &= \delta\mathsf{H} - \boldsymbol{\Gamma}_{\mathrm{r}}\mathsf{H} + (\mathsf{H}^{s}\boldsymbol{\Gamma}_{\mathrm{r}})^{s} + \mathsf{H}\boldsymbol{\Gamma}_{\mathrm{r}},\\
\delta_{\mathrm{r}}\mathsf{H}_{\mathbf{G}} &= \delta\mathsf{H}_{\mathbf{G}} + \boldsymbol{\Gamma}_{\mathrm{r}}^{*}\mathsf{H}_{\mathbf{G}} + (\mathsf{H}^{s}_{\mathbf{G}}\boldsymbol{\Gamma}_{\mathrm{r}})^{s} + \mathsf{H}_{\mathbf{G}}\boldsymbol{\Gamma}_{\mathrm{r}},
\end{aligned}
\tag{5.14}
$$

where the operation S is defined in (2.2). To transform $(5.13)_{1,3}$ into their standard forms, i.e., their forms found commonly in the literature, we require the time-dependent tensors $\overset{\nabla}{\mathbf{T}}_{\mathrm{r}}\colon I \to \mathrm{Lin}(\mathcal{V},\mathcal{V})$ and $\overset{\triangle}{\mathbf{T}}_{\mathrm{r}}\colon I \to \mathrm{Lin}(\mathcal{V},\mathcal{V})$ defined by

$$
\overset{\nabla}{\mathbf{T}}_{\mathrm{r}} := \delta_{\mathrm{r}}(\mathbf{T}\mathbf{G}^{-1})\mathbf{G} \qquad \text{and} \qquad \overset{\triangle}{\mathbf{T}}_{\mathrm{r}} := \mathbf{G}^{-1}\delta_{\mathrm{r}}(\mathbf{G}\mathbf{T}),
\tag{5.15}
$$

respectively, representing such associated forms of the tensors $\delta_{\mathrm{r}}(\mathbf{T}\mathbf{G}^{-1})$ and $\delta_{\mathrm{r}}(\mathbf{G}\mathbf{T})$, respectively. From $(5.15)_{1,2}$ and $(5.13)_{1,3}$, we obtain then

$$
\begin{aligned}
\overset{\nabla}{\mathbf{T}}_{\mathrm{r}} &= \delta\mathbf{T} - \boldsymbol{\Gamma}_{\mathrm{r}}\mathbf{T} - \mathbf{T}\boldsymbol{\Gamma}_{\mathrm{r}}^{T},\\
\overset{\triangle}{\mathbf{T}}_{\mathrm{r}} &= \delta\mathbf{T} + \boldsymbol{\Gamma}_{\mathrm{r}}^{T}\mathbf{T} + \mathbf{T}\boldsymbol{\Gamma}_{\mathrm{r}}
\end{aligned}
\tag{5.16}
$$

using (2.9). The analogous forms of $(5.14)_{1,3}$ for the hyperstress are obtained by means of the time-dependent tensors $\overset{\triangle}{\mathsf{H}}_{\mathrm{r}}\colon I \to \mathrm{Lin}(\mathcal{V},\mathrm{Lin}(\mathcal{V},\mathcal{V}))$ and $\overset{\nabla}{\mathsf{H}}_{\mathrm{r}}\colon I \to \mathrm{Lin}(\mathcal{V},\mathrm{Lin}(\mathcal{V},\mathcal{V}))$, defined as the associated forms

$$
\begin{aligned}
(\overset{\nabla}{\mathsf{H}}_{\mathrm{r}}\,\mathbf{v}_2)\mathbf{v}_1 &:= ((\delta_{\mathrm{r}}\mathsf{H}_{\mathbf{G}^{-1}})(\mathbf{G}\mathbf{v}_2))(\mathbf{G}\mathbf{v}_1),\\
(\overset{\triangle}{\mathsf{H}}_{\mathrm{r}}\,\mathbf{v}_2)\mathbf{v}_1 &:= \mathbf{G}^{-1}((\delta_{\mathrm{r}}\mathsf{H}_{\mathbf{G}})\mathbf{v}_2)\mathbf{v}_1,
\end{aligned}
\tag{5.17}
$$

for all $\mathbf{v}_1, \mathbf{v}_2 \in \mathcal{V}$, of $\delta_{\mathrm{r}}\mathsf{H}_{\mathbf{G}^{-1}}$ and $\delta_{\mathrm{r}}\mathsf{H}_{\mathbf{G}}$, respectively. Substitution of $(5.17)_{1,2}$ into $(5.14)_{1,3}$ yields the expressions

$$
\begin{aligned}
\overset{\nabla}{\mathsf{H}}_{\mathrm{r}} &= \delta\mathsf{H} - \boldsymbol{\Gamma}_{\mathrm{r}}\mathsf{H} - (\mathsf{H}^{s}\boldsymbol{\Gamma}_{\mathrm{r}}^{T})^{s} - \mathsf{H}\boldsymbol{\Gamma}_{\mathrm{r}}^{T},\\
\overset{\triangle}{\mathsf{H}}_{\mathrm{r}} &= \delta\mathsf{H} + \boldsymbol{\Gamma}_{\mathrm{r}}^{T}\mathsf{H} + (\mathsf{H}^{s}\boldsymbol{\Gamma}_{\mathrm{r}})^{s} + \mathsf{H}\boldsymbol{\Gamma}_{\mathrm{r}},
\end{aligned}
\tag{5.18}
$$

for $\overset{\nabla}{\mathsf{H}}_{\mathbf{r}}$ and $\overset{\triangle}{\mathsf{H}}_{\mathbf{r}}$, respectively, *via* (2.9), (5.3) and (5.4). Again, note that the above results (5.14) and (5.18) for the frame derivatives of H and its associated forms apply immediately to the couple stress M := skwH, as well as to symH.

As is clear from the above results, the frame derivative and the formation of associated tensors *do not in general commute*, i.e., the form of the frame derivative is dependent on the particular associated tensor in question (see also MARSDEN and HUGHES [8, Ch. 1, Box 1.6]). In fact, it turns out that these two operation do commute iff the frame derivative of G with respect to the frame in question vanishes. To show this, consider for example $\delta_{\mathbf{r}}(\mathbf{GT})$; since $\delta_{\mathbf{r}}$ obeys Leibniz's rule, we have

$$\delta_{\mathbf{r}}(\mathbf{GT}) = (\delta_{\mathbf{r}}\mathbf{G})\mathbf{T} + \mathbf{G}(\delta_{\mathbf{r}}\mathbf{T}), \tag{5.19}$$

where $\delta_{\mathbf{r}}\mathbf{T}$ is given by $(5.13)_2$. Clearly, then, $\delta_{\mathbf{r}}(\mathbf{GT}) = \mathbf{G}(\delta_{\mathbf{r}}\mathbf{T})$ iff $\delta\mathbf{G}$ vanishes. Now, since $\mathbf{G} \in \mathrm{Sym}^{+}(\mathcal{V}, \mathcal{V}^{*})$, $\delta_{\mathbf{r}}\mathbf{G}$ has the same form as $\delta_{\mathbf{r}}(\mathbf{GT})$ given in $(5.13)_3$, i.e.,

$$\delta_{\mathbf{r}}\mathbf{G} = \boldsymbol{\Gamma}_{\mathbf{r}}^{*}\mathbf{G} + \mathbf{G}\boldsymbol{\Gamma}_{\mathbf{r}} = \mathbf{G}(\boldsymbol{\Gamma}_{\mathbf{r}}^{T} + \boldsymbol{\Gamma}_{\mathbf{r}}) = 2\mathbf{G}\,\mathrm{sym}(\boldsymbol{\Gamma}_{\mathbf{r}}). \tag{5.20}$$

Using (2.9), with $\delta\mathbf{G}$ vanishes since G is constant. The last result implies that $\delta_{\mathbf{r}}\mathbf{G}$ vanishes iff *the frame connection* $\boldsymbol{\Gamma}_{\mathbf{r}}$ *is skew-symmetric*.

To obtain component forms of the above frame derivatives, we introduce an arbitrary frame $\mathbf{b} \in \mathrm{Frm}\mathcal{V}$ of $\mathcal{V}$ and its dual frame $\boldsymbol{\beta} \in \mathrm{Frm}\mathcal{V}^{*}$, i.e., $\boldsymbol{\beta}^{i}\mathbf{b}_{j} = \delta^{i}_{j}$ for $i, j = 1, 2, 3$. Then

$$\begin{aligned} [\mathbf{G}]_{ij} &= (\mathbf{G}\mathbf{b}_{j})\mathbf{b}_{i} = \mathbf{b}_{i} \cdot \mathbf{b}_{j}, \\ [\mathbf{G}^{-1}]^{ij} &= \imath_{(\mathbf{G}^{-1}\boldsymbol{\beta}^{j})}\boldsymbol{\beta}^{i} = \boldsymbol{\beta}^{i}(\mathbf{G}^{-1}\boldsymbol{\beta}^{j}), \end{aligned} \tag{5.21}$$

represent the (i, j)-components of G and its inverse $\mathbf{G}^{-1}$ relative to $\mathbf{b} \in \mathrm{Frm}\mathcal{V}$ and $\boldsymbol{\beta} \in \mathrm{Frm}\mathcal{V}^{*}$; likewise

$$\begin{aligned} [\mathbf{T}]^{i}{}_{j} &:= \sigma(\boldsymbol{\beta}^{i}, \mathbf{b}_{j}) = \imath_{\mathbf{T}\mathbf{b}_{j}}\boldsymbol{\beta}^{i}, \\ [\mathbf{T}\mathbf{G}^{-1}]^{ij} &:= \sigma_{\mathbf{G}^{-1}}(\boldsymbol{\beta}^{i}, \boldsymbol{\beta}^{j}) = \imath_{\mathbf{T}\mathbf{G}^{-1}\boldsymbol{\beta}^{j}}\boldsymbol{\beta}^{i} = [\mathbf{T}]^{i}{}_{m}[\mathbf{G}^{-1}]^{mj}, \\ [\mathbf{G}\mathbf{T}]_{ij} &:= \sigma_{\mathbf{G}}(\mathbf{b}_{i}, \mathbf{b}_{j}) = (\mathbf{G}\mathbf{T}\mathbf{b}_{j})\mathbf{b}_{i} = [\mathbf{G}]_{im}[\mathbf{T}]^{m}{}_{j}, \end{aligned} \tag{5.22}$$

represent the (i, j)-component of the stress and its two associated forms, and

$$\begin{aligned} [\mathsf{H}]^{i}{}_{jk} &:= h(\boldsymbol{\beta}^{i}, \mathbf{b}_{j}, \mathbf{b}_{k}) = \imath_{(\mathsf{H}\mathbf{b}_{k})\mathbf{b}_{j}}\boldsymbol{\beta}^{i}, \\ [\mathsf{H}_{\mathbf{G}^{-1}}]^{ijk} &:= h_{\mathbf{G}^{-1}}(\boldsymbol{\beta}^{i}, \boldsymbol{\beta}^{j}, \boldsymbol{\beta}^{k}) = \imath_{(\mathsf{H}_{\mathbf{G}^{-1}}\boldsymbol{\beta}^{k})\boldsymbol{\beta}^{j}}\boldsymbol{\beta}^{i} = [\mathsf{H}]^{i}{}_{mn}[\mathbf{G}^{-1}]^{mj}[\mathbf{G}^{-1}]^{nk}, \\ [\mathsf{H}_{\mathbf{G}}]_{ijk} &:= h_{\mathbf{G}}(\mathbf{b}_{i}, \mathbf{b}_{j}, \mathbf{b}_{k}) = ((\mathsf{H}_{\mathbf{G}}\mathbf{b}_{k})\mathbf{b}_{j})\mathbf{b}_{i} = [\mathbf{G}]_{im}[\mathsf{H}]^{m}{}_{jk}, \end{aligned} \tag{5.23}$$

the (i,j,k)-component of the hyperstress and its two associated forms, in each case with respect to $\mathbf{b} \in \mathrm{Frm}\mathcal{V}$ and $\boldsymbol{\beta} \in \mathrm{Frm}\mathcal{V}^*$. Note also that $[\mathsf{H}^s]^i{}_{jk} = [\mathsf{H}]^i{}_{kj}$. Lastly,

$$[\boldsymbol{\Gamma}_\mathbf{r}]^i{}_j := \imath_{\boldsymbol{\Gamma}_\mathbf{r}\mathbf{b}_j}\boldsymbol{\beta}^i = \boldsymbol{\beta}^i(\boldsymbol{\Gamma}_\mathbf{r}\mathbf{b}_j) \tag{5.24}$$

represent the (i,j)-component of the frame connection $\boldsymbol{\Gamma}_\mathbf{r}$ relative to $\mathbf{b} \in \mathrm{Frm}\mathcal{V}$ and $\boldsymbol{\beta} \in \mathrm{Frm}\mathcal{V}^*$, and

$$[\boldsymbol{\Gamma}_\mathbf{r}^T]^i{}_j = [\mathbf{G}^{-1}]^{im}[\boldsymbol{\Gamma}_\mathbf{r}^*]^k{}_m[\mathbf{G}]_{kj} = [\mathbf{G}^{-1}]^{im}[\boldsymbol{\Gamma}_\mathbf{r}]_m{}^k[\mathbf{G}]_{kj} \tag{5.25}$$

those of $\boldsymbol{\Gamma}_\mathbf{r}^T$. With these, we obtain

$$\begin{aligned}
[\delta_\mathbf{r}(\mathbf{T}\mathbf{G}^{-1})]^{ij} &= [\delta(\mathbf{T}\mathbf{G}^{-1})]^{ij} - [\boldsymbol{\Gamma}_\mathbf{r}]^i{}_m[\mathbf{T}\mathbf{G}^{-1}]^{mj} - [\mathbf{T}\mathbf{G}^{-1}]^{im}[\boldsymbol{\Gamma}_\mathbf{r}]_m{}^j,\\
[\delta_\mathbf{r}\mathbf{T}]^i{}_j &= [\delta\mathbf{T}]^i{}_j - [\boldsymbol{\Gamma}_\mathbf{r}]^i{}_m[\mathbf{T}]^m{}_j + [\mathbf{T}]^i{}_m[\boldsymbol{\Gamma}_\mathbf{r}]^m{}_j,\\
[\delta_\mathbf{r}(\mathbf{G}\mathbf{T})]_{ij} &= [\delta(\mathbf{G}\mathbf{T})]_{ij} + [\boldsymbol{\Gamma}_\mathbf{r}]_i{}^m[\mathbf{G}\mathbf{T}]_{mj} + [\mathbf{G}\mathbf{T}]_{im}[\boldsymbol{\Gamma}_\mathbf{r}]^m{}_j,
\end{aligned} \tag{5.26}$$

for the component forms of (5.13),

$$\begin{aligned}
[\delta_\mathbf{r}\mathsf{H}_{\mathbf{G}^{-1}}]^{ijk} &= [\delta\mathsf{H}_{\mathbf{G}^{-1}}]^{ijk} - [\boldsymbol{\Gamma}_\mathbf{r}]^i{}_m[\mathsf{H}_{\mathbf{G}^{-1}}]^{mjk} - [\mathsf{H}_{\mathbf{G}^{-1}}]^{imk}[\boldsymbol{\Gamma}_\mathbf{r}]_m{}^j\\
&\qquad -[\mathsf{H}_{\mathbf{G}^{-1}}]^{ijm}[\boldsymbol{\Gamma}_\mathbf{r}]_m{}^k,\\
[\delta_\mathbf{r}\mathsf{H}]^i{}_{jk} &= [\delta\mathsf{H}]^i{}_{jk} - [\boldsymbol{\Gamma}_\mathbf{r}]^i{}_m[\mathsf{H}]^m{}_{jk} + [\mathsf{H}]^i{}_{mk}[\boldsymbol{\Gamma}_\mathbf{r}]^m{}_j + [\mathsf{H}]^i{}_{jm}[\boldsymbol{\Gamma}_\mathbf{r}]^m{}_k,\\
[\delta_\mathbf{r}\mathsf{H}_\mathbf{G}]_{ijk} &= [\delta\mathsf{H}_\mathbf{G}]_{ijk} + [\boldsymbol{\Gamma}_\mathbf{r}]_i{}^m[\mathsf{H}_\mathbf{G}]_{mjk} + [\mathsf{H}_\mathbf{G}]_{imk}[\boldsymbol{\Gamma}_\mathbf{r}]^m{}_j\\
&\qquad +[\mathsf{H}_\mathbf{G}]_{ijm}[\boldsymbol{\Gamma}_\mathbf{r}]^m{}_k,
\end{aligned} \tag{5.27}$$

for the component forms of (5.14). Likewise,

$$\begin{aligned}
[\overset{\nabla}{\mathbf{T}}_\mathbf{r}]^i{}_j &= [\delta\mathbf{T}]^i{}_j - [\boldsymbol{\Gamma}_\mathbf{r}]^i{}_m[\mathbf{T}]^m{}_j - [\mathbf{T}]^i{}_m[\boldsymbol{\Gamma}_\mathbf{r}^T]^m{}_j,\\
[\overset{\triangle}{\mathbf{T}}_\mathbf{r}]^i{}_j &= [\delta\mathbf{T}]^i{}_j + [\boldsymbol{\Gamma}_\mathbf{r}^T]^i{}_m[\mathbf{T}]^m{}_j + [\mathbf{T}]^i{}_m[\boldsymbol{\Gamma}_\mathbf{r}]^m{}_j,
\end{aligned} \tag{5.28}$$

hold for the component forms of (5.16), and

$$\begin{aligned}
[\overset{\nabla}{\mathsf{H}}_\mathbf{r}]^i{}_{jk} &= [\delta\mathsf{H}]^i{}_{jk} - [\boldsymbol{\Gamma}_\mathbf{r}]^i{}_m[\mathsf{H}]^m{}_{jk} - [\mathsf{H}]^i{}_{mk}[\boldsymbol{\Gamma}_\mathbf{r}^T]^m{}_j - [\mathsf{H}]^i{}_{jm}[\boldsymbol{\Gamma}_\mathbf{r}^T]^m{}_k,\\
[\overset{\triangle}{\mathsf{H}}_\mathbf{r}]^i{}_{jk} &= [\delta\mathsf{H}]^i{}_{jk} + [\boldsymbol{\Gamma}_\mathbf{r}^T]^i{}_m[\mathsf{H}]^m{}_{jk} + [\mathsf{H}]^i{}_{mk}[\boldsymbol{\Gamma}_\mathbf{r}]^m{}_j + [\mathsf{H}]^i{}_{jm}[\boldsymbol{\Gamma}_\mathbf{r}]^m{}_k,
\end{aligned} \tag{5.29}$$

for those of (5.18). Of course, the component forms (5.27) and (5.29) for various frame derivatives of H apply immediately to the couple stress $\mathsf{M} := \mathrm{skw}\mathsf{H}$, as well as to $\mathrm{sym}\mathsf{H}$.

6. Special frame derivatives for the Cauchy stress and hyperstress

To obtain familiar special cases of the above general objective frame derivatives, let $\mathbf{b} \in \mathrm{Frm}\mathcal{V}$ be any frame at $b \in B$ in the reference configuration $B \subset E$ of the material body. Now, since $\mathbf{b} \in \mathrm{Frm}\mathcal{V}$ is time-independent, $\mathbf{\Gamma}_{\mathbf{b}}$ vanishes (see (4.4)). In this case, (4.9) yields

$$\mathbf{\Gamma}_{\mathbf{Zb}} = \mathbf{\Lambda}_{\mathbf{Z}} \tag{6.1}$$

for any differentiable $\mathbf{Z} : I \to \mathrm{Lbj}(\mathcal{V}, \mathcal{V})$, where

$$\mathbf{\Lambda}_{\mathbf{Z}} := (\delta\mathbf{Z})\mathbf{Z}^{-1} : I \to \mathrm{Lin}(\mathcal{V}, \mathcal{V}) \tag{6.2}$$

represents the rate of change of $\mathbf{Z} : I \to \mathrm{Lbj}(\mathcal{V}, \mathcal{V})$ relative to itself. Clearly, (6.1) depends only on $\mathbf{Z} : I \to \mathrm{Lbj}(\mathcal{V}, \mathcal{V})$, and not on $\mathbf{b} \in \mathrm{Frm}\mathcal{V}$, a result due mainly to the fact that the reference configuration B is time-independent. Consequently, (6.1) holds for all $\mathbf{b} \in \mathrm{Frm}\mathcal{V}$. We have the following common special cases of $\mathbf{Z}$ and associated connections:

Table 1. Particular connections.

$\mathbf{\Lambda}_{\mathbf{I}} = \mathbf{0}$	:	$I \to \{\mathbf{0}\}$	material
$\mathbf{\Lambda}_{\mathbf{R}} = (\delta\mathbf{R})\mathbf{R}^{-1}$	:	$I \to \mathrm{Skw}(\mathcal{V}, \mathcal{V})$	Green – MacInnis – Dienes
$\mathbf{\Lambda}_{\mathbf{F}} = (\delta\mathbf{F})\mathbf{F}^{-1}$	:	$I \to \mathrm{Lin}(\mathcal{V}, \mathcal{V})$	Oldroyd
$\mathbf{\Lambda}_{\mathbf{P}} = (\delta\mathbf{P})\mathbf{P}^{-1}$	:	$I \to \mathrm{Skw}(\mathcal{V}, \mathcal{V})$	Zaremba – Jaumann

where $\mathbf{F} = \mathbf{RU}$, $\mathbf{\Lambda}_{\mathbf{F}} = \mathbf{L}$ is, as usual, the velocity gradient, and $\mathbf{\Lambda}_{\mathbf{P}} := \mathbf{W} := \mathrm{skw}(\mathbf{L})$ – the vorticity.

Turning next to the frame derivative operator, (4.12) implies

$$\delta_{\mathbf{b}} = \mathcal{K}_{\mathbf{b}} \circ \delta \circ \Theta_{\mathbf{b}} = \mathcal{K}_{\mathbf{b}} \circ \Theta_{\mathbf{b}} \circ \delta = \delta \tag{6.3}$$

for all $\mathbf{b} \in \mathrm{Frm}\mathcal{V}$; consequently, $(4.15)_2$ takes the form

$$\delta_{\mathbf{Zb}} = \mathbf{t}_{\mathbf{Z}} \circ \delta_{\mathbf{b}} \circ \mathbf{t}_{\mathbf{Z}^{-1}} = \mathbf{t}_{\mathbf{Z}} \circ \delta \circ \mathbf{t}_{\mathbf{Z}^{-1}} =: \delta_{\mathbf{Z}}\,, \tag{6.4}$$

a result that, like (6.1), is clearly independent of $\mathbf{b} \in \mathrm{Frm}\mathcal{V}$. As for the frame derivatives of the Cauchy stress and hyperstress tensors in the standard forms (5.16) and (5.18), respectively, we have

$$\begin{aligned} \overset{\nabla}{\mathbf{T}}_{\mathbf{Zb}} &= \delta\mathbf{T} - \mathbf{\Lambda}_{\mathbf{Z}}\mathbf{T} - \mathbf{T}\mathbf{\Lambda}_{\mathbf{Z}}^{T}\,, \\ \overset{\triangle}{\mathbf{T}}_{\mathbf{Zb}} &= \delta\mathbf{T} + \mathbf{\Lambda}_{\mathbf{Z}}^{T}\mathbf{T} + \mathbf{T}\mathbf{\Lambda}_{\mathbf{Z}}\,, \end{aligned} \tag{6.5}$$

and

$$\begin{aligned} \overset{\nabla}{\mathsf{H}}_{\mathbf{Zb}} &= \delta\mathsf{H} - \mathbf{\Lambda}_{\mathbf{Z}}\mathsf{H} - (\mathsf{H}^s\mathbf{\Lambda}_{\mathbf{Z}}^T)^s - \mathsf{H}\mathbf{\Lambda}_{\mathbf{Z}}^T, \\ \overset{\triangle}{\mathsf{H}}_{\mathbf{Zb}} &= \delta\mathsf{H} + \mathbf{\Lambda}_{\mathbf{Z}}^T\mathsf{H} + (\mathsf{H}^s\mathbf{\Lambda}_{\mathbf{Z}})^s + \mathsf{H}\mathbf{\Lambda}_{\mathbf{Z}}, \end{aligned} \tag{6.6}$$

for all $\mathbf{b} \in \mathrm{Frm}\mathcal{V}$ from (5.16) and (5.18), respectively, using (6.2). Again, we emphasize that the results (6.6) also hold for $\mathsf{M} := \mathrm{skw}\mathsf{H}$ and $\mathrm{sym}\mathsf{H}$.

Lastly, note that the frame derivative (5.20) of the Euclidean metric $\mathbf{G}$, together with Table 1 and (6.4), imply

$$\delta_{\mathbf{F}}\mathbf{G} = 2\mathbf{G}\,\mathrm{sym}(\mathbf{L}) = 2\mathbf{GD} \tag{6.7}$$

for the Oldroyd derivative $\mathbf{G}$, as well as

$$\delta_{\mathbf{R}}\mathbf{G} = \mathbf{0} = \delta_{\mathbf{P}}\mathbf{G} \tag{6.8}$$

for the Green–MacInnis–Dienes and Zaremba–Jaumann frame derivatives of the Euclidean metric $\mathbf{G}$. Consequently, as discussed in the last section in the context of (5.19) and (5.20), $\delta_{\mathbf{F}}$ does not commute with the formation of associated tensors, while $\delta_{\mathbf{R}}$ and $\delta_{\mathbf{P}}$ do. In particular, this latter fact implies $\overset{\triangle}{\mathbf{T}}_{\mathbf{Rb}} = \overset{\nabla}{\mathbf{T}}_{\mathbf{Rb}}$, $\overset{\triangle}{\mathbf{T}}_{\mathbf{Pb}} = \overset{\nabla}{\mathbf{T}}_{\mathbf{Pb}}$, $\overset{\triangle}{\mathsf{H}}_{\mathbf{Rb}} = \overset{\nabla}{\mathsf{H}}_{\mathbf{Rb}}$ and $\overset{\triangle}{\mathsf{H}}_{\mathbf{Pb}} = \overset{\nabla}{\mathsf{H}}_{\mathbf{Pb}}$ for all $\mathbf{b} \in \mathrm{Frm}\mathcal{V}$.

References

1. B. SVENDSEN, *A local frame formulation of dual stress-strain pairs and time derivatives*, Acta Mech., 1994 [in press].
2. C.A. TRUESDELL and W. NOLL, *The non-linear field theories of mechanics*, Handbuch der Physik, V. III/3, S. FLÜGGE [Ed.], Springer-Verlag, 1965.
3. I.A. MURDOCH, *A corpuscular approach to continuum mechanics: basic considerations*, Arch. Rat. Mech. Mat., **88**, 81–111, 1985.
4. G. CAPRIZ, *Continua with microstructure*, Springer Tracts in Natural Philosophy, **35**, Springer-Verlag, 1989.
5. R. ABRAHAM, J.E. MARSDEN, T. RATIU, *Manifolds, tensor analysis, and applications*, Appl. Math. Sci., **75**, Springer–Verlag, 1988.
6. W. NOLL, *Finite dimensional spaces: algebra, geometry and analysis*, V.I., M. Nijhoff, 1987.
7. M. SPIVAK, *A comprehensive introduction to differential geometry*, V. 1–5, Publish or Perish, 1979.
8. J.E. MARSDEN, T.J.R. HUGHES, *Mathematical theory of elasticity*, Prentice–Hall, 1983.

TECHNISCHE HOCHSCHULE DARMSTADT,
FACHBEREICH 6, MECHANIK III, DARMSTADT, GERMANY.

Received April 18, 1994.

Arch. Mech., 46, 5, pp. 685–709, Warszawa 1994

Two multispeed discrete Boltzmann models including multiple collisions I. Similarity solutions

H. CORNILLE (GIF-SUR-YVETTE) and
T. PŁATKOWSKI (WARSZAWA)

WE PRESENT a formalism for the determination of exact similarity shock waves solutions for two discrete Boltzmann models (DBMs), when, in addition to binary collisions, multiple collisions are included. For the first time exact solutions corresponding to multiple collisions including quaternary collisions are constructed. We consider the simplest multispeed models with two speeds $1, \sqrt{2}$ and without spurious macroscopic conservation laws, for which exact solutions are known only for binary collisions: (i) the square eight velocity ($8v_i$) model on a plane, with the spatial coordinate along a median of the square, (ii) a three-dimensional fourteen velocity ($14v_i$) model. From the numerical solutions we observe, in addition, overshoots for the microscopic densities.

1. Introduction

THE DISCRETE Boltzmann models [1] (DBMs) with the multiple collisions became recently a popular domain of research [1–3]. Concerning the exact solutions, only a few models with ternary collisions [4] have been studied. Multiple collisions for DBMs can be introduced in order to eliminate spurious macroscopic conservation laws present at the binary level. In this paper we choose models without spurious macroscopic conservation laws, for which the equilibrium states for the models without the multiple collisions are the same as the equilibrium states for the models with the multiple collisions included. For these models we generalize the construction of the exact solutions when higher than ternary collisions are included, and compare the results with general numerical solutions.

We construct a class of similarity shock waves solutions of two multispeed [5–6] DBMs which include binary, ternary and fourth order collisions, and compare the respective shock profiles. Recently [6] hierarchies of multispeed DBMs with binary collisions alone, have been classified following the (1 + 1)-dimensional restriction of their multidimensional PDE satisfied by the microscopic densities. For a hierarchy of models, the nonlinear evolution equations of the planar and of the three-dimensional models are the same, except for a factor which depends on the dimension of the space. *Here we study such a hierarchy of models with two speeds* $1, \sqrt{2}$ *and for which rest particles could be added, differing only by coefficients which depend on the spatial* d *dimension, but with multiple collisions included.* The first model [5] is the square $d = 2$ (d-dimension of the space) $8v_i$ model (cf. Fig. 1a). The second model [6] is a three-dimensional ($d = 3$) $14v_i$ model (cf.

Fig. 1a) which can be interpreted as a superposition of two square models in both the $x_1 = x, x_2$ and $x_1 = x, x_3$ planes, with two common velocities along the x_1-axis. For the $x = x_1$ direction of the shock propagation for these models, there remain five independent densities (cf. Sec. 1): N_1, M_1, R, M_2, N_2.

The evolution equations for these densities, with multiple collisions taken into account, are discussed in Sec. 1, where we also classify all the types of the considered multiple collisions, and discuss different structures of the collision operators.

In Sec. 3, in order to construct exact shock waves solutions, we determine the asymptotic states using the Rankine-Hugoniot (R-H) relations. It is important that for multiple collision terms which contain the binary ones, multiplied by density-dependent factors, the asymptotic states are the same as the binary ones. We recall the general solutions and simple analytical solutions of the R-H relations when only binary collisions occur [7].

In Sec. 4 we present *a formalism for the determination of a class of exact similarity shock wave solutions* which are functions of the variable $w = e^{\gamma\eta}$, $\eta = x - \zeta t$.

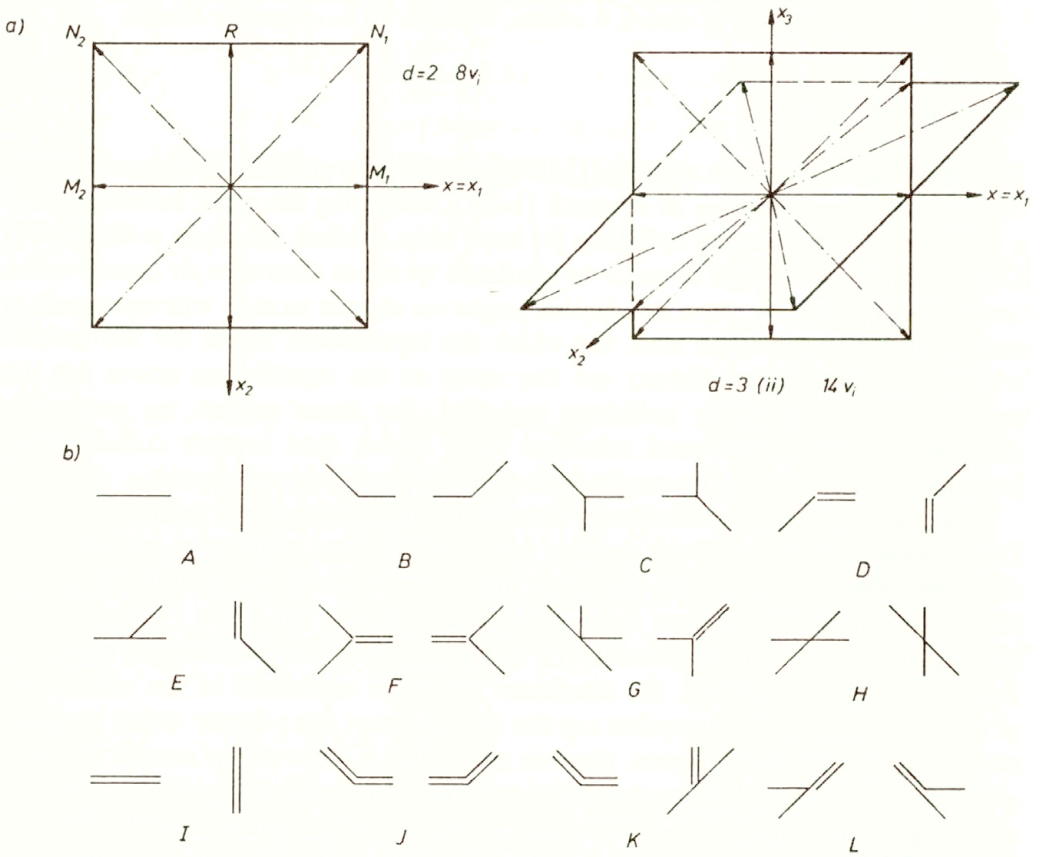

[FIG. 1 a,b]

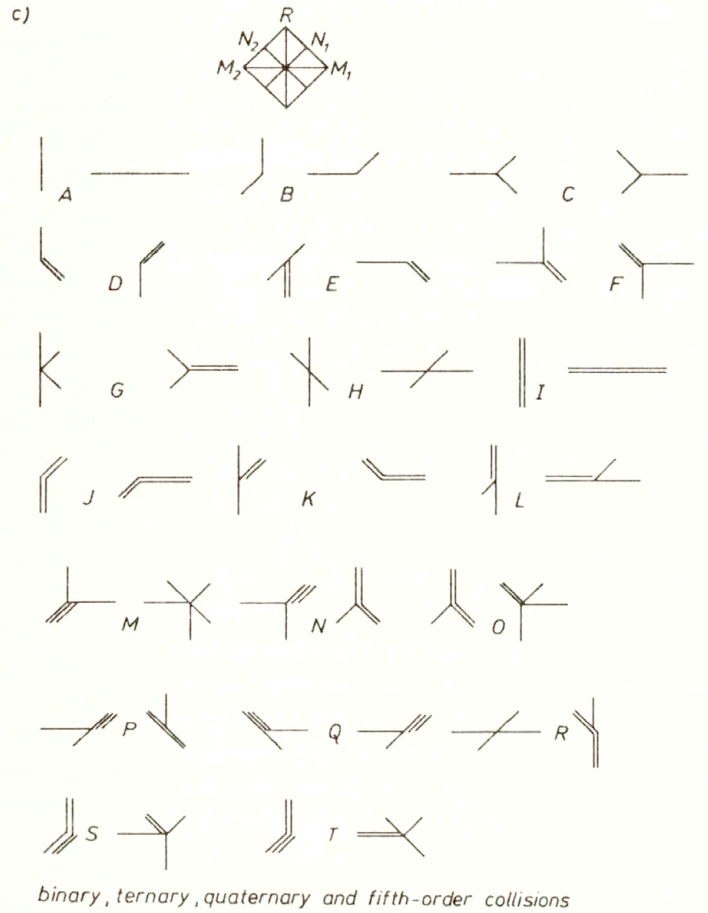

FIG. 1. a) $d = 2$ and $d = 3$ models, b) binary, ternary and quaternary collisions, c) $8v_i$, x-axis along the diagonal.

To explain the method let us note, that the nonlinear equations in (2.1)–(2.5) of Sec. 2 have the following general structure: they contain a first order linear differential term, and nonlinear terms of the p-th order: $p = 2$ for binary collisions, $p = 3$ if ternary collisions are included or $p = 4, 5, \ldots$ with higher order terms. We consider an ansatz of the type: $N_i, M_i, R = \text{const}_1 + \text{const}_2/D^q$, $D = 1 + e^{\gamma\eta}$. The possible values of q are found from the balance between the linear term and the highest nonlinearity, which means $D^{-(q+1)} = D^{-pq}$ or $q = 1/(p-1)$: $q = 1, 1/2, 1/3, 1/4, \ldots$ for $p = 2, 3, 4, 5, \ldots$. In fact, the linear differential term contains two terms: $D^{-1/(p-1)}$, $D^{-p/(p-1)}$ while the nonlinearities contain other terms: $D^{-r/(p-1)}$, $r = 2, 3, \ldots p-1$, $p > 2$ giving $p-2$ relations. For similarity solutions ($\eta = x - \zeta t$) we choose the ansatz:

$$
\begin{aligned}
N_i &= n_{0i} + n_i D^{-q}, \qquad M_i = m_{0i} + m_i D^{-q}, \qquad i = 1, 2, \\
R &= r_0 + r D^{-q}, \qquad D = 1 + e^{\gamma\eta},
\end{aligned}
\tag{1.1}
$$

where the highest monomial nonlinear term is of order p and $n_{0i}, n_i, m_{0i}, i = 1, 2$, r_0, r, γ, ζ are real parameters. Noticing that n_{0i}, m_{0i}, r_0 and $n_{0i}+n_i, m_{0i}+m_i, r_0+r$ are the two equilibrium states (when $|\eta| = \infty$), their determination is known from the Sec. 3 study. However, the nonlinear (2.2), (2.3) equations give new relations which must be satisfied by γ and the cross-sections, the parameters not present in the R-H relations. These relations imply that some of the cross-sections are not arbitrary parameters, however we construct classes of solutions where all the cross-sections are positive. We construct different classes of solutions depending on whether we assume that $p = 2, 3, 4$, or we require that for multiple collisions cross-sections equal to zero, these solutions reduce to the binary ones. *We observe that the addition of multiple collisions decreases the width of the shock.* The exact solutions (1.1) are not the most general similarity solutions of the shock problem for (2.1)–(2.5). It is worthwhile to recall [7], that for exact solutions of DBMs with only binary collisions, other solutions than (1.1), coming from Riccati-coupled equations, exist. For DBMs with multiple collisions (i.e. with higher than quadratic nonlinearities) it is not clear that other exact solutions exist. At least for the simplest ternary case, up to now, no other exact similarity solutions have been found. *Consequently, for the known exact shock wave solutions associated with multiple collisions, the microscopic densities are monotonic.*

In Sec. 5 we present numerical results for the shock problem and, in order to see the possible differences, compare with the results obtained by applying the Runge–Kutta's IVth order procedure. *Contrary to the exact solutions, all the cross-sections are free parameters, and we obtain nonmonotonic profiles of M_i, $i = 1, 2$ densities.*

In Sec. 6 we discuss the results and some generalizations. We show that the present results could be extended to other multispeed models – we give partial results (in particular for the factors of the binary collision terms when multiple collisions are included) for both the Cabannes [8] model and the plane $8v_i$ model with the x-axis along a diagonal of the square.

2. Description of the models and of the multiple collisions

The first model [5] is the square $8v_i$ model (cf. Fig. 1a). We look for one-dimensional shock solutions with the direction of propagation along the x-axis, which we choose along a median of the square. From the symmetry considerations there remain five independent densities N_1, M_1, R, M_2, N_2, associated with the the following velocities in the plane $(x_1 = x, x_2)$:

$$N_1 : (1, \pm 1), \quad N_2 : (-1, \pm 1), \quad M_1 : (1, 0), \quad M_2 : (-1, 0), \quad R : (0, \pm 1).$$

The second model [6] is a $14v_i$ model, $d = 3$, which in the $(x_1 = x, x_2, x_3)$ three-dimensional space can be treated as a superposition of two square models in the x_1, x_2 and x_1, x_3 planes with two common velocities along the x_1-axis (cf.

Fig. 1a). For the $x = x_1$ one-dimensional projection of this model we have the same five independent densities associated with the following velocities in the space:

$$N_1 : (1, \pm 1, 0), (1, 0, \pm 1), \quad N_2 : (-1, \pm 1, 0), (-1, 0, \pm 1),$$
$$M_1 : (1, 0, 0), \quad M_2 : (-1, 0, 0), \quad R : (0, \pm 1, 0), (0, 0, \pm 1),$$

with the same velocity projections of N_1, M_1, R, M_2, N_2 on the x-axis, as for the first model, i.e $1, 1, 0, -1, -1$.

For both models these five densities satisfy three linear relations equivalent to the mass, momentum and energy conservation laws ($p_\pm := \partial_t \pm \partial_x$, $d_* := 2(d-1)$)

$$\begin{aligned} p_+ N_1 + p_- N_2 = 0, \qquad p_+ M_1 + p_- M_2 + d_* R_t = 0, \\ p_+ M_1 - p_- M_2 + 2 d_* p_+ N_1 = 0, \end{aligned} \tag{2.1}$$

and two non-linear equations (cf. Fig. 1b)

$$p_+ N_1 = Q_{1,b} + Q_{1,p} + Q_{1,t} + Q_{1,q}, \qquad \partial_t R = Q_{2,b} + Q_{2,p} + Q_{2,t} + Q_{2,q}, \tag{2.2}$$

where the operators on the rhs of (2.2) correspond, respectively, to binary collisions, (Fig. 1b A, B), pseudotriple collisions (i.e. the collisions in which one particle is in the same state before and after the collision), ternary (Fig. 1b C, D, E), and quaternary (Fig. 1b F, G, H, I, J, K, L) collisions. We define $N_{12}^{\pm} = N_1 \pm N_2$, $M_{12}^{\pm} = M_1 \pm M_2$ and get for the binary collisions:

$$\begin{aligned} Q_{1,b} &= -\sigma_B^{(2)} Q_1, \qquad & Q_1 &= N_1 M_2 - N_2 M_1, \\ Q_{2,b} &= \sigma_B^{(1)} Q_2, & Q_2 &= M_1 M_2 - R^2. \end{aligned} \tag{2.3}$$

For the pseudotriple: $Q_{1,p} = -\sigma_P^{(2)} M Q_1$, $Q_{2,p} = \sigma_P^{(1)} M Q_2$. For the triple collisions

$$\begin{aligned} Q_{1,t} &= -Q_1 (\sigma_C R + \sigma_{DE} M_{12}^+) + \sigma_{DE} Q_2 N_{12}^-, \\ Q_{2,t} &= 2(\sigma_{DE} + \sigma_E) Q_2 N_{12}^+ - 2\sigma_{DE} Q_1 M_{12}^-, \end{aligned} \tag{2.4}$$

with $\sigma_{DE} = \sigma_D + \sigma_E$, and the mass $M = M_1 + M_2 + d_*(R + N_1 + N_2)$. For the quaternary collisions:

$$\begin{aligned} Q_{1,q} &= -Q_1 \left[\sigma_{JF}(M_1 N_2 + M_2 N_1) + \sigma_G R N_{12}^+ + \sigma_L N_1 N_2\right] + \sigma_K Q_2 M_{12}^+ N_{12}^+, \\ Q_{2,q} &= Q_2 \left[\sigma_H N_1 N_2 + \sigma_I (M_1 M_2 + R^2) + 2\sigma_K (N_{12}^+)^2\right] - 2\sigma_K Q_1 N_{12}^+ M_{12}^-. \end{aligned} \tag{2.5}$$

In the above formulas $\sigma_B^{(i)}$, $i = 1, 2$ are the cross-sections for binary collisions, $\sigma_C, \sigma_D, \sigma_E$ are proportional to the transition probabilities (for brevity they will be also called cross-sections) for the ternary collisions C, D, E of Fig. 1b, and

$\sigma_{F,\ldots L}$ correspond to the quaternary Fig. 1b collisions, $\sigma_{JF} = \sigma_J + \sigma_F$. In the collision terms, each drawing of Fig. 1b corresponds to all collisions obtained by applying the transformations of the square symmetry group. In these collisions, called spectatorless collisions, the particles present in the loss term are missing in the gain term.

Using the conservation laws, the nonlinear equations for R, N_1 can be replaced by two equations for other pairs of densities. Below we discuss two important structures of the nonlinear equations associated with the different pairs of the densities.

1. Firstly, there can be only one binary collision term associated with each of the nonlinear equation (Q_1 for N_1 and Q_2 for R in (2.2)). In each equation two classes of multiple collision terms can occur. For the first class, each multiple term is a product of the binary term present in the equation, and a positive factor, depending on some of the microscopic densities. For the second class the multiple collision terms have as a factor another binary term, not present for that density. In the latter case the remaining factors are not necessarily positive.

To see the above properties for $p_+N_1, \partial_t R$, we rewrite the (2.2)–(2.5) nonlinear equations containing linearly the binary ($-Q_1$ for p_+N_1, Q_2 for $\partial_t R$) collision terms:

$$
\begin{aligned}
p_+N_1 &= -Q_1\left[\sigma_B^{(2)} + A_{22}\right] + Q_2A_{21}, \\
\partial_t R &= Q_2\left[\sigma_B^{(1)} + A_{11}\right] - Q_1A_{12},
\end{aligned}
\tag{2.6}
$$

with the coefficients defined in the table below.

2. Secondly, if we take as the nonlinear equations those which describe evolution of M_1, M_2, then both binary collision terms Q_1, Q_2 are present in each equation. A natural question is whether for the multiple collision terms the two corresponding factors (instead of one for p_+N_1 or $\partial_t R$) are also nonnegative? To see this, we write, taking into account the linear (2.1) relations, the nonlinear equations for p_+M_1, p_-M_2:

$$
\begin{aligned}
p_+M_1/d_* &= -Q_2\left[\sigma_B^{(1)} + 2B_{1+}\right]/2 + Q_1\left[\sigma_B^{(2)} + B_{2+}\right], \\
2B_{1\pm} &= A_{11} \pm 2A_{21}, \\
p_-M_2/d_* &= -Q_2\left[\sigma_B^{(1)} + 2B_{1-}\right]/2 - Q_1\left[\sigma_B^{(2)} + B_{2-}\right], \\
B_{2\pm} &= A_{22} \pm A_{12}/2.
\end{aligned}
\tag{2.7}
$$

In the table we present for ternary and quaternary collisions the relevant terms for both structures for the plane $8v_i$ model. Omitting for brevity the multiplicative multipliers proportional to the transition probabilities, and defining $Q_{NM} = M_1N_2 + M_2N_1$, we get from the collisions associated with Fig. 1b –

C...L the following contributions to A_{ij}, $B_{i\mp}$:

Q	A_{11}	A_{12}	A_{21}	A_{22}	B_{1+}	B_{2+}
Q_C	0	0	0	R	0	R
Q_D	$2N_{12}^+$	$2M_{12}^-$	N_{12}^-	M_{12}^+	$2N_1$	$2M_1$
Q_E	$4N_{12}^+$	$2M_{12}^-$	N_{12}^-	M_{12}^+	$3N_1 + N_2$	$2M_1$
Q_F	0	0	0	Q_{NM}	0	Q_{NM}
Q_G	0	0	0	RN_{12}^+	0	RN_{12}^+
Q_H	N_1N_2	0	0	0	N_1N_2	0
Q_I	$M_1M_2 + R^2$	0	0	0	$M_1M_2 + R^2$	0
Q_J	0	0	0	Q_{NM}	0	Q_{NM}
Q_K	$2N_{12}^{+2}$	$2M_{12}^-N_{12}^+$	$N_{12}^+N_{12}^-$	$M_{12}^+N_{12}^+$	$2N_1N_{12}^+$	$2M_1N_{12}^+$
Q_L	0	0	0	N_1N_2	0	N_1N_2

We verify $A_{ii} \geq 0$, $i = 1,2$ while the terms $A_{ij} = 0$ for $N_1 = N_2$, $M_1 = M_2$, $i \neq j$. Note that for the present collisions B_{i+}, $i = 1,2$ are nonnegative, and the transform $N_1 \longleftrightarrow N_2$, $M_1 \longleftrightarrow M_2$ imply $B_{i+} \longleftrightarrow B_{i-}$, so that B_{i-} are also nonnegative. More precisely, for the collisions C, F, G, H, I, J, L with B_{i+} terms invariant under this transform we find $B_{i-} = B_{i+}$, while for D, E, K we get with the above transform respectively: $B_{1-} = 2N_2, 3N_2 + N_1, 2N_2N_{12}^+$ and $B_{2-} = 2M_2, 2M_2, 2M_2N_{12}^+$. However, in the joint paper [11] we introduce fifth order collision terms and we notice a difference with the present ones. *We still find $A_{ii} \geq 0$, and $A_{ij} = 0$ for $N_1 = N_2, M_1 = M_2$. On the contrary, the $B_{i\pm}$ are not always both nonnegative, however at least one of them is nonnegative. The above factorization and nonnegativity properties will be crucial for the study of stability.*

The study of stability, using the Whitham approach, of the asymptotic states will be done in the joint paper [11]. Sufficient conditions for the decrease of the shock thickness will be given in Sec. 3 for the exact solutions. However for both studies, an important tool will be provided mainly by the positivity of the A_{ii} and particular properties of the A_{ij}, factors of the binary collision terms Q_i. It sems worthwhile, at this stage, to give a brief account of these properties which will be developed in the joint paper. Let us define $(m_{0i} \geq 0, n_{0i} \geq 0, r_0 \geq 0)$ – the asymptotic densities of an asymptotic state (M_i, N_i, R) and call $\tilde{A}_{ij}$, $\tilde{B}_{i\pm}$ the corresponding asymptotic values for the A_{ij}, $B_{i\pm}$. From the table we find:

$$\tilde{A}_{ii} \geq 0, \qquad m_{01}\tilde{A}_{21} = \tilde{A}_{12}n_{01}/2, \qquad (n_{01} - n_{02})\tilde{A}_{21} \geq 0,$$
$$m_{01}\tilde{B}_{1\pm} + n_{01}\tilde{B}_{2\pm} \geq 0, \qquad \tilde{A}_{11}\tilde{A}_{22} - \tilde{A}_{21}\tilde{A}_{12} \geq 0, \tag{2.8}$$

$$\tilde{A}_{21} = (n_{01} - n_{02})(\sigma_{DE} + (n_{01} + n_{02})\sigma_K). \tag{2.9}$$

We have found that the properties (2.8) are still valid when all fifth order collisions are included, and for a partial study – of the six order collision terms. On the contrary, (2.9) is peculiar to the ternary and quaternary collisions. For higher order collisions we still find the term $n_{01} - n_{02}$ (or $m_{01} - m_{02} = m_{01}(n_{01} - n_{02})/n_{01}$), but in the second positive factor we must add other fifth (or higher) order cross-sections. Coming back to the nonlinear (2.6) equations, these $\tilde{A}_{ij}$ terms, factors of the binary collision terms not present at the binary level (i.e. if only binary collisions occur), vanish for $n_{01} = n_{02}$ (which implies $m_{01} = m_{02}$ or uniform solutions at the asymptotic state) or are small if $\sigma_{CD} \simeq 0$, $\sigma_K \simeq 0$. In such cases the factors of the binary terms present at the binary level are equal to $\sigma_B^{(i)}$ for the binary collisions and approximated by $\sigma_B^{(i)} + \tilde{A}_{ii} > \sigma_B^{(i)}$ in the multiple collision case. The comparison between binary and such multiple collisions will provide sufficient conditions for the stability of the asymptotic state and the decrease of the shock thickness.

We conjecture that the results (2.8) hold for any p-th order multiple collisions.

Below we prove for the planar $d = 2$ model that there exist no other ternary and quaternary spectatorless collisions, satisfying microscopic conservation laws, than those shown in Fig. 1b. More in details, we determine for the $d = 2$ model all the collisions satisfying 1) spectatorlessness (i.e. all the particles change their velocities in the collision), 2) microscopic energy conservation $\sum v_i^2 = \sum v_i'^2$, 3) momentum conservation $\mathbf{v} = \sum \mathbf{v}_i = \mathbf{v}' = \sum \mathbf{v}_i'$, where primes denote the relevant values, e.g. after collision.

In the following *we say that the collisions satisfying* 1), 2), 3) *are possible.*

Let the symbols [1], [2] denote the particles associated with the speeds respectively $1, \sqrt{2}$. We prove that for ternary collisions only [1] + [1] + [2] = idem are possible, and for quaternary collisions only [1] + [1] + [1] + [2] = idem, are possible.

Remark. ERNST [9] has recently emphasized the existence of spurious microscopic conservation laws for the multispeed DBMs without rest particles. For the present models it means the following. Let a_1, a_2 and a_1', a_2' denote the number of loss and gain particles associated with [1], [2]. From conservation of mass and energy we get: $a_1 + a_2 = a_1' + a_2'$, $a_1 + 2a_2 = a_1' + 2a_2'$, deduce $a_1 = a_1'$, $a_2 = a_2'$ and the number of slow and fast particles is conserved separately.

LEMMA 1. For ternary collisions only [1] + [1] + [2] → idem, is possible (i.e. satisfies 1), 2), 3)). For quaternary collisions only [1] + [1] + [1] + [2] → idem, is not possible.

P r o o f. For ternary collisions the four possible types of collisions are [1]+[1]+[1] = idem, [1]+[1]+[2] = idem, [1]+[2]+[2] = idem, [2]+[2]+[2] = idem. We also note that in the square $8v_i$ model there are only four different velocity vectors $\mathbf{v}_i$ of the [1] type, and four of the [2] type.

Firstly, we prove that the first and the last type of ternary collisions is not possible.

• If $\mathbf{v}_1 \neq \mathbf{v}_2 \neq \mathbf{v}_3 \neq \mathbf{v}_1$, then it follows from 1) that all the postcollisional particles have the same velocity $\mathbf{v}'_4$, therefore 3) is violated.

• For $\mathbf{v}_1 = \mathbf{v}_2 \neq \mathbf{v}_3$ there are two cases: either $\mathbf{v}_1 + \mathbf{v}_3 = 0$, or $\mathbf{v}_1 \perp \mathbf{v}_3$. In the former case 1) implies that $\mathbf{v} = \mathbf{v}_1 \perp \mathbf{v}'$, which contradicts 3). In the latter case 1) implies that for each i either $\mathbf{v}'_i = -\mathbf{v}_1$, or $\mathbf{v}'_i = -\mathbf{v}_3$, which again contradicts 3).

• Finally, if $\mathbf{v}_1 = \mathbf{v}_2 = \mathbf{v}_3$, then $\mathbf{v} = 3\mathbf{v}_1 = \mathbf{v}'$, which contradicts 1).

Secondly, we prove that the third type with two particles [2], with pre- and postcollisional velocities, respectively, $\mathbf{v}_i$, $\mathbf{v}'_i$, $i = 1, 2$, and one particle [1], with the velocities $\mathbf{v}_3$, $\mathbf{v}'_3$ is not possible. There are three cases.

CASE I. $\mathbf{v}_1 + \mathbf{v}_2 = 0$

Then either $\mathbf{v}'_1 + \mathbf{v}'_2 = 0$, which implies $\mathbf{v}_3 = \mathbf{v}'_3$ in contradiction with 1), or $\mathbf{v}'_1 = \mathbf{v}'_2$, which implies $\mathbf{v} = \mathbf{v}_3 \neq 2\mathbf{v}'_1 + \mathbf{v}'_3 = \mathbf{v}'$, which contradict 3).

CASE II. $\mathbf{v}_1 + \mathbf{v}_2 \neq 0$, and $\mathbf{v}_1 \neq \mathbf{v}_2$

Then either $\mathbf{v}'_1 + \mathbf{v}'_2 = 0$ [excluded by the constraint 1)], or $\mathbf{v}'_1 + \mathbf{v}'_2 \neq 0$. The latter inequality implies $\mathbf{v}_1 + \mathbf{v}_2 + \mathbf{v}'_1 + \mathbf{v}'_2 = 0$, but then 3) would imply $\mathbf{v} = \mathbf{v}'$, i.e. 1) would be violated.

CASE III. $\mathbf{v}_1 = \mathbf{v}_2$

In this case, from above only $\mathbf{v}'_1 = \mathbf{v}'_2$ is possible. Adding $\mathbf{v}_3$ and $\mathbf{v}'_3$ with speeds 1 we again find that $\mathbf{v} = \mathbf{v}'$ is not possible.

Thus, there remains only one type of ternary collisions: [1] + [1] + [2] → idem. For the restriction along the $x = x_1$ axis, the three possible subtypes of ternary [1] + [1] + [2] → idem collisions are presented in Fig. 1b-C-D-E, where each diagram represents all the collisions obtained by applying all the symmetries of the square $d = 2$ model. As illustration, we write down the collision terms for N_1 and R:

$$(2.10)\quad N_1: \quad Q_C = R(M_2N_1 - M_1N_2),$$
$$Q_D = (M_1^2N_2 - N_1R^2) + (R^2N_2 - M_2^2N_1), \qquad Q_E = Q_D;$$

$$(2.11)\quad R: \quad Q_C = 0, \qquad Q_D = 2(M_1^2N_2 - R^2N_1) + 2(N_1M_2^2 - R^2N_2),$$
$$Q_E = Q_D + 2(N_1M_1M_2 - R^2N_1) + 2(N_2M_1M_2 - R^2N_2).$$

REMARK. We notice that the absence of the [2] + [2] + [1] = idem type of collisions is peculiar to the square model. For the cubic CABANNES [8] model discussed later on, with speeds 1, $\sqrt{3}$, and the symbols respectively [1], [3], the collisions [3] + [3] + [1] = idem are possible (i.e. satisfy 1), 2), 3)).

For the quaternary collisions we show that [1] + [1] + [1] + [2] → idem is not possible. The collisions [2] + [2] + [2] + [2] = idem give zero contribution to the collision operators when the x-axis is chosen along the median. All other types of the quaternary collisions are presented in Fig. 1b.

Let $\mathbf{v}_i$, $\mathbf{v}'_i$ $i = 1, 2, 3$, be the [1] velocities.

• First if $\mathbf{v}_1 \neq \mathbf{v}_2 \neq \mathbf{v}_3 \neq \mathbf{v}_1$, then their sum is $\mathbf{v}_1$, while $\mathbf{v}'_i$ has multiplicity three and the sum is $-3\mathbf{v}_1$. Adding $\mathbf{v}_4$, $\mathbf{v}'_4$ gives $\mathbf{v} \neq \mathbf{v}'$.

• Second $\mathbf{v}_1 = \mathbf{v}_2 = -\mathbf{v}_3$ with a sum $\mathbf{v}_1$ while the sum of the three $\mathbf{v}'_i$ is either $\mathbf{v}'_1$ or $3\mathbf{v}'_1$ perpendicular to $\mathbf{v}_1$ (we take into account spectatorless collisions). Adding in both cases $\mathbf{v}_4$, $\mathbf{v}'_4$ associated with [2] we necessarily find $\mathbf{v} \neq \mathbf{v}'$.

• Third $\mathbf{v}_1 = \mathbf{v}_2 \neq -\mathbf{v}_3$. For one of the two x_1, x_2 coordinates, the difference between the values of $\sum_1^3 \mathbf{v}_i$, $\sum_1^3 \mathbf{v}'_i$ has modulus 3. Adding $\mathbf{v}_4$, $\mathbf{v}'_4$ belonging to [2], the modulus of this difference is at least 1 and $\mathbf{v} \neq \mathbf{v}'$. ◊

REMARK. Other collisions can occur, for instance the pseudotriple, $\sigma_P^{(i)}$, $i = 1, 2$, not shown in Fig. 1b, with one particle spectator in both loss and gain terms... The multiple collisions can be divided in two other subclasses: one where two (or more) particles with the same velocities can collide, cf. Fig. 1b-D-E-F-G-I-J-K-L, and the other, Fig. 1b-C-H, with only one particle in each direction.

3. Rankine–Hugoniot relations, asymptotic states, shock inequalities

The R-H relations [1, 7] are the three conservation laws for asymptotic values at $\mp\infty$ of the densities functions of a similarity variable η. These asymptotic values satisfy relations coming from vanishing of the collision terms at $\mp\infty$.

We assume that the densities are functions of a similarity variable $\eta = x - \zeta t$ and define for R, N_i, M_i, $i = 1, 2$ two asymptotic states when $|\eta| = \infty$:

$$\begin{aligned} &\text{(i)} : (n_{0i}, m_{0i}, r_0), \\ &\text{(ii)} : (s_i = n_{0i} + n_i,\ p_i = m_{0i} + m_i,\ r_{00} = r_0 + r), \qquad i = 1, 2. \end{aligned} \tag{3.1}$$

We get for n_i, m_i, r, from the linear (2.1) relations ($z := 2(1 - \zeta)/d_*\zeta$):

$$\begin{gathered} n_2/n_1 = y = (1 - \zeta)/(1 + \zeta), \qquad y m_1 = m_2 + 2ry/z, \\ m_1 + 2d_* n_1 + m_2/y = 0. \end{gathered} \tag{3.2}$$

The two collision terms Q_2, Q_1 in (2.2) vanish for the (i) and (ii) states, therefore:

$$(3.3)_1 \quad n_{01} m_{02} = n_{02} m_{01}, \qquad m_{01} m_{02} = r_0^2, \qquad s_1 p_2 = s_2 p_1, \qquad p_1 p_2 = r_{00}^2 .$$

Only n_i, m_i, r enter Eq. (3.2), so that in order to solve (3.2), $(3.3)_1$ it is convenient to introduce new parameters a_{0i}, b_{0i}. These parameters are products of the densities n_{0i}, n_i, m_{0i}, m_i, r_0, r and we can rewrite the two last $(3.3)_1$ relations taking into account the two first:

$$\begin{gathered} a_{0i} + b_{0i} = 0, \qquad i = 1, 2, \\ a_{01} := n_{01} m_2 + m_{02} n_1 - n_{02} m_1 - m_{01} n_2, \qquad b_{01} := n_1 m_2 - n_2 m_1, \\ a_{02} := m_{01} m_2 + m_{02} m_1 - 2 r_0 r, \qquad b_{02} = m_1 m_2 - r^2. \end{gathered} \tag{3.3}_2$$

The multiple collision terms Q_{it}, Q_{iq} written down in (2.4)–(2.5), containing linearly Q_1, Q_2, vanish for the (i), (ii) states. We determine the general solution of (3.2)–(3.3), (Appendix A), with the relations $a_{0i} + b_{0i} = 0$. Thus, the asymptotic (i), (ii) states are determined from one scaling parameter, two arbitrary parameters of one asymptotic state, and from the propagation speed ζ:

$$(3.4) \qquad n_{01} = 1, \qquad m_{01} > 0 \text{ arbitrary}, \qquad n_{02} > 0 \text{ arbitrary}, \qquad |\zeta| < 1.$$

In Appendix A we give the analytical proof of positivity of the asymptotic states with well-defined conditions, for brevity only for two cases: either at the (ii) state only $p_2 \neq 0$ with one arbitrary parameter, or both $s_2 \neq 0$, $p_2 \neq 0$ with two arbitrary parameters.

In order to know whether the (i) or the (ii) state is the upstream or downstream state, we apply the LAX [10] admissibility criterion: let $\zeta^{(j)}_{\pm\infty}$ be the characteristic speeds associated with the state at $\eta = \pm\infty$, then for some index $j = 1, 2, 3$ the following inequality holds: $\zeta^{(j)}_{\infty} < \zeta < \zeta^{(j)}_{-\infty}$. *The supersonic and subsonic inequalities are independent of the values of the cross-sections of all collision terms and depend only on the values of the equilibrium states*. To the two states (i) and (ii) we associate the characteristic velocities $\zeta_{(i)}, \zeta_{(ii)}$, the stream velocities $U_{(i)}, U_{(ii)}$, which are asymptotic values of the stream velocity U: $M = M_1 + M_2 + d_*(R + N_1 + N_2)$, $UM = M_1 - M_2 + d_*(N_1 - N_2)$, the shock velocities $V_{(i)} = \zeta - U_{(i)}$, $V_{(ii)} = \zeta - U_{(ii)}$, and the sound-wave velocities $W_{(i)} = \zeta_{(i)} - U_{(i)}$, $W_{(ii)} = \zeta_{(ii)} - U_{(ii)}$. For the shock inequalities we have to verify $|W| < |V|$ (or $>$) at the upstream (or downstream) state. In all numerical examples presented later on we have verified the shock inequalities. In the joint paper [11] we will study the Whitham stability of the asymptotic states and the properties of the characteristic velocities.

4. Exact similarity shock waves solutions

4.1. Application of the Section 2 R-H relations

Substituting the similarity densities (1.1) into (2.1)–(2.5) we obtain seven R-H relations for the (i), (ii) states which are constructed from the three (3.4) parameters in the general case or from one or two parameters for the particular solutions. We know all quantities associated with the (i) and (ii) states, for instance (see Appendix B1) for the mass $M = m_0 + mD^{-q}$, $D = 1 + e^{\gamma\eta}$ and the shock thickness $w^{(p)} = (1 + q^{-1})^{q+1}/|\gamma^{(p)}|$, both m_0, m are known while $\gamma^{(p)}$, $p = 2$ (binary), $= 3$ (ternary), $= 4$ (quaternary) is unknown. Consequently the ratio $w^{(p)}/w^{(2)}$ is small for multiple collisions if $\gamma^{(p)}/\gamma^{(2)}$ is large. In Sec. 3 we consider only the vanishing of the collision terms. As we shall see this is sufficient to deal with any collision term. As an example we consider

$$Q_2 = M_1 M_2 - R^2 = (m_{01} + m_1 D^{-q})(m_{02} + m_2 D^{-q}) - (r_0 + r D^{-q})^2$$

which becomes a sum of a constant $m_{01}m_{02} - r_0^2 = 0$ (asymptotic state when $D \to \infty$ or $\gamma\eta \to \infty$), a D^{-q} term multiplied by a constant $m_{01}m_2 + m_{02}m_1 - 2rr_0$ and a D^{-2q} term multiplied by another constant $m_1m_2 - r^2$. The other asymptotic state corresponds to $\gamma\eta \to -\infty$ or $D \to 1$. Consequently the two D^{-q}, D^{-2q} constants are opposite and $Q_2 = a_{02}D^{-q}(1 - D^{-q})$ with $a_{02} = m_{01}m_2 + m_{02}m_1 - 2r_0r$. Using the same method for $Q_1 = N_1M_2 - N_2M_1$ we find $a_{01}D^{-q}(1 - D^{-q})$ with $a_{01} = n_{01}m_2 + m_{02}n_1 - n_{02}m_1 - n_2m_{01}$. Similarly for a ternary collision term, the constant vanishes (asymptotic state $D \to \infty$) and the sum of the three constants associated with D^{-kq}, $k = 1, 2, 3$ is zero (asymptotic state associated with $D \to 1$).

New relations will come from the complete study of the nonlinear equations (2.3). In the nonlinear terms the new parameters will be the positive constants $\sigma_C, \ldots \sigma_L$ and γ from the differential terms. Writing these equations as sums of D^{-q} terms with different powers, we put to zero the associated coefficients. These coefficients contain linearly γ and the cross-sections. Consequently all the cross-sections are not arbitrary parameters and we choose subsets of positive cross-sections from which we can determine all other positive cross-sections. For simplicity the positivity study is done numerically.

4.2. Relations coming from the nonlinear (2.3) equations

We rewrite the two nonlinear equations associated with N_1, R:

$$p_+N_1 = Q_{1,b} + Q_{1,p} + Q_{1,t} + Q_{1,q}, \qquad \partial_t R = Q_{2,b} + Q_{2,p} + Q_{2,t} + Q_{2,q}.$$

We recall that $q = 1/(p-1)$ and the linear differential parts give two terms

$$p_+N_1 = (1-\zeta)n_1\gamma q\left[D^{-(q+1)} - D^{-q}\right], \qquad \partial_t R = -r\zeta\gamma q\left[D^{-(q+1)} - D^{-q}\right] \tag{4.1}$$

with $q = 1, 1/2, 1/3$ respectively, for only binary collisions, or adding pseudotriple and ternary collisions, or with quaternary included collisions. In the nonlinear parts of (2.2) we have different possibilities depending upon whether we choose only binary or adding ternary or including also quaternary collisions. For binary alone we have only terms proportional to D^{-q}, D^{-2q}. If ternary or pseudotriple collisions are included, we have D^{-q}, D^{-2q}, D^{-3q} terms and finally, with quaternary collisions, we have in addition a term proportional to D^{-4q}. The relation will be obtained requiring that the coefficients of any power of D^{-q} are the same in both lhs and rhs of (2.2).

Firstly, when only binary colisions occur we get for the nonlinear terms:

$$Q_{1b} = a_{01}(D^{-2q} - D^{-q})\sigma_B^{(2)}, \qquad Q_{2b} = a_{02}(D^{-q} - D^{-2q})\sigma_B^{(1)}, \tag{4.2}$$

with a_{0i} defined in $(3.3)_2$. Equalizing the coefficients of D^{-q}, D^{-2q} in (4.1), (4.2) we find two relations:

$$(1-\zeta)n_1\gamma^{(2)} = \sigma_B^{(2)}a_{01}, \qquad r\zeta\gamma^{(2)} = \sigma_B^{(1)}a_{02}. \tag{4.3}$$

Secondly, adding pseudotriple and ternary collisions we define $Q_{i,b+p+t} = Q_{ib} + Q_{ip} + Q_{it}$, $i = 1,2$ that we write down with (2.3)–(2.4):

$$(4.4)\qquad Q_{1,b+p+t} = -Q_1\left[\sigma_B^{(2)} + M\sigma_P^{(2)} + \sigma_C R + M_{12}^{+}\sigma_{DE}\right] + Q_2 N_{12}^{-}\sigma_{DE}$$
$$= a_{03}D^{-q} - (a_{03} + b_{03})D^{-2q} + b_{03}D^{-3q},$$

$$(4.5)\qquad Q_{2,b+p+t} = -Q_1 2M_{12}^{-}\sigma_{DE} + Q_2\left[\sigma_B^{(1)} + M\sigma_P^{(1)} + 2N_{12}^{+}(\sigma_{DE} + \sigma_E)\right]$$
$$= a_{04}D^{-q} - (a_{04} + b_{04})D^{-2q} + b_{04}D^{-3q}.$$

The coefficients a_{0i}, b_{0i}, $i = 3,4$ are written down in Appendix B, cf. (B.2)–(B.5). They contain linearly the binary coefficients a_{0i}, $i = 1,2$ with factors both linear in the (i) state asymptotic densities n_{0i}, m_{0i}, r_0 and in the cross-sections $\sigma_B^{(i)}$, $\sigma_P^{(i)}$, σ_C, σ_D, σ_E. Equalizing the coefficients of D^{-kq}, $k = 1,2,3$ in (4.1), (4.4), (4.5) we obtain four independent relations:

$$(4.6)\qquad -(1-\zeta)n_1\gamma^{(3)}/2 = a_{03}, \qquad r\zeta\gamma^{(3)}/2 = a_{04}, \qquad a_{0i} + b_{0i} = 0, \qquad i = 1,2.$$

Thirdly, adding quaternary collisions (2.5) we define: $Q_{i,b+p+t+q} = Q_{i,b+p+t} + Q_{iq}$, $i = 1,2$. The $Q_{i,b+p+t}$ are the same as (4.4), (4.5) with the only change $q = 1/2 \to 1/3$. The quaternary terms Q_{iq} are of the type:

$$(4.7)\qquad a_{04+i}D^{-q} + b_{04+i}D^{-4q} + c_{04+i}D^{-3q} - (a_{04+i} + b_{0+4+i} + c_{0+4+i})D^{-2q}, \quad i = 1,2.$$

The particular structure in (4.4)–(4.7) of the coefficients of the D^{-kq} powers comes from the fact that these collision terms vanish at one asymptotic state when $D = 1$. The coefficients a_{0j}, b_{0j}, c_{0j}, $j = 5,6$ are written down (for brevity we put $\sigma_K = \sigma_L = 0$) in Appendix B, cf. (B.6)–(B.9). They still contain factors linear in the cross-sections $\sigma_B^{(i)}$, $\sigma_P^{(i)}$, $\sigma_C, \ldots \sigma_L$, but quadratic in the asymptotic densities of the (i) state. Equalizing the coefficients of D^{-kq}, $k = 1,2,3$ in both the linear terms (4.1) and the nonlinear terms $Q_{i,b+p+t+q}$ we obtain six relations:

$$(4.8)\qquad (1-\zeta)n_1\gamma^{(4)}/3 = a_{03} + a_{05}, \qquad \zeta r\gamma^{(4)}/3 = a_{04} + a_{06},$$
$$b_{02+i} + c_{04+i} = 0, \qquad a_{02+i} + a_{04+i} + b_{04+i} = 0, \qquad i = 1,2.$$

4.3. Solutions for binary and binary plus multiple collisions

Firstly, when we consider only binary collisions, we have three new parameters $\gamma^{(2)}$, $\sigma_B^{(i)} \neq 0$, $i = 1,2$ and two new relations (4.3). *In addition to the arbitrary* (3.4) *parameters, for* $p = 2, q = 1$ *the similarity shock waves are determined with the parameter* $\sigma_B^{(1)}$ and, from (4.3), $\gamma^{(2)}$ and $\sigma_B^{(2)}$ are deduced.

Secondly, for binary, pseudotriple and ternary collisions $p = 3$, $q = 1/2$ we have eight new parameters $\gamma^{(3)}$, $\sigma_B^{(i)}$, $\sigma_P^{(i)}$, σ_C, σ_D, σ_E and four new relations (4.6).

In addition to the (3.4) *parameters, the similarity shock waves are determined by four arbitrary parameters chosen among the cross-sections*. If furthermore we compare the two cases where either the binary collisions are alone or not, while the two equilibrium states ζ and $\sigma_B^{(i)}$ are the same, we only have another parameter $\gamma^{(2)}$ and two new relations (4.3). From (4.3) $\sigma_B^{(2)} = \sigma_B^{(1)} a_{02} n_1 / a_{01} r \zeta$ is fixed, the two γ values are different, in addition to (3.4) we have three arbitrary parameters and we can compare the shock profiles in both cases by evaluating the ratio $w^{(2)}/w^{(3)}$ which is proportional to $\gamma^{(3)}/\gamma^{(2)}$. From (4.3)–(4.6), (B.2) we get $\gamma^{(3)}/2\gamma^{(2)} = -a_{03}/a_{01}\sigma_B^{(2)} > 1$ either if $n_{01} = n_{02}$ (uniform (i) state) or if $\sigma_{DE}/\sigma_B^{(2)} \ll 1$.

Thirdly, for binary, pseudotriple, ternary and quaternary collisions $p = 4$, $q = 1/3$ we have fifteen new parameters $\gamma^{(4)}, \sigma_B^{(i)}, \sigma_P^{(i)}, \sigma_C, \sigma_D, \ldots \sigma_K, \sigma_L$ and six new relations (4.8). *In addition to the* (3.4) *parameters, the similarity shock waves are determined by nine arbitrary parameters chosen among the cross-sections*. If we want to compare it with the case where only binary collisions occur, we still loose one parameter (from (4.3) we see that the ratio $\sigma_B^{(1)}/\sigma_B^{(2)}$ is not arbitrary but fixed). Similarly, as above the ratio $w^{(4)}/w^{(2)}$ is proportional to $\gamma^{(4)}/\gamma^{(2)}$. From (4.3)–(4.8), (B.4)–(B.8) we get: $\gamma^{(4)}/3\gamma^{(2)} = (a_{04} + a_{06})/a_{02}\sigma_B^{(1)} > 1$ if either $n_{01} = n_{02}$ (uniform (i) state) or if $\sigma_{CD}/\sigma_B^{(1)} \ll 1$. If Fig. 1b-K collision is taken into account it is sufficient to have in addition $\sigma_K/\sigma_B^{(1)} \ll 1$.

5. Numerical calculations for compressive shocks

In Figs. 2a-b, 3a-b-c, we present numerical calculations for the exact solutions of Sec. 3, and in Fig. 4a-b those of the Runge-Kutta procedure (Appendix C).

In Figs. 2a-b, for the $d = 2, 3$ models, the two equilibrium states, ζ, $\sigma_B^{(1)} = 1$ and $\sigma_B^{(2)}$ are the same for binary alone and ternary included collisions. In Fig. 2a the R-H solutions are obtained with the general (3.4) formalism and the (i) upstream state is at $+\infty$. We have $\sigma_B^{(i)} = \sigma_P^{(i)} = 1$, $\sigma_E = 0$ and deduce: $\sigma_D = 6 \cdot 10^{-4}$, $\sigma_C = 5 \cdot 10^{-3}$. In Fig. 2b the (ii) upstream state is at $+\infty$ with only $s_2 \neq 0$, $p_2 \neq 0$. We have $\sigma_B^{(2)} = 0.011$, $\sigma_E = 0$, $\sigma_P^{(1)} = 1$, and deduce: $\sigma_P^{(2)} = 7 \cdot 10^{-4}$, $\sigma_D = 54$, $\sigma_C = 61$ and observe small values for the ratios of the two shock thickness. The shock inequalities are satisfied, and we find small ratios of the two shock thicknesses.

Figs.	d	ζ	$\zeta_{(i)}$	$\zeta_{(ii)}$	V_i	W_i	V_{ii}	W_{ii}	$\gamma^{(2)}$	$\gamma^{(3)}$	$w^{(3)}/w^{(2)}$
2a	2	.69	0.43	0.82	1.3	1.03	.64	0.77	131.	510^4	$(1/3)10^{-2}$
2b	3	.997	0.9998	0	.183	0.186	1.9998	1	−.04	−3.5	$(1.6)10^{-2}$

In Fig. 3(a-b-c) with $d = 2$, $n_{01} = 1$, $\sigma_B^{(1)} = 1$ for binary alone (a) or ternary (b) and quaternary ($\sigma_K = \sigma_L = 0$) collisions included (c), the two equilibrium

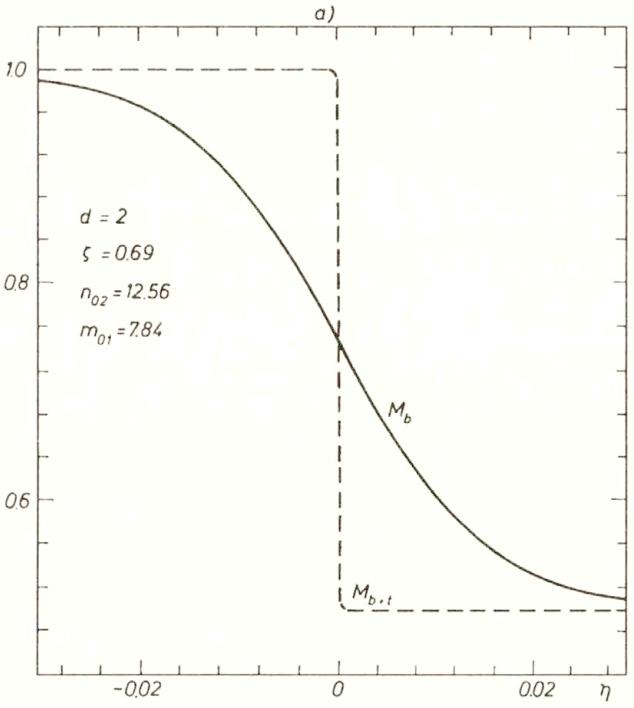

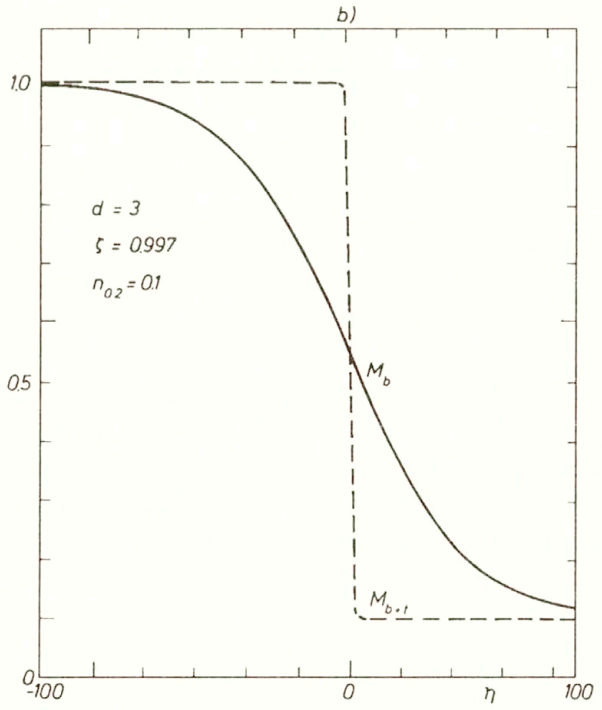

FIG. 2. Binary and ternary.

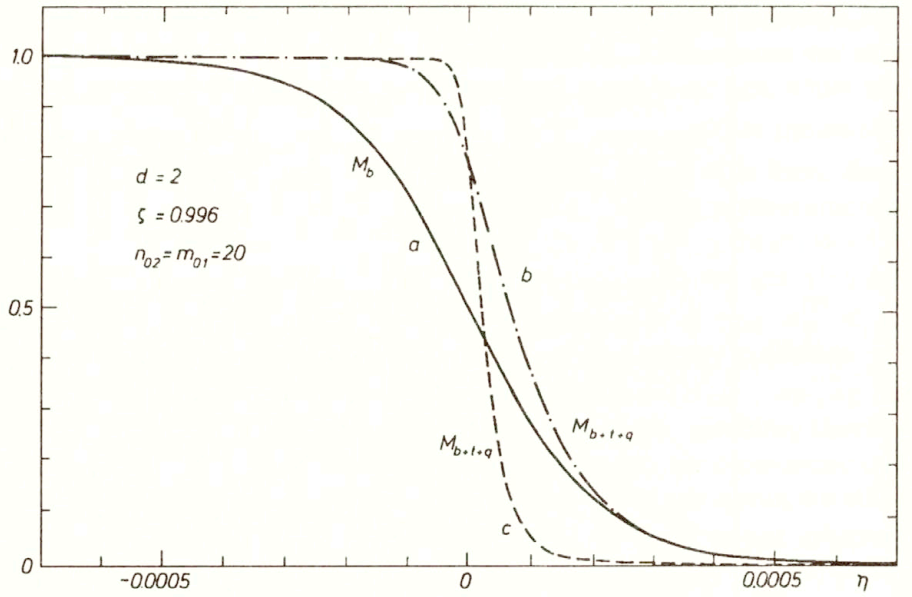

FIG. 3. Binary, ternary and quaternary.

states and ζ are the same. Further in (a-b), $\sigma_B^{(2)} = 0.098$ are the same while in (c) $\sigma_B^{(2)} = 0.05$. We get $\gamma^{(2)} = 9 \cdot 10^3$, $\gamma^{(3)} = 3 \cdot 10^4$, $\gamma^{(4)} = 9 \cdot 10^4$ and for the cross-sections:

	σ_E	σ_C	σ_D	$\sigma_P^{(1)}$	$\sigma_P^{(2)}$	σ_I	σ_{FJ}	σ_H	σ_G
3b	0	0	0	$3 \cdot 10^{-7}$	10^{-8}	$1.5 \cdot 10^{-7}$	$3 \cdot 10^{-9}$	$3.7 \cdot 10^{-7}$	$7.5 \cdot 10^{-9}$
3c	$2 \cdot 10^{-5}$	$9 \cdot 10^{-6}$	$6 \cdot 10^{-4}$	$5 \cdot 10^{-7}$	$1.6 \cdot 10^{-6}$	$5 \cdot 10^{-7}$	10^{-8}	$12.5 \cdot 10^{-7}$	$2.5 \cdot 10^{-8}$

The ratios of the two thicknesses $w^{(4)}/w^{(2)} = 0.53,\ 0.16$ in Figs. 3(b-c) are not small. In Fig. 4a we plot the M_1 densities for the uniform (i) state: $n_{01} = \ldots = r_0 = 1 \ldots$ Profile a corresponds to the binary collisions. In b profile we included triple collisions with $\sigma_P^{(i)} = 0$, $\sigma_C = \sigma_D = \sigma_E = 0.005$ for b, and $\sigma_P^{(i)} = 0$, $\sigma_C = \sigma_D = \sigma_E = 0.02$ for c. While the M_1 overshoot persists for small ternary cross-sections, it disappears for larger values. In d all ternary cross-sections are zero, while $\sigma_I = \sigma_F = \sigma_J = \sigma_H = \sigma_G = 0.02$, $\sigma_K = \sigma_L = 0$.

	m_{01}	n_{02}	ζ	$\zeta_{(i)}$	$\zeta_{(ii)}$	V_i	W_i	V_{ii}	W_{ii}
4a	1	1	0.995	0.913	0.999	0.995	0.913	0.047	0.051
4b	1	1	−0.99	−0.913	−0.998	−0.99	−0.913	−0.098	−0.107

It can be seen that the length of the interval of the density changes in the shock decreases when the multiple collisions are added, cf. Fig. 4a. In Fig. 4b we show

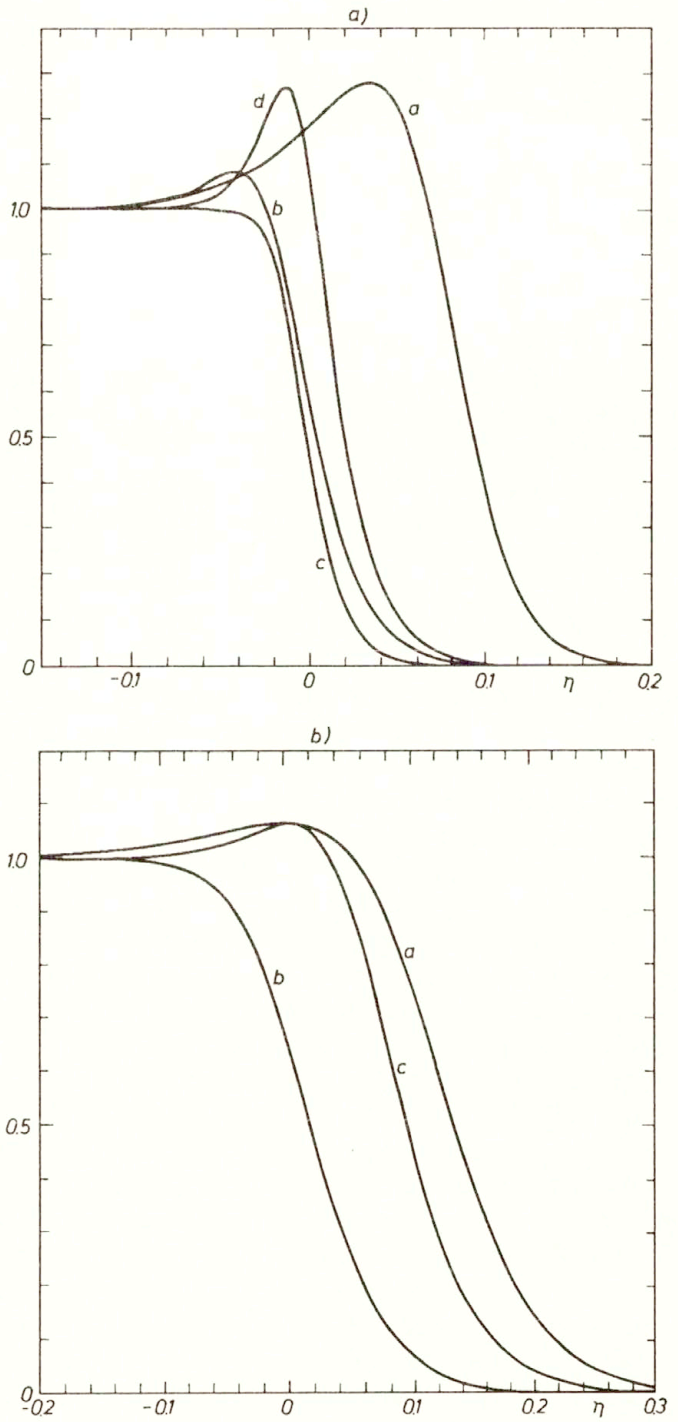

FIG. 4. a) M_1 profiles, $d = 2$, $\zeta = 0.995$, b) M_2 profiles, $d = 2$, $\zeta = 0.99$.

M_2 for the uniform (i) state, and observe analogous phenomena, with a profile as before, b with 0.02 for ternary and zero for quaternary cross-sections, c with zero for ternary and $\sigma_I = \sigma_F = \sigma_J = \sigma_H = \sigma_G = 0.02$, $\sigma_K = \sigma_L = 0$.

6. Discussion and generalizations

6.1. Discussion of the models with x-axis along the median

One motivation of this paper was to show that multiple collisions can be handled by analytical methods. Comparing the (1.1) type of exact solutions to the R-K numerical solutions we see that we loose some properties at the microscopic level (possible overshoots of some densities) but not at the macroscopic one. Furthermore we are able to give sufficient conditions for the decrease of the width of the shock when multiple collisions are present. Adding fifth-order collisions (not presented) we have observed the same features. The present construction of the exact solutions, independent of the fact that the equilibrium states are common to binary alone collisions or multiple included (cf. ternary collisions for the unispeed hexagonal model [4]), can be done for any DBM.

Another motivation for the study of multiple collisions is the generalization of the Whitham stability of the equilibrium states which has only been done for models with binary collisions. This study is presented in the joint paper [11].

The present results are generic for a whole class of DBMs. Requiring spectatorless collisions, microscopic conservation laws and microreversibility, we can construct multiple collisions for a given p-th order. The simplest model associated with the present one is the $9v_i$ model [12] with a rest particle. In a recent work [13] the two $8v_i, 9v_i$ models were compared. In this work [13] a criterion, based on the assumption that equilibrium states are the same for binary and multiple collisions, was established for the H-Theorem. This criterion allows to check, for any multiple collision term, that the contribution associated with any density is correct. As we shall see in the joint paper [11], the joint criterion is satisfied for all Fig. 1b multiple collisions.

In this paper we have verified the following interesting result. *The multiple collision terms associated with a given density contain the binary collision terms multiplied by factors which are densities-dependent. For any nonlinear equation associated with a particular density we always find one nonnegative factor of a binary collision term. For that density, this binary collision term corresponds to a binary collision.* Are these properties peculiar to the present class of models or to the fact that we choose the shock axis along the median of the square model? In the next subsection we study the $14v_i$ Cabannes model [8] with speeds $1, \sqrt{3}$, and in subsection 6.3 – the present models with x-axis along the diagonal of the $8v_i$ square, cf. Fig. 1c. In both cases we find the same results concerning the factors of the binary collision terms when multiple collisions are present.

6.2. Cabannes model

The cubic CABANNES [8] model is a $14v_i, d = 3$ model with densities M_i, R being the same as in Sec. 1. On the contrary, the N_i are associated with the speed $\sqrt{3}$, with different velocities in the space: $N_1 : (1, \pm 1, \pm 1)$, $N_2 : (-1, \pm 1, \pm 1)$, but have the same projections $1, -1$ along the $x = x_1$ axis. Writing [1], [3] for the particles associated with the speeds $1, \sqrt{3}$, for this model, in addition to the multiple collisions studied previously we have new collisions: [1] + [3] + [3] $\rightarrow$ idem, [1] + [1] + [1] + [3] $\rightarrow$ idem. For brevity we consider the ternary collisions. As an example of such collisions we give $\mathbf{v}_1 + \mathbf{v}_2 + \mathbf{v}_3 = \mathbf{v}_1' + \mathbf{v}_2' + \mathbf{v}_3'$ with for the $\mathbf{v}_i$ coordinates: $(1,1,1)$, $(1,-1,-1)$, $(-1,0,0)$ and for $\mathbf{v}_i'$: $(1,-1,1), (-1,1,-1), (1,0,0)$. In addition to the collisions presented in Fig. 1b, there exist collisions with two $\sqrt{3}$ speed particles. The relevant nonlinear equations read:

$$
\begin{aligned}
p_+ N_1 &= \ldots (-Q_1)(N_1 + N_2), \\
\partial_t R &= \ldots + 0, \\
p_+ M_1 &= \ldots 4Q_1(N_1 + N_2),
\end{aligned}
\tag{6.1}
$$

where points represent all Fig. 1b collisions. The three linear conservation laws are satisfied. The additional collisions contain linearly only the binary collision term $-Q_1$, Q_1, present at the binary level respectively for $p_+ N_1, q_+ M_1$, with positive factors proportional to $N_1 + N_2$.

6.3. Multiple collisions for the $8v_i$ square model with x-axis along the diagonal

For brevity we consider only the $d = 2$, $8v_i$ square model, cf. Fig. 1c, with coordinates (x_1, x_2) for the velocities: $(\pm 1, \pm 1)$, $(\pm 2, 0)$, $(0, \pm 2)$. For the solutions with the $x = x_1$ axis along the diagonal of the square, we define the densities [6, 12] M_1, N_1, R, N_2, M_2 associated with the velocities with x_1 coordinates, respectively $2, 1, 0, -1, -2$. We have three linear relations and only two nonlinear independent ones that we write for binary collisions, using notation $q_\pm := \partial_t \pm 2\partial_x$, $p_\pm := \partial_t \pm \partial_x$:

$$
\begin{aligned}
&q_+ M_1 + p_+ N_1 + \partial_t R = 0, \qquad p_+ N_1 + p_- N_2 = 0, \\
&q_- M_2 + p_- N_2 + \partial_t R = 0, \qquad p_+ N_1 = \sigma_B^{(1)}(Q_1 + Q_2), \\
&\partial_t R = \sigma_B^{(2)} Q_3 + \sigma_B^{(1)}(Q_2 - Q_1), \qquad Q_1 = N_2 R - N_1 M_2, \\
&Q_2 = M_1 N_2 - N_1 R, \qquad Q_3 = M_1 M_2 - R^2, \\
&q_+ M_1 = -\sigma_B^{(2)} Q_3 - 2\sigma_B^{(1)} Q_2.
\end{aligned}
\tag{6.2}
$$

Thus, at the binary level we have three Q_i collision terms, $\partial_t R$ has the three terms while $p_+ N_1$ and $q_+ M_1$ have only two. We can expect the following structure when

multiple collisions, cf. Fig. 1c, are present:

$$
\begin{aligned}
p_+N_1 &= Q_1(\sigma_B^{(1)} + A_{11}) + Q_2(\sigma_B^{(1)} + A_{21}) + Q_3A_{31},\\
q_+M_1 &= Q_1A_{12} - 2Q_2(\sigma_B^{(1)} + A_{22}) - Q_3(\sigma_B^{(2)} + A_{32}),\\
R_t &= -Q_1(\sigma_B^{(1)} + A_{13}) + Q_2(\sigma_B^{(1)} + A_{23}) + Q_3(\sigma_B^{(2)} + A_{33})
\end{aligned}
\tag{6.3}
$$

Below we present, cf. Fig. 1c, the collision terms corresponding to the ternary, quaternary and fifth order collisions. We omit for brevity the positive multipliers (ternary, quaternary and fifth order collision rates) in front of the relevant expressions, and report the A_{11}, A_{31}, A_{12}, A_{22}, A_{32}, A_{33} factors of the binary terms for the collisions associated with Fig. 1c-C-D...S-T. With the transform $N_1 \longleftrightarrow N_2$, $M_1 \longleftrightarrow M_2$ we get $A_{11} \longleftrightarrow A_{21}$. From the first linear (6.2) relation we obtain other coefficients: $A_{13} = A_{11} + A_{12}$, $A_{23} = 2A_{22} - A_{21}$ or $A_{13} \longleftrightarrow A_{23}$ and finally with $A_{31} + A_{33} = A_{32}$ we can check the results.

Q	A_{11}	A_{31}	A_{12}	A_{22}	A_{32}	A_{33}
C	N_1	0	$-N_1$	$N_2/2$	0	0
D	$2N_1$	0	$-2N_1$	N_2	0	0
E	N_{12}^+	0	0	N_{12}^+	0	0
F	$2RN_1$	0	$-2RN_1$	RN_2	0	0
G	P_2	0	0	P_1	$2N_1N_2$	$2N_1N_2$
H	0	0	0	0	$2N_1N_2$	$2N_1N_2$
I	0	0	0	0	$2P_3$	$2P_3$
J	$2P_2$	0	0	$2P_1$	0	0
K	$2P_2$	0	0	$2P_1$	$2N_{12}^2$	$2N_{12}^2$
L	M_1M_2	RN_{12}^-	$2M_1M_2$	$2M_1M_2$	P_4	$3RN_{12}^+$
M	$2M_1N_2N_{12}^+$	0	$-2M_1N_2N_{12}^+$	$M_2N_1N_{12}^+$	0	0
N	$P_5 + 3P_0$	0	$-P_6 - 2P_0$	$2(P_7 + P_0)$	0	0
O	$3P_8 + 4P_0$	0	$-P_6 - 2P_0$	$3P_0 + P_9$	0	0
P	$N_1N_2N_{12}^+$	0	0	$N_1N_2N_{12}^+$	0	0
Q	$2N_1^2N_2$	0	$-2N_1^2N_2$	$N_2^2N_1$	0	0
R	$M_1M_2N_{12}^+$	$RN_{12}^+N_{12}^-$	$2M_1M_2N_{12}^+$	$2M_1M_2N_{12}^+$	P_{10}	$3RN_{12}^{+2}$
S	P_{11}	N_{12}^{3-}	$-2P_{12}$	P_{13}	$2N_1^+$	N_{12}^{3+}
T	$2M_{12}^+N_{12}^+N_1$	$2N_{12}^-N_{12}^{+2}$	$-4N_1M_1N_{12}^+$	$2N_2M_1N_{12}^+$	$4N_1^2N_{12}^+$	$2N_{12}^2N_{12}^+$

with $N_{12}^{\pm} = N_1 \pm N_2$, $M_{12}^{\pm} = M_1 \pm M_2$ (as in Sec. 1), while $N_{12}^2 = N_1^2 + N_2^2$, $N_{12}^{3\pm} = N_1^3 \pm N_2^3$, $P_0 = RN_1N_2$, $P_1 = N_1R + N_2M_1$, $P_2 = N_2R + N_1M_2$, $P_3 = M_1M_2 + R^2$, $P_4 = 2R(N_2 + 2N_1)$, $P_5 = N_1^2(4R + 3M_2)$, $P_6 = N_1^2(4R + 2M_2)$, $P_7 = N_2^2(R + M_1)$, $P_8 = N_1^2(R + M_2)$. $P_9 = N_2^2(R + 2M_1)$, $P_{10} = 2RN_{12}^{+}(N_{12}^{+} + N_1)$, $P_{11} = M_1(N_1^2 + 3N_2N_{12}^{+}) + 3M_2N_1^2$, $P_{12} = M_1N_{12}^{+2} + M_2N_1^2$, $P_{13} = N_1N_2M_2 + 2(N_1^2M_2 + N_2^2M_1)$. All these terms, except $M_{12}^{-}, N_{12}^{-}, N_{12}^{3-}$ are positive.

1. Firstly, we discuss the coefficients of the binary terms associated with the p_+N_1, q_+M_1 equations. If only binary collisions occur, then in each equation there are two binary collision terms, cf. (6.2). *With multiple collisions included we observe that all A_{11}, A_{21}, A_{22}, A_{32} factors of these binary collision terms are nonnegative, while A_{31}, A_{12}, coefficients of the third binary collision terms, not present on the binary level, have not a well-defined sign. Consequently, at least two of the three factors are nonnegative.*

2. Secondly we discuss the coefficients of the three binary terms for R_i, which are all present on the binary level. *Although A_{33} is always nonnegative, this is not always true for A_{13} and A_{23}.* We find not well-defined signs in three cases of the fifth order collisions. For A_{13} and the collisions associated with O, S, T we respectively find: $N_1^2M_2 + RN_1(2N_2 - N_1)$, $-N_1^2M_{12}^{-} - M_1N_2N_{12}^{-}$ and $-2N_1N_{12}^{+}M_{12}^{-}$. Furthermore, due to the fact that A_{13}, A_{23} are exchanged when $N_1 \longleftrightarrow N_2$, $M_1 \longleftrightarrow M_2$, these two terms are both nonnegative or not. *Consequently either the three factors are nonnegative or only one.*

In conclusion, in the equation for any density we always find at least one term which is a product of a nonnegative, density-dependent factor, and a binary collision term. This binary collision terms remains also if only binary collisions occur.

With the same assumptions for the 5th order collisions as for the 4th and 3th order in Sec. 2, it can be shown that the collisions presented in Fig. 1c-M-N...S-T are the only possible ones.

From a partial study of the sixth order collision terms, concerning the nonnegativity or not of the A_{ii}, A_{ij} factors, we have found the same results as those presented here.

For the model with the x-axis along the median, with collisions up to the fifth order, we find the same features (presented in the joint paper [11]). Furthermore, for the factors of the binary terms not present at the binary level we still find that they have not a well-defined sign.

Appendix A. R-H relations

For the two (i), (ii) states (3.1) we have 11 parameters: $\zeta, n_{0i}, m_{0i}, n_i, m_i, r_0, r$ and 7 relations (3.2)–(3.3). We choose $n_{01} = 1$, a scaling parameter n_1, define

the associated scaled variables: $n_2 = n_1\overline{n}_2$, $m_i = n_1\overline{m}_i$, $r = n_1\overline{r}$, $a_{0i} = n_1\overline{a}_{0i}$, $b_{0i} = n_1^2\overline{b}_{0i}$, and rewrite the relations in terms of the scaled parameters:

$$\begin{aligned} m_{02} &= n_{02}m_{01}, & r_0 &= \sqrt{n_{02}}m_{01}, \\ \overline{m}_2 &= -y(\overline{m}_1 + 2d_*), & \overline{r} &= z(\overline{m}_1 + d_*), \end{aligned} \tag{A.1}$$

$$n_1 = -n_{01}\overline{a}_{0i}/\overline{b}_{0i}, \qquad i = 1,2 \;\rightarrow \tag{A.2}$$

$$\overline{a}_{01}\overline{b}_{02} - \overline{a}_{02}\overline{b}_{01} = \sum_{k=0}^{3}(A_k - B_k)\overline{m}_1^k = 0,$$

with A_k, B_k written down in the second Ref. (7). *The two asymptotic states are determined from* $n_{01} = 1$ *and three arbitrary parameters* $m_{01} > 0$, $n_{02} > 0$, $|\zeta| < 1$. From (A.2) we get m_{02}, r_0 and all positive parameters for the (i) state. From $\overline{m}_1$, we get $\overline{m}_2$, $\overline{r}$ and $\overline{a}_{0i}$, $\overline{b}_{0i}$, $n_1 = -\overline{a}_{01}/\overline{b}_{01}$ and the five parameters n_i, m_i, r or the (ii) state. For brevity we discuss positivity for two particular solutions. Firstly, if at the (ii) state only $p_2 \neq 0$, then the solution with $n_{01} = 1$ depends on one arbitrary parameter ζ with positivity conditions: $1/\sqrt{1 + d_*^2/4} < \zeta < 1$. The other parameters are deduced from (A.2):

$$\begin{aligned} 1 > n_{02} &= (1-\zeta)/(1+\zeta) > 0, \\ X &:= (2/d_*)\zeta - \sqrt{1-\zeta^2}, \\ m_{01} &= d_*\sqrt{1-\zeta^2}/X > 0, \\ r_0 &= d_*(1-\zeta)/X > 0, \\ m_{02} &= d_*(1-\zeta)^{3/2}/X\sqrt{1+\zeta} > 0, \\ m_2 &= (1-\zeta)(\zeta d_* - \sqrt{1-\zeta^2})/X(1+\zeta) > 0, \\ p_2 &= m_2 + m_{02} > 0. \end{aligned} \tag{A.3}$$

Secondly, if at the (ii) state only $s_2 \neq 0$, $p_2 \neq 0$, then, with $n_{01} = 1$, the solution depends on two arbitrary parameters with conditions for the positivity: $n_{02} > 0$, $\sup[(1-n_{02})/(1+n_{02}), 1/(1+d_*\sqrt{n_{02}}/2)] < \zeta < 1$ and the other found from (A.2):

$$\begin{aligned} m_{01} &= 2(1-\zeta)/\left[\zeta\sqrt{n_{02}} - 2(1-\zeta)/d_*\right] > 0, \\ m_{02} &= n_{02}m_{01} > 0, \\ r_0 &= \sqrt{m_{01}m_{02}} > 0, \\ m_2 &= (1-\zeta)\left[m_{01} + 2d_*\right]/(1+\zeta) > 0, \\ p_2 &= m_2 + m_{02} > 0, \\ s_2 &= n_{02} - (1-\zeta)/(1+\zeta) > 0. \end{aligned} \tag{A.4}$$

Appendix B. Similarity solutions

B1. *Firstly, for DBMs with p-th highest order collision term we write down both the mass M and the shock thickness* $w^{(p)}$:

$$
\begin{aligned}
M &= m_0 + mD^{-q}, \\
m_0 &= m_{01} + m_{02} + d_*(r_0 + n_{01} + n_{02}), \\
m &= m_1 + m_2 + d_*(r + n_1 + n_2), \\
q &= 1/(p-1), \qquad D = 1 + e^{\gamma\eta}, \\
w^{(p)} &= |m|/\max|dM/d\eta| = (1 + q^{-1})^{q+1}/|\gamma|, \\
p &= 2, \qquad w^{(2)} = 4/|\gamma^{(2)}|, \qquad p = 3, \\
w^{(3)} &= 3\sqrt{3}/|\gamma^{(3)}|, \qquad p = 4, \qquad w^{(4)} = 4^{4/3}/|\gamma^{(4)}|,
\end{aligned}
\tag{B.1}
$$

with m_0, m known from Appendix A, but γ has to be determined.

B2. *Secondly, from the* (4.4)–(4.5) $B_{i,b+p+t}$ *relations we determine the coefficients* a_{02+i}, b_{02+i}, $i = 1, 2$ of D^{-kq}, $k = 1, 3$. We define $n_{12}^{\pm} = n_{01} \pm n_{02}$.

For $Q_{1,b+p+t}$ we get from (4.4):

$$
\begin{aligned}
a_{01}D^{-q}(-1 + D^{-q})\Big[\sigma_B^{(2)} + (m_0 + mD^{-q})\sigma_P^{(2)} \\
+\sigma_C(r_0 + rD^{-q}) + \sigma_{DE}(m_{01} + m_{02} + (m_1 + m_2)D^{-q})\Big] \\
+\sigma_{DE}a_{02}D^{-q}(1 - D^{-q})(n_{12}^{-} + (n_1 - n_2)D^{-q}) - a_{03}/a_{01}\sigma_B^{(2)} \\
= 1 + \Big[m_0\sigma_P^{(2)} + \sigma_C r_0 + \sigma_{DE}(m_{01} + m_{02})\Big]/\sigma_B^{(2)} - n_{12}^{-}a_{02}\sigma_{DE}/a_{01}\sigma_B^{(2)},
\end{aligned}
\tag{B.2}
$$

$$
b_{03} = a_{01}\left(m\sigma_P^{(2)} + \sigma_C r + \sigma_{DE}(m_1 + m_2)\right) - a_{02}\sigma_{DE}(n_1 - n - 2). \tag{B.3}
$$

For $Q_{2,b+p+t}$ we get from (4.5):

$$
\begin{aligned}
a_{02}D^{-q}(1 - D^{-q})\Big[\sigma_B^{(1)} + (m_0 + mD^{-q})\sigma_P^{(1)} \\
+2(\sigma_{DE} + \sigma_E)(n_{12}^{+} + (n_1 + n_2)D^{-q})\Big] \\
-a_{01}D^{-q}(1 - D^{-q})2[m_{01} - m_{02} + (m_1 + m_2)D^{-q})]\sigma_{DE}a_{04}/a_{02}\sigma_B^{(1)} \\
= 1 + \Big[m_0\sigma_P^{(1)} + 2(\sigma_{DE} + \sigma_E)n_{12}^{+}\Big]/\sigma_B^{(1)} - a_{01}2\sigma_{DE}n_{12}^{-}m_{01}/n_{01}a_{02}\sigma_B^{(1)},
\end{aligned}
\tag{B.4}
$$

$$
b_{04} = -a_{02}\left[m\sigma_P^{(1)} + 2(\sigma_{DE} + \sigma_E)(n_1 + n_2)\right] + a_{01}2\sigma_{DE}(m_1 - m_2). \tag{B.5}
$$

B3. *Thirdly, for the quaternary terms* $Q_{i,quat}$ *written down in (2.5), (4.7) with* $\sigma_K = \sigma_L = 0$, $\sigma_{FJ} = \sigma_F + \sigma_J$ *we get the coefficients* $a_{04+i}, b_{04+i}, c_{04+i}$, $i = 1, 2$ *of* $D^{-kq}, k = 1, 4, 3$.

From $Q_{1,q} = a_{01}D^{-q}(1-D^{-q})[\sigma_{FJ}(M_1N_2+M_2N_1)+N_{12}^{+}R\sigma_G]$, $\sigma_{FJ} = \sigma_F+\sigma_J$ we get:

$$\begin{aligned} a_{05} &= -a_{01}[2m_{01}n_{02}\sigma_{FJ} + \sigma_G r_0 n_{12}^{+}], \\ b_{05} &= a_{01}[(m_1n_2 + m_2n_1)\sigma_{FJ} + (n_1 + n_2)r\sigma_G], \end{aligned} \tag{B.6}$$

$$\begin{aligned} c_{05} = -b_{05} + a_{01}[\sigma_{FJ}(n_{01}m_2 + n_{02}m_1 + n_1m_{02} + n_2m_1) \\ +\sigma_G(rn_{12}^{+} + r_0(n_1 + n_2))]. \end{aligned} \tag{B.7}$$

From $Q_{2,q} = a_{02}D^{-q}(1 - D^{-q})[\sigma_H N_1N_2 + \sigma_I(R^2 + M_1M_2)]$ we get:

$$\begin{aligned} a_{06}/a_{02} &= [2m_{01}m_{02}\sigma_I + \sigma_H n_{01}n_{02}] > 0, \\ b_{06} &= -a_{02}[(m_1m_2 + r^2)\sigma_I + \sigma_H n_1n_2], \end{aligned} \tag{B.8}$$

$$c_{06} = -b_{06} - a_{02}[\sigma_I(2rr_0 + m_1m_{02} + m_2m_{01}) + \sigma_H(n_1n_{02} + n_2n_{01})]. \tag{B.9}$$

Appendix C. Solution by numerical integration

We solve the classical stationary shock wave problem related to (2.1)–(2.5) by reducing it to a system of two ODE with limiting values corresponding to the equilibrium states (with the parameters related by the R-H equations). Inserting the ansatz for similarity solutions into (2.1)–(2.5), we obtain

$$\begin{aligned} N_2 &= [(1-\zeta)N_1 - C_1]/(1+\zeta), \\ M_2 &= [C_3 - (1-\zeta)M_1 - 2d_*(1-\zeta)N_1]/(1+\zeta), \\ R &= [(1-\zeta)M_1 - (1+\zeta)M_2 - C_2]/d_*\zeta, \\ dN_1/d\eta &= \overline{Q}_1/(1-\zeta), \qquad dM_1/d\eta = \overline{Q}_2/(1-\zeta), \end{aligned} \tag{C.1}$$

where C_i are functions of the parameters of the asymptotic states, determined in Sec. 3, and Q_i are functions of N_1, M_1 with limit conditions:

$$\begin{aligned} \lim_{\eta\to-\infty} N_1 &= n_{01}, \qquad \lim_{\eta\to-\infty} M_1 = m_{01}, \\ \lim_{\eta\to+\infty} N_1 &= s_1, \qquad \lim_{\eta\to+\infty} M_1 = p_1. \end{aligned} \tag{C.2}$$

The free parameters are: $n_{01} = 1$, m_{01}, n_{02}, ζ (cf. Appendix A), and all the cross-sections. We solve (C.1), (C.2) by the Runge–Kutta's IV order procedure, with the initial data $N_1 = n_{01} + \varepsilon_1$, $M_1 = m_{01} + \varepsilon_2$, or $N_1 = s_1 + \varepsilon_1$, $M_1 = p_1 + \varepsilon_2$, ε_i small, depending on the direction of integration. We start from the neighbourhood of the saddle, in the direction which can be calculated by the analysis of the corresponding eigenproblem for the linearized equations, and we end up in the arbitrary close neighbourhood of the node [7].

Acknowledgments

One of the authors (T. Płatkowski) of this paper was supported in part by the KBN under grant No. 2-P301-027-06. This support is a gratefully acknowledged.

References

1. R. GATIGNOL, Lect. Notes in Phys., **36**, 1975; T. PŁATKOWSKI and R. ILLNER, SIAM Rev., **30**, 213, 1988; N. BELLOMO and T. GUSTAFSON, Rev. Math. Phys., **137**, 3, 1991.
2. S. HARRIS, Phys. Fluids, **9**, 1328, 1966; J. HARDY and Y. POMEAU, JMP, **13**, 1042, 1972.
3. U. FRISCH *et al.*, Complex Syst., **1**, 649, 1987; P. CHAUVAT, F. COULOUVRAT and R. GATIGNOL, [in:] Advances in kinetic theory, R. GATIGNOL and SOUBBARAMAYER [Eds.], Springer-Verlag, 1991, p. 139; P. CHAUVAT and R. GATIGNOL, TTSP, **21**, 417, 1992; N. BELLOMO and S. KAWASHIMA, JMP, **31**, 245, 1990; H. CABANNES, Eur. J. Mech., B Fluids, **11**, 415, 1992.
4. H. CORNILLE, JMP, **29**, 1667, 1988, Lect. Notes in Math., G. TOSCANI [Ed.], Springer, 1988, p. 70; D.H. TIEM, CRAS, 313, 995, 1991; H. CORNILLE, CRAS, 313, 743, 1991.
5. B. CHOPPARD and M. DROZ, Phys. Let., **A 126**, 476, 1988.
6. H. CORNILLE, Phys. Let., **154A**, 339, 1991; TTSP, **20**, 325, 1991; JMP, **32**, 3439, 1991.
7. H. CORNILLE, T. PŁATKOWSKI, JMP, **33**, 2587, 1992; J. Stat. Phys., **71**, 733, 1993; TTSP, **23**, 1–3, 75–104, 1994.
8. H. CABANNES, J. Mécanique, **14**, 703, 1975.
9. M. ERNST, Adv. Math. Appl. Sci., **2**, A.S. ALVES [Ed.], World Scientific, 186, 1991.
10. P.D. LAX, CBMS Monograph 11, SIAM 1973.
11. H. CORNILLE, T. PŁATKOWSKI, this issue, Part II.
12. D. D'HUMIÈRES, P. LALLEMAND and U. FRISCH, Europh. Let., **2**, 291, 1986.
13. H. CORNILLE, Saclay preprint, "VII Conf. on Waves", T. RUGGERI [Ed.], Bologna 1993.

SERVICE DE PHYSIQUE THEORIQUE,
CE SACLAY, GIF-SUR-YVETTE, FRANCE
and
DEPARTMENT OF MATHEMATICS, INFORMATICS AND MECHANICS
WARSAW UNIVERSITY, POLAND.

Received April 29, 1994.

Arch. Mech., 46, 5, pp. 711–734, Warszawa 1994

Two multispeed discrete Boltzmann models including multiple collisions II. Stability properties

H. CORNILLE (GIF-SUR-YVETTE) and
T. PŁATKOWSKI (WARSZAWA)

IN THIS PAPER accompanying [1] we analyse the stability poblems for the equilibrium states of the discrete velocity models (DVMs) with multiple collisions, considered in Part I. We provide sufficient conditions for the stability when the multiple collisions are taken into account, using the approach developed by Whitham in the wave theory of propagation of weak perturbations. In the proof we use the factorization properties, developed in Part I. Finally we verify the H-theorem for the considered models and deduce a criterion useful in order to check the correct contribution of each multiple collision term.

1. Introduction

IN THE ANALYSIS of nonlinear fluid flows important role is played by the analysis of the stability of the solutions related to uniform states. The corresponding equations linearized around the uniform state provide informations about stability.

In particular, if the linearized equations are replaced by higher order linear PDE with a sum of products of differential operators of degrees differing by one, the sufficient conditions for stability of the uniform states have been given by WHITHAM [2].

Whitham gave the conditions of exponential damping at large time of the waves associated with the highest order differential operator by the waves provided by the lower order differential operator. The lowest order differential operator, associated with the main waves, provides the characteristic speeds of the propagation.

Applying the Whitham approach to the DVMs, one linearizes the system of evolution equations for the density functions around an asymptotic equilibrium state, and we consider the system of linear PDE for the wave perturbations. The system of equations being equivalent to one linear 5th order equation, we find a sum of a fifth, fourth and third order operators. With the wave ansatz for the perturbation, these operators give the associated polynomials in the variable ζ – the speed of the weak disturbance. The roots of these polynomials characterize the speeds of the propagation, associated with the differential operator of the given order. The Whitham stability conditions for DVMs with binary collisions have been studied in [3, 4, 5] and, in particular, for the models considered in [5].

Our goal is to present, for the first time, a proof of the Whitham stability conditions with multiple collisions. Although the characteristic velocities are (like in the binary case) independent of the cross-sections, *the roots of the fourth order polynomial depend on the cross-sections of the multiple collisions, and we cannot apply the binary results. The Whitham stability conditions being an interlacing of the roots of the corresponding polynomials, we must take into account these multiple collision cross-sections. The second goal is to discuss the H-theorem for the considered models.*

First, we describe the models [6, 7, 1] and specify the equations. To construct a stability criterion, when multiple collisions are taken into account, we recall different structures of the nonlinear equations, studied in Part I and generalized here in Sec. 2. More in details, we recall important factorization properties of the collision terms for the considered models. Let us consider a particular density *not present in all binary collision terms appearing in the nonlinear equation for this density*. For that particular density any multiple collision term has one of the two following properties. Either it contains as a factor only that binary collision term in which the considered density is present (and then the remaining factors are positive), or it includes also another binary component from which that density is absent. In the considered models and with a particular choice of the wave propagation, two such particular densities (with independent nonlinear associated equations) exist.

For the considered models, with two different choices of the wave propagation, our most general factorization result is the following. *In the nonlinear equation for any density, at least one factor of the binary collision terms is nonnegative.*

As we shall see, these different analytical structures of the collision terms are useful for the determination of the signs of quantities which depend on the cross-sections of multiple collisions (crucial for the stability analysis).

Second, we give details of the linearization procedure, which leads to the type of equations, which can be treated by the Whitham method.

In order to determine the sound wave velocities we linearize the model equations around an equilibrium state, and we obtain a sum of three differential operators with associated polynomials P_5, P_4, P_3. The characteristic velocities are the roots of the lowest order cubic polynomial P_3. In order to generalize the Whitham theory, we find inequalities between the roots of P_5, P_4 and the roots of P_4, P_3. If these inequalities are satisfied, then the main wave is provided by the P_3 roots, while the disturbances provided by the higher polynomials are exponentially damped. The main result is that the P_4 roots, contrary to the P_5, P_3 ones, depend on the multiple collisions cross-sections. However, like in the binary collision case, we prove that the inequalities between the P_5, P_4 roots are satisfied so that for the P_5 waves we can refer to the previous results established in the binary case [3–5]. We discuss the properties of the polynomials associated with the subsequent order operators. In particular, in Lemmas 1, 2 the interlacing properties of the subsequent order polynomials are proved.

Third, in Lemmas 3–5 we prove our main results on stability properties. For the Whitham stability conditions we find sufficient conditions in three cases. First, if the cross-sections of particular multiple collisions are small enough and without conditions for the other multiple collisions. Second, provided some well defined constraints on both the multiple collision cross-sections and the densities of the equilibrium state are satisfied. Third, for arbitrary multiple collision cross-sections, we find conditions only for the density values of the asymptotic state.

We would like to give an intuitive explanation of these results (for the rigorous proofs the reader can refer to the tedious details in Sec. 3). For the present models and with a particular choice of the wave propagation, there exist two different binary collision terms with different positive cross-sections. *There exist also two densities for which the associated nonlinear equations contain only one binary term at the binary level.* Concerning the multiple collisions, there exist two different classes. For the first class, concerning these two densities, the multiple collision terms contain only the binary term present at the binary level with a positive factor. In the neighbourhood of an asymptotic state these nonlinear equations look like the binary ones, with the only change that the two positive binary cross-sections are replaced by two positive constants. For this class the proof of Whitham stability for multiple collisions is a trivial extension of the binary one. For the second class, the main difference is that the nonlinear terms contain both factors of the two binary terms. If we assume that the cross-sections (of the factors of the binary terms not present at the binary level) are small enough, for the Whitham stability proof, we come back to the previous case. Now, what happens when these cross-sections are not small. We give two different types of sufficient conditions. Firstly, the conditions mix both the multiple cross-sections and the asymptotic densities of the equilibrium state. Secondly, the multiple collision cross-sections disappear (they can be as large as we want) and only the asymptotic densities of the equilibrium state in the conditions remain. *In conclusion we can always find sufficient conditions for the Whitham stability.*

Finally we report results for the H-theorem [8, 9]. For the models with ternary, fourth order and a particular type of the fifth order collisions, the H-theorem is proved by use of the nonnegativity properties of the terms associated with the considered collision terms (Lemmas 6, 7).

Firstly, for the considered hierarchy of models, we choose the wave propagation along a median of the square. For p-th order collisions, a criterion for the validity of the H-theorem is proved. More in detail, with a particular structure of the expressions associated with each multiple collision (elementary collision terms), we show that each term gives a nonpositive contribution to the evolution of the associated h-functional (Lemma 8, Theorem 1). For the multiple collision terms, up to the fifth order, we have verified this criterion and we report the results in some cases. Secondly, we perform a similar study for the $8v_i$ model

with the wave propagation along the diagonal of the square [1]. We study both the H-theorem and establish the associated criterion (Lemma 9, Theorem 2).

When we determine all multiple collisions of any given order, we have to perform a great number of analytical calculations in order to obtain all possible elementary collision terms. For instance, consider any type of collisions presented in Fig. 1a: either M or N ... or T. For each drawing, taking into account the symmetries of the square, in principle eight collisions are possible. Nevertheless we find at most four different analytical expressions that we call elementary collision terms (cf. Fig. 1b with three elementary collision terms corresponding to Fig. 1a – M). The interest of this criterion is that we can check the correctness of any of these elementary collision terms. On the other hand, we recall [9] that a similar criterion was obtained for another hierarchy of models not considered here.

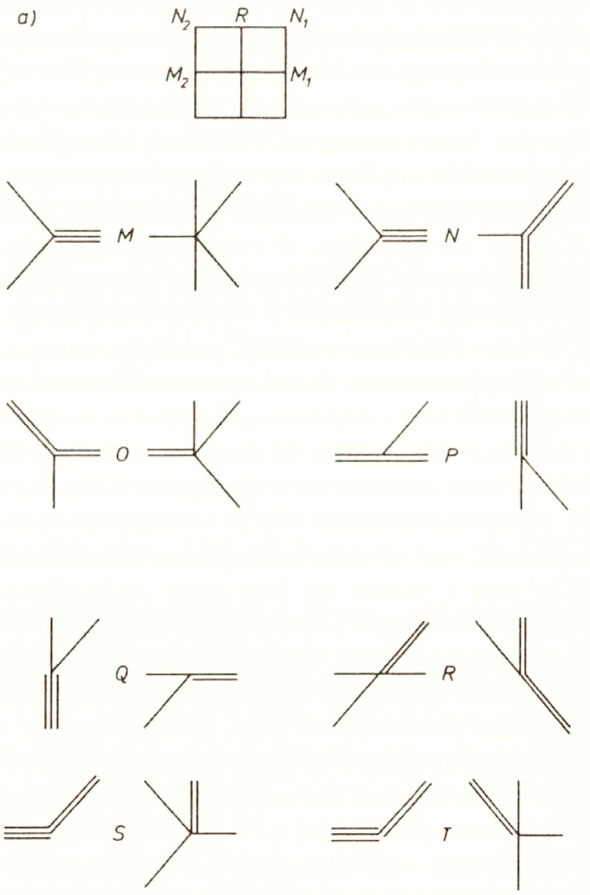

fifth-order collisions

[FIG. 1 a]

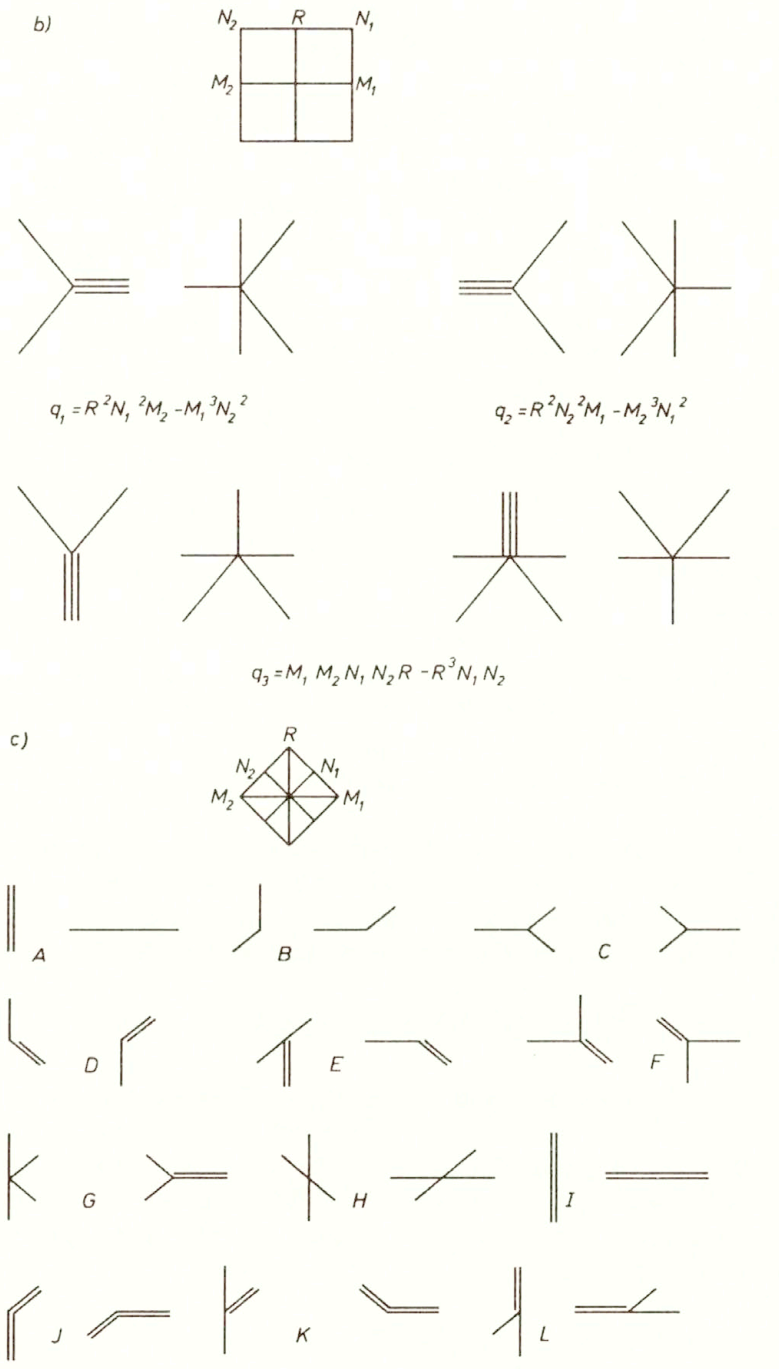

FIG. 1. a) $8v_i$, x-axis along the median, b) $8v_i$, q_i elementary collision terms for Fig. 1a – M, c) b, t, q collisions, $8v_i$, x-axis along the diagonal.

2. Models and equations with multiple collisions

The first model is the square $d = 2$ $8v_i$ model on a plain. For one-dimensional flows along the x-axis [1] there remain five independent densities N_1, M_1, R, M_2, N_2, associated with the x-projections $1, 1, 0, -1, -1$, and the velocities ($x_1 = x, x_2$) in the plane: $N_1 : (1, \pm 1)$, $N_2 : (-1, \pm 1)$, $M_1 : (1, 0)$, $M_2 : (-1, 0)$, $R : (0, \pm 1)$. The second model is a $d = 3, 14v_i$ model with five independent densities for the same 1-d projections: $N_1 : (1, \pm 1, 0), (1, 0, \pm 1)$, $N_2 : (-1, \pm 1, 0), (-1, 0, \pm 1)$, $M_1 : (1, 0, 0)$, $M_2 : (-1, 0, 0)$, $R : (0, \pm 1, 0), (0, 0, \pm 1)$. For both models these five densities satisfy three linear relations [1] ($p_\pm := \partial_t \pm \partial_x, d_* := 2(d-1)$)

$$\begin{aligned} p_+ N_1 + p_- N_2 &= 0, \\ p_+ M_1 + p_- M_2 + d_* R_t &= 0, \\ p_+ M_1 - p_- M_2 + 2 d_* p_+ N_1 &= 0 \end{aligned} \tag{2.1}$$

and two independent nonlinear equations chosen either for $p_+ N_1$, $\partial_t R$, or for $p_+ M_1$, $p_- M_2$.

We recall the two binary collision terms: $Q_1 = N_1 M_2 - N_2 M_1$, $Q_2 = M_1 M_2 - R^2$. We notice that N_1 appears only in Q_1, R only in Q_2, while M_1, M_2 appears in both Q_i. For the models with multiple collisions up to the fourth order taken into account, we recall [1] a factorization property, important for the stability considerations of the next section: only the factors of binary collision terms present at the binary level are nonnegative.

Notice, for the ternary and quaternary collisions, the following discrepancy between the (N_1, R) and (M_1, M_2) couples of the associated nonlinear equations: For the $p_+ N_1, \partial_t R$ equations we have only one nonnegative factor, whereas there are two such factors for the equations associated with $p_+ M_1, p_- M_2$.

$$\partial_t R = Q_2 \left[\sigma_B^{(1)} + A_{11}\right] - Q_1 A_{12}, \qquad p_+ N_1 = -Q_1 \left[\sigma_B^{(2)} + A_{22}\right] + Q_2 A_{21} \tag{2.2}$$

with A_{ij} m-th order polynomials in N_i, M_i, R, $m = 2$ for quaternary collisions. We have verified that for the fifth order collisions included (shown in Fig. 1a), we have still the form (2.2) of the nonlinear equations for R, N_1, with the order $m = 3$ for A_{ij} polynomials. For collisions up to the fifth order we have found $A_{ii} > 0$.

Taking into account the linear (2.1) relations we write the associated nonlinear equations for $p_+ M_1, p_- M_2$

$$\begin{aligned} p_+ M_1 / d_* &= -Q_2 \left[\sigma_B^{(1)} + 2B_{1+}\right]/2 + Q_1 \left[\sigma_B^{(2)} + B_{2+}\right], \\ 2B_{1\pm} &= A_{11} \pm 2A_{21}, \\ p_- M_2 / d_* &= -Q_2 \left[\sigma_B^{(1)} + 2B_{1-}\right]/2 - Q_1 \left[\sigma_B^{(2)} + B_{2-}\right], \\ B_{2\pm} &= A_{22} \pm A_{12}/2, \end{aligned} \tag{2.3}$$

where, up to the fourth order collisions, we have found $B_{i\pm} > 0$. *The main new result, coming from fifth order collisions, is that for* N_1, R *nonlinear equations we still find* $A_{ii} > 0$ *but for the* M_1, M_2 *ones, in each equation only one of the two factors* $B_{1\pm}$ *or* $B_{2\pm}$ *is always nonnegative*. This means that with the fifth order collisions included, for each nonlinear equation associated with N_1, R, M_1, M_2, at least one factor of the binary collision term is nonnegative. However, there exist also a combination of $B_{1\pm}$, $B_{2\pm}$ and a quadratic expression of A_{ii}, A_{ij} which are nonnegative:

$$
\begin{aligned}
B_+ &= M_1(M_2 B_{1+} + N_2 B_{2+}), \\
B_- &= M_2(M_1 B_{1-} + N_1 B_{2-}), \\
A &= A_{11}A_{22} - A_{12}A_{21}.
\end{aligned} \tag{2.4}
$$

These results will be very important, for the study of the stability, in the next section. In Fig. 1a each of M, N, ... S, T diagrams represents all the fifth order collisions obtained by applying the transformations of the symmetry group of the square to the given collisional configuration.

In Appendix A we determine all the fifth order collisions satisfying 1) spectatorlessness (i.e. all the particles change their velocities in the collision), 2) microscopic energy conservation, 3) momentum conservation.

Analysing all the diagrams we can write the contributions of all the considered fifth order collisions to the relevant collision operators. We omit the positive constant multipliers, proportional to the multiple cross-sections. We begin with the coefficients A_{ij} in (2.2) and A in (2.4)

Q	A_{11}	A_{22}	A_{12}	A_{21}	A
M	$P_5^+ + 2P_0$	$Q^+ M_{12}^+$	$Q^+ M_{12}^-$	P_5^-	≥ 0
N	$2P_5^+ + 4P_0$	$Q^+(R + 2M_{12}^+)$	$2Q^+ M_{12}^- + 2RQ^-$	$2P_5^-$	≥ 0
O	0	$4Q^+ R + R^2 N_{12}^+$	0	0	0
P	$8Q_{MR} N_{12}^+$	$M_1 M_2 M_{12}^+$	$4M_1 M_2 M_{12}^-$	$Q_{MR} N_{12}^-$	≥ 0
Q	$4Q_{MR} N_{12}^+$	$M_1 M_2 M_{12}^+$	$4M_1 M_2 M_{12}^-$	$Q_{MR} N_{12}^-$	≥ 0
R	$4N_1 N_2 N_{12}^+$	$N_1 N_2 M_{12}^+$	$2N_1 N_2 N_{12}^-$	$N_1 N_2 N_{12}^-$	≥ 0
S	P_S	$2Q^+ M_{12}^+ + P^+$	$2M_{12}^- Q^+ + 2P^-$	$2P_5^- + RN_{12}^{2-}$	≥ 0
T	$2P_5^+ + 2RN_{12}^2$	$2M_{12}^+ Q^+$	$2M_{12}^- Q^+$	$2P_5^-$	≥ 0

with $Q_{MR} = M_1 M_2 + R^2$, $P_0 = RN_1 N_2$, $P_5^\pm = M_2 N_1^2 \pm M_1 N_2^2$, $P_S = 2N_2^2(M_1 + R) + 2N_1^2(M_2 + R)$, $Q^\pm = N_2 M_1 \pm N_1 M_2$, $M_{12}^\mp = M_1 \mp M_2$, $N_{12}^\mp = N_1 \mp N_2$, $P^\mp = R(N_1 M_1 \mp N_2 M_2)$, $N_{12}^{2-} = N_1^2 - N_2^2$. We notice that N_{12}^-, M_{12}^-, P_5^-, Q^-, P^- are not sums of positive products of the densities and that they are present only in A_{12}, A_{21}.

We verify $A_{ii} \geq 0$, $i = 1, 2$, $A = A_{11}A_{22} - A_{12}A_{21} > 0$ while the terms $A_{ij} = 0$ for $N_1 = N_2$, $M_1 = M_2$, $i \neq j$. The A_{ij} factors depend linearly on the multiple collision cross-sections so that both A_{ii} and $A_{ij} \to 0$ when they vanish.

We go on with the coefficients B_{i+}, $i = 1, 2$, $B_+ = M_1(M_2B_{1+} + N_2B_{2+})$ of (2.2)–(2.3):

Q	B_{1+}	B_{2+}	B_+
M	$Q^-_{MN}/2 + P_0$	$Q^+(3M_1 + M_2)/2$	≥ 0
N	$Q^-_{MN} + 2P_0$	$Q^+(3M_1 + M_2) + 2P_0$	≥ 0
O	0	$8RQ^+ + 2R^2N^+_{12}$	≥ 0
P	$Q_{MR}(5N_1 + 3N_2)$	$M_1M_2(3M_1 - M_2)$	≥ 0
Q	$Q_{MR}(3N_1 + N_2)$	$M_1M_2(3M_1 - M_2)$	≥ 0
R	$N_1N_2(3N_1 + N_2)$	$2M_1N_1N_2$	≥ 0
S	$Q^-_{MN} + 2R^2N_1$	$Q^+(M_2 + 3M_1) + 2N_1M_2R$	≥ 0
R	$Q^-_{MN} + RN^2_{12}$	$Q^+(M_2 + 4M_1)$	≥ 0

where only $Q^-_{MN} = 3M_2N_1^2 - M_1N_2^2$ and $3M_1 - M_2$ are not sums of positive terms. We notice that either the two B_{i+} are nonnegative or only one. On the contrary B_+ is always nonnegative. If we apply the transform $N_i \longleftrightarrow N_j$, $M_i \longleftrightarrow M_j$ we get $B_{i+} \longleftrightarrow B_{i-}$, $B_+ \longleftrightarrow B_-$. It follows that always one of the two B_{i-} is nonnegative while all $B_\pm$ are nonnegative.

In the same way one can consider multiple collisions of higher orders. If p particles collide, we say that the collision is of the p-th order. We assume that the corresponding evolution equations with the p-th order collisions taken into account satisfy equations of the (2.2) type with collision terms containing linearly the binary Q_1, Q_2 ones and the A_{ij} being polynomials in N_i, M_i, R, the highest monomial being of order $p-2$. They contain multiple collision cross-sections, such that A_{ij} vanish when all these cross-sections vanish. Analysing the contributions of the considered multiple collisions up to the fifth order, in terms of the densities N_i, M_i, R, we have found positivity properties, crucial for the stability analysis of the next section:

$$A_{ii} > 0, \qquad B_\pm > 0, \qquad A \geq 0. \tag{2.5}$$

A partial analysis of the sixth order collision terms confirms these positivity results. As we shall see in the next section, there exist also for an asymptotic state, taking into account the above relations, two other important properties linking the asymptotic values of $A_{12}, A_{21}, N_1 - N_2, M_1 - M_2$.

3. Whitham stability conditions

We consider an asymptotic state (n_{0i}, m_{0i}, r_0) (called (i) state in Ref. 1) for the (N_i, M_i, R_0) densities. In the asymptotic state the two binary collisions terms

vanish:

$$(3.1) \qquad Q_2 = 0 \;\rightarrow\; n_{01}m_{02} = n_{02}m_{01}, \qquad Q_1 = 0 \;\rightarrow\; m_{01}m_{02} = r_0^2.$$

The study of stability of the asymptotic states, using the Whitham approach, will be done in the next subsections. Important tools will be provided by the positivity (2.5) of the five terms A_{ii}, $B_{\pm}$, A and some other related coefficients, defined below. Let us call $\tilde{A}_{ij}$, $\tilde{B}_{\pm}$, $\tilde{A}$, the asymptotic values of A_{ij}, $B_{\pm}$, A. The A_{ij} terms have not a well-defined sign, but for the asymptotic states (3.1) vanish for $n_{01} = n_{02}$. From (2.4) we get as first results:

$$(3.2) \qquad \tilde{A}_{ii} > 0, \qquad \tilde{B}_{\pm} > 0, \qquad \tilde{A} = \tilde{A}_{11}\tilde{A}_{22} - \tilde{A}_{12}A_{21} > 0.$$

For purposes of the next subsections it is convenient to define new constants:

$$\tilde{a}_{12} = n_{01}m_{02}\tilde{A}_{12}, \qquad \tilde{a}_{21} = m_{01}m_{02}\tilde{A}_{21}$$

and

$$(3.3) \qquad \tilde{\sigma}_1 = m_{01}m_{02}\left[\sigma_B^{(1)} + \tilde{A}_{11}\right] > 0, \qquad \tilde{\sigma}_2 = n_{01}m_{02}\left[\sigma_B^{(2)} + \tilde{A}_{22}\right] > 0,$$

$$(3.4) \qquad \lambda = \tilde{\sigma}_1\tilde{\sigma}_2 - \tilde{a}_{12}\tilde{a}_{21} > m_{01}^2 m_{02}n_{01}\tilde{A} > 0,$$

$$(3.5) \qquad \tilde{\sigma}_{\pm} = \tilde{\sigma}_1/2 + \tilde{\sigma}_2 \pm (\tilde{a}_{21} + \tilde{a}_{12}/2) > \tilde{B}_{\pm} > 0.$$

We see that the positivity of these five constants $\tilde{\sigma}_i$, $\tilde{\sigma}_{\pm}$, λ is a direct consequence of (3.2) or of the positivity properties of the density-dependent quantities (2.4). Another important property is obtained by taking into account the two relations (3.1) of the asymptotic states. For each collision term considered we have verified the following relation:

$$(3.6) \qquad \tilde{a}_{21} = \tilde{a}_{12}/2, \qquad (n_{01} - n_{02})\tilde{a}_{21} > 0$$

and the corresponding values, obtained from the A_{ij} values of ternary, quaternary and fifth order collisions, are reported below with the cross-sections of the $DE, K, ..T$ of Fig. 1b [1] and the present Fig. 1a. We define $n_{12}^{\pm} = n_{01} \pm n_{02}$ and find:

$$(3.7) \qquad \tilde{a}_{21}/m_{01}m_{02}n_{12}^{-} = \sigma_{DE} + n_{12}^{+}\sigma_K + m_{01}n_{02}(\sigma_M + 2\sigma_N) + 2m_{01}m_{02}\sigma_{PQ} + n_{01}n_{02}\sigma_R + (r_0 n_{12}^{+} + 2m_{02}n_{01})\sigma_S + 2m_{02}n_{02}\sigma_T > 0.$$

CONJECTURE. We conjecture that for the asymptotic quantities, the positivity properties (3.3)–(3.6) proved only up to the fifth order, hold for any p-th order multiple collisions.

3.1. Linearization around an asymptotic state

We consider small perturbations around the asymptotic state (n_{0i}, m_{0i}, r_0): $N_i \simeq n_{0i}(1 + X_i(x,t))$, $M_i \simeq m_{0i}(1 + Y_i(x,t))$, $R \simeq r_0(1 + Y_0(x,t))$, and substitute these densities in the five nonlinear equations associated with (N_i, M_i, R_0). We keep the terms linear in (X_i, Y_i, Y_0). We can replace three nonlinear equations by the three linear (2.1) equations which will remain linear in (X_i, Y_i, Y_0), and there will remain only two nonlinear equations chosen to be either (2.2) or (2.3). We define linear differential operators of the first order:

$$d_+ = n_{01}p_+, \quad d_- = n_{02}p_-, \quad \delta_+ = m_{01}p_+, \quad \delta_- = m_{02}p_-, \quad \delta_0 = r_0\partial_t \tag{3.8}$$

and obtain from (2.1) three equations linear in (X_i, Y_i, Y_0):

$$\begin{aligned} d_+X_1 + d_-X_2 &= 0, \\ 2d_*d_+X_1 + \delta_+Y_1 - \delta_-Y_2 &= 0, \\ \delta_+Y_1 + \delta_-Y_2 + d_*Y_0 &= 0. \end{aligned} \tag{3.9}$$

For the nonlinear equations, taking into account (3.1), we first determine the Q_i binary collision terms and retain the first order terms:

$$\begin{aligned} Q_1 &\simeq n_{01}m_{02}(X_1 + Y_2 - X_2 - Y_1), \\ Q_2 &\simeq m_{01}m_{02}(Y_1 + Y_2 - 2Y_0). \end{aligned} \tag{3.10}$$

We can now write down the linearized version of the nonlinear (2.2) equations

$$-d_+X_1 + \tilde{\sigma}_2(X_2 - X_1 + Y_1 - Y_2) + \tilde{a}_{21}(Y_1 + Y_2 - 2Y_0) = 0, \tag{3.11}$$

$$-\delta_0Y_0 + \tilde{\sigma}_1(Y_1 + Y_2 - 2Y_0) + \tilde{a}_{12}(X_2 - X_1 + Y_1 - Y_2) = 0, \tag{3.12}$$

where $\tilde{a}_{21} = \tilde{a}_{12}/2$.

With the three linear (3.9) relations and the two linear (2.11), (2.12) relations we have a homogeneous linear system of the type: $\mathbf{L}\,\mathbf{X} = 0$ with $\mathbf{X}$ a column vector with components: X_1, X_2, Y_1, Y_2, Y_0 and $\mathbf{L}$ the formal matrix with differential operators written down below in (3.13). The condition $\det \mathbf{L} = 0$ gives $\Delta = 0$ with:

$$\Delta = \begin{vmatrix} d_+ & d_- & 0 & 0 & 0 \\ -2d_*d_+ & 0 & -\delta_+ & \delta_- & 0 \\ 0 & 0 & \delta_+ & \delta_- & d_*\delta_0 \\ -d_+ - \tilde{\sigma}_2 & \tilde{\sigma}_2 & \tilde{\sigma}_2 + \tilde{a}_{21} & -\tilde{\sigma}_2 + \tilde{a}_{21} & -2\tilde{a}_{21} \\ -\tilde{a}_{12} & \tilde{a}_{12} & \tilde{\sigma}_1 + \tilde{a}_{12} & \tilde{\sigma}_1 - \tilde{a}_{12} & -2\tilde{\sigma}_1 - \delta_0 \end{vmatrix}. \tag{3.13}$$

This determinant is the sum of a fifth, fourth and third order differential operators: Δ_k, $k = 5, 4, 3$ with $\Delta_5 = 2d_+d_-\delta_+\delta_-\delta_0$; recalling $\tilde{a}_{21} = \tilde{a}_{12}/2$, $\tilde{\sigma}_\pm = \tilde{\sigma}_1/2 + \tilde{\sigma}_2 \pm 2\tilde{a}_{21} > 0$, we further find:

$$\Delta_4 = 2\delta_+\delta_-d_+d_-\tilde{\sigma}_1 + \delta_0\delta_+\delta_-(d_+ + d_-)\tilde{\sigma}_2 + \delta_0 d_* d_+ d_-[\delta_+\tilde{\sigma}_- + \delta_-\tilde{\sigma}_+].$$

For $\Delta_3 = 2\lambda\tilde{\Delta}_3$ we find the (3.4) positive factor $\lambda = \tilde{\sigma}_1\tilde{\sigma}_2 - \tilde{a}_{12}\tilde{a}_{21}$ and

$$\tilde{\Delta}_3 = [d_+ + d_-][2\delta_+\delta_- + (\delta_+ + \delta_-)d_*\delta_0/2] + 2d_*d_+d_-[\delta_+ + \delta_- + d_*\delta_0].$$

3.2. General properties for the associated polynomials

As was explained by Whitham [2], *for the stability of the equilibrium state we must show that the wave motions associated with the higher order operators are exponentially damped, at large time, by the main waves provided by the lower order operator.* For each differential operator of a given order [2, 3] we must seek $\Delta_k(h(\eta)) = 0$, $\eta = x - \zeta t$, for h an η-dependent function. So with each Δ_k operator [2] we associate the polynomials $P_k(\zeta)$ and seek the roots. In order to obtain these roots we substitute in Δ_k formally: $d_+ \to n_{01}(1-\zeta)$, $d_- \to -n_{02}(1+\zeta)$, $\delta_+ \to m_{01}(1-\zeta)$, $\delta_- \to -m_{02}(1+\zeta)$, $\delta_0 \to -r_0\zeta$. We find that $P_5 = \zeta(1-\zeta^2)^2 = 0$ has roots $-1, -1, 0, 1, 1$ which are the same as for binary collisions and are independent of the multiple collisions. We find that Δ_4 depends linearly on $\tilde{\sigma}_i, \tilde{a}_{ij}$ or equivalently on $\tilde{\sigma}_i, \tilde{\sigma}_\pm$. As we shall see, P_4 has the roots $-1, +1$ and two other $\zeta^\pm$ in the interval $]-1, +1[$ which depend on the cross-sections of the multiple collisions. In a recent paper [5], for the same models but without multiple collisions, comparing the P_5, P_4 waves we have obtained the damping, provided the Whitham interlacing property $-1 < \zeta^- < 0 < \zeta^+ < 1$ is satisfied. Here we will show that this interlacing property holds. On the contrary, the roots of the cubic $P_3(\zeta_{(i)})$ polynomial, which are the characteristic velocities of the weak shock theory, are independent of the multiple cross-sections. For completeness we will report the proof [5] that they also belong to $]-1, +1[$. In summary, if we compare with the previous results for binary collisions, the main problem is that the P_4 roots depend on the cross-sections of the multiple collisions and we cannot apply directly the binary results. *For the waves associated with P_4, P_3, Whitham has given the interlacing conditions for the roots which lead to the statibily.* Let $-1, \zeta^-, \zeta^+, 1$ and $\zeta^{(j)}$, $j = 1, 2, 3$ be the roots of $P_4 = (1-\zeta^2)P_2(\zeta)$, P_3. We must verify that:

$$-1 < \zeta^{(1)} < \zeta^- < \zeta^{(2)} < \zeta^+ < \zeta^{(3)} < 1. \tag{3.14}$$

For the $P_4 = (1-\zeta_{(i)}^2)P_2$ polynomial the roots are $-1, +1$ and two other $\zeta^\pm$ from $P_2(\zeta^\pm) = 0$. For the study of P_2 we define two auxiliary polynomials $P_1(\zeta)$, $P_{22}(\zeta)$ with roots $P_1(a) = 0$, $P_{22}(a^\pm) = 0$:

$$P_1 = n_{01}(1-\zeta) - n_{02}(1+\zeta), \qquad a = \frac{n_{01} - n_{02}}{n_{01} + n_{02}}, \qquad a^2 < 1, \tag{3.15}$$

$$P_{22} = 2(1-\zeta^2)m_{01}n_{02} + \zeta d_* r_0 P_1/2. \tag{3.16}$$

The P_2 polynomials can be written in two equivalent forms:

$$\begin{aligned} P_2/m_{01}n_{02} &= \tilde{\sigma}_1 P_{22} + \zeta r_0[P_1\tilde{\sigma}_2(d_* + m_{02}/n_{02}) \\ &\quad -d_*((1-\zeta)n_{01} + (1+\zeta)n_{02})2\tilde{a}_{21}] \\ &= \tilde{\sigma}_1 2m_{02}n_{01}(1-\zeta^2) + \zeta r_0[\tilde{\sigma}_2 P_1 m_{02}/n_{02} \\ &\quad +d_*(n_{01}(1-\zeta)\tilde{\sigma}_- - n_{02}(1+\zeta)\tilde{\sigma}_+]. \end{aligned} \tag{3.17}$$

For the roots $a, a^\pm$ of P_1, P_{22} we deduce simple properties:

$$\begin{aligned} &P_{22}(0) > 0, \quad |a^\pm| < 1, \quad a^+ > 0, \quad a^- < 0, \\ &a^- < a < a^+, \quad P_{22}(a) > 0, \quad a^\pm P_1(a^\pm) < 0, \\ &P_1(\pm 1) \lesseqgtr 0, \quad P_{22}(\pm 1) < 0, \quad aP_1(0) > 0. \end{aligned} \tag{3.18}$$

LEMMA 1. The P_5, P_4 interlacing properties $-1 < \zeta^- < 0 < \zeta^+ < 1$ are satisfied.

Due to $\tilde{\sigma}_i > 0$, $\tilde{\sigma}_\pm > 0$ and $P_1(\pm 1) \lesseqgtr 0$ we have:

$$\begin{aligned} P_2(0) &= \tilde{\sigma}_1 2m_{02}n_{01} > 0, \\ P_2(1) &= r_0[\tilde{\sigma}_2 P_1(1)m_{02}/n_{02} - 2d_* n_{02}\tilde{\sigma}_+] < 0, \end{aligned} \tag{3.19}$$

$$P_2(-1) = -r_0[\tilde{\sigma}_2 P_1(-1)m_{02}/n_{02} + 2d_* n_{01}\tilde{\sigma}_-] < 0, \tag{3.20}$$

and the P_5, P_4 interlacing properties follow from $P_2(0) > 0$, $P_2(\pm 1) < 0$.

We write the cubic P_3 polynomial, with roots $\zeta^{(i)}$, in terms of the above P_1, P_{22}:

$$P_3/m_{01} = P_1 P_{22}/n_{01} + 2d_* n_{02}(1-\zeta^2)[P_1 - \zeta d_* r_0 n_{01}/m_{01}]. \tag{3.21}$$

LEMMA 2. The P_3 roots are real and belong to $]-1, +1[$, furthermore $P_3(a^\mp) \gtreqless 0$ and we have the following inequalities:

$$\begin{aligned} &P_3(\pm 1) \gtreqless 0, \quad aP_3(0) > 0, \quad aP_3(a) < 0, \\ &a > 0 \ : \ -1 < \zeta^{(1)} < 0 < \zeta^{(2)} < a < \zeta^{(3)} < 1, \\ &a < 0 \ : \ -1 < \zeta^{(1)} < a < \zeta^{(2)} < 0 < \zeta^{(3)} < 1. \end{aligned} \tag{3.22}$$

For the proof of the first result we start from $P_3(\pm 1) = (m_{01}/n_{01})\, P_1(\pm 1)\, P_2(\pm 1)$, $P_3(0)/P_1(0) = P_{22}(0)/n_{01} + 2d_* n_{02} > 0$, $aP_3(a) = -2d_* n_{02}(1-a^2)a^2 r_0 n_{01} < 0$, and with (3.18) we deduce (3.22).

For the proof of the last results we write $P_3(a^\pm) = 2d_* n_{02}(1-(a^\pm)^2)[P_1(a^\pm) - a^\pm d_* r_0 n_{01}/m_{01}]$ and apply (3.18).

3.3. Sufficient conditions for the Whitham interlacing properties of P_4, P_3

We precise the (3.22) relations recalling that $a^- < a < a^+$:

$$
\begin{aligned}
&a > 0 \ : \ \zeta^{(1)} < a^- < 0 < \zeta^{(2)} < a < a^+ < \zeta^{(3)}, \\
&a < 0 \ : \ \zeta^{(1)} < a^- < a < \zeta^{(2)} < 0 < a^+ < \zeta^{(3)}.
\end{aligned} \tag{3.23}
$$

LEMMA 3. Sufficient conditions for the interlacing (3.14) are $P_2(a) > 0$, $P_2(a^\pm) < 0$.

Firstly we consider $a > 0$. From (3.23) we have $\zeta^{(2)} < a < a^+ < \zeta^{(3)}$. If $P_2(a) > 0$ and $P_2(a^+) < 0$, we get $a < \zeta^+ < a^+$ and it follows $0 < \zeta^{(2)} < \zeta^+ < \zeta^{(3)}$. Similarly from (3.23) we have $\zeta^{(1)} < a^-$ and if $P_2(a^-) < 0$, we get $a^- < \zeta^-$ and it follows $\zeta^{(1)} < \zeta^- < 0$. Secondly we consider $a < 0$. From (3.23) and the assumptions of Lemma 3 we get: $\zeta^{(1)} < a^- < a < \zeta^{(2)} < 0$, $a^- < \zeta^- < a$ and both $a^+ < \zeta^{(3)}$, $0 < \zeta^+ < a^+$.

COROLLARY 1. The Whitham conditions are satisfied if $\tilde{a}_{21}$, $i \neq j$ is small enough.

From the first expression of P_2 written down in (3.17) we get for $\tilde{a}_{21}$ small enough: $P_2(a) \simeq \tilde{\sigma}_1 P_{22}(a) > 0$ and $P_2(a^\pm) \simeq m_{01} r_0 (d_* n_{02} + m_{02}) \tilde{\sigma}_2 a^\pm P_1(a^\pm) < 0$ with (3.18) and we apply Lemma 3.

For ternary and quaternary collisions the conditions of Corollary 1 become with (3.7): σ_{CD}, σ_K small enough and σ_M, σ_N, σ_{PQ}, σ_R, σ_S, σ_T – small enough if fifth order collisions are included.

We seek sufficient conditions for the Whitham conditions (3.14), with any $\tilde{a}_{21}$.

LEMMA 4. Sufficient conditions for the Whitham conditions (3.14) are:

$$
\begin{aligned}
&P_2(a) > 0 \quad \text{and} \quad P_2(a^-) < 0 \quad \text{for} \quad a > 0, \\
&P_2(a) > 0 \quad \text{and} \quad P_2(a^+) < 0 \quad \text{for} \quad a < 0.
\end{aligned}
$$

For the proof, rewriting the first expression of P_2 in (3.17) we get:

$$
\operatorname{sign}[a^\pm P_2(a^\pm)] = \operatorname{sign}[(a - a^\pm)\tilde{\sigma}_2 (m_{02}/n_{02} d_* + 1) + 2\tilde{a}_{21}(a a^\pm - 1)]. \tag{3.24}
$$

First, we consider $a > 0, a^+ > 0$ and get $a - a^+ < 0$ from (3.18), $a a^+ - 1 < 0$, $\tilde{a}_{21} > 0$. It follows that $P_2(a^+) < 0$, one condition of Lemma 3 is satisfied and only the two conditions of Lemma 4 remain. Second, we consider $a < 0$, $a^- < 0$ and get $a - a^- > 0$ from (3.18), $a a^- - 1 < 0$, $\tilde{a}_{21} < 0$ (recalling $a(n_{01} - n_{02}) > 0$ from (3.15)). It follows that $P_2(a^-) < 0$, one condition of Lemma 3 is satisfied and only the two conditions of Lemma 4 remain.

COROLLARY 2. Sufficient conditions for the Whitham conditions (3.14) are provided by

$$
\begin{aligned}
a > 0 \quad \text{or} \quad & a < 0: \; n_{02} m_{01} \tilde{sigma}_1 > r_0 d_* (n_{01} - n_{02}) \tilde{a}_{21} \to P_2(a) > 0, \\
& a > 0: \; \tilde{\sigma}_2 > \bar{c} \tilde{a}_{21} (1 - a a^-)/(a - a^-), \\
& \qquad \bar{c} = 2/(m_{01}/n_{01} d_* + 1) \to P_2(a^-) < 0, \\
& a < 0: \; \tilde{\sigma}_2 > \bar{c} \tilde{a}_{21} (1 - a a^+)/(a - a^+) \to P_2(a^+) < 0.
\end{aligned} \tag{3.25}
$$

For the proof of the first condition $P_2(a) > 0$ we rewrite the first (3.17) expression:

$$
\operatorname{sign}[P_2(a)] = \operatorname{sign}[2\tilde{\sigma}_1 m_{01} n_{02} - 2 r_0 d_* \tilde{a}_{21} (n_{01} - n_{02})]. \tag{3.26}
$$

For the two other we apply (3.24).

In order to explicate these results we must take into account the multiple cross-sections in $\tilde{\sigma}_i$ and $\tilde{a}_{21}$. We try to find sufficient conditions independent of these cross-sections, which means valid if they are very large. These cross-sections are contained linearly in $\tilde{\sigma}_i$ and $\tilde{a}_{21}$. We consider ternary, quaternary and fifth order collisions and use the following method. We seek lower bounds for $\tilde{\sigma}_i$ which factorize a term containing linearly the cross-sections with positive coefficients functions of the microscopic densities. We determine this positive term to factorize also the cross-section-dependent part of $(n_{01} - n_{02})\tilde{a}_{ij}$. If we succeed in finding such a factor, it can be eliminated from (3.25) and we obtain sufficient conditions independent of the cross-sections.

Firstly, we consider only the ternary and quaternary collisions with $\tilde{a}_{21}$ *written in* (3.7). The (3.25) conditions are satisfied if σ_{CD} and $\tilde{\sigma}_K$ are small. However, as we shall see they can be also satisfied if they are large, provided conditions on the asymptotic state are required. The five parameters n_{0i}, m_{0i}, r_0 satisfy the two (3.1) relations and it remains to choose three arbitrary parameters n_{01}, n_{02}, m_{01}, from which we obtain the two other:

$$
m_{02} = m_{01} n_{02}/n_{01}, \qquad r_0 = m_{01} \sqrt{n_{02}/n_{01}}\,. \tag{3.27}
$$

We wish to obtain from (3.25) conditions independent of the cross-sections. The first (3.25) condition becomes:

$$
\tilde{\sigma}_1 > r_0 d_* (n_{01} - n_{02}) \tilde{a}_{21}/n_{02} m_{01}\,. \tag{3.28}_1
$$

$\tilde{a}_{21}$ is written in (3.7) but for ternary and quaternary collisions we retain only the terms $\sigma_{DE} = \sigma_D + \sigma_E$, σ_K. $\tilde{\sigma}_1$ is written in (3.3) but for $\tilde{A}_{11}$ we have [1] terms coming from other ternary and quaternary cross-sections $\sigma_E, \sigma_H, \sigma_I$:

$$
\begin{aligned}
\tilde{a}_{21} &= m_{01} m_{02} (n_{01} - n_{02})(\sigma_{DE} + (n_{01} + n_{02})\sigma_K), \\
\tilde{\sigma}_1 &= m_{01} m_{02} \Big[\sigma_B^{(1)} + 2(n_{01} + n_{02})(\sigma_{DE} + \sigma_E + \sigma_K (n_{01} + n_{02})) \\
&\qquad + 2 n_{01} n_{02} \sigma_H + 2 m_{01} m_{02} \sigma_I \Big].
\end{aligned} \tag{3.28}_2
$$

For $\tilde{\sigma}_1$ we obtain a lower bound if we retain only the terms coming from σ_{DE}, σ_K:

$$2m_{01}m_{02}(n_{01}+n_{02})(\sigma_{DE}+\sigma_K(n_{01}+n_{02})) = 2(n_{01}+n_{02})\tilde{a}_{21}/(n_{01}-n_{02}) > 0.$$

If we require that in $(3.28)_1$ the inequality should be satisfied with this lower bound, it will be automatically satisfied for the $\tilde{\sigma}_1$ larger than this lower bound. With this lower bound substituted in $(3.28)_1$ we see that the positive factors $\tilde{a}_{21}/(n_{01}-n_{02})$ at the lhs and $(n_{01}-n_{02})\tilde{a}_{21}$ at the rhs are present. Consequently the constraint $(3.28)_1$ becomes independent of $\tilde{a}_{21}$, or of the cross-sections σ_{DE}, σ_K. In such a way we obtain the conditions for ternary and quaternary collisions:

ternary and quaternary:

$$(3.29)_1 \qquad P_2(a) > 0 \qquad \text{if} \qquad 1 < 2(n_{01}+n_{02})\sqrt{n_{01}n_{02}}/d_*(n_{01}-n_{02})^2.$$

Secondly, we include the fifth order collisions and the lower bound becomes $\tilde{\sigma}_1 > (n_{01}+n_{02})\tilde{a}_{21}/(n_{01}-n_{02}) > 0$, the only change being a factor 2, and $(3.29)_1$ becomes:

fifth order:

$$(3.29)_2 \qquad P_2(a) > 0 \qquad \text{if} \qquad 1 < (n_{01}+n_{02})\sqrt{n_{01}n_{02}}/d_*(n_{01}-n_{02})^2.$$

Similarly $\tilde{\sigma}_2$ has also a lower bound related to $a\tilde{a}_{21}$: $\tilde{\sigma}_2 > C\tilde{a}_{21}/a$ with C a parameter which depends on the multiple collisions considered. For ternary and quaternary collisions $C = 1$. For only fifth order collisions Fig. 1 M-N-T we find $C = 2$. If all ternary, quaternary and fifth order collisions are considered, then $C = 1/2$. Taking into account this lower bound in (3.25), we get constraints independent of the cross-sections:

$$(3.30) \qquad \begin{aligned} &a > 0, \qquad P_2(a^-) < 0 \quad \text{if} \quad a(C-\bar{c}) - a^-(C-a^2\bar{c}) > 0, \\ &a < 0, \qquad P_2(a^+) < 0 \quad \text{if} \quad -a(C-\bar{c}) + a^+(C-a^2\bar{c}) > 0. \end{aligned}$$

Recalling that the $a^\pm$ roots of P_{22} written in (3.16) depend only on the parameters of the asymptotic state, we obtain the following Lemma:

LEMMA 5. Sufficient conditions for the Whitham conditions (3.14), valid for any ternary, quaternary and fifth order cross-sections values, are provided by the (3.29), (3.30) conditions on the arbitrary parameters of the asymptotic state.

For $P_2(a) > 0$, $d = 2$, and ternary and quaternary collisions we get as sufficient condition: $0.23 = 1/4.35 < n_{02}/n_{01} < 4.35$ (better than $n_{02}/n_{01} = 1$ for $A_{ij} = 0$). If we include fifth order collisions we get: $0.36 < n_{02}/n_{01} < 2.77$. For $P_2(a^\pm) < 0$ we can either consider $\bar{c} < C$, $m_{01}/d_*n_{01} > 2/C - 1$ or take into account the $a^\pm$ values which depend on the n_{01}, n_{02}, m_{01} parameters.

4. H-theorem and criterion for elementary collision term

In the present introduction of elementary collision term and in subsections 4.1, 4.2 we consider the models with x-axis along the median of the square, while in subsection 4.3 we will report the results for the $8v_i$ model with x-axis along the diagonal. This model was previously studied in our first paper [1] subsection 6.3, and the drawing of the multiple collision terms in Fig. 1c.

Each drawing of Fig. 1a corresponds to a collision term of the type $q = X - Y$ with X and Y products of the densities. Let us call q_{N_1}, q_R, q_{M_1} the nonlinear terms associated with p_+N_1, R_t, q_+M_1. For each drawing these terms are equal to q multiplied by constants $q_{N_1} = \lambda q$, $q_R = \nu q$, $q_{M_1} = \zeta q$. For instance, for the drawing represented in Fig. 1a – M we find $q_1 = R^2N_1^2M_2 - M_1^3N_2^2$ with $\lambda = -1$, $\nu = -1$, $\zeta = 3$. Now taking into account the symmetries of the square, other collisions can occur. For instance cf. Fig. 1b for the three elementary collision terms of Fig. 1a – M. Firstly, it can happen that the same analytical q is present in other drawings and for the sum we must verify that the corresponding coefficients λ, ν, ζ are such that the conservation laws are satisfied. We call such a q term *elementary collision term*. Secondly, other analytically different q collision terms can exist. For instance with the transform $N_1 \longleftrightarrow N_2$, $M_1 \longleftrightarrow M_2$, from the previous q term we find another one $q_2 = R^2N_2^2M_1 - M_2^3N_1^2$ that we still call elementary collision term $q = X - Y$ with X and Y only products of the densities. Thirdly still, with the symmetries of the square, we find also another elementary collision term $q_3 = M_1M_2N_1N_2R - R^3N_1N_2$ which simply factorizes Q_2. Let us write for the two first collision terms, containing factors of both Q_1, Q_2 $q = X(1 - X/Y)$ with $Y/X = N_1^{\alpha_1}R^{\gamma}...$ where for brevity we do not write the powers of M_i, N_2. For each of the two q terms we plot the $\alpha_1, \lambda_1, \nu, \gamma$ values:

Coll.	q	α_1	λ	ν	γ
M, q_1	$R^2N_1^2M_2 - M_1^3N_2^2$	-2	-1	-1	-2
M, q_2	$R^2N_2^2M_1 - M_2^3N_1^2$	2	1	-1	-2

We remark that $\alpha_1/\lambda = \gamma/\nu$, and the same relation being found for other elementary collision terms, we will study later the theoretical reason for this result. Finally for collisions of the M type we must sum all these terms with the associated λ, ν, ζ constants and if we write $X - Y$ for the respective sums of q_{N_1}, q_R, q_{M_1}; in general they are not proportional to one analytic term and X, Y are not simply products of the densities. For the H-theorem we can either show that each elementary q collision term gives a negative contribution to the evolution of the h-functional, or the same property for the sum of these elementary terms attached to the same type of collision; for instance for the Fig. 1 fifth order collisions M or N ... or T. We begin with this last case.

4.1. H-theorem: Models with x-axis along the median

We define Q_{M_i}, Q_{N_i}, Q_R for the nonlinear part of the nonlinear equations associated with the densities M_i, N_i, R. For brevity we do not introduce double subcripts corresponding to the sums over all elementary collisions terms and to the sums over all types of collisions:$C, D, ...L$ for ternary, quaternary and $M, ...T$ for fifth order. The main reason, as we shall see, being that it is sufficient for each type of collisions to prove that it gives a negative contribution. From the conservation laws we have the linear relations $Q_{N_2} = -Q_{N_1}$, $Q_{M_1} = -d_*(Q_R/2 + Q_{N_1})$, $Q_{M_2} = -d_*(Q_R/2 - Q_{N_1})$. We define the h-functional $h/d_* = R\log R + \sum N_i \log N_i + \sum M_i \log M_1/d_*$ that we introduce into the nonlinear equations of the models. For the h-functional we must prove:

$$A = N_1 \log N_1 - N_2 \log N_2 + (M_1 \log M_1 - M_2 \log M_2)/d_*,$$

$$(4.1)\quad (\partial_t h + \partial_x A)/d_* = Q_R \log R + \sum Q_{M_i} \log M_i/d_* + Q_{N_i} \log N_i < 0$$

$$\rightarrow \text{ H-theorem.}$$

Using the above linear equations we can eliminate Q_{N_2} and Q_{M_i}. Keeping only Q_{N_1}, Q_R the rhs of (4.1) becomes:

$$(4.2)\qquad Q_{N_1} \log(M_2 N_1/M_1 N_2) + (1/2) Q_R \log(R^2/M_1 M_2).$$

We recall that Q_{N_1} and Q_R contain linearly the binary collision terms: $Q_R = Q_2(\sigma_B^{(1)} + A_{11}) - Q_1 A_{12}$, $Q_{N_1} = -Q_1(\sigma_B^{(2)} + A_{22}) + Q_2 A_{21}$ that we substitute into (4.2):

$$(4.3)\qquad \left[Q_1(\sigma_B^{(2)} + A_{22}) - Q_2 A_{21}\right] \log(M_1 N_2/M_2 N_1) + \left[Q_2(\sigma_B^{(1)} + A_{11}) - Q_1 A_{12}\right] (1/2) \log(R^2/M_1 M_2).$$

LEMMA 6. If $A_{ii} > 0$, $A_{ij} = 0$, the H-theorem is satisfied. As application for the triple and quadruple collisions C, F, G, H, I, J, L as well as for the fifth order O collisions, the H-theorem is satisfied.

In these cases, recalling that $Q_1 = N_1 M_2 - N_2 M_1$, $Q_2 = M_1 M_2 - R^2$, we see that the rhs of (4.1) written in (4.3) is negative.

For $A_{ij} \neq 0$ we give the proof for the remaining DE, K cases of the ternary and quaternary collisions, and below we shall study the fifth order collisions using a criterion for the elementary collision terms.

We rewrite the rhs of (4.1)–(4.3), from the linear relations $Q_R = -(Q_{M_1} + Q_{M_2})/d_*$, $Q_{N_1} + (Q_{M_2} - Q_{M_1})/2d_*$, in terms of Q_{M_i}

$$(4.4)\qquad 2(\partial_t h + \partial_x A) = Q_{M_1} \log(M_1^2 N_2/R^2 N_1) + Q_{M_2} \log(M_2^2 N_1/R^2 N_2).$$

LEMMA 7. For the ternary and quaternary collision terms with cross-sections σ_{DE}, σ_K, the H-theorem is satisfied.

We find $Q_{M_i}/2d_* = [\sigma_{DE} + (N_1 + N_2)\sigma_K](N_i R^2 - M_i^2 N_j)$, $j \neq i$ and the contributions to the rhs of (4.4) are negative.

4.2. Criterion for elementary collision term: x-axis along the median

For the elementary collision terms we establish a criterion for the validity of the H-theorem, from the property that the binary and multiple collisions have the same equilibrium states. This means that the equilibrium states are determined only by the two independent relations: $N_1M_2/N_2M_1 = 1$, $R^2/M_1M_2 = 1$. As explained above, let $q = X - Y$ be any elementary multiple collision term (X, Y only products of the densities) and define:

$$Y/X = N_1^{\alpha_1}N_2^{\alpha_2}M_1^{\beta_1}M_2^{\beta_2}R^{\gamma}. \tag{4.5}$$

LEMMA 8. For any elementary collision term $q = X - Y$, necessarily Y/X is the product of R^2/M_1M_2 and N_1M_2/N_2M_1 in some arbitrary powers. Furthermore we have:

$$Y/X = [R^2/M_1M_2]^{\gamma/2}[N_1M_2/N_2M_1]^{\alpha_1}. \tag{4.6}$$

Firstly, otherwise at equilibrium state we eliminate $R = \sqrt{M_1M_2}$, and between the N_i, M_i there will exist another relation than $M_1N_2 = M_2N_1$, and different equilibrium states. Secondly we apply (4.5). We discard, in the following, the trivial cases with only one factor in (4.6), because in this case q simply factorizes one of the two binary q_i terms and it is sufficient to apply Lemma 6. Let us define, for this elementary collision term, the constants proportional to q for the nonlinear equations associated with p_+N_1, R_t:

$$q_{N_1} = \lambda q, \qquad q_R = \nu q. \tag{4.7}$$

From the ν, λ coefficients, with the linear relations corresponding to the conservation laws recalled above, we deduce the corresponding ones $-\lambda$, $-d_*(\lambda + \nu/2)$, $d_*(\lambda - \nu/2)$ for q_{N_2}, q_{M_1}, q_{M_2}.

THEOREM 1. *The elementary $q = X - Y$ collision term gives a negative contribution to the H-theorem if* $[\lambda/c = \alpha_1,\ \nu/c = \gamma,\ c > 0]$.

Firstly, in (4.1) we replace q_R, q_{N_i}, q_{M_i} by q multiplied by the corresponding λ, ν constants written in (4.6) and above. We explicitly write the contribution coming from q

$$\partial_t h + \partial_x A = d_*X(1 - Y/X)\log\left[(R^2/M_1M_2)^{\nu/2}(N_1M_2/N_2M_1)^{\lambda}\right] + \ldots \tag{4.8}$$

but the complete rhs is a sum of such terms with different λ, ν values. Secondly, considering Y/X written in (4.6) and the relations between the λ, ν and α_1, γ parameters written in the Theorem, we see that the rhs of (4.8) is negative for the contribution coming from Q.

We want to apply this criterion to all multiple collision terms not proportional to only one binary collision term. For a collision DE or K or M, N ... or T we

have different q elementary collisions terms. We do not report both values for two q terms obtained by the exchange $N_1 \longleftrightarrow N_2$, $M_1 \longleftrightarrow M_2$.

Coll.	q	α_1	λ	ν	γ
DE	$M_1^2N_2 - N_1R^2$	1	1	2	2
K	$M_1^2N_2^2 - R^2N_1$	1	1	2	2
K	$R^2N_1^2 - M^2N_1N_2$	−1	−1	−2	−2
M	$R^2N_1^2M_2 - M_1^3N_2^2$	−2	−1	−1	−2
N	$R^2N_1^2M_2 - M_1^3N_2^2$	−2	−2	−2	−2
N	$RM_1^2N_2^2 - R^3N_1N_2$	1	1	2	2
P,Q	$R^4N_1 - N_2M_2M_1^3$	−1	−1	−4	−4
R	$M_1^2N_1^2N_2 - R^2N_1^2N_2$	1	1	2	2
S	$M_2^2RN_1N_2 - R^3N_2^2$	−1	−1	2	2
S,T	$M_2^3N_1^2 - R^2M_1N_2^2$	−2	−2	2	2

All these elementary collision terms can be written as linear combinations of the two binary ones and we verify the criterion: $\alpha_1/\lambda = \gamma/\nu$. For the terms obtained with $N_1 \longleftrightarrow N_2$, $M_1 \longleftrightarrow M_2$, $R \longleftrightarrow R$ we see that $\alpha_1 \longleftrightarrow -\alpha_1\gamma \longleftrightarrow \gamma$ and we have verified that $\lambda \longleftrightarrow -\lambda$, $\nu \longleftrightarrow \nu$ so that the two ratios do not change. In conclusion all the ternary, quaternary and fifth order collisions satisfy the H-theorem.

4.3. H-theorem and criterion for the model with x-axis along the diagonal

We call Q_R, Q_{N_i}, Q_{M_i} the nonlinear part associated with the equations R_t, p_+N_1, p_-N_2, q_+M_1, q_-M_2. We recall both the three linear relations [1] and the analytical structure of Q_R, Q_{N_1}, combinations of the three binary collision terms Q_i, $i = 1,2,3$

$$
\begin{aligned}
Q_{N_1} + Q_{N_2} &= Q_{M_1} + Q_{N_1} + Q_R = Q_{M_2} + Q_{N_2} + Q_R = 0,\\
Q_1 &= N_2R - N_1M_2, \qquad Q_2 = M_1N_2 - N_1R,\\
Q_3 &= M_1M_2 - R^2,\\
Q_{N_1} &= Q_1\left(\sigma_B^{(1)} + A_{11}\right) + Q_2\left(\sigma_B^{(1)} + A_{21}\right) + Q_3A_{31},\\
Q_R &= -Q_1\left(\sigma_B^{(1)} + A_{13}\right) + Q_2\left(\sigma_B^{(1)} + A_{23}\right) + Q_3\left(\sigma_B^{(2)} + A_{33}\right).
\end{aligned}
\tag{4.9}
$$

The coefficients A_{ij} which depend on the densities N_i, M_i, R have been reported in a table [1]. We define the functional $h = \sum(M_i \log M_i + 2N_i \log N_i) + 2R \log R$

and we must prove that

$$A = 2(M_1 \log M_1 - M_2 \log M_2 + N_1 \log N_1 - N_2 \log N_2),$$

$$\partial_t h + \partial_x A = 2Q_R \log R + \sum (Q_{M_i} \log M_i + 2Q_{N_i} \log N_i < 0 \quad (4.10)$$

$$\rightarrow \text{ H-theorem.}$$

Using the (4.9) linear relations we eliminate Q_{N_2}, Q_{M_i} and rewrite the rhs in terms of Q_{N_1}, Q_R:

$$\partial_t h + \partial_x A = Q_{N_1} \log(M_2 N_1^2 / M_1 N_2^2) + Q_R \log(R^2 / M_1 M_2). \quad (4.11)$$

We recall that all ternary and quaternary collisions Fig. 1c – C-D...L as well as fifth order collisions Fig. 1c – M-N...T were studied [1]. For the H-theorem, like in the two preceding subsections, we can, for a given type of collision, either sum over all elementary collision terms or verify the criterion for each elementary term. We begin with the first case.

LEMMA 9. In both cases: (i) $Q_{N_1} = C_1 \sum N_i Q_i, Q_R = C_2 Q_3, C_i \geq 0$, (ii) $Q_{N_1} = C_1 Q_1 + C_2 Q_2, Q_R = C_2 Q_2 - C_1 Q_1 + C_3 Q_3, \ C_i \geq 0$, the rhs of (4.11) is negative and the H-theorem is satisfied.

For the proof we first consider case (i) and the rhs (4.11) becomes:

$$2C_1[Q_2 \log(RN_1/M_1 N_2) + Q_1 \log(M_2 N_1 / RN_2)] + C_3 Q_3 < 0.$$

We can apply this result to Fig. 1c – C-D with $C_1 = 1, C_2 = 0$, to Fig. 1c – F with $C_1 = R, C_2 = 0$, to Fig. 1c – H with $C_1 = 0, C_2 = M_1 M_2 + R^2$, and to Fig. 1c – I with $C_1 = 0$, $C_2 = 2N_1 N_2$.

Secondly, we consider case (ii) where the rhs (4.11) becomes:

$$2C_1 Q_1 \log(M_2 N_1 / RN_2) + 2C_2 Q_2 \log(RN_1 / M_1 N_2) + C_3 Q_3 \log(R^2 / M_1 M_2) < 0.$$

We can apply this result to: Fig. 1c – E with $C_1 = C_2 = N_1 + N_2$, $C_3 = 0$, Fig. 1c – P with $C_1 = C_2 = N_1 N_2 (N_1 + N_2)$, $C_3 = 0$, Figs. 1c – J-G-K with $C_i = N_j R + N_i M_j$, $i \neq j$ and, respectively, $C_3 = 0, 2N_1 N_2, N_1^2 + N_2^2$. All ternary collisions and all quaternary (except Fig. 1c – L) are covered by this lemma. For the missing quaternary collisions and all fifth order collisions we will apply a criterion for elementary collision terms. We sketch briefly the proof which is similar to the previous one with the x-axis along the median of the square.

Firstly, the equilibrium states being the same for binary or multiple collisions, for any elementary collision term $q = X - Y$ the ratio Y/X is the product of $N_1^2 M_2 / N_2^2 M_1$ and $R^2 / M_1 M_2$ at some arbitrary powers. Indeed, from $Q_i = 0$, $i = 1, 2, 3$ at equilibrium we have $R = M_1 N_2 / N_1 = N_1 M_2 / N_2$ and only one relation between N_i, M_i. If the above product is not true, eliminating

$R = \sqrt{M_1 M_2}$ at equilibrium, we will have another N_i, M_i relation. Secondly, writing $Y/X = N_1^{\alpha_1} N_2^{\alpha_2} M^{\beta_1} M^{\beta_2} R^{\gamma}$, we have

$$Y/X = \left(N_1^2 M_2 / N_2^2 M_1\right)^{\alpha_1/2} \left(R^2/M_1 M_2\right)^{\gamma/2}. \tag{4.12}$$

Thirdly we define the constants $q_{N_1} = \lambda q$, $q_R = \nu q$ and finally get the

THEOREM 2. *The elementary $q = X - Y$ collision terms give a negative contribution to the h-functional if $\lambda/c = \alpha_1$, $\nu/c = \gamma$, $c > 0$.*

For the proof, we substitute in (4.11) Q_{N_1}, Q_R by q multiplied by λ, ν and apply (4.12).

$$\partial_t h + \partial_x A = d_* X(1 - Y/X) \log[(R^2/M_1 M_2)^{\nu} (N_1^2 M_2 / N_2^2 M_1)^{\lambda}] < 0. \tag{4.13}$$

As a particular case, if $\gamma = 0$ we must have $\nu = 0$. This happens for the Fig. 1c – Q collision with $q = N_1 N_2^3 M_1 - N_2 N_1^3 M_2$ with $\alpha_1 = \lambda = -2$. We apply this criterion to all other cases not covered by Lemma 9. We discard also elementary collision terms proportional to only one binary term and report only one case for the two q which can be deduced from $N_1 \longleftrightarrow N_2$, $M_1 \longleftrightarrow M_2$:

Coll.	q	α_1	λ	γ	ν
L	$R^3 N_2 - M_1 M_2^2 N_1$	1	1	−3	−3
O	$N_1^3 M_2^2 - R N_2^3 M_1$	−3	−3	1	1
R	$R^3 N_2^2 - M_1 N_1 N_2 M_2^2$	1	1	−3	−3
R	$R^3 N_1 N_2 - M_1 N_1^2 M_2^2$	1	1	−3	−3
S	$N_1 N_2^2 M_2 R - N_2^3 R^2$	−1	−1	1	1
S	$N_1^3 M_2 R - N_2^3 M_1^2$	−3	−3	−1	−1
T	$M_2^2 N_1^2 N_2 - N_2^3 R^2$	−2	−2	2	2
T	$R^2 N_1^2 N_2 - N_2^3 M_1^2$	−2	−2	−2	−2

We verify in all cases the criterion: $\alpha_1/\lambda = \gamma/\nu$.

Appendix A. Fifth order collisions

We determine all the fifth order collisions satisfying 1) spectatorlessness (i.e. all the particles change their velocities in the collision), 2) microscopic energy conservation $\sum v_i^2 = \sum v_i'^2$, 3) momentum conservation $\mathbf{v} = \sum \mathbf{v}_i = \mathbf{v}' = \sum \mathbf{v}_i'$, where primes denote the relevant values, e.g. after collision. We remind that in the square $8v_i$ model there are only four different velocity vectors $\mathbf{v}_i$ of the [1] type, and four of the [2] type.

CASE I. We show that for 5th order collisions there are no collisions [1] + [1] + [1] + [1] + [1] = idem, and [2] + [2] + [2] + [2] + [2] = idem, satisfying 1), 2), 3).

We note that if there are five [1] particles in the same direction (say, M_1) with projection of the total momentum **v** on the x axis $v_x = 5$ before collision, then, in order for 1) to be satisfied, the only possible directions for the postcollisional particles are those which correspond to R, inverse of R, and M_2. This results in $v'_x \leq 0$, therefore 3) is not satisfied. If there are four or three [1] particles in the same direction, then with 1) satisfied, 3) is violated. More in detail, in the former case there are two different possibilities of the fifth [1] particle, and the projection of the total momentum on the direction of the four [1] particles is 4 or 3, which, by 1), can not be satisfied in any of the postcollisional configurations. In the latter case there are four possible configurations of the remaining two [1] particles, and in each case with 1) satisfied, the projection of the total momentum on the direction of the three [1] particles can not be satisfied. For two pairs of [1] particles in two directions, there are two possibilities of the precollisional directions of both [1] pairs: parallel or perpendicular. The fifth particle occupies the third direction, therefore, with 1) satisfied, there is only one possible direction for all the [1′] postcollisional particles, and again 3) is violated. For at most one pair of two [1] particles in one direction, 1) can not be satisfied, since all four directions possible for [1] particles before collision are occupied. Similar considerations hold for [2] + [2] + [2] + [2] + [2] = idem case.

CASE II. There are no collisions [1] + [2] + [2] + [2] + [2] = idem, satisfying 1), 2), 3). If there are four [2] particles with the same precollisional direction, say that of N_1, or three in the same and one in the opposite direction, then, with 1) satisfied, the projection of **v** on N_1 is not conserved. For three [2] particles in N_1 direction and one [2] perpendicular, the projection of **v** either on x or on y axis is not conserved. Conservation of momentum excludes also two [2] particles in the same direction [along the scheme discussed above for Case I: with 1) satisfied, 3) can not hold, we omit details]. Finally, for four [2] particles, each in a different direction, 1) can be not satisfied.

CASE III. [1] + [1] + [2] + [2] + [2] = idem. First we assume three of [2] particles in the same (e.g. N_1) direction. There are six different configurations of the remaining two [1] particles: one, in which two [1] particles have velocities opposite to each other (we identify symmetrical cases), three with perpendicular velocities of [1] particles, and two with their velocities in the same direction. With 1) satisfied, we eliminate all these configurations by checking that either the projection of **v** on N_1, or on one of the coordinate axis is not satisfied.

Second, we assume each of [2] particles in a different direction. Again, with 1) satisfied, the postcollisional velocities of all [2] particles must be the same which, for any configuration of the two [1] particles, results in violation of 3).

Third, for two particles [2] in one (say N_1) direction, the third of [2] is either perpendicular, or has the opposite direction along N_1. In the former case the

projection of v on x is at least 1, whereas, with 1) satisfied, the projection of v′ on x is at most -1. Thus, 3) is not satisfied. In the latter case either three of [2′] has the same (perpendicular to N_1) direction (the case already excluded), or two of [2′] are perpendicular to N_1, and third [2′] has the direction opposite to both [2′]. Examination of all configurations and outcomes for both [1] particles implies that the only collision compatible with 1), 2), 3) is that shown in diagram R of Fig. 1a.

First we analyse all the precollisional configurations of the remaining [1] particles, associated with the given configuration of the three [2] ones. There are six different configurations of [1] particles. If both [1] are in M_1 direction, then, due to 1), there can be no v_x momentum conservation. If the [1] particles have different directions (there are four different configurations of this kind), then, with 1) satisfied, the possible [1′] directions exclude the momentum conservation in the v_y direction. There remains the configuration of both [1] particles in M_2 direction. In this case we have $v_x = -1$, $v_y = 1$. We now analyse all the configurations of the [1′] particles (we remind that [2′] directions are already fixed). For each possible configuration we calculate the momentum projections on the x and y axis. When these projections agree with the precollisional ones, we check 1) in addition. With that procedure we obtain the R-diagram as the only one which satisfies 1) and 2).

CASE IV. [1] + [1] + [1] + [2] + [2] = idem. If each of [1] has a different direction, then with the remaining unoccupied direction as the only one (by 1)) for all [1′] particles, 3) can not be satisfied. For two of [1] in the same direction, the only collisions satisfying 1), 2), 3) are those corresponding to diagram O in Fig. 1a.

Finally, with three of [1] particles in one direction, we obtain diagrams M, N, S, T of Fig. 1a as the only ones for the considered type of the collisions. In all the other cases, with 1) satisfied, 3) is violated. The proof follows the lines reported above for the R-diagram, therefore we omit details.

CASE V. [1] + [1] + [1] + [1] + [2] = idem. First, all different directions of [1] are excluded by 1). Second, with three of [1] in the same direction, e.g. the y-axis, either the fourth one is perpendicular, or has the opposite direction along y. In the former case y-projection of v can not be conserved. The latter leads to diagrams P, Q only. Finally, the case of two [1] particles in one direction gives no new diagrams.

Acknowledgments

One of the authors (T. Płatkowski) of this paper was supported in part by the KBN under grant No. 2-P301-027-06. This support is a gratefully acknowledged.

References

1. H. CORNILLE, T. PŁATKOWSKI, Part I, this volume.
2. G.B. WHITHAM, Comm. Pure Appl. Math., **12**, 113, 1959; T.T. WU, Comm. Pure Appl. Math., **14**, 745–747, 1961.
3. R. GATIGNOL, Lect. Notes in Phys., **36**, Springer, 1975.
4. I.E. BROADWELL, Phys. Fluids, 7, 1243–1247, 1964.
5. H. CORNILLE, T. PŁATKOWSKI, J. Stat. Phys, **71**, 733, 1993.
6. B. CHOPPARD and M. DROZ, Phys. Let., **A126**, 476, 1988.
7. H. CORNILLE, JMP, **32**, 3439, 1991.
8. P. CHAUVAT, F. COULOUVRAT and R. GATIGNOL, [in:] Advance in Kinetic Theory, R. GATIGNOL and SOUBBARAMAYER [Eds.], Springer Verlag, 1991 p. 139; P. CHAUVAT and R. GATIGNOL, TTSP, **21**, 417, 1992; H. CABANNES, Eur. J. Mech. B Fluids, **11**, 415, 1992; P. CHAUVAT, Thesis, Paris 1993.
9. H. CORNILLE, Saclay preprint 1993.

SERVICE DE PHYSIQUE THEORIQUE,
CE SACLAY, GIF-SUR-YVETTE, FRANCE
and
DEPARTMENT OF MATHEMATICS, INFORMATICS AND MECHANICS
WARSAW UNIVERSITY, POLAND.

Received April 29, 1994.

Arch. Mech., 46, 5, pp. 735–755, Warszawa 1994

Flutter analysis of a two-dimensional airfoil with nonlinear springs based on center-manifold reduction

J. GRZĘDZIŃSKI (WARSZAWA)

METHODS OF LOCAL BIFURCATION theory are applied to a nonlinear integro-differential flutter equation of a thin airfoil placed in an incompressible flow. Center-manifold reduction leads to the two-dimensional normal form of the classical Hopf bifurcation. Limit cycle amplitude and frequency are calculated and compared with those of time marching finite difference scheme and harmonic balance method.

1. Introduction

THE SIMPLEST aeroelastic model of a two-dimensional airfoil representing typical wing section of an aircraft is extensively used since the earliest days of flutter analysis [1]. Under some simplifying assumptions, limiting in general the analysis to the small amplitude harmonic motion of an airfoil of infinitesimal thickness placed in a plane ideal gas flow, the problem is fully linearized and the essential part – the unsteady aerodynamic forces – is given analytically. The stability boundary in terms of flutter velocity – the critical velocity above which the steady aircraft motion becomes unstable – is then determined by solving repeatedly an eigenvalue problem for a complex-valued matrix.

Although recent flutter analysis of an aircraft is much more sophisticated and includes many degrees of freedom, this simplest two-dimensional model serves frequently as a basis for testing new computational methods of aeroelastic analysis, usually relaxing some of the linearizing assumptions. This is also the case of the present paper.

Even if it is linearized, the aerodynamic operator relating the unsteady aerodynamic forces to the deflection of an aircraft structure (generalized coordinates) always determines feasible methods for flutter analysis of nonlinear structures. In the unsteady subsonic motion, the aerodynamic forces depend on the history of motion as a result of the shedding of the vortical wake behind an aircraft. Consequently, the aerodynamic operator is always of the form of convolution integral and cannot be simplified without additional assumptions. Thus, in the time domain, the flutter equation is an integro-differential equation. This causes no difficulty in the absence of nonlinear terms – after applying Laplace transform the whole problem transforms as a linear algebraic equation into frequency domain.

The great simplicity of working in the frequency domain influenced probably the development of the harmonic balance method dealing with certain structural nonlinearities and introduced for the first time in 1959 [2]. This method, capable

of handling only concentrated nonlinearities, replaces each nonlinear restoring force by the first term of its Fourier transform. If there is only one nonlinear force present in a system, then for any given limit cycle amplitude the flutter equation can be solved for the corresponding flight velocity. Multiple nonlinearities result in greater complexity of calculations. The amplitudes of aircraft deflections at concentration points are not known prior to the calculations since their ratios are determined by the resulting flutter mode. Therefore, any method of solution uses iterative procedures, usually focussed on the aeroelastic system under considerations [3].

An alternative approach relies on numerical algorithms worked out for nonlinear algebraic equations not related to any particular dynamical system. Recently, the most promising are the continuation methods available also as a ready-for-use package of subroutines [4]. Continuation methods were successfully applied to the linear flutter equation [5, 6]. It is worth noting here that this equation, although linear with respect to generalized coordinates, contains aerodynamic forces being nonlinear functions of the frequency of oscillatory motion. Therefore, any method of solving this equation is essentially a nonlinear procedure. A preliminary study of continuation method applied to the flutter analysis of a two-dimensional airfoil with nonlinear springs can be found in Ref. [7].

All linearization techniques in frequency domain assume pure harmonic motion of aeroelastic structure and characterize each nonlinear force during oscillations by a certain average value over a single period of time. If such a simplification is nonsatisfactory, then it is necessary to return back to the integro-differential equation in time domain. The most general approach solves this equation by numerical integration in time with appropriate initial conditions. This time-consuming method encounters one more difficulty concerning calculations of unsteady aerodynamic forces for an arbitrary motion – in order to perform calculations the matrix of the impulsive response functions of the system must be known. This is not a serious problem in the case of two-dimensional airfoil placed in an incompressible flow since the response matrix is then given in terms of well-known Wagner function [8]. However, analogous calculations dealing with compressible flow and aeroelastic systems with many degrees of freedom are of much greater complexity.

The problem simplifies significantly if the response functions are replaced by their approximations having the form of a sum of exponential functions of time. Such an approximation is usually performed in frequency domain because Laplace transform changes the exponential terms into rational functions resulting in much simpler task [9].

Moreover, the rational approximation in frequency domain simplifies the flutter equation in time domain since it gives a system of first-order ordinary differential equations instead of an integro-differential equation. There exists a great variety of methods worked out for nonlinear ordinary differential equations and, therefore, the above approach is frequently used in flutter analysis [10]. On the

other hand, the rational approximation changes qualitatively the aerodynamic operator replacing its logarithmic singularity by a finite number of poles located in an arbitrary manner in the complex Laplace plane. It is known that such a simplification may influence the stability analysis of an aeroelastic system and, therefore, it would be preferable to retain the original form of the aerodynamic operator.

The critical flutter velocity determines a branching point in the phase space of a nonlinear aeroelastic system. In a small neighbourhood of this point two types of solution to the flutter equation are permissible. The first one describes a steady motion that can be stable or unstable, while the second one represents an oscillatory motion and tends asymptotically to the limit cycle oscillations, being in turn also stable or unstable. This type of instability is referred to as the Hopf bifurcation and belongs to bifurcations of the best qualitative understanding [11]. Hopf bifurcation is two-dimensional, what means that limit cycle oscillations are described by only two generalized coordinates, no matter how many degrees of freedom are used in order to describe the original aeroelastic system. A two-dimensional subspace containing these asymptotic oscillations is called center manifold. Thus, as far as an asymptotic analysis is considered, it is possible to obtain the limit cycle for an entire aircraft from only two differential equations. The method of deriving these equations uses the techniques of center manifold reduction and normal form theory [12]. For an aeroelastic system of N degrees of freedom this approach contains several steps:

- formulation of the problem in terms of a system of $2N$ nonlinear integro-differential equations of the first order, instead of a system of N equations of the second order – this is the requirement of the methods of bifurcation theory worked out for such equations;
- identification of the bifurcation point – this is done by solving the fully linearized flutter equation;
- increasing the number of generalized coordinates by one by adding the flight velocity U as a new variable, and also increasing the number of equations to $2N + 1$ by introducing a new equation $dU/dt = 0$ – this is done in order to work on the interval in velocity space in the vicinity of bifurcation point;
- restriction of the aeroelastic system to the appropriate center manifold – this step requires creation of a special nonlinear transformation of the initial $2N+1$-dimensional system of integro-differential equations into a two-dimensional system of ordinary differential equations of the first kind;
- normalization of the reduced system – this step puts the reduced aeroelastic system into a simpler form by applying the so-called near-identity change of coordinates. The simplicity achieved lies in the phase-shift symmetry of the resulting system of equations;
- calculation of the limit cycle amplitude and frequency for a given flight velocity – this task, because of the symmetry of the final equations, is equivalent to finding roots of a polynomial with real coefficients.

The last three steps deal with formal power series expansions of nonlinear terms with respect to generalized coordinates and, therefore, restrict the analysis to a certain neighbourhood of the bifurcation point. The range of validity of the results has to be estimated for each aeroelastic system separately.

2. Flutter equation

The geometrical scheme of a thin two-dimensional airfoil is shown in Fig. 1. Semi-chord b of the airfoil serves as a reference length. The pitch angle and

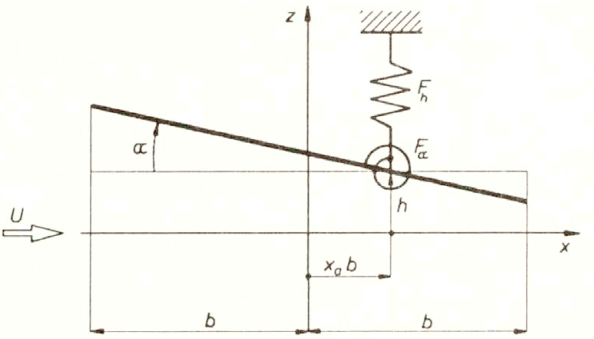

FIG. 1. Two-dimensional thin airfoil.

the plunge displacement during oscillations are described by α and h, respectively. Nondimensional distance measured from airfoil mid-chord to the elastic axis is denoted by x_α. Four nondimensional parameters describe linear dynamical properties of the airfoil:

$$\mu = \frac{m}{\pi \rho b^2} \quad \text{airfoil – air mass ratio,}$$

$$x_\alpha = \frac{S_\alpha}{mb} \quad \text{nondimensional distance measured from the elastic axis to the centre of mass,}$$

$$r_\alpha = \sqrt{\frac{I_\alpha}{mb^2}} \quad \text{radius of gyration about the elastic axis,}$$

$$\Omega = \frac{\omega_h}{\omega_\alpha} \quad \text{uncoupled natural frequency ratio corresponding to linear springs,}$$

where

ρ air density,
m mass of airfoil per unit span,
S_α static moment about the elastic axis per unit span,
I_α moment of inertia about the elastic axis per unit span,
ω_h uncoupled natural frequency of plunging motion,
ω_α uncoupled natural frequency of pitching motion.

For given uncoupled natural frequencies ω_h and ω_α, the corresponding spring constants K_h and K_α can be written as

$$K_h = m\omega_h^2, \qquad K_\alpha = I_\alpha \omega_\alpha^2 .$$

Both springs are assumed to be nonlinear and produce cubic restoring forces F_h and F_α in the plunge and pitch degree of freedom, respectively:

$$F_h = K_h(h + c_h h^3), \qquad F_\alpha = K_\alpha(\alpha + c_\alpha \alpha^3), \tag{2.1}$$

where c_h and c_α are known constants.

Displacements of the airfoil during an unsteady motion are described by the N-dimensional ($N = 2$) vector of geometrical coordinates $\mathbf{u}(t)$ being function of time t:

$$\mathbf{u}(t) = \begin{Bmatrix} h(t) \\ \alpha(t) \end{Bmatrix}. \tag{2.2}$$

In the absence of external aerodynamic forces and under the assumption that $c_h = c_\alpha = 0$ (linear springs), the natural frequencies ω_j and modes $\mathbf{\Phi}_j$ ($j = 1, 2$) can be calculated from the eigenvalue problem

$$\omega_j^2 \mathbf{M}\mathbf{\Phi}_j = \mathbf{K}\mathbf{\Phi}_j , \tag{2.3}$$

where $\mathbf{M}$ and $\mathbf{K}$ are mass and stiffness matrices, respectively:

$$\mathbf{M} = \begin{bmatrix} m & -S_\alpha \\ -S_\alpha & I_\alpha \end{bmatrix}, \qquad \mathbf{K} = \begin{bmatrix} K_h & 0 \\ 0 & K_\alpha \end{bmatrix}.$$

It is convenient to introduce modal coordinates, although in the present case this is equivalent only to a formal linear change of coordinates. For systems with many degrees of freedom such a procedure is frequently used in order to reduce the total number of coordinates, even in the presence of nonlinearities [10]. The vector $\mathbf{q}(t)$ of modal coordinates is defined by the relation

$$\mathbf{u}(t) = \left[\mathbf{\Phi}_1 \,\middle|\, \mathbf{\Phi}_2\right]\mathbf{q}(t), \tag{2.4}$$

and in the absence of structural damping forces it satisfies the equation of motion [13]

$$\ddot{\mathbf{q}}\,(t) + \mathsf{K}\mathbf{q}(t) + \mathbf{k}(\mathbf{q}) = \mathbf{F}_A(\mathbf{q}), \tag{2.5}$$

where $\mathbf{F}_A(\mathbf{q})$ is the vector of generalized unsteady aerodynamic forces. The generalized stiffness matrix K is expressed by natural frequencies ω_1 and ω_2,

$$\mathsf{K} = \begin{bmatrix} \omega_1^2 & 0 \\ 0 & \omega_2^2 \end{bmatrix}. \tag{2.6}$$

The nonlinear term corresponding to Eqs. (2.1) is given by

$$\mathbf{k}(\mathbf{q}) = \left[\Phi_1 \mid \Phi_2\right]^T \left\{ \begin{array}{l} K_h c_h \left(\Phi_1^{(1)} q_1 + \Phi_1^{(2)} q_2\right)^3 \\ K_\alpha c_\alpha \left(\Phi_2^{(1)} q_1 + \Phi_2^{(2)} q_2\right)^3 \end{array} \right\}, \tag{2.7}$$

where $\Phi_j^{(i)}$ denotes the j-th component of the i-th natural mode.

The aim is to find the critical flutter speed for the Eq. (2.5), and also the limit cycle amplitude and frequency in the neighbourhood of the critical point.

Since the aeroelastic system is nonlinear, it is not possible to assume harmonic motion during limit cycle oscillations. Therefore, unsteady aerodynamic forces must be written in a general form valid for an arbitrary motion:

$$\mathbf{F}_A(\mathbf{q}) = \frac{\rho U^2}{2} \int_{-\infty}^{0} \mathbf{g}(-\tau)\mathbf{q}\left(t + \frac{b}{U}\tau\right) d\tau, \tag{2.8}$$

where U denotes the flow velocity. Elements of the matrix $\mathbf{g}$ are response functions corresponding to the impulsive changes of generalized coordinates $\mathbf{q}$. For a thin airfoil in a two-dimensional incompressible flow these functions can be expressed in terms of well-known Wagner function [8]. Finally, the equation of motion (2.5) takes the form of an integro-differential equation containing an integral of convolution type.

The point of interest of this paper is an asymptotic motion of the airfoil. In the analysis of this kind of motion the methods of local bifurcation theory of dynamical systems will be used [14]. Bifurcation theory has been developed for the first-order equations and the flutter equation (2.5) has to be transformed into such a system. This can be easily done by introducing a $2N$-dimensional vector of new coordinates $\mathbf{y}(t)$,

$$\mathbf{y}(t) = \left\{ \begin{array}{c} \mathbf{y}_1(t) \\ \hline \mathbf{y}_2(t) \end{array} \right\}, \tag{2.9}$$

where $\mathbf{y}_1(t) = \mathbf{q}(t)$, $\mathbf{y}_2(t) = \dot{\mathbf{q}}(t)$. The resulting first-order flutter equation is

$$\dot{\mathbf{y}}(t) = \mathbf{D}_U \mathbf{y}(t) + \int_{-\infty}^{0} \mathbf{G}_U(-\Theta; U)\mathbf{y}(t + \Theta)d\Theta + \mathbf{f}_U(\mathbf{y}), \tag{2.10}$$

where square matrices of the order $2N$, $\mathbf{D}_U$, $\mathbf{G}_U$ and the nonlinear term $\mathbf{f}_U(\mathbf{y})$ are given by

$$\mathbf{D}_U = \left[\begin{array}{c|c} \mathbf{0} & \mathbf{I} \\ \hline -\mathsf{K} & \mathbf{0} \end{array} \right], \qquad \mathbf{f}_U(\mathbf{y}) = \left\{ \begin{array}{c} \mathbf{0} \\ \hline -\mathbf{k}(\mathbf{q}) \end{array} \right\},$$

$$\mathbf{G}_U(-\Theta;U) = \left[\begin{array}{c|c} \mathbf{0} & \mathbf{0} \\ \hline \dfrac{\rho U^3}{2b}\mathbf{g}\left(-\dfrac{U}{b}\Theta\right) & \mathbf{0} \end{array}\right],$$

with K and $\mathbf{k}(\mathbf{q})$ given by Eq. (2.6) and Eq. (2.7), respectively.

The critical flutter conditions are fully determined by the linearized flutter equation obtained from Eq. (2.5) for oscillatory motion

$$\mathbf{q}(t) = \hat{\mathbf{q}}e^{st}, \tag{2.11}$$

where

$$s = \gamma + i\omega, \tag{2.12}$$

in the absence of nonlinear term ($\mathbf{k}(\mathbf{q}) = 0$). The vector of unsteady aerodynamic forces is then given by the simple linear relation

$$\mathbf{F}_A(\mathbf{q}) = \mathsf{A}(s;U)\hat{\mathbf{q}}e^{st},$$

where

$$\mathsf{A}(s;U) = \frac{\rho U^2}{2}\int_0^\infty \mathbf{g}(\tau)e^{-\frac{sb}{U}\tau}d\tau \tag{2.13}$$

is called aerodynamic matrix. Usually, this matrix is calculated directly, hence there is no need to evaluate the response matrix $\mathbf{g}$. In the present case the aerodynamic matrix is given by

$$\mathsf{A}(p;U) = -\pi\rho b^2U^2\left[\boldsymbol{\Phi}_1 \,|\, \boldsymbol{\Phi}_2\right]^T \begin{bmatrix} p^2 + 2pC(p) & p + (2+p)C(p) \\ -pC(p) & \dfrac{p^2}{8} + \dfrac{p}{2}\left(1 + \dfrac{p}{2}\right)C(p) \end{bmatrix} \left[\boldsymbol{\Phi}_1 \,|\, \boldsymbol{\Phi}_2\right],$$

where

$$C(p) = \frac{K_1(p)}{K_0(p) + K_1(p)} \tag{2.14}$$

is the generalized Theodorsen function [8] of a complex argument

$$p = \frac{sb}{U}, \tag{2.15}$$

with $K_0(p)$ and $K_1(p)$ being the modified Bessel functions.

Finally, the flutter equation reduces to the eigenvalue problem

$$(\mathsf{A}(s;U) - \mathsf{K})\hat{\mathbf{q}} = s^2\hat{\mathbf{q}}. \tag{2.16}$$

Loss of stability occurs when damping drops to zero ($\gamma = 0$ in Eq.(2.12)) and the flutter boundary is determined by the real negative eigenvalue of Eq. (2.16)

$$s^2 = -\omega_0^2, \tag{2.17}$$

corresponding to the critical flutter velocity $U = U_0$.

The critical bifurcation point of the first order equation (2.10) is defined by the eigenvalues of its linear part corresponding to $\mathbf{f}_U(\mathbf{y}) = 0$. It can be shown [11, 15] that also in the presence of convolution integral within the linear part, the eigenfunctions have the form

$$\mathbf{y}(t) = \hat{\mathbf{y}} e^{st},$$

where s is given by (2.12). The resulting eigenvalue problem is the following:

$$\left[\begin{array}{c|c} \mathbf{0} & \mathbf{I} \\ \hline \mathsf{A}(s;U) - \mathsf{K} & \mathbf{0} \end{array}\right] \hat{\mathbf{y}} = s\hat{\mathbf{y}}. \tag{2.18}$$

It follows from comparison with (2.17) that at the flutter boundary the characteristic matrix of linearized first-order flutter equation has a complex-conjugate, pure imaginary pair of eigenvalues $s = \pm i\omega_0$. Therefore, the Hopf bifurcation of time-periodic solution occurs in the nonlinear aeroelastic system [11].

3. Center-manifold reduction

The Hopf bifurcation is two-dimensional. It means that in the space of solutions to Eq. (2.10), all bifurcating solutions tend asymptotically to a two-dimensional attracting subspace, called center manifold, and generated by eigenvectors corresponding to eigenvalues of zero real parts [14]. Moreover, these asymptotic solutions satisfy certain system of two nonlinear ordinary differential equations of the first order, which can be derived from the integro-differential equation (2.10), written for many degrees of freedom. This procedure of obtaining a low-dimensional system of equations from initial multi-dimensional system is called center-manifold reduction. The most important is that the center-manifold reduction preserves entirely all information about the asymptotic behaviour of the full initial system.

There are two problems associated with center-manifold reduction. Since the aim is to calculate asymptotic limit cycle oscillations for a general form of the nonlinear term $\mathbf{f}_U(\mathbf{y})$, this term is assumed to have a formal power series expansion with respect to generalized coordinates $\mathbf{y}$. Consequently, the method of center-manifold reduction is also based on such expansions. The second problem concerns the way the velocity U should be treated in. The critical flutter conditions correspond to a certain critical value of the velocity $U = U_0$, which in turn

determines the existence of pure imaginary eigenvalues of Eq. (2.18) and the center manifold, as well. At this critical branching point the amplitude of oscillations tends to zero and, in order to obtain finite amplitude limit cycle oscillations, the velocity value must be different from critical. Unfortunately, if $U \neq U_0$, the characteristic matrix of Eq. (2.18) no longer possesses pure imaginary eigenvalues and the center manifold simply does not exist. On the other hand, the existence of the center manifold has been proven in a certain neighbourhood of equilibrium solution $\mathbf{y}_0(t)$, corresponding to $U = U_0$, in the space of solutions $\mathbf{y}(t)$ [11, 16]. For that reason the center-manifold reduction usually applies to the so-called suspended systems [17]. Suspended aeroelastic system is derived from Eq. (2.10) by introducing the difference

$$u = U - U_0 \tag{3.1}$$

as an additional variable satisfying the equation $\dot{u} = 0$. The $2N + 1$-dimensional vector of new generalized coordinates is the following:

$$\mathbf{x}(t) = \begin{Bmatrix} \mathbf{y}_1(t) \\ \hline \mathbf{y}_2(t) \\ \hline u \end{Bmatrix}, \tag{3.2}$$

and it satisfies the equation

$$\dot{\mathbf{x}}(t) = \mathbf{D}\mathbf{x}(t) + \int_{-\infty}^{0} \mathbf{G}(-\Theta; u)\mathbf{x}(t + \Theta)\, d\Theta + \mathbf{f}(\mathbf{x}), \tag{3.3}$$

where square matrices of order $2N + 1$, $\mathbf{D}$, $\mathbf{G}$ and the nonlinear term $\mathbf{f}(\mathbf{x})$ are given by

$$\mathbf{D} = \left[\begin{array}{c|c|c} \mathbf{0} & \mathbf{I} & \mathbf{0} \\ \hline -\mathsf{K} & \mathbf{0} & \mathbf{0} \\ \hline \mathbf{0} & \mathbf{0} & 0 \end{array}\right], \qquad \mathbf{f}(\mathbf{x}) = \begin{Bmatrix} \mathbf{0} \\ \hline -\mathbf{k}(\mathbf{q}) \\ \hline 0 \end{Bmatrix},$$

$$\mathbf{G}_U(-\Theta; u) = \left[\begin{array}{c|c|c} \multicolumn{1}{c|}{\multirow{2}{*}{$\mathbf{0}$}} & \mathbf{0} & \mathbf{0} \\ & & \\ \hline \frac{\rho(U_0 + u)^3}{2b}\mathbf{g}\left(-\frac{U_0 + u}{b}\Theta\right) & \mathbf{0} & \mathbf{0} \\ \hline \multicolumn{1}{c|}{\mathbf{0}} & \mathbf{0} & 0 \end{array}\right].$$

Since the matrix $\mathbf{G}(-\Theta; u)$ now includes the independent variable u instead of the bifurcation parameter U, the integral in Eq. (3.3) is no longer linear with

respect to x. In what follows, the matrix **G** is replaced by the Taylor series

$$\mathbf{G}(-\Theta;u) = \mathbf{G}(-\Theta;0) + \sum_{j=1}^{\infty} \frac{1}{j!} \frac{d^j \mathbf{G}(-\Theta;0)}{du^j} u^j . \tag{3.4}$$

It is also assumed that the multi-variable power series expansion for the nonlinear function **f**(**x**) on the right-hand side of Eq. (3.3) is known:

$$\mathbf{f}(\mathbf{x}) = \sum_{\nu \geq 2} \frac{1}{\nu!} \mathbf{f}_\nu \mathbf{x}^\nu , \tag{3.5}$$

where

$$\mathbf{x}^\nu = \{x_1^{\nu_1} \cdot x_2^{\nu_2} \ldots x_{2N+1}^{\nu_{2N+1}}\} , \qquad \sum_{j=1}^{2N+1} \nu_j = \nu, \qquad \nu_j \geq 0.$$

The number of components of the vector $\mathbf{x}^\nu$ and also the number of columns of each matrix $\mathbf{f}_\nu$ changes from one term to another and equals to the number $c_{\nu,2N+1}$ of compositions of ν into $2N + 1$ parts. The elements of matrices $\mathbf{f}_\nu$ can be easily calculated from Eq. (2.7). For cubic restoring forces the only nonzero matrix is $\mathbf{f}_3$. Substitution of series (3.4) into Eq. (3.3) yields the integro-differential equation valid in a certain neighbourhood of the critical bifurcation point,

$$\dot{\mathbf{x}}(t) = \mathbf{D}\mathbf{x}(t) + \int_{-\infty}^{0} \mathbf{G}(-\Theta;0)\mathbf{x}(t+\Theta)\, d\Theta + \mathbf{f}(\mathbf{x}) + \mathbf{h}(\mathbf{x}), \tag{3.6}$$

where **f**(**x**) is given by Eq. (3.5), while **h**(**x**) equals

$$\mathbf{h}(\mathbf{x}) = \sum_{\eta \geq 2} \frac{1}{(\eta-1)!} \int_{-\infty}^{0} \frac{d^{\eta-1}\mathbf{G}(\Theta;0)}{du^{\eta-1}} \mathbf{x}^\eta(t+\Theta)\, d\Theta, \tag{3.7}$$

where $\mathbf{x}^\eta = \{x_1^{\eta_1} \cdot x_2^{\eta_2} \ldots x_{2N+1}^{\eta_{2N+1}}\}$, and always $\eta = \eta_{2N+1} + 1$ ($x_{2N+1} \equiv u$) which implies that $\sum_{j=1}^{2N+1} \eta_j = 1$. Equation (3.6) will be reduced on the center manifold.

The linear spectrum of Eq. (3.3) now includes one more eigenvalue with zero real part than the previous spectrum of not suspended system (2.10). Hence the center manifold corresponding to Eq. (3.6) is larger than that of Eq. (2.10) and has the dimension of three.

From a quite formal point of view, the center-manifold reduction is equivalent to the appropriate nonlinear change of coordinates given in the form of a series

$$\mathbf{x}(t+\Theta) = \sum_{\mu \geq 1} \frac{1}{\mu!} \mathbf{w}_\mu(\Theta)\mathbf{z}^\mu(t), \tag{3.8}$$

where the vector $\mathbf{z}(t)$ of new coordinates has only three components. The matrices $\mathbf{w}_\mu(\Theta)$ of order $(2N+1) \times c_{\mu,3}$, where $c_{\mu,3}$ denotes the number of compositions of μ into 3 parts, are composed of continuous functions defined over the interval $\Theta \in (-\infty, 0]$. The algorithm of center-manifold reduction, described in details in Ref. [15], provides the way of calculating these functions and also the method of simultaneous deriving the first-order ordinary differential equation describing the limit-cycle oscillations in terms of new variables $\mathbf{z}$:

$$\dot{\mathbf{z}}(t) = \mathbf{\Lambda}\,\mathbf{z}(t) + \sum_{\mu \geq 2} \frac{1}{\mu!} \mathbf{d}_\mu \mathbf{z}^\mu , \tag{3.9}$$

where $\mathbf{\Lambda}$ denotes the diagonal matrix of eigenvalues $i\omega_0$, $-i\omega_0$, 0, and $\mathbf{d}_\mu$ are rectangular matrices build up with already known complex numbers. The way the suspended system has been introduced implies that $z_3 \equiv u$ and also $\dot{z}_3(t) = 0$, which means that an asymptotic motion is essentially two-dimensional. The third variable u acts once again as a parameter while the suspended system serves as a convenient tool for deriving series expansion with respect to it.

The next important conclusion drawn from the algorithm of center-manifold reduction says that there is no need to know the response functions forming elements of the matrix $\mathbf{G}(-\Theta; 0)$. This is because the columns $\mathbf{w}_{\mu k}(\Theta)$, $k = 1, 2, \ldots, c_{\mu,2N+1}$, $\mu \geq 1$, of each matrix $\mathbf{w}_\mu(\Theta)$ of the transformation (3.8), can be only of the elementary form:

$$\mathbf{w}_{\mu k}(\Theta) = \hat{\mathbf{w}}_{\mu k} \Theta^j e^{s\Theta} ,$$

with an integer $j \geq 0$, and s being a complex imaginary number [15]. Consequently, all integrals appearing within the algorithm can be carried out as follows:

$$\int_{-\infty}^{0} \frac{d^r \mathbf{G}(-\Theta; 0)}{du^r} \Theta^j e^{s\Theta} = \frac{\partial^{r+j} \mathbf{A}(s; U_0)}{\partial U^r \partial s^j} ,$$

where $r \geq 0$, and the only non-zero block of the matrix

$$\mathbf{A}(s; U_0) = \left[\begin{array}{c|c|c} \mathbf{0} & \mathbf{0} & \mathbf{0} \\ \hline \mathsf{A}(s; U_0) & \mathbf{0} & \mathbf{0} \\ \hline \mathbf{0} & \mathbf{0} & 0 \end{array}\right]$$

is the aerodynamic matrix $\mathsf{A}(s; U)$ given by Eq. (2.13) and calculated for a pure harmonic motion and the critical velocity U_0.

Since Eq. (3.9) is an ordinary differential equation, it can be easily transformed to the so-called Poincaré normal form either by Lie transforms [12] or by recursive

change of coordinates [18]. Both methods introduce new variables $\boldsymbol{\zeta}(t)$ related to $\mathbf{z}(t)$ by the near-identity transformation

$$\mathbf{z}(t) = \boldsymbol{\zeta}(t) + \sum_{\nu \geq 2} \frac{1}{\nu!} \mathbf{b}_\nu \boldsymbol{\zeta}^\nu(t). \tag{3.10}$$

This transformation retains the form of Eq. (3.9) also with respect to new coordinates $\boldsymbol{\zeta}(t)$. The requirement for calculating elements of matrices $\mathbf{b}_\nu$ is to make as many coefficients $\mathbf{d}_\mu$ equal to zero as possible. However, the simplification achieved lies not in a small number of terms of the resulting normal form, which in fact remains infinite, but rather in the phase-shift symmetry introduced by the transformation (3.10). The normal form of Hopf bifurcation in polar coordinates r, θ

$$\zeta_1 = re^{i\theta}, \qquad \zeta_2 = \overline{\zeta}_1, \tag{3.11}$$

may be written as [14]:

$$\begin{aligned} \dot{r} &= r\left(\gamma(u) + \sum_{j=1}^{\infty} a_j(u) r^{2j}\right), \\ \dot{\theta} &= \omega(u) + \sum_{j=1}^{\infty} b_j(u) r^{2j}, \end{aligned} \tag{3.12}$$

where $\gamma(u) \pm i\omega(u)$ is the complex-conjugate pair of eigenvalues ($\gamma(0) = 0$, $\omega(0) = \omega_0$). All functions $\gamma(u)$, $\omega(u)$, $a_j(u)$, $b_j(u)$ are real and have the form of power series expansions with respect to u. In practical calculations Eqs. (3.12) are implemented up to some finite order $j \leq n$. Therefore, the amplitude r_H of the limit cycle oscillations satisfies an algebraic equation obtained from Eq. $(3.12)_1$ by setting $\dot{r} = 0$:

$$\gamma(u) + \sum_{j=1}^{n} a_j(u) r_H^{2j} = 0. \tag{3.13}$$

For any given u the left-hand side of Eq. (3.13) is of the form of a polynomial with respect to r_H. Hence all possible limit cycle amplitudes are determined by the real positive roots of this polynomial. Since limit cycle oscillations $\zeta_1 = \zeta_H(t)$ on the center manifold are pure harmonic [11],

$$\zeta_H = r_H e^{i\omega_H t}, \tag{3.14}$$

then for each amplitude r_H the corresponding frequency ω_H is calculated from

$$\omega_H = \omega(u) + \sum_{j=1}^{n} b_j(u) r_H^{2j}. \tag{3.15}$$

The sequence of transformations of variables given by Eqs. (3.11), (3.10), (3.8), (2.9) and (2.4) yields the final limit cycle oscillations of physical variables $\mathbf{u}(t)$ given by Eq. (2.2). Since two of these trnsformations are nonlinear, the physical variables do not oscillate harmonically in time, contrary to the center-manifold variables $\zeta(t)$.

4. Numerical examples

The main new data that must be supplied to the algorithm of center-manifold reduction are derivatives of the aerodynamic matrix $\mathsf{A}(s; U)$ with respect to variables s and U. It can be seen from Eq. (2.13) that these derivatives can be easily evaluated if derivatives of the aerodynamic matrix with respect to a single complex variable p (2.15) are known up to the desired order of approximation. For the n-th order of approximation of the Eqs. (3.12) the highest derivatives are of order $2n - 1$. In the numerical examples in the paper two-dimensional incompressible aerodynamic theory is used and, therefore, all elements of the aerodynamic matrix are given analytically in terms of the generalized Theodorsen function $C(p)$ (2.14). By using the following relations for the modified Bessel functions $K_0(p)$ and $K_1(p)$:

$$\frac{dK_0(p)}{dp} = -K_1(p), \qquad \frac{dK_1(p)}{dp} = -K_0(p) - \frac{K_1(p)}{p},$$

the first two derivatives of the Theodorsen function can be obtained

$$\frac{dC(p)}{dp} = 2C(p) - 1 + \frac{1}{p}(C(p) - 1)C(p),$$

$$\frac{d^2C(p)}{dp^2} = \frac{2C(p) - 1}{p} + 2\frac{dC(p)}{dp}\left(1 + \frac{C(p) - 1}{p}\right).$$

The higher order derivatives satisfy the following recurrence formula, valid for $k > 1$:

$$\frac{d^{k+1}C(p)}{dp^{k+1}} = \left(2 - \frac{k+1}{p}\right)\frac{d^kC(p)}{dp^k} + \frac{1}{p}\frac{d^kC^2(p)}{dp^k} + \frac{2k}{p}\frac{d^{k-1}C(p)}{dp^{k-1}}.$$

The first numerical example has been chosen in order to compare the center-manifold reduction with direct integration of equations of motion. The report of LEE and LEBLANC (Ref. [19]) presents flutter analysis of a two-dimensional thin airfoil based on a time marching finite difference scheme. Only cubic nonlinear restoring force in the pitch degree of freedom has been taken into account, which corresponds to $c_h = 0$, $c_\alpha \neq 0$ in Eq. (2.1). Although equations of motion have been written in the report in the integro-differential form, they are equivalent

to the system of ordinary differential equations because of exponential approximation of Wagner function applied in calculations. The airfoil data values are the following: $x_a = -0.5$, $\mu = 100$, $x_\alpha = 0.25$, $r_\alpha = 0.5$, $\Omega = 1.2$ and $c_\alpha = 3$. These values have been chosen because they generate a relatively strong nonlinear effect as compared to those presented in the report.

Variations of the limit cycle amplitudes in plunge h/b and pitch α with the ratio of the velocity U to the critical bifurcation velocity U_0 are illustrated in Fig. 2 and Fig. 3, respectively.

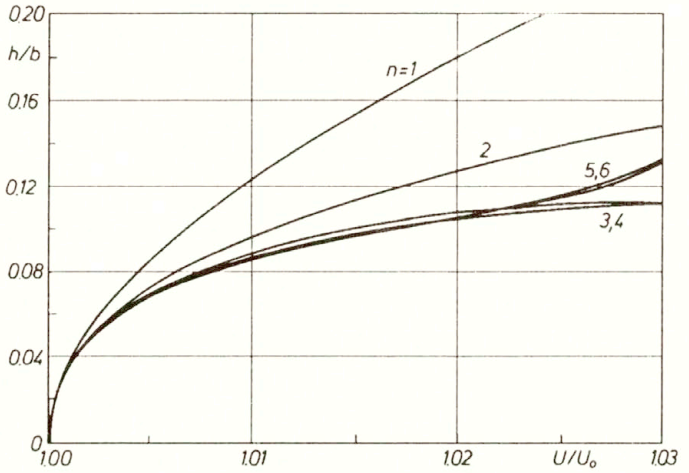

FIG. 2. Limit cycle amplitude in plunge.

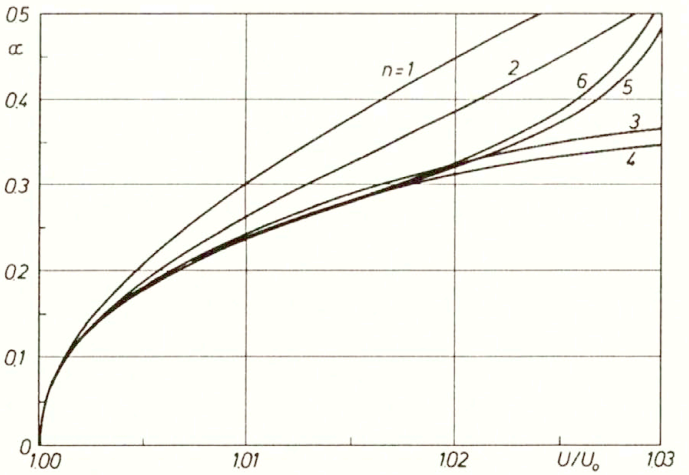

FIG. 3. Limit cycle amplitude in pitch.

The sequence of lines for $n = 1 \ldots 6$ corresponds to the different numbers of terms included in the series of Eqs. (3.12). The related Hopf limit cycle amplitude

r_H and frequency ω_H, given on the center manifold by Eqs. (3.13) and (3.15), are shown in Fig. 4 and Fig. 5, respectively.

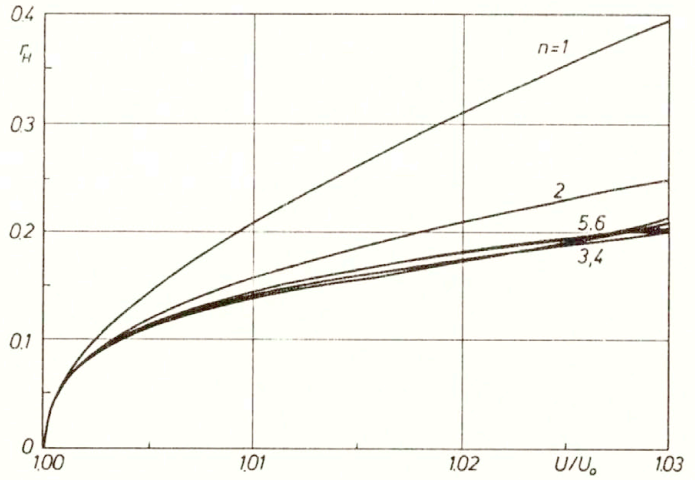

FIG. 4. Amplitude of center manifold Hopf limit cycle.

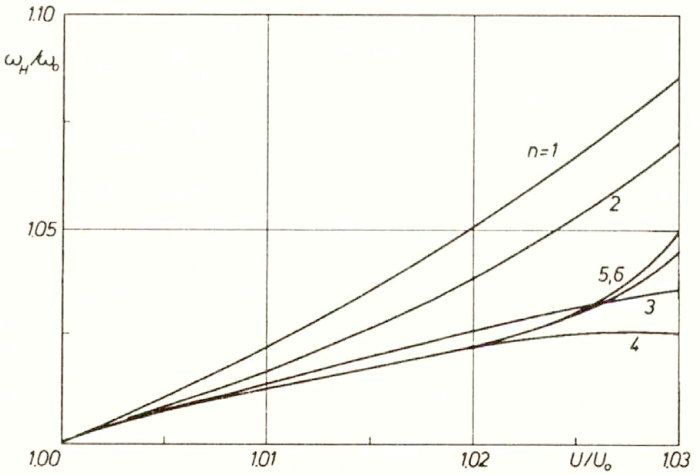

FIG. 5. Frequency of center manifold Hopf limit cycle.

The significant change of slopes of two curves corresponding to $n = 5$ and 6 in Figs. 2 and 3, for the velocity ratio greater than 1.02, breaks the converging trend of the first four curves. Such behaviour illustrates an important property of power series expansions used in the center-manifold reduction – these series usually do not converge. More often the divergence is generated by the normal form transformation given by Eq. (3.10) [14]. Nevertheless, the finite order approximation can be considered as a part of an asymptotic expansion, and the optimal number of terms should be estimated for each aeroelastic system separately. The number

of terms strongly depends on the interval of variation of the bifurcatian parameter. For the numerical example presented above the four-order approximation seems to give the best results.

The next two pictures (Figs. 6 and 7) show the comparison of the limit cycle amplitudes calculated by this four-order approximation, with analogous results of the numerical integration of flutter equation [19], and also with results of the harmonic balance method [7].

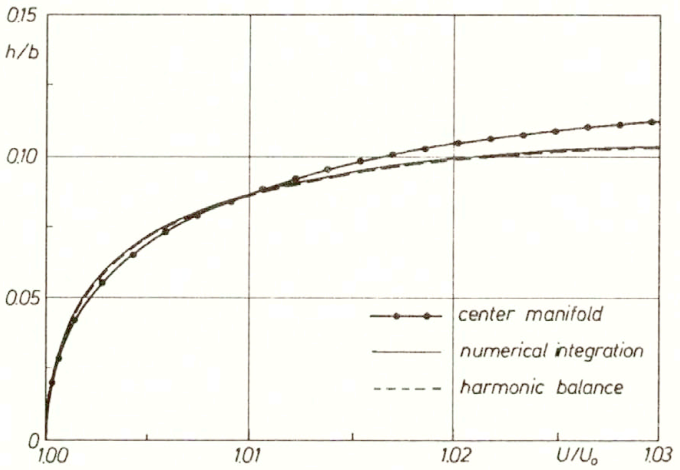

FIG. 6. Limit cycle amplitude in plunge.

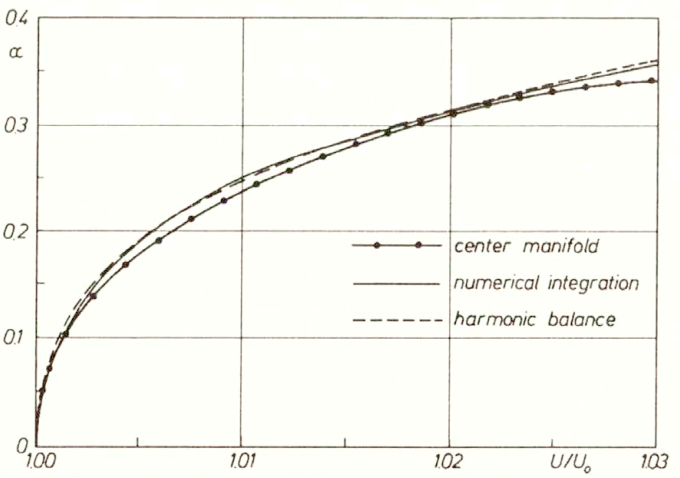

FIG. 7. Limit cycle amplitude in pitch.

In the second example both springs are nonlinear. The airfoil data values are the following:

$$x_a = -0.1, \quad \mu = 20, \quad x_\alpha = 0.25,$$
$$r_\alpha = 0.5, \quad \Omega = 1.5, \quad c_h = 0.3 \quad \text{and} \quad c_\alpha = 5.$$

Variations of limit cycle amplitudes in physical variables h/b and α, and also the Hopf limit cycle amplitude r_H and frequency ω_H on the center manifold, with the velocity ratio U/U_0, are illustrated in Figs. 8–11. For this data the six-term approximation gives satisfactory results in a wide range of variation of the bifurcation parameter U.

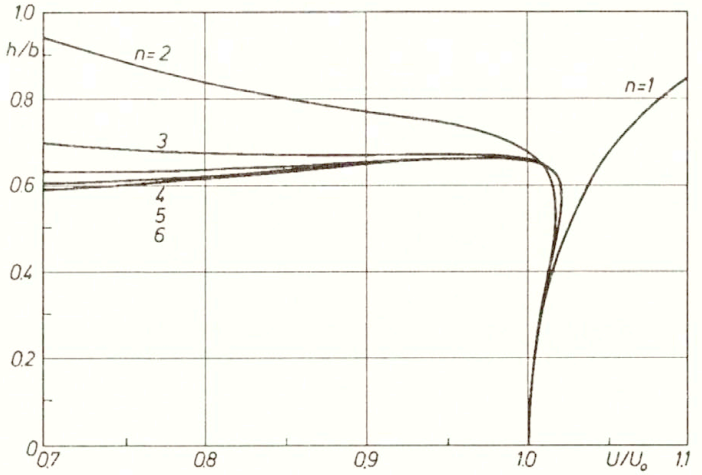

FIG. 8. Limit cycle amplitude in plunge.

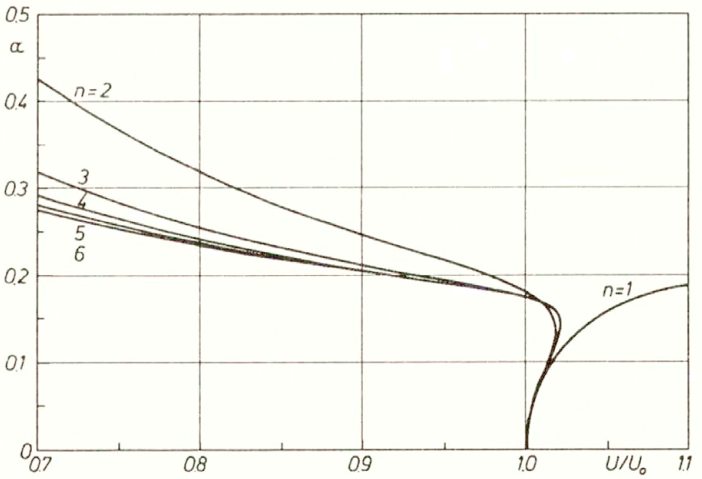

FIG. 9. Limit cycle amplitude in pitch.

The next two pictures (Figs. 12 and 13) illustrate the comparison of the limit cycle amplitudes corresponding to the six-order center manifold approximation with analogous results of the harmonic balance method of Ref. [7]. This example shows that sometimes it is not enough to take into account only the first term in the series expansions of Eqs. (3.12), even for only qualitative analysis. The

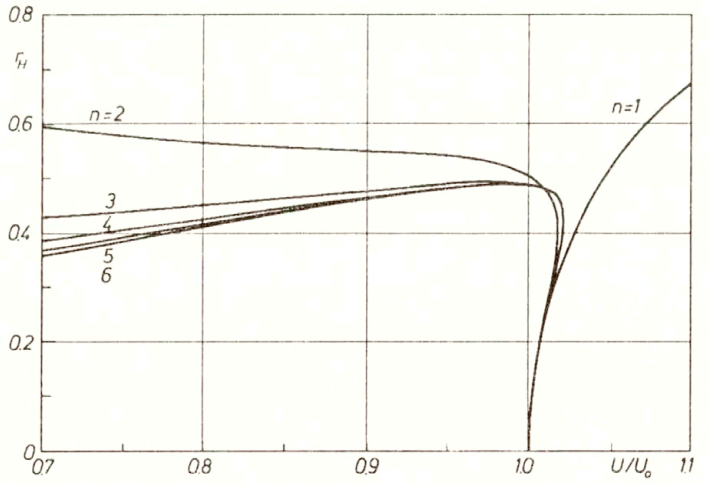

FIG. 10. Amplitude of center manifold Hopf limit cycle.

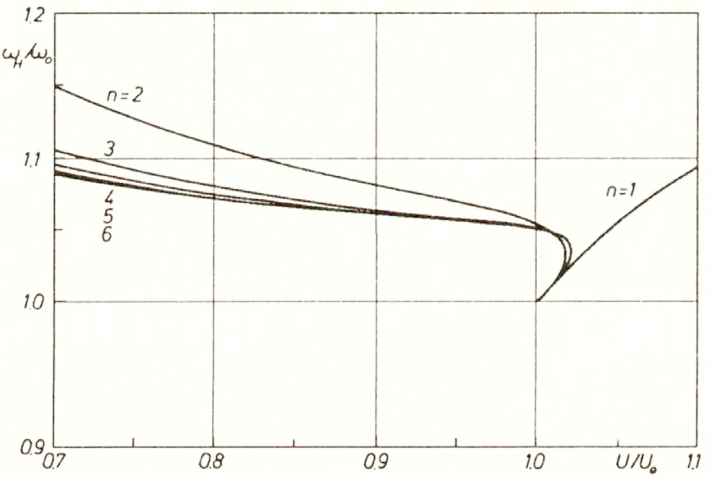

FIG. 11. Frequency of center manifold Hopf limit cycle.

single-term approximation gives a square-root dependence of the Hopf limit-cycle amplitude r_H on the bifurcation parameter u, obtained from Eq. (3.13):

$$r_H = \sqrt{-\frac{1}{a_1(0)}\frac{d\gamma(0)}{du}u},$$

valid for small u (note that $\gamma(0) = 0$). In the present example, the above formula is satisfied within a small interval above the bifurcation point, resulting in a stable limit cycle, while in a wide range below this point the unstable limit cycle oscillations occur.

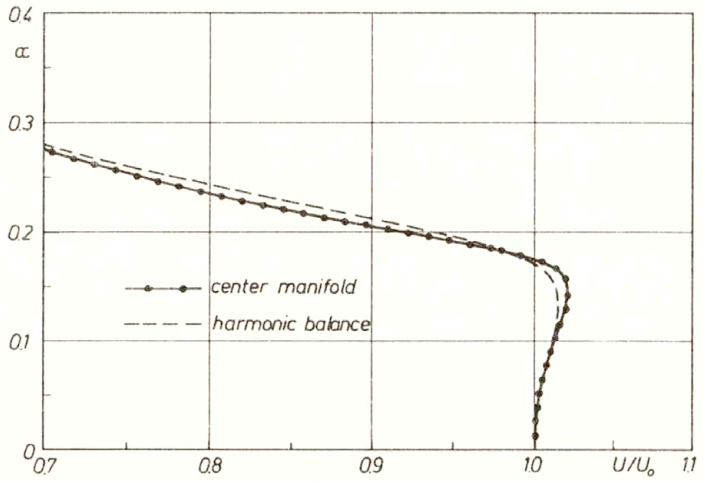

FIG. 12. Limit cycle amplitude in plunge.

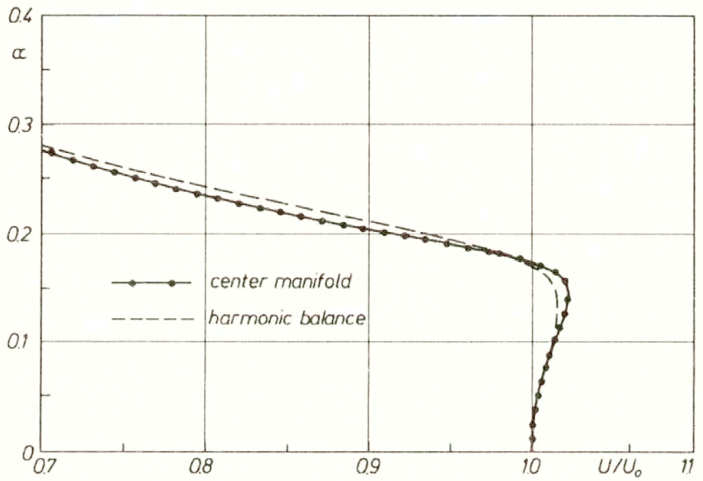

FIG. 13. Limit cycle amplitude in pitch.

5. Concluding remarks

Three different methods compared in the paper, although applied to the same numerical examples, are not expected to give exactly the same results. The method of numerical integration of equations of motion should give, in general, the most reliable results. However, the implementation of Ref. [19] simplifies significantly the aerodynamic operator and, therefore, cannot serve as a reference method. The harmonic balance method assumes pure harmonic oscillations of an airfoil and also treats nonlinear springs in a simplified manner. Finally, the method of center-manifold reduction is based on asymptotic series expansions

producing errors that can be estimated only numerically. Nevertheless, there is a good agreement between these three methods. Hence the main advantage of the center-manifold reduction lies in a possibility of extension of this method to such aeroelastic systems that the harmonic balance method cannot handle and the direct numerical integration method cannot be used in sufficiently effective way.

The method of center-manifold reduction applied to nonlinear asymptotic stability analysis is especially focussed on aeroelastic systems with many degrees of freedom, because it finally reduces the analysis to a low-dimensional system of differential equations describing finite amplitude limit cycle oscillations of an entire aircraft. The method is general in the sense that it allows for any source of concentrated and also distributed nonlinearities. In particular, both aerodynamic and structural nonlinearities are treated in the same way. Moreover, the method does not introduce simplifications of the aerodynamic model. Therefore, the main source of the instability of motion – the energy transfer from the gas flow to the aircraft structure – remains undisturbed.

The draw-back of center-manifold reduction, however not related to the method ifself but rather to the most widely used procedure of obtaining an effective solution, is a power series representation of nonlinear terms. For that reason the present analysis has been restricted only to structural nonlinearities, which seem to be easier to handle in this way than the nonlinear unsteady transonic aerodynamic forces.

Acknowledgements

This work has been supported in part by the State Committee for Scientific Research, Poland, under Grant 3 P404 001 04.

References

1. T. THEODORSEN, *General theory of aerodynamic instability and the mechanism of flutter*, NACA Rept. No. 496, 1935.
2. S.F. SHEN, *An approximate analysis of nonlinear flutter problems*, J. Aerospace Sciences, **28**, 25–32, January 1959.
3. C.L. LEE, *An iterative procedure for nonlinear flutter analysis*, AIAA J., **24**, 5, 833–840, May 1986.
4. W.C. RHEINBOLDT, *A locally parametrized continuation process*, ACM Trans. Math. Software, **9**, 2, 215–235, 1983.
5. C.C. MANTEGAZZA, *Continuation and direct solution of the flutter equation*, Computer and Structures, **8**, 185–192, 1978.
6. E.E. MEYER, *Application of a new continuation method to flutter equations*, 29th Structural Dynamics and Material Conference, Williamsburg, Virginia, April 18–20, 1988.
7. W. POTKAŃSKI, *Investigations of nonlinearities in aeroelastic equations by a continuation method* [private communication].
8. Y.C. FUNG, *An introduction to the theory of aeroelasticity*, J. Wiley and Sons, New York 1955.
9. R. VEPA, *Finite state modeling of aeroelastic systems*, NASA CR-2779, 1977.

10. F. POIRION, *Effects of structural nonlinearities on flutter analysis*, Proc. Intern. Forum on Aeroelasticity and Structural Dynamics, Strasbourg, May 24–26, 1993.
11. B.D. HASSARD, N.D. KAZARINOFF, Y.-H. WAN, *Theory and applications of Hopf bifurcation*, Cambridge University Press, 1981.
12. S.-N. CHOW, J.K. HALE, *Methods of bifurcation theory*, Grundlehren der mathematischen Wissenschaften 251, Springer-Verlag, 1982.
13. V.J.E. STARK, *General equations of motion for an elastic wing and method of solution*, AIAAJ., **22**, 8, 1146–1153, August 1984.
14. J.D. CRAWFORD, *Introduction to bifurcation theory*, Rev. of Modern Physics, **63**, 4, October 1991.
15. J. GRZĘDZIŃSKI, *Calculation of coefficients of a power series approximation of a center manifold for nonlinear integro-differential equations*, Arch. Mech., **45**, 2, 235–250, 1993.
16. N. CHAFEE, *A bifurcation problem for a functional differential equation of finitely retarded type*, J. Math. Anal. and Appl., **35**, 312–348, 1971.
17. D. RUELLE, F. TAKENS, *On the nature of turbulence*, Commun. Math. Phys., **20**, 3, 167–192, May 1971.
18. L. HSU, L. FAVRETTO, *Recursive formulae for normal form and center manifold theory*, J. Math. Anal. and Appl., **101**, 2, 562–574, July 1984.
19. B.H.K. LEE, P. LEBLANC, *Flutter analysis of a two-dimensional airfoil with cubic non-linear restoring force*, National Research Council Canada, NAE-AN-36, Feb. 1986.

POLISH ACADEMY OF SCIENCES
INSTITUTE OF FUNDAMENTAL TECHNOLOGICAL RESEARCH.

Received May 3, 1994.

Arch. Mech., 46, 5, pp. 757–773, Warszawa 1994

Travelling waves in a two-temperature model of laser-sustained plasma

B. KAŹMIERCZAK and Z. PERADZYŃSKI (WARSZAWA)

IN THIS PAPER we prove the existence of travelling fronts in a two-temperature model of a laser-sustained plasma. We use the implicit function theorem starting from a solution of a one-temperature model. We estimate the temperature difference as a function of electron-heavy particle collision frequency (which is treated as a perturbation parameter) and its influence on the speed of front propagation.

1. Introduction

IN THIS PAPER we consider the problem of existence of solutions of combustion fronts type for the equations describing laser-sustained plasma. Here, plasma is composed of electrons and heavy particles with temperatures T_1 and T_2, respectively. To obtain the existence result we use perturbation technique, taking one temperature approximation as a starting point. This is an interesting case of perturbation around an infinite value of a perturbation parameter, which in our case can be interpreted as the collision frequency.

2. The physical problem

Let T_1, T_2 denote the temperatures of electrons and heavy particles, respectively. Then, assuming that the pressure p is constant, T_1 and T_2 satisfy the following system of equations [1, 2, 3]:

$$\begin{aligned}
&\left(\frac{\partial}{\partial t} + \mathbf{v}\cdot\operatorname{grad}\right)\left\{\frac{3}{2}k_B n_1 T_1 + n_1 E\right\} \\
&\qquad = \operatorname{div}(k_{11}\operatorname{grad}T_1 + k_{12}\operatorname{grad}T_2) + f - (T_1 - T_2)\mathcal{W}, \\
&\left(\frac{\partial}{\partial t} + \mathbf{v}\cdot\operatorname{grad}\right)\left\{\frac{3}{2}k_B n_2 T_2\right\} \\
&\qquad = \operatorname{div}(k_{21}\operatorname{grad}T_1 + k_{22}\operatorname{grad}T_2) + (T_1 - T_2)\mathcal{W}.
\end{aligned} \tag{2.1}$$

In the above equations by k_{ij} we have denoted entries of the effective heat conductivity matrix, by n_1, n_2 – the number densities of electrons and heavy particles, and by $\mathbf{v}$ – their common convectional velocity. E is ionizaton energy and k_B is the Boltzmann constant. I denotes the laser beam intensity. The source function f is responsible for the outer balance of plasma energy; $f = \kappa I - \mathcal{E}_{\text{rad}}$, where the first term represents absorption of energy from the laser beam of intensity I, and the latter one – the energy losses due to plasma radiation.

All the functions appearing above are assumed to depend on the temperatures T_1, T_2 only.

As a matter of fact, f depends only on T_1, i.e. $f = f(T_1)$. Both κ and $\mathcal{E}_{\text{rad}}$ are strongly dependent on T_1. They are almost zero for $T_1 < T_0$, where $T_0 > 0$ (e.g. for Argon plasma $T_0 \approx 10000\,\text{K}$) and they grow rapidly for higher temperatures. (For example the dependence of κ on T_1 is shown in Fig. 1). Therefore, with a reasonable approximation, which is very commonly used, one can assume that $f(T_1) \equiv 0$ for $T_1 < T_0$. However, this apparent simplification creates some mathematical difficulties mainly connected with the fact that $f_{,T}(T) \equiv 0$ for $T < T_0$. In [4] we made the assumption $f_{,T}(T_*) < 0$ (where $T_* < T_0$ is the temperature of the ambient gas), which was essential in the proof. That proof does not work in the case of the source function considered here.

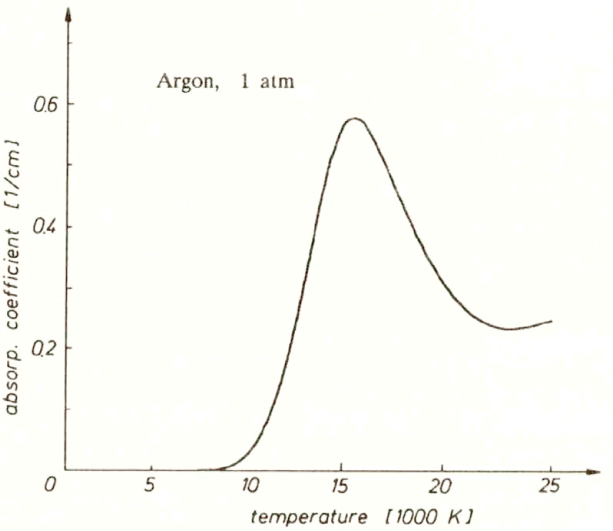

FIG. 1.

The term $(T_1 - T_2)\mathcal{W}$ describes collisional energy exchange between electrons and heavy particles. $\mathcal{W}$ is proportional to the frequency of electron-heavy particle collisions. This frequency tends to infinity as the pressure tends to infinity. So, it is possible to write $\mathcal{W}(p; u, r) = \lambda(p)W(u, r)$, where λ is a dimensionless parameter, $\lambda(p) \to \infty$ as $p \to \infty$. Thus λ is a relative measure of the electron-heavy particle collisions. Consequently, for high pressures the temperatures of electrons and heavy particles are nearly the same and we have to do with one temperature model.

2.1. Travelling waves solutions

Solutions to Eqs. (2.1) may be sought in the form of travelling waves. Thus, for $\mathbf{n} \in \mathbb{R}^3$ and $\chi \in \mathbb{R}^1$, let us assume that $T_1(\mathbf{x}, t) = u_1(\mathbf{x} \cdot \mathbf{n} + \chi t)$, $T_2(\mathbf{x}, t) = u_2(\mathbf{x} \cdot$

$\mathbf{n} + \chi t$) ($\mathbf{n}$ is called the direction of propagation and χ the speed of a travelling wave). Inserting these relations into (2.1) we arrive at the following system of ODEs:

$$
\begin{aligned}
(k_{11}u_1' + k_{12}u_2')' - q\{C_{11}u_1' + C_{12}u_2'\} + f - \lambda(u_1 - u_2)W &= 0,\\
(k_{21}u_1' + k_{22}u_2')' - q\{C_{21}u_1' + C_{22}u_2'\} + \lambda(u_1 - u_2)W &= 0.
\end{aligned} \tag{2.2}
$$

Here symbol $'$ means differentiation with respect to $\xi \in \mathbb{R}^1$, $\xi := \mathbf{x} \cdot \mathbf{n} + \chi t$, while

$$
q := (\chi + \mathbf{v} \cdot \mathbf{n})\rho, \qquad C_{ij} = \rho^{-1}\left\{\frac{3}{2}k_B n_i T_i + \delta_{i1} n_i E\right\}_{,T_j}, \tag{2.3}
$$

where by ρ we have denoted the mass density and δ_{i1} is the Kronecker's delta. By the continuity equation we have $q = \text{const}$, so q will be treated as a real parameter. Physically q is the mass flux.

DEFINITION 1. *A $C^2(\mathbb{R}^1)$ solution $(u_1(\xi), u_2(\xi))$ to* Eqs. (2.2) *is called heteroclinic, if it tends to different constant vectors (asymptotic states) as $\xi \to \pm\infty$ and its derivatives vanish at $\pm\infty$.* ■

Thus to have travelling waves for Eqs. (2.1) we must find heteroclinic solutions to Eqs. (2.2). It is known that for a given λ such solutions can exist only for certain values of the parameter q, as we have to do with a kind of an eigenvalue problem. Thus q should be treated as an unknown, whose value must be determined. The aim of this work is to prove existence of heteroclinic triples (q, u_1, u_2) satisfying Eqs. (2.2) under the condition that λ is sufficiently large.

DEFINITION 2. *Let us denote*

$$
\begin{gathered}
u := u_1, \qquad r := u_1 - u_2,\\
k_1 := k_{11} + k_{12}, \qquad k_2 := k_{12} + k_{22},\\
K := k_1 + k_2, \qquad d := k_{11}k_{22} - k_{12}k_{21}, \qquad C := \sum_{i,j} C_{ij},\\
k(u) := K(u, r = 0), \qquad c(u) := C(u, r = 0). \quad \blacksquare
\end{gathered} \tag{2.4}
$$

By adding Eqs. $(2.2)_1$, $(2.2)_2$ we arrive at the equation:

$$
u'' + \{-qc(u)u' + (K(u,r))'u' + f(u) + N_1\}(K(u,r))^{-1} = 0, \tag{2.5}
$$

or the equivalent equation

$$
(K(u,r)u')' - qc(u)u' + f(u) + N_1 = 0, \tag{2.5$_1$}
$$

where

$$N_1 = -[k_{12}(u,r)r' + k_{22}(u,r)r']' - qC(u,r)u' + qc(u)u' + q\{C_{12}(u,r) + C_{22}(u,r)\}r'.$$

The equation for r is obtained by finding k_2u'' from $(2.2)_1$ and substituting it into $(2.2)_2$. It has the following form:

$$r'' - \lambda WK(d)^{-1}r + N_2 = 0, \tag{2.6}$$

where

$$N_2 = -k_2(d)^{-1}\{qC_{11}(u,r)u' + qC_{12}(u,r)(u-r)' - (k_1(u,r))'u' - f(u)) + (k_{12}(u,r))'r'\} + k_1(d)^{-1}\{(-k_2(u,r))'u' + (k_{22}(u,r))'r' + qC_{21}(u,r)u' + qC_{22}(u,r)(u-r)'\}.$$

3. Heteroclinic orbits in a one-temperature model

The difference r between the temperatures must tend 0 as λ tends to infinity. Thus, for $\lambda = \infty$ we must formally put $r = 0$. Then $N_1 = 0$ and Eq. $(2.5)_1$ reduces to

$$(k(u)u')' - qc(u)u' + f(u) = 0. \tag{3.1}$$

3.1. Properties of the function f

Asymptotic values of any heteroclinic solution to (3.1) must solve the algebraic equation $f(u) = 0$, i.e. the equation:

$$f(u) = \kappa(u)I - \mathcal{E}_{\text{rad}}(u) = 0. \tag{3.2}$$

Let $J(u) := [\mathcal{E}_{\text{rad}}(u)](\kappa(u))^{-1}$ and let $J_0 := \min_{u>0} J(u) = J(u_0)$. It is known ([5]), that for $u \geq u_0$, $J(u)$ is a parabola-like function of u. Then, for $u \geq u_0$, we have $f(u) = \kappa(u)(I - J(u))$ and for every $I > J_0$ the equation $(I - J\phi(u)) = 0$ possesses a solution $u_+ > u_0$. So, we assume $u(\infty) = u_+$. This solution is stable because $f_{,u}(u_+) < 0$. As we have mentioned in the Introduction, the absorption coefficient κ vanishes for temperatures smaller than a certain temperature T_0, i.e. $f(u) \equiv 0$ for $u < T_0$. Thus, the "left-hand" zero of the function $f(u)$ is nonunique. Its value must be determined by the physical boundary condition at $(-\infty)$. Consequently, we assume that $u(-\infty) := u_- = T_* < T_0$, where T_* is the temperature of the "cold" incoming gas.

Now, the following two remarks will be of crucial importance for our further consideratons

REMARK 1. Physical arguments show that effective conductivity coefficients $k_1(u, r)$, $k_2(u, r)$, $c(u)$ (the total specific heat of the plasma divided by its density) and W (scaled frequency of collisions) are positive for $u > 0$, $u - r > 0$. Also, $d = k_{11}k_{22} - k_{12}k_{21}$ is positive due to the fact that k_{12} and k_{21} are relatively small. Finally, it is quite natural to suppose that all the considered functions are sufficiently smooth. ■

REMARK 2. By the use of a standard integral transformation, Eq. (3.1) can be changed to the equation of the type:

$$M'' - q\gamma(M)M' + \phi(M) = 0. \tag{3.3}$$

In fact, let $u \to M(u) := \int_{u_-}^{u} k(y)\,dy$. As $k > 0$ for $u > 0$, then $M_{,u} > 0$ and this transformation has the inverse $M \to u(M)$. It is easy to check that $\gamma(M) = c(u(M))[k(u(M))]^{-1}$ and $\phi(M) = f(u(M))$. According to Remark 1, γ is smooth, bounded and positive, whereas, according to the above properties of the function $f(u)$, the function $\phi(M)$ is nonnegative for $M \in (0, M_+)$ and identically equal to zero for $M \in (0, M^*)$ and some $M^* \in (0, M_+)$. Eq. (3.3) appears in the combustion theory and it is relatively well analyzed. Due to the properties of f we have $\phi(M) < 0$ for $M > M_+ = \int_{u_-}^{u^+} k(y)\,dy$. Then, by means of phase plane analysis (see [6, 7] and references therein), one can prove the existence of a unique mass speed $q = q_0$ and a unique monotonic heteroclinic orbit $M(\xi)$ to Eq. (3.3) such that $M \to 0$ as $\xi \to \infty$ and $M \to M_+$ as $\xi \to \infty$. It is easy to note that $q > 0$. ■

Now, one can ask a question, what happens, when $\lambda < \infty$, but is still sufficiently large. To be precise, the question is whether we can find an appropriate value of q for which there exists a solution $(u(\xi), r(\xi))$ to (2.5), (2.6) such that $u(\xi)$ tends to u_+ or u_- as $\xi \pm \infty$, respectively, and $r'(\xi) \to \infty$ as $|\xi| \to \infty$. We will consider this problem in the subsequent section.

4. Existence theorem and its proof

This section is devoted to the proof of existence of heteroclinic orbits to the system of ODEs:

$$u'' + E(q, u, u', r, r', r'') = 0, \tag{4.1}$$

$$r'' - \lambda b(u, r)r + P(q, u, u', r, r') = 0. \tag{4.2}$$

One can see that this system generalizes the system (2.5), (2.6). However, it will be considered below independently of the latter system.

The asymptotic states to the system (4.1), (4.2) are the solutions of the system:

$$E(q,u,0,r,0,0) = 0, \tag{4.3}$$

$$b(u,r)r + \varepsilon^2 P(q,u,0,r,0) = 0, \tag{4.4}$$

where

$$\varepsilon^{-2} = \lambda.$$

Let us note that generalization of (2.5), (2.6) to (4.1), (4.2) consists, among others, in the fact that solutions to (4.3), (4.4) may depend on the parameter q.

Our aim is to show that heteroclinic solutions to the system (2.2) can be constructed from appropriate solution to the equation

$$u'' + E_0(q,u,u') = 0, \tag{4.5}$$

where

$$E_0(q,u,u') := E(q,u,u',0,0,0).$$

This equation is obtained by putting formally $r \equiv 0$ in Eq. (4.1). The main tool of our analysis will be the implicit function theorem.

If $\varepsilon = 0$ and b is strictly positive, then the system (4.3), (4.4) can be satisfied only by the pairs $(u,0)$, where u fulfils the "reduced" equation:

$$E(q,u,0,0,0,0) = E_0(q,u,0) = 0. \tag{4.6}$$

H1. For $q = q_0$ the equation (3.6) has at least two solutions, which, without losing generality, may be taken to be 0 and 1, such that

$$E_{0,u}(q_0,0,0) \leq 0, \qquad E_{0,u}(q_0,1,0) \leq 0. \quad \blacksquare$$

H2. For $q = q_0$ Eq. (4.5) has a heteroclinic solution $G(\xi)$. Without losing generality we may assume that $G(-\infty) = 0$, $G(\infty) = 1$.

There exist finite nonzero constants α, β, C_1, and C_2 such that $\alpha, \beta > 0$ and

$$(G'(\xi)C_1 e^{-2\alpha\xi} - 1) = o(1) \quad \text{as} \quad \xi \to -\infty,$$
$$(G'(\xi)C_2 e^{2\beta\xi} - 1) = o(1) \quad \text{as} \quad \xi \to \infty. \quad \blacksquare$$

REMARK 3. As it is known, the asymptotic behaviour of G as $\xi \to \infty$ or $\xi \to -\infty$ is determined by characteristic roots of the linearized version of Eq. (4.5) near $(u,u') = (1,0)$ and $(0,0)$. Thus, (2α) is a the positive characteristic root of linearization near $(0,0)$, and (-2β) is the negative root of linearization around $(1,0)$. $\blacksquare$

H3. $E \in C^{1+\tau}$, $\tau > 0$, $b \in C^2$, $P \in C^2$. $\blacksquare$

H4. $b(u,r) > b > 0$ for all (u,r) in a certain C^0-neighbourhood of $(G,0)$. $\blacksquare$

DEFINITION 2. *For α and β determined in* H2 *and for $i = 0, 1, 2$, let B_i denote the subspace of $C^i(\mathbb{R}^1)$ consisting of functions y for which the expressions*

$$y_n := \max\left\{\sup_{p\geq 0} e^{\beta p}|y^{(n)}(p)|,\ \sup_{p\leq 0} e^{-\alpha p}|y^{(n)}(p)|\right\}, \quad n \leq i,$$

are finite (the symbol $y^{(n)}$ denotes the n-th derivative of y).

B_i is a Banach space with the norm $\|y\|_i := \sum_{n\leq i} y_n$. ■

H5. For all (ε, q) near $(0, q_0)$ there exist two families of solutions to system (4.3), (4.4): $[u_-(\varepsilon, q), r_-(\varepsilon, q)]$ and $[u_+(\varepsilon, q), r_+(\varepsilon, q)]$, such that $[u_-(\varepsilon, q), r_-(\varepsilon, q)] \to [0, 0]$ and $[u_+(\varepsilon, q), r_+(\varepsilon, q)] \to [1, 0]$ as $(\varepsilon, q) \to (0, q_0)$. We assume that the dependence of these functions on (ε, q) is at least C^2 smooth. ■

H5 is in particular fulfilled, when $[u_-(\varepsilon, q), r_-(\varepsilon, q)]$ and $[u_+(\varepsilon, q), r_+(\varepsilon, q)]$ are independent of ε and q. Such a situation takes place in the case of our plasma system (2.5), (2.6) . ■

DEFINITION 3. *For $[u_-(\varepsilon, q), r_-(\varepsilon, q)]$ and $[u_+(\varepsilon, q), r_+(\varepsilon, q)]$ determined in* H5 *and G defined in* H2, *let*

$$L(\varepsilon, q; \xi) := u_-(\varepsilon, q) + G(\xi)[u_+(\varepsilon, q) - u_-(\varepsilon, q)],$$
$$S(\varepsilon, q; \xi) := r_-(\varepsilon, q) + G(\xi)[r_+(\varepsilon, q) - r_-(\varepsilon, q)].$$ ■

REMARK 4. Due to Eq. (4.4) and H4, $S_{,q}(0, q; \xi)$ is identically equal to 0 for q and all ξ, so by H2, H3, H5 $S_{,q}(\varepsilon, q; \xi) = O(\varepsilon^2)$, $S_{,q\xi}(\varepsilon, q; \xi) = O(\varepsilon^2)$ and $S_{,q\xi\xi}(\varepsilon, q; \xi) = O(\varepsilon^2)$ as $\varepsilon \to 0$. ■

In [4] we assumed that $E_{0,u}(q_0, 0, 0) < 0$ and $E_{0,u}(q_0, 1, 0) < 0$. Now we admit these quantities to be equal to 0. Consequently, the constant solutions (0 or 1) to Eq. (4.5) may not be exponentially stable. This causes the difficulties connected with convergence of some integrals (cf. the proof of Lemma 3 and Remark 7 in Appendix 2). To remedy the situation, we will decompose u and r in the following way:

$$u(\xi) := U(\xi) + L(\varepsilon, q; \xi), \qquad r := R(\xi) + S(\varepsilon, q, \xi), \tag{4.7}$$

and assume that U and R belong to the space B_2. Let us note that L and S satisfy appropriate boundary conditions, i.e. they tend (as $\xi \pm \infty$) to appropriate solutions of system (4.3), (4.4). We can thus look for U and R instead of u and r.

The system (4.1), (4.2) is an autonomous one. So, if it is satisfied by $(u(\xi), r(\xi))$, then it is also satisfied by the function $(u(\xi + \xi_0), r(\xi + \xi_0))$ with any finite ξ_0. To get rid of this ambiguity and to fix the position of u in the ξ-space, U will be subjected to an additional condition of the form: $U(0)G'(0) + U'(0)G''(0) = 0$. This can be interpreted as the condition of orthogonality of the vector $(U(0), U'(0))$ to

the vector $(G'(0), G''(0))$. As a matter of fact, the vector $(G'(0), G''(0))$ can be replaced by any nonzero vector, which is not orthogonal to $(G'(0), G''(0))$. This condition guarantees that G', being a solution to the linearized equation

$$U'' + E_{,u}(q_0, G, G')U + E_{,u'}(q_0, G, G')U' = 0$$

is excluded from the considered spaces of functions.

DEFINITION 4. *Let B_2^0 denote the subspace of B_2 consisting of functions y such that $y(0)G'(0) + y'(0)G''(0) = 0$.* ■

Now, we will transform the system (4.1), (4.2) so that the implicit function theorem can be applied. For given functions U and r and $\varepsilon \neq 0$ we may define a linear operator $A(U, R, \varepsilon) : B_2 \to B_0$ determined by the relation

$$y \to A(U, R, \varepsilon) := y'' - \varepsilon^{-2} b(U + L, R + S, \varepsilon)y, \tag{4.8}$$

where the dependence of L and S on (ε, q) was not explicitly written. If U and R are sufficiently close to 0 then, due to H3 and H4 and all $\varepsilon \neq 0$, this operator has a well defined inverse $A^{-1}(U, R, \varepsilon)$ (see e.g. [8] p. 69, 50, [9] Ch. XI; see also Appendix 1). Taking advantage of this fact for $\varepsilon \neq 0$ we can write the system (4.1), (4.2) in the following form:

$$Q_1(q, U, R, \varepsilon) = 0, \qquad Q_2(q, U, R, \varepsilon) = 0, \tag{4.9}$$

where we defined

$$\begin{aligned} (4.10)_1 \qquad Q_1(q, U, R, \varepsilon) &:= (U + L)'' \\ &\quad + E\,(q, U + L, (U + L)', R + S, (R + S)', (R + S)'')\,, \end{aligned}$$

$$(4.10)_2 \qquad Q_2(q, U, R, \varepsilon) := R - A^{-1}(U, R, \varepsilon)N(q, U + L, R + S) + S, \qquad \varepsilon \neq 0,$$

and

$$(4.10)_3 \qquad N(q, U, R) := -P\,(q, U + L, (U + L)', R + S, (R + S)')\,.$$

Before applying the implicit function theorem we have to prove continuity and differentiability of the mappings Q_1 and Q_2. First, we must extend the definition of Q_2 for $\varepsilon = 0$. Let us define

$$Q_2(q, U, R, 0) = 0. \tag{4.11}$$

In Appendix 1 we will prove the following lemma:

LEMMA 1. Let the assumptions H3 and H4 be fulfilled. Let Q_2 be defined by (4.8), $(4.10)_1$, $(4.10)_3$ and (4.11). Then for all (q, U, R, ε) from some neighbourhood of $(q_0, 0, 0, 0)$ in $\mathbb{R}^1 \times B_2^0 \times B_2 \times \mathbb{R}^1$:

i. Q_2 is a continuous mapping from $\mathbb{R}^1 \times B_2^0 \times B_2 \times \mathbb{R}^1$ to B_2, and $\|Q_2(q, U, R, 0) - R\|_2 = O(|\varepsilon|)$ for $\varepsilon \to 0$.

ii. Q_2 is continuously Frechet differentiable with respect to (q, U, R). If

$$DQ_2(q, U, R, \varepsilon)[\tilde{q}, \tilde{U}, \tilde{R}]$$

denotes the Frechet derivative with respect to (q, U, R) at a point (q, U, R, ε) acting on $[\tilde{q}, \tilde{U}, \tilde{R}]$ (which is equal to $\lim_{\eta \to 0} \frac{\partial}{\partial \eta} Q_2(q + \eta\tilde{q}, U + \eta\tilde{U}, R + \eta\tilde{R}, \varepsilon)$), then $\|DQ_2(q, U, R, \varepsilon)[\tilde{q}, \tilde{U}, \tilde{R}] - \tilde{R}\|_2 = |\varepsilon|\, O(|\tilde{q}| + \|\tilde{U}\|_2 + \|\tilde{R}\|_2)$. ■

It is also clear that, according to assumptions H3 and H5,

LEMMA 2. Q_1 is a continuous mapping from $\mathbb{R}^1 \times B_2^0 \times B_2 \times \mathbb{R}^1$ to B_0, continuously Frechet differentiable with respect to (q, U, R). ■

Hence the mapping $Q(q, U, R, \varepsilon) := [Q_1(q, U, R, \varepsilon), Q_2(q, U, R, \varepsilon)]$ is a well defined mapping from $\mathbb{R}^1 \times B_2^0 \times B_2 \times \mathbb{R}^1$ to $B_0 \times B_2$, continuously Frechet differentiable with respect to (q, U, R). Moreover, for $\varepsilon = 0$, the equation $Q(q, U, R, \varepsilon) = 0$ is satisfied by the triple $(q = q_0,\ U = 0,\ R = 0)$. The last thing we have to prove is to show that the linearized system defined by the Frechet derivative of Q at $(q_0, 0, 0, 0)$, i.e.

$$DQ(q_0, 0, 0, 0)[\tilde{q}, \tilde{U}, \tilde{R}] = (f_1, f_2), \tag{4.12}$$

has for all $(f_1, f_2) \in B_0 \times B_2$ a uniquely determined solution $(\tilde{q}, \tilde{U}, \tilde{R}) \in \mathbb{R}^1 \times B_2^0 \times B_2$. We need several subsidiary symbols:

$$\begin{aligned} a(\xi) &:= E_{0,u'}(q_0, G(\xi), G'(\xi)), \\ e(\xi) &:= E_{0,u}(q_0, G(\xi), G'(\xi)), \\ h(\xi) &:= E_{0,q}(q_0, G(\xi), G'(\xi)), \\ p(\xi) &:= \exp\left(\int_0^\xi a(s)\, ds\right), \\ m_i(\xi) &:= E_{,r^{(i)}}(q_0, G(\xi), G'(\xi), 0, 0, 0), \qquad i = 0, 1, 2, \end{aligned} \tag{4.13}$$

where $r^{(i)}$ denotes the i-th derivative of r, and $E_{,r^{(i)}}$ – the derivative of E with respect to $r^{(i)}$.

As we will see, it is also necessary to assume that

H6. $\int_{-\infty}^{\infty} G'(\xi) h(\xi) p(\xi)\, d\xi \neq 0$. ■

LEMMA 3. Suppose that assumptions H1–H6 are true. Then, for all $(f_1, f_2) \in B_0 \times B_2$ the system (4.12) has a uniquely determined solution $(\tilde{q}, \tilde{U}, \tilde{R}) \in \mathbb{R}^1 \times B_2^0 \times B_2$, thus the operator $DQ(q_0, 0, 0, 0)$ has a bounded inverse. ■

The proof of Lemma 3 will be given in Appendix 2.

DEFINITION 5. *For $i = 1, 2$, let $\mathcal{B}_i$ denote the subspace of $C^2(\mathbb{R}^1)$ consisting of functions ϕ such that $\phi' \in B_{i-1}$. $\mathcal{B}_i$ is a Banach space with the norm $\|\phi\|_{\mathcal{B}_i} = \|\phi\|_{C^0} + \|\phi'\|_{B_{i-1}}$.* ■

Now, by Lemma 3 and the implicit function theorem (conf. e.g. [10] p. 17, 18, 19) we conclude that for all sufficiently small $|\varepsilon|$, there exists a unique solution $(q(\varepsilon), U(\varepsilon), R(\varepsilon))$ for Eqs. (4.9) belonging to the space $\mathbb{R}^1 \times B_2 \times B_2^0$, and thus a unique (up to translation in ξ) solution (q, u, r), with $u(\varepsilon) = U(\varepsilon) + L(\varepsilon, q(\varepsilon))$, $r = R(\varepsilon) + S(\varepsilon, q(\varepsilon))$, for Eqs. (4.1), (4.2) belonging to the space $\mathbb{R}^1 \times \mathcal{B}_2 \times \mathcal{B}_2$. The asymptotic values of $u(\varepsilon)$ and $r(\varepsilon)$ fulfill the system (4.3), (4.4) with $q = q(\varepsilon)$.

As $\varepsilon^2 = \lambda^{-1}$, we have proved the following existence result for heteroclinic solutions to the system (4.1), (4.2).

THEOREM 1. *Assume that assumptions* H1–H6 *are fulfilled. Then for $\lambda > 0$ sufficiently large there exist a unique (up to a translation in ξ) triple $(q_\lambda, u_\lambda, r_\lambda)$ satisfying the system* (4.1), (4.2) *such that:*

i. *the functions u_λ and r_λ belong to the space $\mathcal{B}_2$;*

ii. $(q_\lambda, u_\lambda, r_\lambda) \underset{\lambda \to \infty}{\longrightarrow} (q_0, G, 0)$ *in the norm of* $\mathbb{R}^1 \times \mathcal{B}_2 \times \mathcal{B}_2$;

iii. $(u_\lambda(-\infty), r_\lambda(-\infty))$ *and* $(u_\lambda(\infty), r_\lambda(\infty))$ *are equal to the appropriate solutions of the system* (4.3), (4.4) *with $q = q_\lambda$.* ■

By returning to the initial variables u_1 and u_2 we can obtain the similar existence result of heteroclinic solutions for the system $(2.2)_{1,2}$.

REMARK 5. Theorem 1 can be proved also when the functions appearing in the system (4.1), (4.2) depend on $\lambda = \varepsilon^{-2}$, provided that for all ε close to 0 they are sufficiently smooth with respect to the other variables (as in H3). ■

It is easy to note that, according to Remarks 1 and 2, assumptions H1–H6 are satisfied for our plasma system of ODEs given by (2.5), (2.6). First, by appropriate affine change of variables we can suppose that $u_- = 0$ and $u_+ = 1$. Thus Remarks 1 and 2 imply H1–H4. The properties of $f(u)$ imply H5. Also assumption H6 is fulfilled because k and c are positive. Thus the above theorem ensures the existence of heteroclinic solution to Eqs. (2.5), (2.6).

5. Estimations of temperature difference in travelling fronts for laser-sustained plasma

In the case of the plasma system (2.5), (2.6), the problem is simplified, since this time $r_- = r_+ = 0$, and the function $S(\varepsilon, q; \xi)$ is equal to zero and $r \equiv R$. Moreover, the function $L(\varepsilon, q; \xi)$ is constant in (ε, q) and neither N_1 nor N_2 (with u substituted by $U + L$) depend on the parameter ε. (N_1 and N_2 are written after Eqs. $(2.5)_1$ and (2.6)). According to the implicit function theorem (see e.g.

[10]), the triple (q, U, R) is the uniform (with respect to ε) limit of the sequence $\{(q, U, r)_n\}$, where $(q, U, r)_0 = (q_0, 0, 0)$ and, for $n \geq 1$,

$$(q, u, r)_n = (q, u, r)_{(n-1)} - (dQ(q_0, G, 0, 0))^{-1}[Q((q, u, r)_{n-1}, \varepsilon)].$$

Thus, in the first approximation ($n = 1$), according to Lemma 2, we have $r = Q_2(q_0, U = 0, r = 0, \varepsilon) = A^{-1}(0, 0, \varepsilon)N_2(q_0, [U = 0, r = 0])$, i.e. r is given as a B_2 solution to the equation

$$r'' - B(\xi)r = -N_2(\xi), \tag{5.1}$$

where for a fixed ε we have put $B(\xi) = B(G, 0)(\xi) = \varepsilon^{-2}[WKd^{-1}](\xi)$ and the functions W, K and d are taken at the point $(U = 0, r = 0)$. Similarly we have denoted $N_2(\xi) = N_2(q_0, [U = 0, r = 0])(\xi)$.

Taking advantage of the WKB-method (see Lemma 4 in Appendix 1), we can find an approximate (in C^0) solution to Eq. (5.1)

$$r(\xi) = +2^{-1}\left\{Y_-(\xi)\int_{-\infty}^{\xi} Y_+(s)N_2(s)\,ds + Y_+(\xi)\int_{\xi}^{\infty} Y_-(s)N_2(s)\,ds\right\}, \tag{5.2}$$

where

$$Y_\pm(\xi) = B^{-\frac{1}{4}}(\xi)\exp\left[\pm\int_0^{\xi}\sqrt{B(s)}\,ds\right].$$

Differentiating (5.1) we obtain the equation for $z = r'$, from which we have

$$z(\xi) = 2^{-1}\left\{Y_-(\xi)\int_{-\infty}^{\xi} Y_+(s)T(s)\,ds + Y_+(\xi)\int_{\xi}^{\infty} Y_-(s)T(s)\,ds\right\},$$

where $T(s) = (N_2(s))' - (B(s))'r(s)$. Then, by means of (4.1) we can find an approximation for r''.

Further, $N_2(q_0, [G, 0], \varepsilon)$ has the following form:

$$N_2(q_0, [G, 0], \varepsilon) = -k_2(d)^{-1}\left\{q_0C_1G' - k_{1,u}G'^2 - f\right\} + k_1(d)^{-1}\left\{-k_{2,u}G'^2 + q_0C_2G'\right\},$$

where $C_1 = C_{11} + C_{12}$, $C_2 = C_{21} + C_{22}$.

It is easy to note (see Appendix 1) that for small $|\varepsilon|$ we have, according to (5.2),

$$r = \varepsilon^2(WK)\{-k_2[q_0C_1G' - k_{1,u}G'^2 - f] + k_1[-k_{2,u}G'^2 + q_0C_2G']\} + O(\varepsilon^3).$$

It is seen that the same formula can be derived, when we set $q = q_0$ and $u_1 = u_2 = G$ (everywhere except in $W(u_1 - u_2)$), multiply the first equation by k_2, the second by k_1 and subtract it from the first.

Now, let us estimate δq – a change in a mass flux q (see Eq. (2.3)) due to the finitness of λ. First, we note that Eq. (2.5) can be written in the form:

$$u'' - qc(u)(k(u))^{-1} + (k(u))^{-1}k_{,u}u'^2 + f(u)(k(u))^{-1} + \mathcal{P}(q,[u,r]) = 0.$$

It can be checked that the linearization of $\mathcal{P}$ at $q = q_0$, $u = G$ (i.e, $U = 0$), $r = 0$ is equal to

$$\begin{aligned}\mathcal{P}_0 := {} & K_{,r}(G,0)r(k(G))^{-1}\{G''\} + G'^2(k(G))^{-1}K_{,ur}(G,0)r \\ & + r'G'(k(G))^{-1}K_{,r}(G,0) + (k(G))^{-1}\{k_2(G,0)[B(G,0)r - N_2(q_0,G,0,\varepsilon)] \\ & - q_0C_{,r}(G,0)G'r + q_0C_2^*(G,0)r'\},\end{aligned}$$

where $C_2^* = C_{12} + C_{22}$ and we have used Eq. (5.1) to eliminate r''. According to (4.13) we have

$$p(\xi) = \exp\left[\int_0^\xi \left\{-q_0c(u_0)(k(u_0))^{-1} + 2u_0'(k(u_0))^{-1}k_{,u}(u_0)\right\} ds\right],$$

$$h := \int_{-\infty}^{\infty} \left[pG'^2c(G)(k(G))^{-1}\right](\xi)\, d\xi.$$

Then, according to the proof of Lemma 3 (Appendix 2), we have in the first approximation:

$$\delta q = h^{-1}\int (pG'\mathcal{P}_0)(\xi)\, d\xi.$$

Appendix 1. Proof of Lemma 1

First, let us consider the linear equation:

$$y'' - \varepsilon^{-2}b(\xi)y = f(\xi), \tag{A.1}$$

with $b(\xi) > b > 0$ for all $\xi, b \in \mathcal{B}_2$, $f \in \mathcal{B}_1$ (see Definition 5) and ε^{-2} large.

If $b = \text{const}$, then the homogeneous form of Eq. (A.1) is fulfilled by the functions $y_\pm = \exp(\pm\xi\sqrt{b})$, and the unique bounded solution (A.1) takes the form

$$y(\varepsilon,\xi) = -(2\sqrt{b})^{-1}|\varepsilon|\left\{y_-(\xi)\int_{-\infty}^{\xi} y_+(s)f(s)\, ds + y_+(\xi)\int_{\xi}^{\infty} y_-(s)f(s)\, ds\right\}.$$

Hence in this case $\|y(\varepsilon,\cdot)\|_1 = O(|\varepsilon|)$ as $\varepsilon \to 0$.

The general solution to Eq. (A.1) can be constructed by the use of two independent solutions to its homogeneous version. The asymptotic form (for $\varepsilon \to 0$) of these solutions can be estimated from the WKB theory.

LEMMA 4. Let $b(\xi) > b > 0$ for all ξ, $b \in \mathcal{B}_2$, $f \in \mathcal{B}_1$. Then, for all sufficiently small $|\varepsilon|$ the unique C^2 solution to Eq. (A.1), which is bounded for all ξ, has the following representation:

$$\text{(A.2)} \qquad y(\varepsilon,\xi) = -|\varepsilon|^2(1+\eta|\varepsilon|)\left\{Y_-(\xi)\int_{-\infty}^{\xi} Y_+(s)f(s)\,ds + Y_+(\xi)\int_{\xi}^{\infty} Y_-(s)f(s)\,ds\right\},$$

where

$$Y_-(\xi) = \left(\sqrt[4]{b(\xi)}\right)^{-1}\exp\left\{-|\varepsilon|^{-1}\int_0^{\xi}\left(\sqrt{b(s)}+\varepsilon^2\rho_-(s)\right)ds\right\},$$

$$Y_+(\xi) = \left(\sqrt[4]{b(\xi)}\right)^{-1}\exp\left\{+|\varepsilon|^{-1}\int_0^{\xi}\left(\sqrt{b(s)}+\varepsilon^2\rho_+(s)\right)ds\right\},$$

ρ_-, ρ_+ are continuous bounded functions independent of ε, and η is a constant independent of ε. ■

The proof of this lemma follows from [9] p. 327 and the estimations given in [11] section II.2 (with slight modifications). ■

LEMMA 5. Let $b \in \mathcal{B}_2$, $b(\xi) > b > 0$. Let $f \in \mathcal{B}_1$ (see Def. 5). Then, for $y(\varepsilon,\cdot)$ determined by (A.2) and for $\varepsilon \to 0$ the following relations hold:

$$\text{(A.3)} \qquad y \in \mathcal{B}_2,$$

$$\text{(A.4)} \qquad \|y(\varepsilon;\cdot)\|_{\mathcal{B}_2} = 0(|\varepsilon|)\|f\|_{\mathcal{B}_1},$$

$$\text{(A.5)} \qquad \|y(\varepsilon;\cdot)\|_{\mathcal{B}_1} = 0(\varepsilon^2)\|f\|_{\mathcal{B}_1}. \quad ■$$

P r o o f. From (A.2) one can conclude, that

$$y(\varepsilon,\xi) = \varepsilon^2 f(\xi)(b(\xi))^{-1} + O(|\varepsilon|^3)w(\xi),$$

where $|w(\xi)| \le \exp(\alpha\xi)$ for $\xi \le 0$ and $|w(\xi)| \le \exp(-\beta\xi)$ for $\xi \ge 0$ (see Definition 2). Hence from Eq. (A.1) we obtain $y''(\xi) = O(|\varepsilon|)w(\xi)$. Then, differentiating Eq. (A.1) we obtain the equation $z'' - \varepsilon^{-2}bz = f' + \varepsilon^{-2}b'y$, where $z := y'$. The right-hand side of this equation has its B_0 norm finite (and independent of ε).

If z is its solution, then it can be expressed by relation (A.2) with f replaced by $(f' + \varepsilon^{-2}b'y)$. Thus, we obtain (A.5) and hence (A.4). As $y'' \in B_0$, hence (A.3). The lemma is proved. ∎

Now, we take $b(\xi) := b[U + L(\varepsilon, q), R + S(\varepsilon, q)](\xi)$. According to assumption H4 for all (q, U, R, ε) sufficiently close to $(q_0, 0, 0, 0)$, we have $b(\xi) > b$ for all ξ and $b \in \mathcal{B}_2$. Thus, by Lemma 4 and Lemma 5 point i. of Lemma 1 is proved.

Now, we will prove point ii. of Lemma 1. Let

$$\Sigma(\varepsilon, q, \xi) = S''(\varepsilon, q, \xi) - \varepsilon^{-2}b[U + L(\varepsilon, q), R + S(\varepsilon, q)]S(\varepsilon, q, \xi)$$

and

$$\underline{\Sigma}(\varepsilon, \underline{q}, \xi) = S''(\varepsilon, q, \xi) - \varepsilon^{-2}b[\underline{U} + L(\varepsilon, \underline{q}), \underline{R} + S(\varepsilon, \underline{q})]S(\varepsilon, \underline{q}, \xi).$$

Then, let $\zeta(\xi)$, $\underline{\zeta}(\xi)$ be the unique solutions in $\mathcal{B}_2$ (Def. 5) of the equations:

$$\zeta'' - \varepsilon^{-2}b[U + L(\varepsilon, q), R + S(\varepsilon, q)]\zeta = N[q, U + L(\varepsilon, q), R + S(\varepsilon, q), \varepsilon],$$
$$\underline{\zeta}'' - \varepsilon^{-2}b[\underline{U} + L(\varepsilon, \underline{q}), \underline{R} + S(\varepsilon, \underline{q})]\underline{\zeta} = N[\underline{q}, U + L(\varepsilon, \underline{q}), \underline{R} + S(\varepsilon, \underline{q}), \varepsilon],$$

respectively. The difference $Y := (\zeta + S(\varepsilon, q)) - (\underline{\zeta} + S(\varepsilon, \underline{q}))$ satisfies the equation

$$\begin{aligned} Y'' - \varepsilon^{-2}b(\underline{u}, \underline{R})(\xi)Y = (&N[q, U + L(\varepsilon, q), R + S(\varepsilon, q), \varepsilon] \\ &- N[\underline{q}, U + L(\varepsilon, \underline{q}), \underline{R} + S(\varepsilon, \underline{q}), \varepsilon] + \varepsilon^{-2}(\zeta + S(\varepsilon, q))(b[U + L(\varepsilon, q), R \\ &+ S(\varepsilon, q)] - b[\underline{U} + L(\varepsilon, \underline{q}), \underline{R} + S(\varepsilon, \underline{q})]) + \Sigma(\varepsilon, q) - \underline{\Sigma}(\varepsilon, q))(\xi). \end{aligned}$$

Owing to H2, H3, H4, H5, Definition 3, Remark 4 and Lemma 5, the mappings $(N + \Sigma)$ and b are Frechet differentiable with respect to (q, U, R) (as mappings from $\mathbb{R}^1 \times B_2^0 \times B_2$ to B_1 and to $\mathcal{B}_2$, respectively), thus according to the definition of A (relation (4.8)) we obtain from the last equation:

$$\begin{aligned} Y = A^{-1}(\underline{U}, \underline{R}, \varepsilon)\left((D(N + \Sigma) + \varepsilon^{-2}(\zeta + S)Db)[\tilde{q}, \tilde{U}, \tilde{R}]\right) \\ + A^{-1}(\underline{U}, \underline{R}, \varepsilon)\left(R_N(\tilde{q}, \tilde{U}, \tilde{R}) + R_b(\tilde{q}, \tilde{U}, \tilde{R})\right). \end{aligned}$$

Here $\tilde{q} := q - \underline{q}$, $\tilde{U} := U - \underline{U}$, $\tilde{R} := R - \underline{R}$, $D(N + \Sigma)$ and Db denote the Frechet derivatives of $(N + \Sigma)$ and b at the point $(\underline{q}, \underline{U}, \underline{R})$, whereas $\|R_N(\tilde{q}, \tilde{U}, \tilde{R})\|_1$ and $\|R_b(\tilde{U}, \tilde{R})\|_1$ are terms of the order $o(|\tilde{q}| + \|\tilde{U}\|_2 + \|\tilde{R}\|_2)$ as $(|\tilde{q}| + \|\tilde{U}\|_2 + \|\tilde{R}\|_2) \to 0$. Further, taking advantage of (A.5) and substituting $\zeta + S = \underline{\zeta} + \underline{S} + Y$, we obtain

$$Y = \left(A^{-1}(\underline{U}, \underline{R}, \varepsilon)(D(N + \Sigma) + \varepsilon^{-2}(\underline{\zeta} + \underline{S})Db)\right)[\tilde{q}, \tilde{U}, \tilde{R}] + \delta(\tilde{q}, \tilde{U}, \tilde{R}),$$

where $\|\delta(\tilde{q}, \tilde{U}, \tilde{R})\|_1 = o(|\tilde{q}| + \|\tilde{U}\|_2 + \|\tilde{R}\|_2)$ as $(|\tilde{q}| + \|\tilde{U}\|_2 + \|\tilde{R}\|_2) \to 0$. Thus, the Frechet derivative of $(\zeta + S)$ with respect to (q, U, R) at the point $(\underline{q}, \underline{U}, \underline{R}, \varepsilon)$ is equal to $A^{-1}(\underline{U}, \underline{R}, \varepsilon)(D(N + \Sigma) + \varepsilon^{-2}(\underline{\zeta} + \underline{S})Db)$. Due to the fact that $\zeta = A^{-1}(U, R, \varepsilon)N(q, U, R, \varepsilon)$, H5, Lemma 5, Remark 4 and definition of Q_2, we have proved the Frechet differentiability of Q_2. By the use of (A.4) and (A.5) we obtain point ii. of Lemma 1. Thus the whole lemma is proved.

Appendix 2. Proof of Lemma 3

Due to point i. of Lemma 1, the form of Q_1, Remark 4 and (4.13), the system (4.12) can be written as:

$$D\tilde{U} = \Phi(\tilde{q}, f_1, \tilde{R})(\xi), \tag{A.7}$$

$$\tilde{R} = f_2(\xi), \tag{A.8}$$

where

$$DU := \tilde{U}'' + a(\xi)\tilde{U}' + e(\xi)\tilde{U} \tag{A.9}$$

and

$$\Phi(\tilde{q}, f_1, \tilde{R})(\xi) := f_1(\xi) - \sum_{i=0}^{2} m_i(\xi)\left[\tilde{R}^{(i)}(\xi)\right] - h(\xi)\tilde{q} - D\left[L_{,q}(0, q_0, \xi)\right]\tilde{q}.$$

Let us note that G' fulfils the homogeneous version of Eq. (A.7), but it does not belong to B_2^0, since $(G'(0))^2 + (G''(0))^2 \neq 0$ (otherwise G would be identically equal to a constant). According to assumption H2, for μ sufficiently large the functions

$$\vartheta_{1,2}(\xi) = G'(\xi)\int_{\pm\mu}^{\xi} [p(z)G'^2(z)]^{-1}\,dz$$

are also well determined solutions to the homogeneous version of Eq. (A.7) for $\xi \in (\pm\mu, \pm\infty)$. These solutions can be extended to functions $\vartheta_{1,2}$ determined on the whole $\mathbb{R}^1$-line. It is easy to note that $\vartheta_1(\xi)$ ($\vartheta_2(\xi)$) tends to some nonzero constant or grows exponentially as $\xi \to \infty$ ($\xi \to -\infty$). Thus, by choosing appropriate linear combination of ϑ_1 and ϑ_2, we obtain a solution ϑ such that

$$\begin{aligned} \vartheta(\xi) &= m_1 e^{\gamma_1 \xi}(1 + o(1)) \qquad \text{as} \quad \xi \to \infty, \\ \vartheta(\xi) &= m_2 e^{\gamma_2 \xi}(1 + o(1)) \qquad \text{as} \quad \xi \to -\infty, \end{aligned} \tag{A.10}$$

for some nonzero constants m_1 and m_2. Here $\gamma_1 = 2\beta - a(\infty)$, $\gamma_2 = -2\alpha - a(-\infty)$, where a is defined by $(4.13)_1$. Without losing generality we may also assume that the Wronskian $G'\vartheta' - G''\vartheta$ is equal to 1 for $\xi = 0$.

Knowing two linearly independent solutions of the homogeneous equation we can write down the general solution of Eqs. (A.8), (A.7). Namely:

$$\tilde{R}(\xi) = f_2(\xi),$$

$$\tilde{U}(\xi) = -G'(\xi)\int_0^{\xi} \vartheta(z)p(z)\Phi(\tilde{q}, f_1, f_2)(z)\,dz + c_1 G'(\xi)$$

$$+\vartheta(\xi)\left(-c_2 + \int_0^{\xi} G'(z)p(z)\Phi(\tilde{q}, f_1, f_2)(z)\,dz\right).$$

Let us note that Φ belongs to the space B_0. Due to assumptions H2 and H3, $\vartheta(\xi)$ behaves like a nonzero constant or grows exponentially for $|\xi| \to \infty$, so c_2 should be chosen properly so that $\tilde{U} \in B_2$. Thus c_2 must obey the conditions:

$$c_2 = \int_0^{\infty} G'(z)p(z)\Phi(\tilde{q}, f_1, f_2)(z)\,dz,$$

$$c_2 = \int_0^{-\infty} G'(z)p(z)\Phi(\tilde{q}, f_1, f_2)(z)\,dz.$$

Hence we obtain $\int_{-\infty}^{\infty} G'(z)p(z)\Phi(\tilde{q}, f_1, f_2)(z)dz = 0$. This condition, together with assumption H5, allows us to determine in a unique way the value of $\tilde{q}$:

$$\tilde{q} = \left[\int_{-\infty}^{\infty} G'p\Phi(0, f_1, f_2)\,dz\right]\left[\int_{-\infty}^{\infty} G'gp\,dz\right]^{-1}.$$

Since $\tilde{U}$ must belong to B_2^0, then the constant c_1 is also uniquely determined. It is easy to check that with the above choice of constatnts $\tilde{U}$ belongs to B_2. The first statement of the lemma is proved.

Thus, the operator $DQ(q_0, 0, 0, 0)$ is invertible on the whole $B_0 \times B_2$. Due to Theorem 4.2–H p. 180 in [12], the operator $(DQ(q_0, 0, 0, 0))^{-1}$ is continuous and thus bounded. The whole lemma is proved. ■

REMARK 7. Let us see more precisely what happens when $E_{0,u}(q_0, 0, 0)$ or $E_{0,u}(q_0, 0, 1)$ become equal to 0. According to H2 and (A.10) the terms

$$\vartheta(\xi)\left(-c_2 + \int_0^{\xi} G'p\Phi\,dz\right) = \vartheta(\xi)\left(\int_{-\infty}^{\xi} G'p\Phi\,dz\right) = -\vartheta(\xi)\left(\int_{\xi}^{\infty} G'p\Phi\,dz\right)$$

can be written, for $|\xi|$ sufficiently large, as terms proportional to

$$(1 + o(1))\left(\int_{-\infty}^{\xi} (1 + o(1))\Phi(z)\,dz\right) \quad \text{or} \quad (1 + o(1))\left(\int_{\xi}^{\infty} (1 + o(1))\Phi(z)\,dz\right).$$

We want these integrals to belong to B_2, so at least to B_0. As $\Phi \in B_0$, then it follows that Φ vanishes exponentially at $\pm\infty$.

Acknowledgements

This work was supported by grant KBN No 336249203.

References

1. S.I. BRAGINSKII, [in:] Reviews of Plasma Physics, M.A. LEONTOVICH [Ed.], 1, p. 205. Consultants Bureau, New York 1965.
2. O. CHANG, *Relaxation thermique dans un jet rarefie de plasma d'azote*, Rapport de Stage de D.E.A. de Mecanique, Universite P.M. Curie, juin 1991.
3. A.A. VEDENOV, G.G. GLADUŠ, *Physical processes accompanying the laser treatment of materials* [in Russian], Energoatomizdat, 1985.
4. B. KAŹMIERCZAK, Z. PERADZYŃSKI, *Heteroclinic solutions to strongly coupled systems of ODEs*, [subm. to Math. Meth. in the Appl. Sci.].
5. YU.P. RAIZER, *Physics of gas discharge* [in Russian], Nauka, Moskva 1987.
6. P. FIFE, *Mathematical aspects of reacting and diffusing systems*, Lect. Notes in Biomath., **28**, Springer 1979.
7. H. BERESTYCKI, B. NICOLAENKO, B. SCHERER, *Travelling waves solutions to combustion models and their singular limits*, SIAM J. Math. Anal., **16**, 6, 1983.
8. W.A. COPPEL, *Dichotomies in Stability Theory*, Lect. Notes in Math., **629**, Springer 1978.
9. PH HARTMAN, *Ordinary differential equations*, J. Wiley and Sons Inc., New York-London-Sydney 1964.
10. M. CRANDALL, *An introduction to constructive aspects of bifurcation theory and implicit function theorem*, [in:] Applications of bifurcation theory, P. RABINOWITZ [Ed.], Acad. Press, pp. 1–35, New York 1977.
11. M.W. FEDORJUK, *Asymptotical methods for linear O.D.E.* [in Russian], Moskva 1983.
12. A.E. TAYLOR, *Introduction to functional analysis*, J. Wiley and Sons Inc., New York 1958.

POLISH ACADEMY OF SCIENCES
INSTITUTE OF FUNDAMENTAL TECHNOLOGICAL RESEARCH

Received May 27, 1994.

Arch. Mech., 46, 5, pp. 775–788, Warszawa 1994

New formulation of the space-time finite element method for problems of evolution (*)

CZ. BAJER and R. BOGACZ (WARSZAWA)

IN THE PAPER the space-time finite element method was developed for problems of evolution. The equilibrium equations were determined in terms of velocity. Non-stationary partition into spatial finite elements, which arises from the evolution of the shape of material, was assumed. Properties of the solution scheme, particularly its convergence and stability, depends on the form of the distribution of virtual velocity. The system of one degree of freedom, described both by linear and nonlinear differential equation, was investigated. The damping of higher-mode oscillations and the amplitude and phase error were estimated. The solution of testing and real problems were performed. High efficiency of the proposed method for complex problems, also with internal contact, were proved.

1. Introduction

THE SPACE-TIME discretization of the structure has some advantages. First, it enables the non-stationary partition of a structure. It allows to solve in a simple way quite new problems: problems with moving edge, mesh adaptation in hyperbolic problems, mesh condensation which moves together with a travelling force. Second, the evolution of the domain considered in nonlinear problems can be efficiently modelled by the continuous change of geometry in time. The method of the space-time finite elements, described for the first time by ODEN [1] and then developed in papers [2, 3, 4, 5], has considerably been changed as compared with its first formulation. The fundamental difference concerns the approximation of characteristic parameters. In commonly used time integration schemes it has the form

$$\mathbf{u}(\mathbf{x}, t) = \mathbf{N}(\mathbf{x}) \cdot \mathbf{q}(t), \tag{1.1}$$

whereas in the space-time approximation we use

$$\mathbf{u}(\mathbf{x}, t) = \mathbf{N}(\mathbf{x}, t) \cdot \mathbf{q}_e. \tag{1.2}$$

The same question concerns both the state parameters and the geometry of a structure. Thus the evolution of the geometry has a continuous representation in the formulation and in the equilibrium equation.

In the paper we will discuss some numerical properties of the time integration method derived from the formula (1.2). The first approach to the formulation developed here can be found in [6, 7]. The reader can also find there the historical

(*) The work has been done as a part of the project No PB–309389101, granted by KBN.

background. It should be emphasized that we do not apply directly the Hamilton principle (nor any other energy methods). The method has various possibilities of modification. The order of the error can be evaluated and changed according to our requirements. The artificial damping can easily be introduced and controlled. Engineering problems with the evolution of geometry can be solved with much more higher efficiency than by means of other numerical tools. The approach can be extended to nonlinear evolution of geometry within the time interval. It could allow us to increase considerably the time step of calculation with material and geometrical nonlinearities. Thermo-mechanical coupling, temperature problems, problems with phase change can be modelled in a natural way by using non-rectangular space-time elements.

Let us shortly recall and develop the formulation.

2. Formulation

We start from the differential equation of motion

$$m\frac{dv}{dt} + kx = 0\,. \tag{2.1}$$

The principle of virtual power gives the form

$$\left(m\frac{dv}{dt} + kx\right) v^* = 0\,, \tag{2.2}$$

where v^* is the function of virtual velocity.

We assume the linear distribution of real velocity v over the time interval $0 \leq t \leq h$,

$$v = \left(1 - \frac{t}{h}\right) v_0 + \frac{t}{h} v_1\,. \tag{2.3}$$

The displacement $x(t)$ is described by the integral

$$x(t) = \int_0^t v\,dt = h_0 + \frac{h}{2}\left[1 - \left(1 - \frac{t}{h}\right)^2\right] v_0 + \frac{t^2}{2h} v_1\,. \tag{2.4}$$

Here the proper choice of distribution of the virtual velocity v^* is the fundamental problem of the method. The convergence, efficiency, accuracy of time integration and accuracy of the solution in the case of geometrical nonlinearities depend on the form of v^*. The simplest one is the Dirac distribution:

$$v^* = v_1\,\delta\left(\frac{t}{h} - \alpha\right), \qquad 0 \leq \alpha \leq 1. \tag{2.5}$$

The form (2.5) is convenient for our purpose since it reduces the computational effort and allows us to select the parameter α according to the stability condition.

The integration of (2.2) in time interval $[0, h]$ with respect to (2.3), (2.4) and (2.5) gives the following formula:

$$v_1 = \frac{1 - \frac{kh^2}{2m}[1 - (1-\alpha)^2]}{1 + \frac{k\alpha^2 h^2}{2m}} v_0 - \frac{k}{m} \frac{h}{\left(1 + \frac{k\alpha^2 h^2}{2m}\right)} x_0, \tag{2.6}$$

which allows us to compute v_1 if the initial conditions v_0, x_0 for time step $[0, h]$ are known. Now the geometry x_1 is the last unknown value we must determine to proceed to the next step $[h, 2h]$. The average value of the velocity taken at point βh, $0 \leq \beta \leq 1$ results in the formula

$$x_1 = x_0 + h[(1-\beta)v_0 + \beta v_1]. \tag{2.7}$$

The energy at the end of the time interval is preserved if $\beta = 1 - \alpha$. Then we have finally

$$x_1 = x_0 + h[\alpha v_0 + (1-\alpha)v_1]. \tag{2.8}$$

It was proved in [7] that the unconditional stability of the process (2.6), (2.8) occurs for $\frac{\sqrt{2}}{2} \leq \alpha \leq 1$. For $\alpha = 1$ we have the explicit formula while for other values ($0 \leq \alpha < 1$) the scheme is implicit and requires iterations to determine the geometry x_1.

3. Numerical dissipation

Numerical damping of higher frequencies with zero damping of the basic frequency of the structure is the important question for each time integration method. Several papers on this subject exist (for example [8]). The ideal solution is when we can control the damping properties of the procedure (in particular cases the damping should be equal to zero). Lower frequencies should not be damped while higher should be damped relatively stronger. With respect to the shape of the damping diagram, we can divide all methods in two groups: the first one (Wilson, Houbolt method) with the zero slope of the damping function for small h/T, growing with the increase of h/T, and the second one (Newmark, trapezoidal rule) with a certain slope of the damping function for $h/T \to 0$. The practical experiences indicate that the first group damps higher modes too much, and the second group does the same with lower modes. Other methods, which use more artificial parameters in their formulations, improve the damping

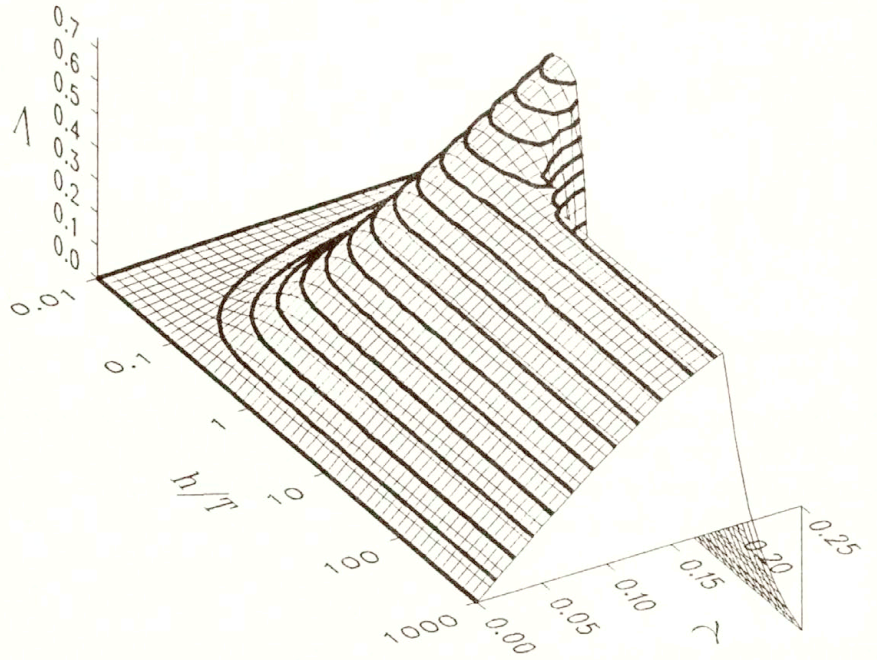

FIG. 1. Logarithmic decrement Λ as a function of damping parameter γ for $\alpha = 0.8$.

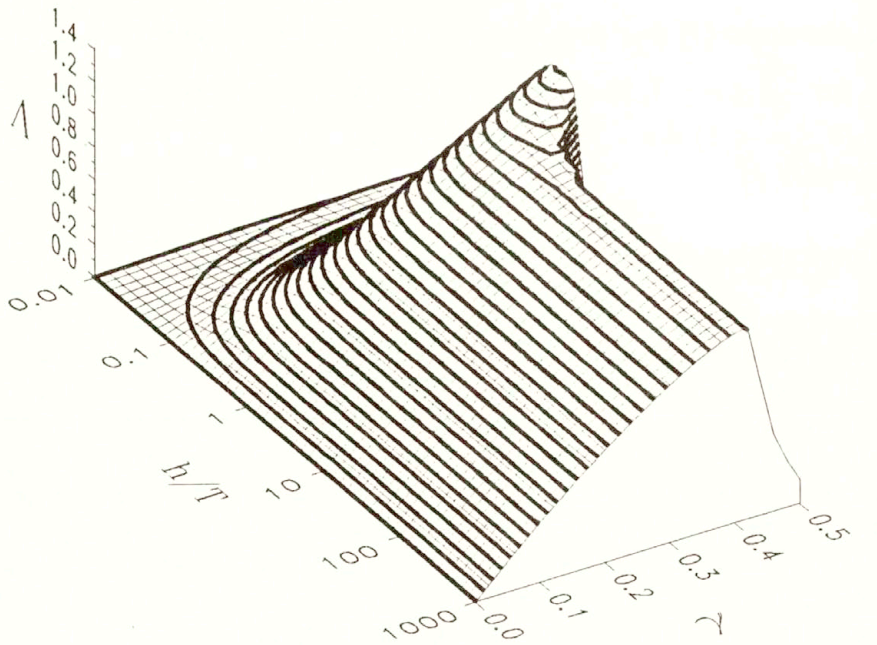

FIG. 2. Logarithmic decrement Λ as a function of damping parameter γ for $\alpha = 0.9$.

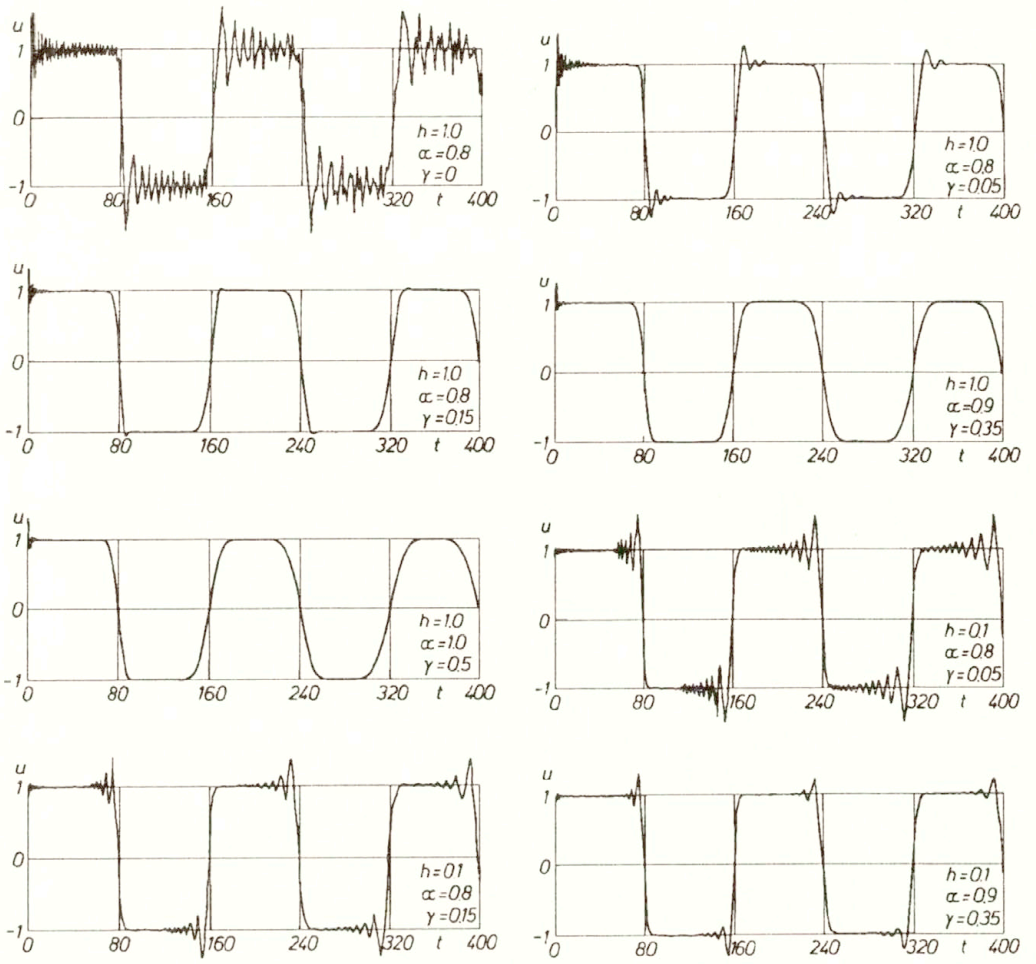

FIG. 3. Displacements in time of the free end of the 40-element bar with selected parameters α and γ for time step $h = 0.1$ and 1.0.

properties but their use is dangerous since the regular dependence of properties on the parameters does not exist.

Here, let us modify the Eq. (2.7) by

$$\beta = 1 - \frac{\alpha}{1+\gamma}, \qquad 0 \leq \gamma \leq 1. \tag{3.1}$$

The system (2.6), (2.7), (3.1) has the artificial damping which depends on the parameter γ and on the moment αh in which the equation of motion is considered. Figures 1 and 2 present the damping decrement as a function of γ for two values at α: 0.8 and 0.9. It can be interesting to compare the response of a 40-element model of a bar fixed at one end and subjected to an impulse. The most characteristic results are depicted in Fig. 3. Even small value of γ allows

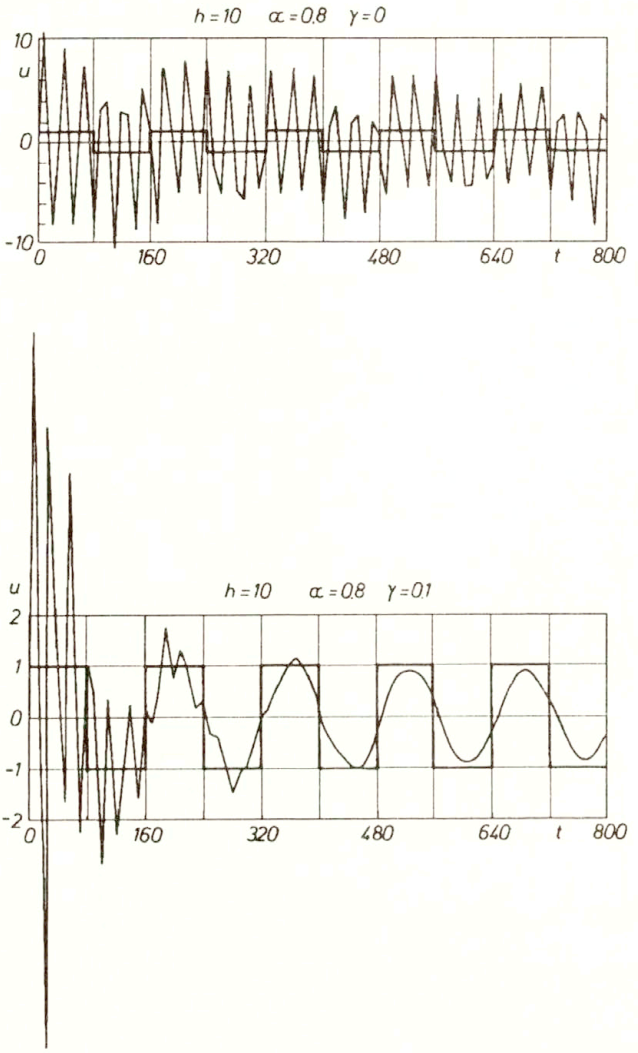

FIG. 4. Displacements in time of the free end of a 40-element bar computed with a long time step: without damping and with $\gamma = 0.1$ (thick line – theoretical solution).

to reduce the spurious vibrations of higher modes. For the Courant number $\kappa = 1$ ($\kappa = ch/b$, c – wave speed, b – length of the finite element) it suffices to take $\gamma = 0.05 \div 0.10$. For short time steps γ should be increased. Figure 4 presents the displacement in time of the free end of the same bar. However, the calculation was performed with a long time step. Small artificial damping with $\gamma = 0.1$ stabilizes vibration after several steps. Otherwise the response of the numerical model does not correspond with the response of the mathematical one.

4. Convergence

Simple error analysis enables us to determine the reminder of the Taylor expansion of the exact solution which is not represented in the numerical solution. The order of the error and respective coefficients for different parameters α are given in Table 1. The best case is for $\alpha = 1/2$. However, the scheme is

Table 1. The order of convergence for different parameters α.

method	error order	coefficient
$\alpha = 0$	Δt^2	$\frac{1}{2}$
$\alpha = \frac{1}{4}$	Δt^2	$\frac{1}{4}$
$\alpha = \frac{1}{2}$	Δt^3	$\frac{1}{12}$
$\alpha = \frac{3}{4}$	Δt^2	$\frac{1}{4}$
$\alpha = 1$	Δt^2	$\frac{1}{2}$

conditionally stable. We can decrease the error order and improve the stability by a linear combination of several Dirac peaks introduced to (2.5). Then the virtual velocity has the form

$$v^* = v_1 \sum_i w_i \delta\left(\frac{t}{h} - \alpha_i\right), \tag{4.1}$$

where w_i are the weights and α_i are the coordinates of peaks. The formula which corresponds to (2.6) is of the form

$$v_1 = \frac{1 - \frac{h^2}{2}[1 - \sum_i w_i(1-\alpha_i)^2]}{1 + \frac{h^2}{2}\sum_i w_i \alpha_i^2} v_0 - \frac{h}{1 + \frac{h^2}{2}\sum_i w_i \alpha_i^2} x_0 . \tag{4.2}$$

Both k and m are, for simplicity, equal to 1. For example, if we take $\alpha_1 = 0$, $\alpha_2 = 1/2$, $\alpha_3 = 1$, we can determine $w_1 = 5/6$, $w_2 = -2/3$, $w_3 = 5/6$. The solution has the error $O(h^4)$. The time integration scheme

$$v_1 = \frac{1 - \frac{h^2}{6}}{1 + \frac{h^2}{3}} v_0 - \frac{h}{1 + \frac{h^2}{3}} x_0 , \qquad x_1 = x_0 + \frac{1}{2}h(v_0 + v_1) \tag{4.3}$$

is identical with the classical space-time finite element scheme described in [9]. We should strongly emphasize here that the coincidence occurs for the simplest case of a linear, one-degree-of-freedom system. Here we investigate such a case for the reason of its simplicity and possibility of comparison of the results. We can notice that in the case of linear vibration of simple oscillator, the central difference method is identical with the velocity formulation for $\alpha = 0$. The Newmark method ($\beta = 1/4$, $\gamma = 1/2$) and the trapezoid rule are identical with the case of $\alpha = \sqrt{2}/2$.

Higher ranges of approximation are also available. In the case described above by (4.3) the cost of calculations is doubled (in a general case of multi-degree-of-freedom system). Matrices have to be determined for $t = h/2$ and $t = h$. The matrix for $t = 0$ is taken from the previous step.

The phase error P for the method described by (2.6), (2.8) is given by the relation

$$P = \frac{\sqrt{\kappa}}{\operatorname{arctg}\left(\dfrac{\sqrt{\kappa(2\alpha^2\kappa + 4 - \kappa)}}{\alpha^2\kappa + 2 - \kappa}\right)}, \qquad \kappa = \frac{ch}{b}. \tag{4.4}$$

In the limit $\lim_{\kappa \to 0} P = 0$.

5. Multidimensional case

As a multidimensional case, let us consider the change of the geometry in time (Fig. 5). The equation of virtual work and the recurrence solution scheme is derived in the same way as in the case of one degree of freedom. The integration

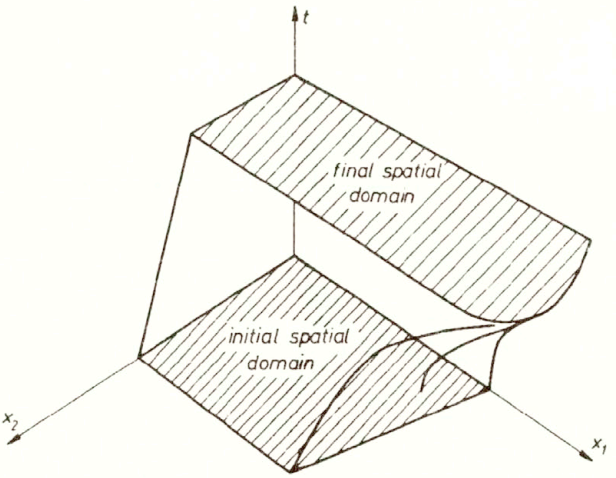

FIG. 5. Evolution of the spatial domain in two dimensions.

is carried out over the space time volume Ω:

$$\int_{\Omega} (\mathbf{v}^*)^T \rho \frac{\partial \mathbf{v}}{\partial t} \, d\Omega + \int_{\Omega} (\dot{\boldsymbol{\varepsilon}}^*)^T \boldsymbol{\sigma} \, d\Omega = \int_{\Omega} (\mathbf{v}^*)^T \mathbf{f} \, d\Omega \,. \tag{5.1}$$

The displacement is described by the integral

$$\mathbf{u}(t) = \mathbf{u}_0 + \int_0^t \mathbf{v} \, dt \,. \tag{5.2}$$

The interpolation formulas

$$\mathbf{v} = \mathbf{N} \dot{\mathbf{q}} \qquad \text{and} \qquad \mathbf{v}^* = \mathbf{N}^* \dot{\mathbf{q}} \tag{5.3}$$

and constitutive equation $\boldsymbol{\sigma} = \mathbf{E}\boldsymbol{\varepsilon}$ allow us to write the equilibrium of forces in the time layer $[0, h]$ in the form

$$(\mathbf{K} + \mathbf{M}) \dot{\mathbf{q}} = \mathbf{F} - \mathbf{s}, \tag{5.4}$$

where

$$\mathbf{K} = \int\int_{V_{\alpha h}} (\mathcal{D}\mathbf{N}_{\alpha h}(\mathbf{x}))^T \mathbf{E} \mathcal{D}\mathbf{N} \left(\mathbf{x}, \frac{\alpha h}{2}\right) dV \cdot \alpha h \,, \tag{5.5}$$

$$\mathbf{M} = \int\int_{V_{\alpha h}} \mathbf{N}_{\alpha h}^T(\mathbf{x}) \rho \frac{\partial \mathbf{N}(\mathbf{x}, \alpha h)}{\partial t}) \, dV, \tag{5.6}$$

$$\mathbf{s} = \int\int_{V_{\alpha h}} (\mathcal{D}\mathbf{N}_{\alpha h}(\mathbf{x})^T \mathbf{E} \boldsymbol{\varepsilon}_0 \, dV, \tag{5.7}$$

$$\mathbf{F} = \int\int_{V_{\alpha h}} \mathbf{N}_{\alpha h}^T(\mathbf{x}) \cdot \mathbf{f}(\mathbf{x}, \alpha h) \, dV. \tag{5.8}$$

K, **M**, s and **F** are the stiffness matrix, mass matrix, initial internal force vector and external force vector, respectively. Here the integration is carried out over the spatial volume V. Shape matrices $\mathbf{N}_{\alpha h}$ are determined for the spatial geometry in $t = \alpha h$ and $\mathbf{N}(\mathbf{x}, \cdot)$ for the space-time volume in a given time.

Two numerical tests prove the efficiency of the method. The first one presents vibration of a bar element, fixed at one end. Very soft material ensures large displacements, comparing with the initial element length $b = 1.0$. Two plots in Fig. 6 present the motion in the phase plane. They are obtained for the initial condition $v_0 = 1.0$. The first one was performed for $h = 0.1$ and for different values of α. The second one compares the results for $h = 0.5$ obtained by the space-time procedure (solid line) and by the modified Newton–Raphson method

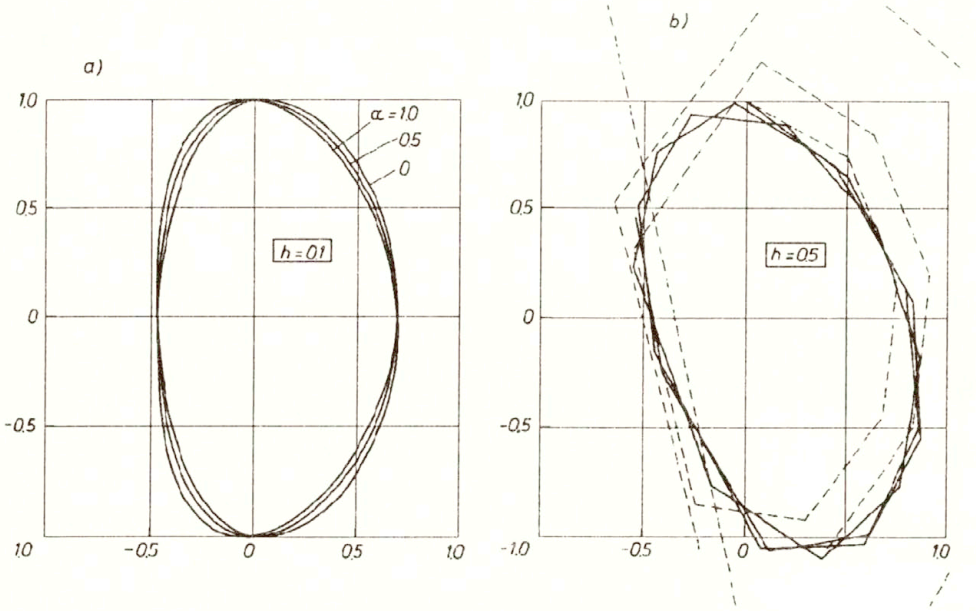

FIG. 6. Motion of a bar in the phase plane.

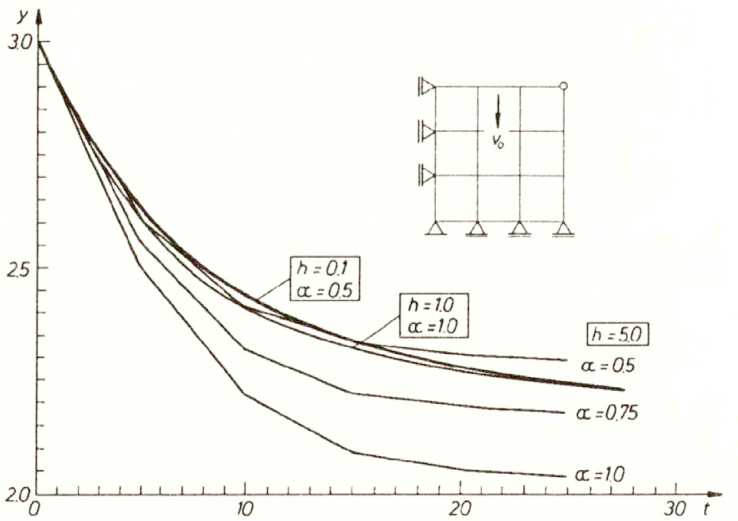

FIG. 7. Test of viscoplastic deformation.

with central difference method for time integration (dashed line). The precision of the calculation is sufficiently high in spite of the large geometry change per step. The second test was performed for the viscoplastic material. The Norton constitutive law [10] was taken for calculation. The 3×3 finite element square hits a rigid base with the initial speed v_0. Displacement of the upper corner as a function of time is depicted in Fig. 7. Different time steps were taken. The fastest

calculation was obtained for $h = 5$ with $\alpha = 0.5$ (5 steps with 3–4 iterations per step). The second interesting case is for $h = 1.0$ and $\alpha = 1.0$. Here we have the explicit formula (no iterations) for which we need 15 time steps.

6. Numerical examples

More complex numerical examples prove high efficiency of the presented approach to problems of evolution of geometry. Two examples of viscoplastic deformation are presented below. The first one is the benchmark. The cylinder ($H = 3.24\,\text{cm}$, $R = 0.32\,\text{cm}$, $\rho = 8.93\,\text{g/cm}^3$, $K = 0.005$, $m = 0.1$) hits a rigid base with a speed $v = 0.0227\,\text{cm/}\mu\text{s}$. The computation was performed with $\alpha = 0.5$ and $h = 1\,\mu\text{s}$ in 80 steps (Fig. 8). Finally, the following results were ob-

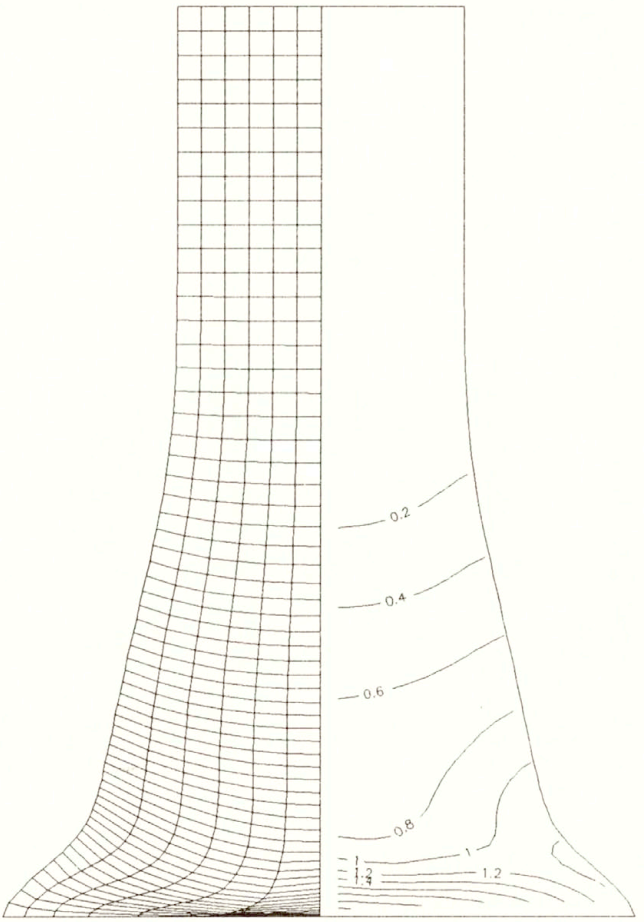

FIG. 8. Impact of a bar – deformed mesh and generalized strain.

tained: height 2.12 cm, radius 0.71 cm, maximum strain 3.0. Other authors got the following range of values: height 2.08–2.16 cm, radius 0.67–0.72 cm, maximum strain 2.6–3.2. It is essential that other methods (for example [11, 12]) require 9500 steps or 3200–12600 cycles. On this background the space-time approach is much more efficient. The second example has 1250 spatial quadrangular elements. The axi-symmetric viscoplastic cylinder (H = 10 cm, R_{int} = 2 cm, R_{ext} = 2.2 cm) is crashed with a speed v = 180 km/h. The calculation lasts longer in this case since an internal contact is considered. There is no friction between parts of the material. The deformed mesh and 3-dimensional view is depicted in Fig. 8, 9 and 10.

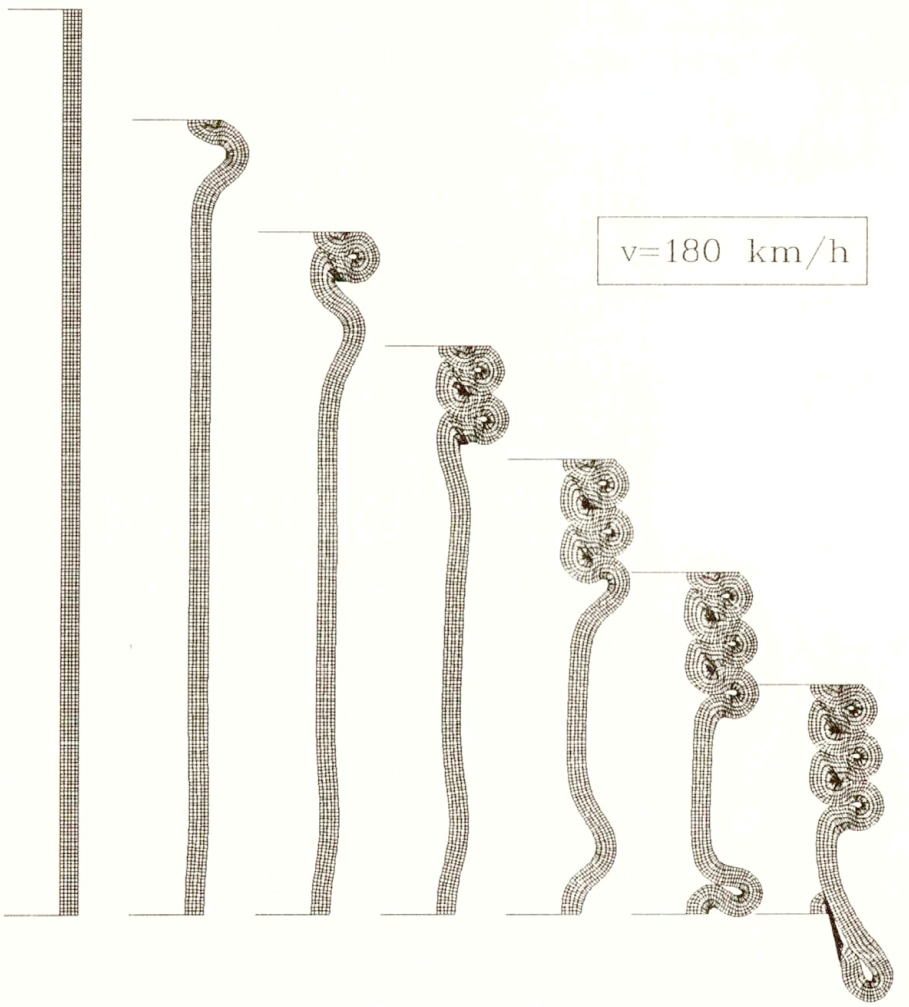

Fig. 9. Finite element mesh in successive stages.

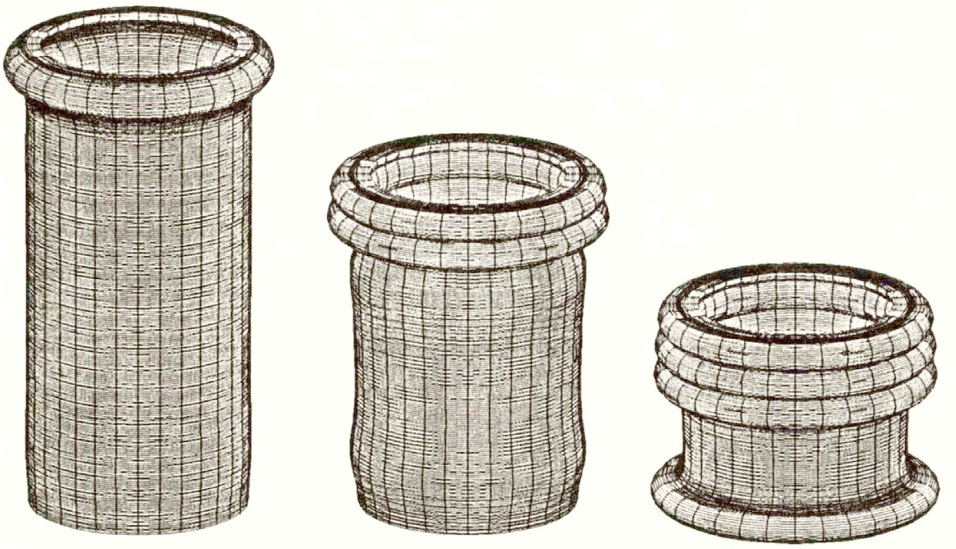

FIG. 10. 3-D view of the axi-symmetric cylinder in chosen moments.

7. Conclusions

In the paper we have presented a new approach to the space-time finite element method. The formulation is based on the velocity vector as a basic parameter. Problems with nonlinear geometry evolution can simply and efficiently be solved. In this case we can choose both the explicit and implicit scheme. Real engineering problems can be solved with a small number of time steps and small number of iterations per step.

The properties of the time integration scheme depend on the parameters of the formulation. The accuracy, degree of approximation, reduction of higher mode oscilations were investigated. Comparison with other numerical time integration methods can be done but direct relation between the methods is impossible. All the methods developed to date are derived for the integration with constant coefficients. The method presented in the paper is prepared for problems of evolution. One-degree-of-freedom system is only the particular case.

References

1. J.T. ODEN, *A generalized theory of finite elements, II. Applications*, Int. J. Numer. Meth. Engng., 1, 247–259, 1969.
2. Z. KĄCZKOWSKI, *The method of finite space-time elements in dynamics of structures*, J. Tech. Phys., **16**, 1, 69–84, 1975.
3. Z. KĄCZKOWSKI, *General formulation of the stiffness matrix for the space-time finite elements*, Arch. Inż. Ląd., **25**, 3, 351–357, 1979.
4. C.I. BAJER, *Adaptive mesh in dynamic problem by the space-time approach*, Comput. and Struct., **33**, 2, 319–325, 1989.

5. C. BAJER and A. PODHORECKI, *Space-time element method in structural dynamics*, Arch. Mech., **41**, 863–889, 1989.
6. C. BOHATIER, *A large deformation formulation and solution with space-time finite elements*, Arch. Mech., **44**, 31–41, 1992.
7. C. BAJER, *Space-time finite element formulation for the dynamical evolutionary process*, Appl. Math. and Comp. Sci., **3**, 2, 251–268, 1993.
8. H.M. HILBER, T.J.R. HUGHES and R.L. TAYLOR, *Improved numerical dissipation for time integration algorithms in structural dynamics*, Earthquake Engng. and Struct. Dyn., 5, 283–292, 1977.
9. Z. KACPRZYK and T. LEWIŃSKI, *Comparison of some numerical integration methods for the equations of motion of systems with a finite number of degrees of freedom*, Engng. Trans., **31**, 2, 213–240, 1983.
10. N.J. HOFF, *Approximate analysis of structures in the presence of moderately large creep deformation*, Q. Appl. Math., **12**, 1, 49, 1954.
11. R.E. DICK and W.H. HARRIS, *Fully automated rezoning of evolving geometry problems*, [in:] Numerical Methods in Industrial Forming Processes, pp. 243–248. Balkema, 1992.
12. J.-PH. PONTHOT, *The use of the Eulerian – Lagrangian formulation including contact: Applications to forming simulation via FEM*, [in:] Numerical Methods in Industrial Forming Processes, pp. 293–300. Balkema, 1992.

POLISH ACADEMY OF SCIENCES
INSTITUTE OF FUNDAMENTAL TECHNOLOGICAL RESEARCH

Received December 23, 1993; *new version June* 6, 1994.

Arch. Mech., 46, 5, pp. 789–795, Warszawa 1994

A counter-example to the "fundamental theorem of stochastic calculus of variations"

P. KAZIMIERCZYK (WARSZAWA)

A COUNTER-EXAMPLE is given to the statement called "the fundamental theorem of stochastic calculus of variations". The weak point of the proof of this theorem is indicated as well. The importance of the counter-example is also discussed from the point of wiew of the main application of the theorem – characterization of stationary points of "Yasue action" functionals.

1. Introduction

THE CLASSICAL calculus of variations has apparently been exceptionally useful as a unifying principle in mechanics, as well as a guide for formulation or determination of new laws of physics. To extend this powerful methodology to the class of processes important in stochastic mechanics, in particular to the class of diffusion process, a specific calculus is necessary as the sample-paths of diffusions exclude the path-wise use of common rules of differentiation and integration – the diffusion processes are defined via the Itô stochastic calculus.

In the introduction to one of the famous monographs on the classical calculus of variations ([1]), the authors emphasize that the proofs of fundamental results (like the derivation of Euler–Lagrange equation, say) require tedious, long and subtle arguments concerning the consecutive limit passages. In the case of stochastic processes, especially where the sample-wise approach is excluded, one more parameter (an element of a probability space) has to be kept under analysis and, simultaneously, the nature of the limits becomes less uniform. Moreover, a variety of probabilistic concepts of convergence can be employed. Thus, one should expect a further increase of complication in proofs of variational calculus rules.

Motivated by such a conviction, a group of theoretical mechanists asked me (a mathematician) to join their seminar devoted to the assessment of some variational results, seemingly established in the field of statistical mechanics.

One of the approaches assessed was that originated in sixties by E. NELSON – see his monograph [2], theorem 11.12. The idea was developed by K. YASUE in 1980 through three parallell publications – one ([3]) concerning just "the fundamental lemma of stochastic calculus of variations" and the consequent ([4] and [5]) employing this result to characterize the stationary points of "Yasue action" functionals. The argument of [3] was invoked indiscriminately in a series of later publications (cf. [6÷8] in [6] the name Y-E-N – Yasue–Euler–Nelson was given to the result). During the eighties the "stochastic calculus of variations" went

through many editions, and in particular, made its way into monographs (see [9], Chapter V).

It was, thus, rather an unexpected discovery that this result is false! The theorem, as it was stated in publication [3], applies to a wide family of stochastic processes including diffusions. The simplest diffusion – the Wiener process itself, is used in what follows to construct a counter-example. Although the gap in the proof is easy to notice and the example is equally easy to construct, a number of publications utilizing the false result call for an explicit communication. According to the valuable remarks of the reviewer, there exist many publications, in which additional assumptions are employed prior to the usage of the variational lemma under consideration. This work does not prove that the results of such applications of the false theorem are necessarily false: under stronger assumptions, the thesis may hold true. There exist, however, some publications, where the theorem of [3] is applied to the classical diffusions. In such cases, the counterexample that follows, constitutes a serious warning.

2. The Y-E-N Theorem

To construct a counter-example it is necessary to prove that all assumptions of the theorem considered are satisfied. Thus, the main part of the paper [3] has to be recalled. The "proof" from [3] is also cited below in order to facilitate the indication of the gap leading to the erroneous thesis. It seems probable that the knowledge of the source of error may, in future, encourage one to modify the theorem and the proof.

Let $x(t)$, $a \leq t \leq b$, be a random process defined in the probability space $(\Omega, \mathcal{A}, \Pr)$, where Ω is the totality of sample paths, $\mathcal{A}$ is a σ-algebra of measurable events, and Pr is a probability measure defined on $\mathcal{A}$.

DEFINITION. *$x(t)$, $a \leq t \leq b$, is an* (S0) *process if each $x(t)$ belongs to $L_1(\Omega, \Pr)$ and the mapping $t \mapsto x(t)$ from $\mathbb{R}$ to $L_1(\Omega, \Pr)$ is continuous.*

Let $\mathcal{P}_t$ and $\mathcal{F}_t$ be σ-algebras of measurable events generated by $\{x(u)|\ a \leq u \leq t\}$, and $\{x(u)|\ t \leq u \leq b\}$, respectively. The conditional expectation with respect to any σ-algebra $\mathcal{B} \subset \mathcal{A}$ is denoted by $E[\cdot\,|\mathcal{B}]$.

DEFINITION. *$x(t)$, $a \leq t \leq b$, is an* (S1) *process if it is an* (S0) *process such that*

$$Dx(t) = \lim_{h \to 0^+} h^{-1} E[x(t+h) - x(t)|\,\mathcal{P}_t] \tag{2.1}$$

and

$$D_\star x(t) = \lim_{h \to 0^+} h^{-1} E[x(t) - x(t-h)|\,\mathcal{F}_t] \tag{2.2}$$

exist in $L_1(\Omega, \Pr)$, and the mappings $t \mapsto Dx(t)$ and $t \mapsto D_\star x(t)$ are both continuous (from $\mathbb{R}$ to $L_1(\Omega, \Pr)$).

The totality of (S1) processes with continuous sample paths, such that $x(t)$, $Dx(t)$ and $D_\star x(t)$, $a \le t \le b$, all lie in $L_2(\Omega, \Pr)$ and are continuous functions of t in $L_2(\Omega, \Pr)$, is denoted by $L_2(\mathrm{S1})$. The main object of interest is the so-called action functional

$$I = E\left[\int_a^b L(x(t), Dx(t), D_\star x(t))\, dt\right], \tag{2.3}$$

where $L : \mathbb{R} \times \mathbb{R} \times \mathbb{R} \to \mathbb{R}$ is a smooth function playing role of the Lagrangian.

DEFINITION. *A functional $J : L_2(\mathrm{S1}) \to \mathbb{R}$ is differentiable if*

$$\begin{aligned} \delta J &= J(x(\cdot) + \delta x(\cdot)) - J(x(\cdot)) \\ &= dJ(\delta x(\cdot), x(\cdot)) + R(\delta x(\cdot), x(\cdot)) \end{aligned} \tag{2.4}$$

for any $x(\cdot)$ and $\delta x(\cdot) \in L_2(\mathrm{S1})$, where dJ is a linear functional of $\delta x(t)$, $a \le t \le b$, $R(\delta x(\cdot), x(\cdot)) = o(\|\delta x\|)$ and $\|\cdot\|$ is the $L_2(\Omega, \Pr)$-norm. The linear part dJ is called a (functional) derivative of the functional J.

Under the above assumptions, the following statement is called the fundamental theorem of stochastic calculus of variations ([3]).

THEOREM. *The action integral I is differentiable and has a derivative*

$$\begin{aligned} dI = E\Bigg[\int_a^b \left\{\frac{\partial L}{\partial x(t)} - D\left(\frac{\partial L}{\partial D_\star x(t)}\right) - D_\star\left(\frac{\partial L}{\partial Dx(t)}\right)\right\} \delta x(t)\, dt \\ + \left(\frac{\partial L}{\partial D_\star x(t)} + \frac{\partial L}{\partial Dx(t)}\right) \delta x(t)\Big|_a^b\Bigg]. \end{aligned} \tag{2.5}$$

P r o o f of the Theorem (cited in accordance with [3]). By the Taylor expansion

$$\begin{aligned} \delta I = E\Bigg[\int_a^b \Big(\frac{\partial L}{\partial x(t)}\partial x(t) + \frac{\partial L}{\partial Dx(t)} D\partial x(t) \\ + \frac{\partial L}{\partial D_\star x(t)} D_\star \delta x(t)\Big)\, dt\Bigg] + o(\|\delta x\|). \end{aligned}$$

The rest of the proof is the direct application of the following lemma – a slight modification of Theorem 11.12 of NELSON [2]. Both the original [2] and the following versions [3] were associated by the same justification (see below).

LEMMA. Let $x(t)$ and $y(t)$, $a \le t \le b$, be random processes in $L_2(\mathrm{S1})$ and $f, g : \mathbb{R} \to \mathbb{R}$ be smooth functions, then

$$E\left[f(x(t))g(y(t))\Big|_a^b\right] = E\left[\int_a^b \{g(y(t))Df(x(t) + f(x(t))D_\star g(y(t))\}\, dt\right]. \tag{2.6}$$

The proof of the lemma consists (both in [2] and [3]) of the following sequence of equalities:

$$E\left[f(x(t))g(y(t))\Big|_a^b\right] = \lim_{n\to\infty}\sum_{j=1}^{n-1} E[f(x(t_{j+1}))g(y(t_j)) - f(x(t_j))g(y(t_{j-1}))] \tag{2.7}$$

$$= \lim_{n\to\infty}\sum_{j=1}^{n-1} E[(f(x(t_{j+1})) - f(x(t_j)))\frac{1}{2}(g(y(t_j)) + g(y(t_{j-1}))) + \frac{1}{2}(f(x(t_{j+1})) + f(x(t_j)))(g(x(t_j)) - g(y(t_{j-1})))]$$

$$= \lim_{n\to\infty}\sum_{j=1}^{n-1} E[g(y(t_j))Df(x(t_j)) + f(x(t_j)) \times D_\star g(y(t_j)))](b-a)/n \tag{2.8}$$

$$= E\left[\int_a^b \{g(y(t))Df(x(t) + f(x(t))D_\star g(y(t))\}\,dt\right].$$

The weak point of the above argument is the equality between (2.7) and (2.8). Under the general assumptions of the lemma, this equality does not always hold true. The factor $(f(x(t_{j+1})) - f(x(t_j)))(b-a)/n$ is, under the expectation operator, replaced by the limit of its smoothed (conditionally averaged) value $Df(x(t_j))$ and, similarly, $(g(x(t_j)) - g(y(t_{j-1})))n/(b-a)$ is replaced by $D_\star g(y(t_j))$. However, the differences $(f(x(t_{j+1})) - f(x(t_j)))(b-a)/n - Df(x(t_j))$ and $(g(x(t_j)) - g(y(t_{j-1})))(b-a)/n - D_\star g(y(t_j))$ are not negligible when multiplied by general (possibly neither centered nor independent) factors, and when the number of such terms in the series tends to infinity. It is likely that to conclude the proof along a similar line, at least the statistical independence of processes x and y should additionally be assumed.

3. The counter-example

Let us consider the following two stochastic processes:

$$X_t(\omega) = W_t(\omega) \qquad \text{and} \qquad Y_t(\omega) = W_t^3(\omega),$$

where $\{W_t(\omega), \{\mathcal{F}_t\}, \{\mathcal{P}_t\}, t \in [0,T]\}$ is a standard Wiener process (cf. [2, 10]). It is easy to verify that both these processes belong to the class $L_2(\mathrm{S1})$. Firstly, the function $x \mapsto x^3$ is of class C^∞. Secondly, the Wiener process W is continuous both path-wise and in the mean-square sense. These properties assure that both

X and Y are (S0) processes. To see that they are also (S1) processes, it is enough to calculate

$$D\,W_t = \lim_{h\to 0^+} h^{-1}E\,[W_{t+h} - W_t \,|\, \mathcal{P}_t] = 0, \tag{3.1}$$

$$D_\star W_t = \lim_{h\to 0^+} h^{-1}E\,[W_t - W_{t-h} \,|\, \mathcal{F}_t], \tag{3.2}$$

$$D_\star W_t = \lim_{h\to 0^+} h^{-1}E\,[W_t - W_{t-h} \,|\, \sigma(W_t)] = \frac{1}{t}W_t, \tag{3.3}$$

$$D\,W_t^3 = 0, \tag{3.4}$$

$$\begin{aligned} D_\star W_t^3 &= \lim_{h\to 0^+} h^{-1}E\,[W_t^3 - W_{t-h}^3 \,|\, \mathcal{F}_t], \\ D_\star W_t^3 &= \lim_{h\to 0^+} h^{-1}E\,[W_t^3 - W_{t-h}^3 \,|\, \sigma(W_t)], \end{aligned} \tag{3.5}$$

$$D_\star W_t^3 = \lim_{h\to 0^+} h^{-1}[3h^2\frac{t-h}{t}W_t + W_t^3 h^3] = 0. \tag{3.6}$$

Equalities (3.1) and (3.4) follow from the fact that the Wiener process is of independent, Gaussian, zero mean increments. Equalities (3.2) and (3.5) follow from the Markov property. Equalities (3.3) and (3.6) can be deduced from the formulae (2.54) and (2.55) of [7] (in (2.54) the sign Δ should be replaced by ∇), but can also be derived via the following elementary calculation.

Directly from the definition of the Wiener process one knows that the probability density function of the vector $[W_t, W_s - W_t]$ is as follows:

$$p_{W_t;W_s-W_t}(a,c) = \frac{1}{2\pi\sqrt{t(s-t)}}\exp\left\{-\frac{1}{2}[a^2(s-t) + c^2 t]\right\}.$$

Thus, the probability density function of the vector $W_s - W_t$, W_s has the form

$$\begin{aligned} p_{W_s-W_t;W_s}(c,b) &= p_{W_t;W_s-W_t}(b-c,c)\begin{vmatrix} 1 & 0 \\ -1 & 1 \end{vmatrix} \\ &= \frac{1}{2\pi\sqrt{t(s-t)}}\exp\left\{-\frac{1}{2}\left[(b-c)^2(s-t) + c^2 t\right]\right\}. \end{aligned}$$

Next, using elementary operations one obtains the conditional density (the conditional distributions for Gaussian random variables are very well known; we invoke them just to show that the example can really be constructed in an elementary way):

$$\begin{aligned} p_{W_s-W_t|W_s}(c|b) &= \frac{P_{w_s-w_T;w_s}(C,B)}{\int_{-\infty}^{\infty} p_{W_s-W_t;W_s}(c,b)\,db} \\ &= \frac{1}{\sqrt{2\pi}}\sqrt{\frac{s}{t(s-t)}}\exp\left\{-\frac{1}{2}\frac{s}{t(s-t)}\left(c - b\frac{s-t}{s}\right)^2\right\}. \end{aligned}$$

Thus, one easily calculates (for a Gaussian random variable Z with mean m and variance σ^2, the mean value of Z^3 is equal to $EZ^3 = 3m\sigma^2 + m^3$)

$$E(W_s - W_t|W_s) = W_s\frac{s-t}{s}, \tag{3.7}$$

$$E((W_s - W_t)^2|W_s) = 3W_s\frac{t(s-t)^2}{s^2} + W_s^3\frac{(s-t)^3}{s^3}. \tag{3.8}$$

Formulae (3.7), (3.8) applied to (3.2) and (3.5) yield (3.3) and (3.4), respectively. The constant function 0 and the process $\frac{1}{t}W_t$ are both continuous (sample-wise and in the mean-square sense). Thus, it is evident that both processes X and Y belong to the family $L_2(S1)$.

Now, we are ready to state the counter-example. Let $f = g = Id$ (identity operator) in the lemma of Nelson and Yasue. Then, according to this lemma, one should obtain

$$E\,W_t^4|_a^b = E\,W_t^3W_t|_a^b = E\,Y_tX_t|_a^b = E\int_a^b Y_t\,D_\star X_t\,dt = E\int_a^b W_t^3\frac{1}{t}W_t\,dt. \tag{3.9}$$

But,

$$E\,W_t^4|_a^b = E[W_b^4 - W_a^4] = 3(b^2 - a^2), \tag{3.10}$$

while

$$E\int_a^b \frac{1}{t}W_t^4\,dt = \int_a^b \frac{3}{t}t^2\,dt = \frac{3}{2}(b^2 - a^2). \tag{3.11}$$

Obviously, (3.10) with (3.11) contradict (3.9). Thus, the lemma cited above is false.

To show that also the theorem is false it is enough to notice that the lemma is used directly in the proof of the theorem, and to use the same two processes X and Y: as the perturbation element $\delta x(t)$, and as the point at which the functional L is calculated. Let, for instance, the functional L be defined as follows (cf. [2÷9].

$$L(x(t),\,D\,x(t),\,D_\star x(t)) = \frac{1}{2}\left(\frac{1}{2}m|D\,x(t)|^2 + \frac{1}{2}m|D_\star x(t)|^2\right) - V(x).$$

Then, according to the proof given to the theorem in [3], the lemma should be applied, in particular, to justify the following (false) equality:

$$E\int_a^b \frac{\partial L}{\partial D_\star x(t)}\,D_\star\delta x(t)\,dt = E\left[\frac{\partial L}{\partial D_\star x(t)}\,\delta x(t)|_a^b \int_a^b D\frac{\partial L}{\partial D_\star x(t)}\,\delta x(t)\,dt\right].$$

Let $x(t) = X_t$, $\delta x(t) = \varepsilon Y_t$ (where X and Y are the processes defined above). Then

$$\frac{\partial L}{\partial D_\star x(t)} = mD_\star X_t = \frac{m}{t} X_t$$

and we arrive at exactly the same situation as the one analyzed while constructing the counter-example to the lemma. Therefore, the theorem is false.

References

1. I.M. Gelfand and S.V. Fomin, *Calculus of variations*, Prentice-Hall Inc., New Yersey 1963.
2. E. Nelson, *Dynamical theories of Brownian motion*, Princeton University Press, 1967.
3. K. Yasue, *Stochastic calculus of variations*, Lett. Math. Phys., **4**, 4, 357–360, 1980.
4. K. Yasue, *Quantum mechanics and stochastic control theory*, J. Math. Phys., **22**, 1010–1020, 1981.
5. K. Yasue, *Stochastic calculus of variations*, J. Func. Anal., **41**, 327–340, 1981.
6. J.-C. Zambrini, *Stochastic calculus of variations with constraints*, Lett. Math. Phys., **4**, 6, 457–463, 1980.
7. W.H. Fleming, *Stochastic calculus of variations and mechanics*, J. Optimiz. Th. Appl., **41**, 1, 55–74, 1983.
8. J.-C. Zambrini, *"Stochastic dynamics", A review of stochastic calculus of variations*, Intern. J. Theoretical Phys., **24**, 277–327, 1985.
9. Ph. Blanchard, Ph. Combe and W. Zheng, *Mathematical and physical aspects of stochastic mechanics*, Lect. Notes in Phys., 281, Springer-Verlag, 1987.
10. N. Ikeda and Sh. Watanabe, *Stochastic differential equations and diffusion processes*, North-Holland/Kodansha, 1981.

POLISH ACADEMY OF SCIENCES
INSTITUTE OF FUNDAMENTAL TECHNOLOGICAL RESEARCH.

Received November 8, 1993; *new version June* 6, 1994.

Arch. Mech., 46, 5, pp. 797–804, Warszawa 1994

An existence theorem of periodic travelling wave solutions to the power Kadomtsev–Petviashvili equation

Y. CHEN, J. WU (FAYETTEVILLE) and S-L. WEN (ATHENS)

THE POWER Kadomtsev–Petviashvili equation $[u_t + (n+1)(n+2)u^n u_x + u_{xxx}]_x + 3u_{yy} = 0$ is considered. The authors convert the equation into an ordinary differential equation and show the existence of nonconstant periodic travelling wave solutions using elementary arguments. An explicit solution is given for the case $n = 4$.

1. Introduction

THE KORTEWEG–DE VRIES equation is a nonlinear evolution equation governing long one-dimensional, small amplitude, surface gravity waves propagating in a shallow channel of water [1]. It arises in the study of many physical problems, such as water waves, plasma waves, lattice waves, waves in elastic rods, etc. For a general review we cite the article by MIURA [2].

A two-dimensional generalization of the Korteweg–de Vries equation is the Kadomtsev–Petviashvili equation (referred to as KP equation henceforth), which was obtained in 1970 in the study of plasmas [3]. The evolution described by the KP equation is weakly nonlinear, weakly dispersive, and weakly two-dimensional, with all three effects being of the same order. The KP equation has also been proposed as a model for the surface waves and internal waves in channels of varying depth and width [4]. In this paper the authors consider the power KP equation of the form

$$[u_t + (n+1)(n+2)u^n u_x + u_{xxx}]_x + 3u_{yy} = 0, \tag{1.1}$$

where n is a positive integer. Equation (1.1) reduces to the KP equation when $n = 1$, and the modified KP equation when $n = 2$. In this paper, we shall prove an existence theorem of nonconstant periodic travelling wave solution to the power KP equation for $n > 2$ using elementary methods. It should be noted that nonconstant periodic travelling wave solutions to the KP ($n = 1$) and modified KP ($n = 2$) equations have been discussed by two of the authors [5, 6]. The drawbacks in using functional analysis methods to prove existence theorems seem to involve more restrictions on the solution u and its derivatives (see Theorem 4 in Ref. [6], for example). The approach of this paper follows more or less the line used in Ref. [5]. As in Ref. [5], we shall also establish a criterion for the existence of a single soliton solution, namely, $C = (a\omega - 3b^2)/a^2 > 0$.

The plan of the paper is as follows. In Sec. 2, we reduce the study of Eq. (1.1) to that of a second order ordinary differential equation. The existence of solitary

wave solutions is discussed in Sec. 3 and the existence of periodic traveling wave solutions for $n > 2$ is proved in Sec. 4. A special case ($n = 4$) is incluced as an example which gives an explicit periodic solution. The results we have obtained here seem to be new.

2. Formulation of the problem

We consider a power KP equation of the form [3, 5]

$$[u_t + (n+1)(n+2)u^n u_x + u_{xxx}]_x + 3u_{yy} = 0, \tag{2.1}$$

where $u = u(x, y, t)$ is a function of x, y and t. We look for real-valued solutions of the form $U(\xi) = u(x, y, t)$, where $\xi = ax + by - \omega t$ with a, b and ω being real constants. Without loss of generality we assume $a > 0$. Equation (2.1) can thus be written as

$$-(a\omega - 3b^2)U'' + a^2(n+1)(n+2)(U^n U')' + a^4 U^{(4)} = 0. \tag{2.2}$$

Integration of both sides of Eq. (2.2) twice with respect to ξ yields

$$-(a\omega - 3b^2)U + a^2(n+2)U^{n+1} + a^4 U'' = A\xi + Ba^2, \tag{2.3}$$

where A and B are integration constants.

3. Existence of solitary wave solutions

Seeking a solitary wave solution, we impose the boundary conditions U, U', U'', and $U''' \to 0$ as $\xi \to \pm\infty$. These yield $A = B = 0$ in Eq. (2.3). In view of $U''(\xi) = \dfrac{1}{2}\dfrac{d[U']^2}{dU}$, we obtain

$$\frac{1}{2}[U'(\xi)]^2 = \frac{1}{a^2}\left[-U^{n+2}(\xi) + \frac{C}{2}U^2(\xi)\right], \tag{3.1}$$

where $C = (a\omega - 3b^2)/a^2$.

There are three cases to consider:

First, if $C < 0$, a nonconstant real solution to Eq. (3.1) exists only when n is odd, and the solution is

$$U(\xi) = \left\{\frac{C}{2}\sec^2\left[\frac{n\sqrt{-C}}{2a}(\xi - \xi_0)\right]\right\}^{1/n},$$

where ξ_0 is an integration constant.

Second, if $C = 0$, a nonconstant real solution to Eq. (3.1) exists also only when n is odd, and the solution is

$$U(\xi) = \frac{1}{\{(n^2/2a^2)(\xi - \xi_0)^2\}^{1/n}}.$$

Clearly, the solutions of these two cases are unbounded, and therefore, they are not of much physical interest.

Third, if $C > 0$, we have the solitary wave solution to Eq. (3.1) as

$$U(\xi) = \left\{ \frac{C}{2} \operatorname{sech}^2 \left(\frac{n\sqrt{C}}{2a} (\xi - \xi_0) \right) \right\}^{1/n}.$$

We note that $C > 0$ gives a condition under which a nontrivial solitary wave solution exists. This condition indicates a relationship that must be satisfied by the wave numbers a, b and the frequency ω, namely, $a\omega > 3b^2$, for the existence of nonconstant solitary wave solutions. On the other hand, if $a\omega \leq 3b^2$, either no real solution exists or the solutions are unbounded.

4. Existence of periodic wave solutions

To obtain bounded solutions we assume $A = 0$ in Eq. (2.3). Then we have from Eq. (2.3)

$$\frac{1}{2}U'^2 = \frac{1}{a^2}\left(-U^{n+2} + \frac{C}{2}U^2 + BU + D\right) = \frac{1}{a^2}F(U), \tag{4.1}$$

where $C = (a\omega - 3b^2)/a^2$ and D is an integration constant. The Eq. (4.1) leads to

$$\frac{\sqrt{2}}{a}d\xi = \frac{dU}{\sqrt{F(U)}}. \tag{4.2}$$

For the existence of periodic solutions the zeros of the polynomial $F(U)$ on the right-hand side of Eq. (4.1) play an important role. The polynomial $F(U)$ has at most four terms. When n is odd, the number of variations in signs occuring in the coefficients of $F(U)$ and $F(-U)$ is at most three, and when n is even, the number of variations is at most four. Therefore, $F(U)$ has at most three real zeros if n is odd and at most four real zeros if n is even.

If n is odd, applying a similar argument as that given in the Appendix A of [5], we can see that $F(U) \geq 0$ when $F(U)$ has three distinct real simple zeros $U_1 > U_2 > U_3$ and $U_1 \geq U \geq U_2$, where U_1 is a simple maximum and U_2 is a simple minimum of U.

Furthermore, $U' = \left(\sqrt{2}/a\right)\sqrt{F(U)}$, and $\sqrt{F(U)}$ changes its sign when U goes on a path of an infinitesimal circle around the point U_1 or U_2 in the complex U-plane. This implies that U' changes its sign at U_1 and U_2. Hence, $U(\xi)$ is periodic. In this case $U(\xi)$ can be obtained from the integral equation

$$\frac{\sqrt{2}}{a}(\xi - \xi_1) = \int_U^{U_1} \frac{dU}{\sqrt{F(U)}}, \tag{4.3}$$

where $U(\xi_1) = U_1$. And the period T in ξ is given by

$$T = \sqrt{2}a \int_{U_2}^{U_1} \frac{dU}{\sqrt{F(U)}}. \tag{4.4}$$

It should be noted here that there is no restriction on C which can be positive, zero, or negative.

If n is even, periodic solutions to Eq. (4.1) exist in the following four cases:

1. $F(U)$ has only two simple real zeros $U_1 > U_2$. Equation (4.1) has a periodic real solution $U(\xi)$ which can be obtained from the integral equation (4.3) with period T in ξ given by Eq. (4.4).

2. $F(U)$ has real zeros $U_1 > U_2 > U_3$ with U_3 being a double zero. Equation (4.1) has a periodic real solution $U(\xi)$ such that $U_2 \leq U \leq U_1$, and $U(\xi)$ can also be obtained from Eq. (4.3) with the period T in ξ given by Eq. (4.4).

3. $F(U)$ has real zeros $U_1 > U_3 > U_4$ with U_1 being a double zero. Equation (4.1) has then a periodic real solution $U(\xi)$ such that $U_4 \leq U \leq U_3$, and $U(\xi)$ is given by the integral equation

$$\frac{\sqrt{2}}{a}(\xi - \xi_3) = \int_U^{U_3} \frac{dU}{\sqrt{F(U)}}, \tag{4.5}$$

where $U(\xi_3) = U_3$. The period T in ξ is given by

$$T = \sqrt{2}a \int_{U_4}^{U_3} \frac{dU}{\sqrt{F(U)}}. \tag{4.6}$$

4. $F(U)$ has four distinct real simple zeros such that $U_1 > U_2 > U_3 > U_4$. Since $F(U) = -U^{n+2} + (C/2)U^2 + BU + D$, it can be shown that when $U_4 \leq U \leq U_3$ or $U_2 \leq U \leq U_1$, we have $F(U) \geq 0$.

First, if $U_2 \leq U \leq U_1$, U_1 is a simple maximum and U_2 is a simple minimum of U. U' changes its sign at U_1 and U_2, and hence, $U(\xi)$ is periodic. $U(\xi)$ thus can be obtained from Eq. (4.3) with the period T given by Eq. (4.4).

Second, if $U_4 \leq U \leq U_3$, then similarly, U' changes its sign at simple maximum U_3 and simple minimum U_4, and hence $U(\xi)$ is periodic. In this case, $U(\xi)$ can be obtained from Eq. (4.5) with T given by Eq. (4.6).

It should be noted that in the Case 1 when $F(U)$ has only two simple real zeros, there is no restriction on C which can be positive, zero, or negative. In the Cases 2, 3, and 4, in order to have $F(U) \geq 0$ when $U_3 \geq U \geq U_4$ or $U_1 \geq U \geq U_2$, and therefore have periodic wave solutions, the coefficient C must be positive. Thus, similarly to the solitary wave solution, we note that $C > 0$ gives a condition under which a nontrivial periodic wave solution exists when $F(U)$ has more than two simple zeros and n is even. This condition indicates a relationship that must be satisfied by the wave numbers a, b and the frequency ω, namely, $a\omega > 3b^2$, for the existence of nontrivial periodic solutions.

EXAMPLE. Let $n = 4$ and assume $B = 0$. If $F(U)$ has four real zeros, it must be the case $U_1 > U_2 > U_3 > U_4$ with $U_4 = -U_1$ and $U_3 = -U_2$ because $F(U)$ is an even function. We choose $U_1 \geq U \geq U_2$, a solution of Eq. (4.1) can then be written as

$$\frac{\sqrt{2}}{a}(\xi - \xi_1) = \int_{U_2}^{U} \frac{dU}{\sqrt{-U^6 + (C/2)U^2 + D}}. \tag{4.7}$$

Let $z(\xi) = U^2(\xi)$, then $dU = dz/(2\sqrt{z})$, and hence

$$\frac{\sqrt{2}}{a}(\xi - \xi_1) = \frac{1}{2}\int_{Z_2}^{Z} \frac{dz}{\sqrt{z(-z^3 + (C/2)z + D)}}. \tag{4.8}$$

It is shown in Appendix that the function $G(z) = z(-z^3 + (C/2)z + D)$ has four distinct real zeros $Z_1 = U_1^2 > Z_2 = U_2^2 > Z_3 = 0 > Z_4 = -(U_1^2 + U_2^2)$ and $Z_1 \geq z \geq Z_2$. Therefore, the function $z(\xi)$ can be obtained as

$$z(\xi) = \frac{Z_2}{1 - \beta \mathrm{sn}^2\left[(\sqrt{2}\alpha/a)(\xi - \xi_1), r\right]},$$

and hence,

$$U(\xi) = \frac{U_2}{\sqrt{1 - \beta \mathrm{sn}^2\left[\frac{\sqrt{2}\alpha}{a}(\xi - \xi_1), r\right]}},$$

where

$$\alpha = \sqrt{Z_1(Z_2 - Z_4)} = U_1\sqrt{U_1^2 + 2U_2^2},$$

$$\beta = \frac{Z_1 - Z_2}{Z_1} = \frac{U_1^2 - U_2^2}{U_1^2},$$

and

$$r = \sqrt{-\frac{(Z_1 - Z_2)Z_4}{Z_1(Z_2 - Z_4)}} = \sqrt{\frac{U_1^4 - U_2^4}{U_1^2(U_1^2 + 2U_2^2)}}.$$

Therefore, $U(\xi)$ can be written as

$$\begin{aligned} U(\xi) &= \frac{U_2}{\sqrt{1 - \frac{U_1^2 - U_2^2}{U_1^2}\mathrm{sn}^2\left[\frac{\sqrt{2}\alpha}{a}(\xi - \xi_1), r\right]}} \\ &= \frac{U_1 U_2}{\sqrt{U_1^2 - (U_1^2 - U_2^2)\mathrm{sn}^2\left[\frac{\sqrt{2}\alpha}{a}(\xi - \xi_1), r\right)}} \\ &= \frac{U_1 U_2}{\sqrt{U_2^2 + (U_1^2 - U_2^2)\mathrm{cn}^2\left[\frac{\sqrt{2}\alpha}{a}(\xi - \xi_1), r\right)}}. \end{aligned}$$

Since $U_1^2 > U_2^2 > 0$, it is easy to see that $U(\xi)$ is a bounded periodic solution.

Appendix

Since the function $F(U) = -U^6 + (C/2)U^2 + D$ has four distinct real solutions $U_1 > U_2 > U_3 > U_4$ with $U_4 = -U_1$ and $U_3 = -U_2$, it can be written as

$$\begin{aligned} F(U) &= (U_1^2 - U^2)(U^2 - U_2^2)(U^2 + MU + N) \\ &= -U^6 - MU^5 + (U_1^2 + U_2^2 - N)U^4 + (U_1^2 + U_2^2)MU^3 \\ &\quad + \left[(U_1^2 + U_2^2)N - U_1^2 U_2^2\right] U_2^2 - U_1^2 U_2^2 MU - U_1^2 U_2^2 N. \end{aligned}$$

Because the coefficients of U^5, U^4, U^3 and U must be zero, we have $M = 0$, $N = U_1^2 + U_2^2 > 0$, $C/2 = U_1^4 + U_1^2 U_2^2 + U_2^4 > 0$, and $D = -U_1^2 U_2^2 N < 0$. Therefore, $F(U)$ must have a pair of conjugate imaginary zeros $U_5 = i\sqrt{U_1^2 + U_2^2}$ and $U_6 = -i\sqrt{U_1^2 + U_2^2}$.

Let $G(z) = z(-z^3 + (C/2)z + D)$. Since $z = U^2$, the polynomial $G(z)$ has four distinct real zeros $Z_1 = U_1^2$, $Z_2 = U_2^2$, $Z_3 = 0$, $Z_4 = -(U_1^2 + U_2^2)$, and

$Z_1 \geq z \geq Z_2$. Thus, Eq. (4.8) can be written as [7, 8]

$$\frac{\sqrt{2}}{a}(\xi - \xi_1) = \frac{1}{2}\int_{Z_2}^{z} \frac{z}{\sqrt{z(-z^3 + (C/2)z + D}}$$

$$= \frac{1}{2}\int_{Z_2}^{z} \frac{dz}{\sqrt{(Z_1 - z)(z - Z_2)(z - Z_3)(z - Z_4)}}$$

$$= \frac{1}{\sqrt{(Z_1 - Z_3)(Z_2 - Z_4)}} F(\lambda, r),$$

where $F(\lambda, r) = \mathrm{sn}^{-1}(\sin\lambda, r)$ is the normal elliptic integral of the first kind with modulus r,

$$\lambda = \arcsin\sqrt{\frac{(Z_1 - Z_3)(z - Z_2)}{(Z_1 - Z_2)(z - Z_3)}}$$

and

$$r^2 = \frac{(Z_1 - Z_2)(Z_3 - Z_4)}{(Z_1 - Z_3)(Z_2 - Z_4)}.$$

Let $\alpha = \sqrt{(Z_1 - Z_3)(Z_2 - Z_4)} = \sqrt{Z_1(Z_2 - Z_4)}$, $\beta = \dfrac{Z_1 - Z_2}{Z_1 - Z_3} = \dfrac{Z_1 - Z_2}{Z_1}$, and $\nu = F(\lambda, r) = \dfrac{\sqrt{2}\alpha}{a}(\xi - \xi_1)$, then we obtain

$$z(\xi) = \frac{Z_2 - \beta Z_3 \mathrm{sn}^2(\nu, r)}{1 - \beta \mathrm{sn}^2(\nu, r)} = \frac{Z_2}{1 - \beta \mathrm{sn}^2(\nu, r)}.$$

Thus, the solution to Eq. (4.1) becomes

$$U(\xi) = \frac{U_2}{\sqrt{1 - \beta \mathrm{sn}^2(\nu, r)}},$$

where $\mathrm{sn}(\nu, r) = \sin\lambda$.

References

1. D.J. KORTEWEG and G. DEVRIES, *On the change of form of long waves advancing in a rectangular canal, and on a new type of long stationary waves*, Philosophical Magazine, **39**, 422–443, 1895.
2. R.N. MIURA, *The Korteweg–deVries equation; a survey of results*, SIAM Rev., **18**, 412–459, 1976.
3. B.B. KADOMTSEV and V.I. PETVIASHVILI, *On the stability of solitary waves in weak dispersing media*, Soviet. Phys. Dokl., **15**, 6, 539–541, 1970.
4. P.M. SANTINI, *On the evolution of two-dimensional packets of water waves over an uneven bottom*, Lett. Nuovo Cimento, **30**, 236–240, 1981.
5. YUNKAI CHEN and SHIH-LIANG WEN, *Travelling wave solutions to the two-dimensional Korteweg–de Vries equation*, J. Math. Anal. and Appl., **127**, 1, 226–236, 1987.

6. YUNKAI CHEN and SHIH-LIANG WEN, *On existence theorems of periodic travelling wave solutions to the two-dimensional Korteweg–de Vries equation*, Applicable Analysis, **31**, 1–10, 1988.
7. I.S. GRADSHIEYN and I.K. RYZHIK, *Tables of integrals, series and products*, Academic Press, New York-London 1965.
8. P.F. BYRD and M.D. FRIEDMAN, *Handbook of elliptic integrals for engineers and scientists*, 2nd ed., Springer Verlag, New York-Berlin 1971.

DEPARTMENT OF MATHEMATICS AND COMPUTER SCIENCE
FAYETTEVILLE STATE UNIVERSITY, FAYETTEVILLE, NC, USA,
DEPARTMENT OF NATURAL SCIENCES
FAYETTEVILLE STATE UNIVERSITY, FAYETTEVILLE, NC, USA
and
DEPARTMENT OF MATHEMATICS
OHIO UNIVERSITY, ATHENS, OHIO, USA.

Received June 29, 1994.

Arch. Mech., 46, 5, pp. 805–810, Warszawa 1994

BRIEF NOTES

Mechanical modelling of domain patterns in strained epitaxy of thin films (*)

W. POMPE, M. SEMSCH (DRESDEN),
H. BALKE and K. BRÄMER (CHEMNITZ)

IN THIS PAPER we analyse the stability of domain patterns of single crystalline tetragonal films on single crystalline cubic substrates. Two parts of the total energy of the domain patterns are considered: the elastic relaxation energy and the twin energy of the domain walls. It is shown by means of a three-dimensional elastic FEM-analysis that square domain patterns have energy minima with smaller values than the stripe patterns. Therefore, the square patterns are energetically favoured over the stripe patterns.

1. Introduction

TODAY, NEW TECHNIQUES allow for the manufacturing of polycrystalline and single-crystal thin films on single-crystal substrates. The substrates are coated with a precursor film and subsequently heated. If the film and the substrate structure are very similar, single-crystal films can form [1]. Lattice misfit causes twin domain patterns in the film [2]. However, from a theoretical point of view, different twin domain patterns are possible. Here we consider square (shear) domain patterns of a tetragonal film on a cubic substrate. We calculate the normalized total average energy change of the pattern formation as a function of the domain size. Stable domain patterns are expected for relative minima of this energy.

2. Type of domain patterns

We consider two possible arrangements of tetragonal film crystals on a cubic substrate (Fig. 1). In both cases the lattice axes with the lattice parameters a and c, of the film crystals lie in the directions of the coordinates x or y. The crystal axes of the cubic substrate with the lattice parameter b are parallel to the coordinate axes x, y and z. The two arrangements differ in their c-directions. For the a_1-domain the c-direction is parallel to the x-axis and perpendicular to the c-direction of the a_2-domain.

(*) Paper presented at the 6th Polish-German Symposium on "Mechanics of Inelastic Solids and Structures".

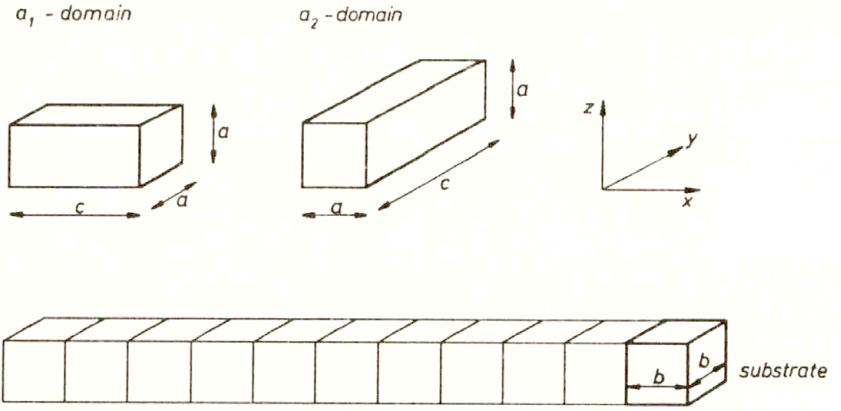

FIG. 1. Possible arrangements of a_1- and a_2-domains.

In our model the twin walls between the a_1- and a_2-domains are taken to be orthogonal to the interface and inclined by 45° to the x-coordinate (square pattern in Fig. 2a). In Fig. 2b the arrangement of the stripe a_1-a_2-pattern is also given. It is needed for the comparison of our results with the conclusion of [2].

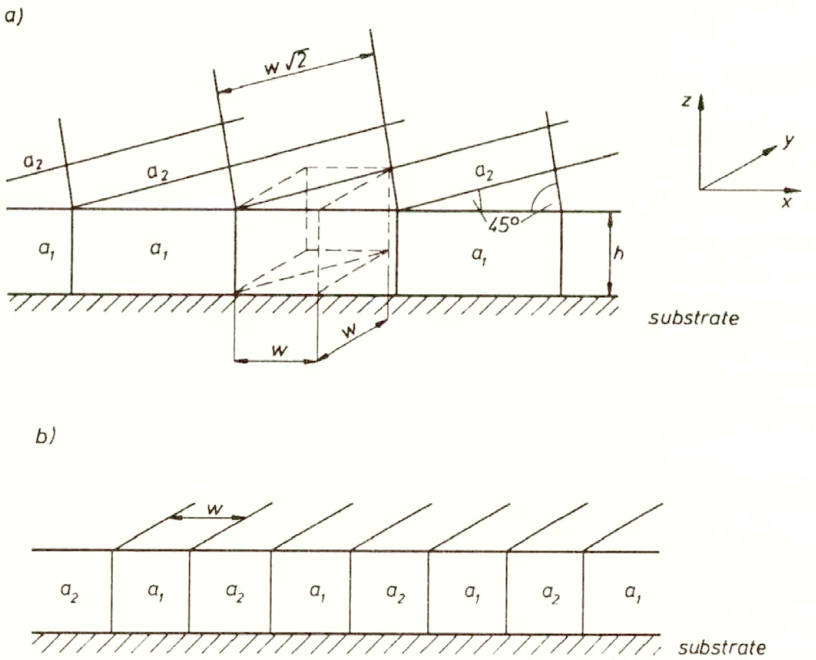

FIG. 2. Types of domain patterns, a) square, b) stripe.

In both arrangements film thickness and domain width are denoted by h and w, respectively.

3. Square a_1-a_2-pattern

In the initial state the thin film is homogeneously strained by the misfit strains ε_a and ε_c

$$\varepsilon_a = \frac{b-a}{b}, \qquad \varepsilon_c = \frac{b-c}{b}, \tag{3.1}$$

and stressed by

$$\sigma_x = \frac{E}{1-\nu^2}(\varepsilon_a + \nu\varepsilon_c), \qquad \sigma_y = \frac{E}{1-\nu^2}(\varepsilon_c + \nu\varepsilon_a), \tag{3.2}$$

E – Young's modulus, ν – Poisson's ratio (Fig. 3a).

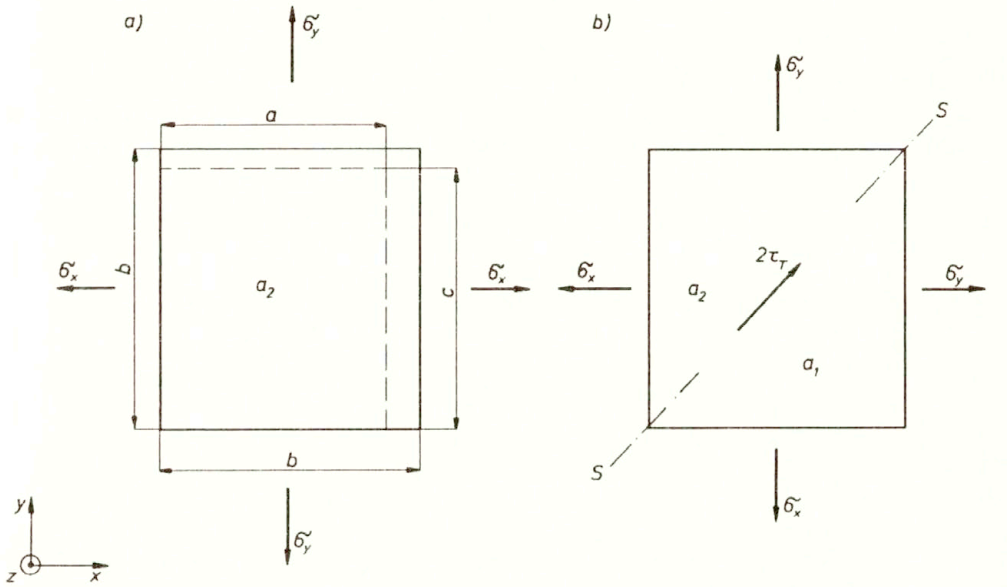

FIG. 3. Eigen-stresses in the film, a) a_2-domain, b) square with a_1- and a_2-quarter domain before relaxation of the external shear traction $2\tau_T$.

In the presence of a twin boundary on the internal diagonal plane parallel to the line SS and the z-axis, the lattice orientation in the lower part of the square is rotated by 90° around the z-axis. For maintaining the static equilibrium, an external shear traction

$$2\tau_T = \frac{E}{1+\nu}\varepsilon_T, \qquad \varepsilon_T = \varepsilon_a - \varepsilon_c, \tag{3.3}$$

is applied at the internal diagonal plane (Fig. 3b). The elastic relaxation of this traction provides the energy available for transformation to twin energy.

4. Domain energy

The total energy change in a square a_1-a_2-domain is the sum of the released elastic energy U and the twin energy of the domain wall U_γ

$$U_{\text{total}} = U + U_\gamma, \tag{4.1}$$

where U is the difference between the stored elastic energy of the final state with the twinned square pattern U_{fin} and the stored elastic energy of the initial stress state in the film U_{in} with $U = U_{\text{fin}} - U_{\text{in}}$.

The size of the square a_1-a_2-domain amounts to w^2. Therefore the total average energy change per domain size w^2, normalized by $hE\varepsilon_T^2$, is

$$\overline{U}_{\text{total}} = \frac{U + \gamma h w\sqrt{2}}{w^2 h E \varepsilon_T^2}, \tag{4.2}$$

where γ is the specific wall energy.

If we neglect the coupling of one individual domain to its surroundings, we obtain a rough analytical estimate of a lower limit for the released energy

$$U > -\frac{1}{2} \cdot \frac{2(1+\nu)}{E} \tau_T^2 w^2 h = -\frac{w^2 h E \varepsilon_T^2}{4(1+\nu)}.$$

Upon substituting this into (4.2) we have

$$\overline{U}_{\text{total}} > -\frac{1}{4(1+\nu)} + \frac{\gamma\sqrt{2}}{hE\varepsilon_T^2} \cdot \frac{h}{w}$$

with

$$\overline{U}_{\text{total}} \to \infty \qquad \text{for} \quad \frac{w}{h} \to 0.$$

For $h \ll w$, the elastically relaxed volume is in the order of magnitude of wh^2. Therefore $\overline{U}_{\text{total}}$ from (4.2) tends to zero for $w/h \to \infty$.

The three-dimensional finite element model gives a more precise result. A triangular prism with a height of about $3\sqrt{2}w$ was modelled [3]. The upper boundary was free. In order to get bounds for the released energy, the lower boundary was taken free or clamped. At the lateral faces the normal displacements and the shear stresses were equal to zero except for the shear loaded part of the size $hw\sqrt{2}$ of the diagonal face, see Fig. 2a and 3b. Various meshes composed of 8 nodal points elements were used. The number of degrees of freedom was about 16 000.

In Fig. 4 the normalized total average energy change per domain size w^2 is shown as a function of w/h for different specific wall energies $\gamma/E\varepsilon_T^2 h$. We can find an equilibrium domain energy minimum and an equilibrium domain width for any film thickness.

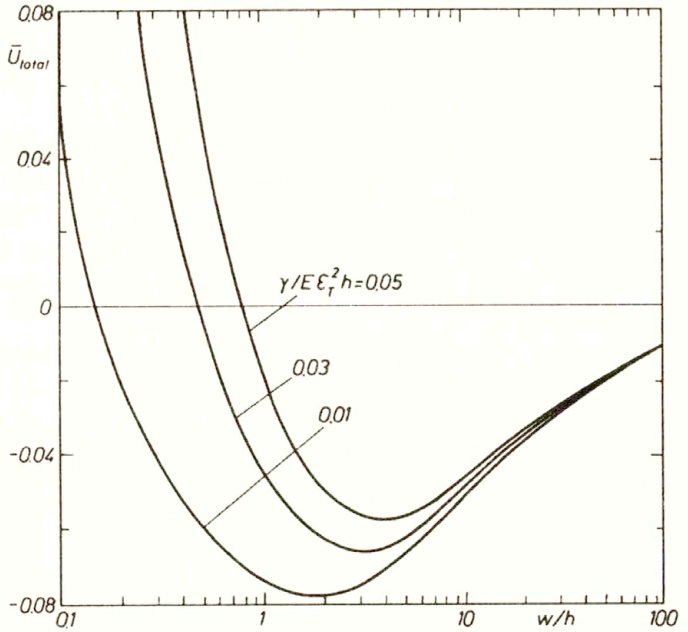

FIG. 4. Normalized total average energy change of the square domain pattern after (4.2) as a function of the normalized domain width ($\nu = 0.32$).

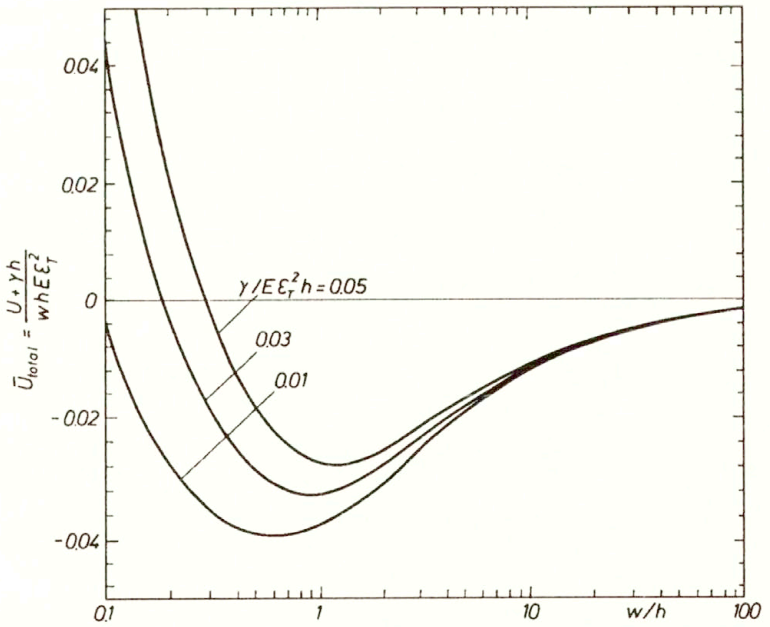

FIG. 5. Normalized total average energy change of the stripe domain pattern after [2] as a function of the normalized domain width (here, U is the released energy per unit length, $\nu = 0.3$).

5. Comparison of the domain energies

In [2] the total average energy change per unit length and domain size w, normalized by $hE\varepsilon_T^2$, was calculated for the stripe a_1-a_2-domain patterns. The result is plotted in Fig. 5. By comparison of Fig. 4 with Fig. 5 we see that the equilibrium energy of the square domain patterns is smaller than the equilibrium energy of the stripe domain patterns by a factor of about two. Therefore the square patterns are energetically favoured.

Acknowledgement

We would like to thank Professor F.F. LANGE for the initiation of this work and Professor J.S. SPECK for the fruitful exchange of ideas.

References

1. A. SEIFERT, F.F. LANGE and J.S. SPECK, *Liquid precursor route for heteroepitaxy of $Zr(Y)O_2$ thin films on (001) cubic zirconia*, J. Am. Ceram. Soc., **76**, 443–448,1993.
2. W. POMPE, X. GONG, Z. SUO and J.S. SPECK, *Elastic energy release due to domain formation in the strained epitaxy of ferroelectric and ferroelastic films*, J. Appl. Phys., **74**, 6012–6019, 1993.
3. Swanson Analysis Systems, ANSYS, Revision 4.4.A 1990.

MAX-PLANCK RESEARCH GROUP "MECHANICS OF HETEREOGENEOUS SOLIDS" DRESDEN,
TECHNICAL UNIVERSITY DRESDEN,
and
TECHNICAL UNIVERSITY CHEMNITZ-ZWICKAU, GERMANY.

Received January 3, 1994; *new version July* 6, 1994.

Centre International des Sciences Mecaniques

International Centre for Mechanical Sciences

PRELIMINARY PROGRAMME 1995

Courses

New Design Concepts for High Speed Air Transport
Coordinator: H. Sobieczky (Göttingen) — June 5 - 9, 1995

Bone Cell and Tissue Mechanics
Coordinator: S.C. Cowin (New York) — July 10 - 14, 1995

Liquid Bridge Theory and Applications
Coordinator: J. Meseguer (Madrid) — July 17- 21, 1995

Mathematical Modelling for Arch Dam design and Safety Control
Coordinators: M. E.R. de Arantes e Oliveira, J.O. Pedro (Lisboa) — Sept. 4 - 8, 1995

Mechanics of Solids with Phase Changes
Coordinators: M. Berveiller (Metz), F.D. Fischer (Leoben) — Sept. 11 - 15, 1995

Modelling and Simulation of Hypersonic Flows for Spatial Flights
Coordinator: R. Brun (Marseille) — Sept. 18 - 22, 1995

Control of Flow Instabilities and Unsteady Flows
Coordinators:
G.E.A. Meier (Göttingen), G.H. Schnerr (Karlshruhe) — Sept. 18 - 22, 1995

Advanced Methods of Tunnelling
Coordinator: K. Kovari (Zürich) — Sept. 25 - 29, 1995

Earthquake Resistant Design
Coordinator: R.T. Duarte (Lisboa) — Oct. 2 - 6, 1995

The Flow of Particles in Suspension
Coordinator: G. Cognet (Grenoble) — Oct. 9 - 13, 1995

Meetings Hosted by CISM

Workshop on "Multimedia GIS Data"
International Society for Photogrammetry and Remote Sensing – Commission I
Coordinators: R. Galetto (Pavia), F. Crosilla (Udine) — June 12 - 16, 1995

10th International Conference on Artifical Intelligence in Engineering
Chairmen: C.A. Brebbia (Southampton), C. Tasso (Udine) — July 4 - 6, 1995

Additional and more detailed information will be available in November 1994

I-33100 Udine (Italy), Palazzo del Torso, Piazza Garibaldi, 18
Tel: + 39 0432 - Secretariat 294989 or 508251 - Administration 294795 - Printing Office 45533 - Fax 501523
Partita I.V.A. 00401650304

Computer Assisted Mechanics and Engineering Sciences (CAMES)

to be published quarterly starting in 1994

Editor: M. Kleiber, Warsaw Associate Editor: H.A. Mang, Vienna

Scope of the Journal

Computer Assisted Mechanics and Engineering Sciences (CAMES) is a refereed international journal, published quarterly, providing an international forum and an authoritative source of information in the field of computational mechanics and related problems of applied science and engineering.

The specific objective of the journal is to support researchers and practitioners based in Central Europe by offering them a means facilitating (a) access to newest research results by leading experts in the field (b) publishing their own contributions and (c) dissemination of information relevant to the scope of the journal.

Papers published in the journal will fall largely into three main categories. The first will contain state-of-the-art reviews with the emphasis on providing the Central European readership with a guidance on important research directions as observed in the current world literature on computer assisted mechanics and engineering sciences.

The second category will contain contribution presenting new developments in the broadly understood field of computational mechanics including solid and structural mechanics, multi-body system dynamics, fluid dynamics, constitutive modeling, structural control and optimization, transport phenomena, heat transfer, etc. Variational formulations and numerical algorithms related to implementation of the finite and boundary element methods, finite difference method, hybrid numerical methods and other methodologies of computational mechanics will clearly be the core areas covered by the journal.

The third category will contain articles describing novel applications of computational techniques in engineering practice; areas of interest will include mechanical, aerospace, civil, naval, chemical and architectural engineering as well as software development.

The journal will also publish book reviews and information on activities of the Central European Association of Computational Mechanics.

Subscription and sale of single issues is managed by the Editorial Office.
Price of single issue: 25 USD (in Poland: 40 000 zł)

Address: Editorial Office, CAMES
Polish Academy of Sciences
Institute of Fundamental Technological Research
ul. Świętokrzyska 21, PL 00-049 Warsaw, Poland
Our Bankers: IV Oddz. Pekao SA Warszawa 501132-40054492-3111

INTERNATIONAL CONFERENCE
ON LIGHTWEIGHT STRUCTURES
IN CIVIL ENGINEERING

25–29 September, 1995
WARSAW, POLAND

The Conference is aimed at bringing together leading researches and practitioners in the fields of structural analysis and design, architecture, construction and all related subjected pertinent to rationally designed and executed civil engineering and building structures. In particular, it is intended that the following topics be included: spatial lattice structures, plate and shell structures, domes and membranes, high-rise buildings, towers, reservoirs, bridges, cable and pneumatic structures. The Conference will provide a forum for discussion of the current state-of-the-art in the fields of metal, reinforced concrete, timber, prestressed, composite and textile structures. Presentations of analytical, numerical and experimental techniques relevant to the computer-aided design will also be welcomed, including the finite element method.

Further information may be obtained from:

Prof. Jan B. Obrębski
Warsaw University of Technology
Faculty of Civil Engineering
Institute of Structural Mechanics
Al. Armii Ludowej 16, p.144
00–637 Warsaw, Poland

INSTITUTE OF FUNDAMENTAL TECHNOLOGICAL RESEARCH
is publishing the following periodicals:

ARCHIVES OF MECHANICS — bimonthly (in English)
JOURNAL OF TECHNICAL PHYSICS — quarterly (in English)
ARCHIVES OF ACOUSTICS — quarterly (in English)
ENGINEERING TRANSACTION — quarterly (in English)
ADVANCES IN MECHANICS — quarterly (in English)
ARCHIVES OF CIVIL ENGINEERING — quarterly (in English)

Subscription orders for all the magazines published in Poland available trought the local press distributors or directly trought the *Foreign Enterprise ARS POLONA*, Krakowskie Przedmieście 7, 00-068 Warszawa, Poland.

Adress of the Editorial Office:

Institute of Fundamental Technological Research,
Świętokrzyska 21, p. 508,
00-049 WARSZAWA, Poland.

DIRECTIONS FOR THE AUTHORS

The periodical *ARCHIVES OF MECHANICS (ARCHIWUM MECHANIKI STOSOWANEJ)* deals with the printing of original papers which should not appear in any other publications. The authors may publish in the Bull. Acad. Polon. Sci. short papers only, announcing the solutions of any problems as well as informing that the full text will be inserted in the columns of the *ARCHIVES OF MECHANICS (ARCHIWUM MECHANIKI STOSOWANEJ)*.

As a rule, the volume of a paper should not exceed 40 000 typographic signs, that is about 20 type-written pages, format: 210 × 297 mm, leaded. The papers should be submitted in two copies. They must be set in accordance with the norms established by the Editorial Office. Special importance is attached to the following directions:

1. The title of the paper should be as short as possible.

2. The text should be preceded by a brief introduction; it is also desirable that a list of notations used in the paper be given.

3. Short papers should be divided into sections and subsections, long papers into sections, subsections and points. Each section, subsection or point must bear a title.

4. The formula number consists of two figures: the first represents the section number and the other the formula number under that section. Thus the division into subsections does not influence the numbering of formulae. Only such formulae should be numbered to which the author refers throughout the paper, also the resulting formulae. The formula number should be written on the left-hand side of the formula; brackets are to be only to avoid any misunderstanding. For instance, if the author refers to formula 3 of the set (2.1), a subscript should be added to denote the set of formula, viz. $(2.1)_3$.

5. All the notations should be written very distinctly. Special care must be taken to write small and capital letters as precisely as possible. Semi-bold type must be underlined in black pencil. Explanations should be given on the margin of the manuscript in case of special type face.

6. It has been established to denote vectors semi-bold type, transforms of the corresponding functions by tilded symbols. Trigonometric functions are denoted by sin, cos, tg and ctg, inverse functions – by arc sin, arc cos, arc tg and arc ctg; hyperbolic functions are denoted by sh, ch, th and cth, inverse functions – by Arsh, Arch, Arth and Arcth.

7. Figures in brackets denote reference titles. Items appearing in the reference list should include the initials of the Christian name of the author and his surname, also the full title of the paper (in the language of the original paper); moreover;

a) in the case of books, the publisher's name, the place and year of publication should be given, e.g.,
5. S. Ziemba, *Vibration analysis*, PWN, Warszawa 1970;

b) in the case of a periodical, the full title of the periodical, consecutive volume number, current issue number, pp. from ... to ..., year of publication should be mentioned; the annual volume number must be marked in black pencil so as to distinguish it from the current issue number, e.g.,
6. M. Sokołowski, *A thermoelastic problem for a strip with discontinuous boundary conditions*, Arch. Mech., **13**, 3, 337–354, 1961.

8. The authors should enclose a summary of the paper. The volume of the summary is to be about 100 words.

9. If the paper is to be translated into another language than that of the manuscript, the author is requested to include a glossary of special terms.

Upon receipt of the paper, the Editorial Office forwards it to the reviewer. His opinion is the basic for the Editorial Committee to determine whether the paper can be accepted for publication or not.

The printing of the paper completed, the author receives 25 copies of reprints free of charge. The authors wishing to get more copies should advise the Editorial Office accordingly, not later than the date of obtaining the galley proofs.

The papers submitted for publication in the journal should be written in English. No royalty are paid to the authors.

If possible, please send us, in addition to the typescript, the same text prepared on a diskette (floppy disk) 3 1/2″ or 5 1/4″.

EDITORIAL COMMITTEE
ARCHIVES OF MECHANICS
(ARCHIWUM MECHANIKI STOSOWANEJ)